



RESEARCH REPORT

**Evaluation of Fracturing Methods
For the Stimulation of Devonian Shale
In Northern Ohio**

Columbia/DOE Contract DE-AC21-78MC08385



**EVALUATION OF FRACTURING METHODS
FOR THE STIMULATION OF DEVONIAN SHALE
IN NORTHERN OHIO**

COLUMBIA/DOE CONTRACT #DE-AC21-78MC08385

FINAL REPORT

**Compiled By:
ERIC C. SMITH**

**Reviewed By:
R. M. FORREST**

**Approved By:
W. F. MORSE**

FEBRUARY, 1982

**RESEARCH DEPARTMENT
COLUMBIA GAS SYSTEM
SERVICE CORPORATION**

1
2
3
4
5
6
7
8
9
10
11
12
13
14
15
16
17
18
19
20
21
22
23
24
25
26
27
28
29
30
31
32
33
34
35
36
37
38
39
40
41
42
43
44
45
46
47
48
49
50
51
52
53
54
55
56
57
58
59
60
61
62
63
64
65
66
67
68
69
70
71
72
73
74
75
76
77
78
79
80
81
82
83
84
85
86
87
88
89
90
91
92
93
94
95
96
97
98
99
100

TABLE OF CONTENTS

Foreword.	1
General Conclusions and Recommendations	3
Program Design and Execution.	5
Pre-Drilling Preparation.	8
Drilling Operations	14
Completion Operations	30
Geological Characterization	43
Stimulation Design and Execution.	53
Results of Cryogenic and Foam Fracturing Treatments of the Devonian Shale in Lorain County	58
Results of Displaced Explosive and Foam Stimulation of the Devonian Shale in Trumbull County	66
Summary	77
Appendix A - Matrix Gas Contents of Core Samples from Well #20143	A-1
Appendix B - Matrix Gas Contents of Core Samples from Well #20149	B-1
Appendix C - Matrix Gas Contents in Cuttings from Well #20151	C-1
Appendix D - Cliffs Minerals, Inc., Eastern Gas Shales Project Ohio Well #7, Trumbull County, Phase II Report, Preliminary Laboratory Results, August 1980.	D-1
Appendix E - Cliffs Minerals, Inc., Eastern Gas Shales Project Ohio Well #5, Lorain County, Phase II Report, Preliminary Laboratory Results, April 1980	E-1
Appendix F - M. D. Wood, Inc., Final Report, February 27, 1981.	F-1

1
2
3
4
5
6
7
8
9
10
11
12
13
14
15
16
17
18
19
20
21
22
23
24
25
26
27
28
29
30
31
32
33
34
35
36
37
38
39
40
41
42
43
44
45
46
47
48
49
50
51
52
53
54
55
56
57
58
59
60
61
62
63
64
65
66
67
68
69
70
71
72
73
74
75
76
77
78
79
80
81
82
83
84
85
86
87
88
89
90
91
92
93
94
95
96
97
98
99
100

LIST OF TABLES

<u>TABLE</u>		<u>PAGE</u>
I	Summary of Drilling and Logging Information.	15
II	Drilling and Casing Summary for Lorain County Wells.	16
III	Drilling and Casing Summary for Trumbull County Wells.	17
IV	Wellbore Surveys for Trumbull County Wells	18
V	Wellbore Surveys for Lorain County Wells	19
VI	Average Matrix Gas Contents in Core and Cuttings Samples from Lorain and Trumbull Counties, Ohio	46
VII	Average Matrix Gas Contents in Core from Prior Shale Programs. . .	47
VIII	Composition of Matrix Gas from Columbia Shale Cores.	48
IX	Average Gas Content of Pyrolysis Products.	50
X	Summary of Treatment Parameters.	54
XI	Test Data Summary - 10 Well Northern Ohio Shale Program.	55
XII	Perforated Depths (in feet) for Wells in Lorain County	59
XIII	Results of Radioactive Tracer Surveys in Lorain County Wells . . .	63
XIV	Perforated Depths (in feet) for Wells in Trumbull County	67
XV	Results of Radioactive Tracer Surveys in Trumbull County Wells . .	73
XVI	Well 20144T-Interference Test #1 Data. (Packer at 2449 feet)	75
XVII	Well 20144T-Interference Test #2 Data. (Packer at 2387 feet)	76

1. The first part of the document discusses the importance of maintaining accurate records of all transactions and activities. It emphasizes that this is crucial for ensuring transparency and accountability in the organization's operations.

LIST OF FIGURES

<u>FIGURE</u>		<u>PAGE</u>
1	Location Map 10-Well Shale Program, Trumbull County, Ohio.	9
2	Location Map 10-Well Shale Program, Lorain County, Ohio.	10
3	Geological Section in Ohio Test Areas.	11
4	Data Summary for Well No. 20143 Trumbull Co., Ohio	20
5	Data Summary for Well No. 20144 Trumbull Co., Ohio	21
6	Data Summary for Well No. 20145 Trumbull Co., Ohio	22
7	Data Summary for Well No. 20146 Trumbull Co., Ohio	23
8	Data Summary for Well No. 20147 Trumbull Co., Ohio	24
9	Data Summary for Well No. 20148 Lorain Co., Ohio	25
10	Data Summary for Well No. 20149 Lorain Co., Ohio	26
11	Data Summary for Well No. 20150 Lorain Co., Ohio	27
12	Data Summary for Well No. 20151 Lorain Co., Ohio	28
13	Data Summary for Well No. 20152 Lorain Co., Ohio	29
14	Cleanup Summary Well No. 20143	35
15	Cleanup Summary Well No. 20144	36
16	Cleanup Summary Well No. 20145	37
17	Cleanup Summary Well No. 20148	38
18	Cleanup Summary Well No. 20149	39
19	Cleanup Summary Well No. 20150	40
20	Cleanup Summary Well No. 20151	41
21	Cleanup Summary Well No. 20152	42
22	Well Sites in Grafton Township, Lorain County.	62
23	Wellbore Configuration for GOEX Displaced Explosives Treatments. .	69

1
2
3
4
5
6
7
8
9
10
11
12
13
14
15
16
17
18
19
20
21
22
23
24
25
26
27
28
29
30
31
32
33
34
35
36
37
38
39
40
41
42
43
44
45
46
47
48
49
50
51
52
53
54
55
56
57
58
59
60
61
62
63
64
65
66
67
68
69
70
71
72
73
74
75
76
77
78
79
80
81
82
83
84
85
86
87
88
89
90
91
92
93
94
95
96
97
98
99
100

FOREWORD

This report documents the events and results of the research performed by the Columbia Gas System Service Corporation on the Devonian shale at test locations in Lorain and Trumbull Counties, Ohio, and for the Northern Ohio Research Program as a whole. Columbia, the United States Department of Energy, the Gas Research Institute, Mitchell Energy, and Texas Gas Transmission Corporation jointly funded this program through individual agreements including U.S. DOE contract #DE-AC21-78MC08385 and GRI contract #5080-321-0324.

The drilling and completion of these wells in Trumbull and Lorain Counties, Ohio was designed to evaluate and inventory the shale gas reserves throughout the untested portions of the Appalachian Basin.

The objectives of this program were to: (1) evaluate the Devonian shale section's gas potential; (2) compare the cost effectiveness of different stimulation techniques; and, (3) advance well logging and testing methods.

Columbia drilled, stimulated, and evaluated five wells in each county test area. We cored and extensively logged one well in each county. The program for the remaining wells consisted of standard logging tools. Foam-type hydraulic fracturing served as a standard stimulation method for both areas for comparing the effects of cryogenic and displaced explosive fracturing.

Columbia wishes to thank Mr. C. A. Komar of the Morgantown Energy Technology Center and John Sharer of the Gas Research Institute for their assistance in directing this program.

We also wish to express thanks to the Columbia Gas Transmission Corporation operating personnel, including John Foster, Mian Ahmad, Steve Eads, Charles Bellinger, Marvin Grayson, Mark Brand, and Jim Weekley for their efforts in the planning and execution of much of our field effort.

Finally, we would like to acknowledge the support of the Columbia Research Department technicians and engineers in bringing this program to its successful completion.

GENERAL CONCLUSIONS AND RECOMMENDATIONS

A comparison of core analyses from Lorain and Trumbull Counties with those from gas producing areas showed that the shale sections in both areas contain adequate matrix gas for commercial production. Although we observed large natural gas shows in Lorain County and measured high concentrations of matrix off-gas in the core from both project areas, no significant gas production resulted from 15 individual stimulations in the Devonian shale sections of 10 wells in Trumbull and Lorain Counties, Ohio. These results indicate that hydraulic fracturing treatments using a foam medium (as performed under this contract) were unsuccessful in achieving commercial production in either area. We obtained similarly unproductive results using a CO₂-water medium for fracturing in Lorain County. Two operational failures prevented our obtaining a valid test of the displaced explosive fracturing concept. These negative experiences could result from a combination of: (1) failure to effectively contact the target horizons with the stimulations, (2) formation damage due to the completion operations, and (3) a limited extent of natural permeability planes, but not from the level of matrix gas concentrations in the treated formations.

Core samples from both counties gave little evidence of natural fracture development. Permeable zones within silty horizons may control the location of the local gas shows. Further shale research in northern Ohio should first focus on actual producing areas, and attempt to delineate the permeability trends. Future tests of stimulation methods should include borehole shooting. Although shooting may not induce extensive fractures, it should ensure at least some contact with nearly all of the treated section. In so doing, it may serve as a reasonable basis of comparison with other treatment techniques.

In view of our recent results, future shale research should focus on defining the factors which give rise to productive geological settings. Such information should provide the basic understanding of reservoir behavior required to design workable exploration and completion techniques. One could then proceed toward a meaningful assessment of the overall Devonian shale reserves.

This approach should begin with a detailed study of the available geological and geophysical data for several areas containing shale wells with both high and low cumulative production. Each area study would involve the preparation of maps and cross sections based on drilling, logging, completion, and production records for wells which have produced at least ten years. Supplementary field operations would probably include geophysical, remote sensing, and wellbore surveys ("fracture" locating devices and down-hole instruments for measuring gas influx). From this, one could hopefully explain why, how, and finally, where effective permeability channels tend to form.

PROGRAM DESIGN AND EXECUTION

Columbia and others have estimated that the Devonian shale contains several hundred trillion cubic feet of natural gas within the Appalachian Basin. However, several geological, technological, and economic factors limit the producible portion of this gas-in-place. Columbia, U.S. DOE, and GRI commenced this research as part of a comprehensive effort to define the economic reserves of the Eastern Gas Shales and to find the most practical method of producing them. Our program design called for replicate field tests of two or more stimulation methods in each area. Furthermore, we wanted to test representative areas with varied geological settings.

The National Petroleum Council recently published a thorough study of the Devonian shale gas resources. They reported total gas contents of 225 to 1860 trillion cubic feet, with a producible volume of 25 to 50 trillion cubic feet. These stated volumes depend upon projections of the shale's organic richness, gas content, and production capacity. A truly definitive study would require widespread production data across the basin. Also, the potential gas figures involve assumptions about the effects of fracturing techniques. We still need to evaluate these techniques in each prospective area to define the reserves. The present study is aimed at enhancing the hydrocarbon recovery per well in prospective areas. Devonian shale wells can help offset a substantial portion of the void left by declining conventional gas sources, provided that industry and government have properly outlined the productive regions and recovery methods by studies such as this.

Columbia's interest in gas shale research dates back to 1972. Early studies included limited coring, shale retorting, and comparisons of

several stimulation methods on a small scale. Since 1972, we have participated in four research contracts involving shale gas which were supported in part by the United States Department of Energy, the Ohio Energy Research and Development Administration, Mitchell Energy, the Gas Research Institute, and Texas Gas Transmission Company. During the course of these programs, we have drilled, logged, and completed 22 wells, recovered and examined about 7000 feet of core samples, and performed various analyses and reservoir tests. In addition, numerous other contractors funded by U.S. DOE and GRI have provided useful auxiliary data. Data generated from these and other non-proprietary programs have contributed to our current assessment of the Devonian shale's energy potential.

In the original research proposal to U.S. DOE, Columbia proposed to drill and complete ten wells in each of four areas. We planned to fracture the same stratigraphic intervals in all of the wells within each county. Our schedule called for multiple tests of at least two of the following hydraulic stimulation types per area: foam, dendritic, cryogenic, liquid explosives, and massive hydraulic. Each area included three cryogenic treatments as a standard of comparison. By varying the treatment sizes we hoped to gain some insight into the most effective stimulation volume. After contract negotiations and meetings with DOE, GRI, Mitchell Energy, and Texas Gas, the proposal evolved to a ten-well program with five wells located in eastern Ohio and five in northeastern Ohio. Both locations would have foam treatments in two wells as a standard, plus three cryogenic fractures in Lorain and three explosive fractures in Trumbull County. Columbia and DOE had a provision in their contract for further work in Steuben County, New York and Garrett County, Maryland if both parties were to agree at some later date.

Further program revisions occurred after drilling and casing the ten wells. According to the final schedule for Trumbull County, one well had a single-staged foam treatment, two wells had dual-staged foam treatments, and two wells had single-staged liquid explosive treatments. In Lorain County two wells had dual-staged foam treatments, two wells were completed with a single-staged cryogenic treatment, and one well had a dual-staged foam treatment. GRI agreed to fund all costs relating to the additional five stimulations not called for in the original program.

The following sequence of events comprised our activities under the subject research contract: (1) pre-drilling preparation, (2) drilling operations, (3) completion operations, and (4) analysis and data evaluation.

During the pre-drilling phase, Columbia selected the project areas and specific well sites. After receiving archaeological, environmental, and site approvals we surveyed the locations, obtained the required drilling permits and prepared the sites and well roads.

PRE-DRILLING PREPARATION

The initial choice of test areas considered several geological factors which could influence gas production. We intended to evaluate the effects of varying depths, organic shale thicknesses, structural settings, and thermal maturities on the shale production in areas throughout the Appalachian Basin.

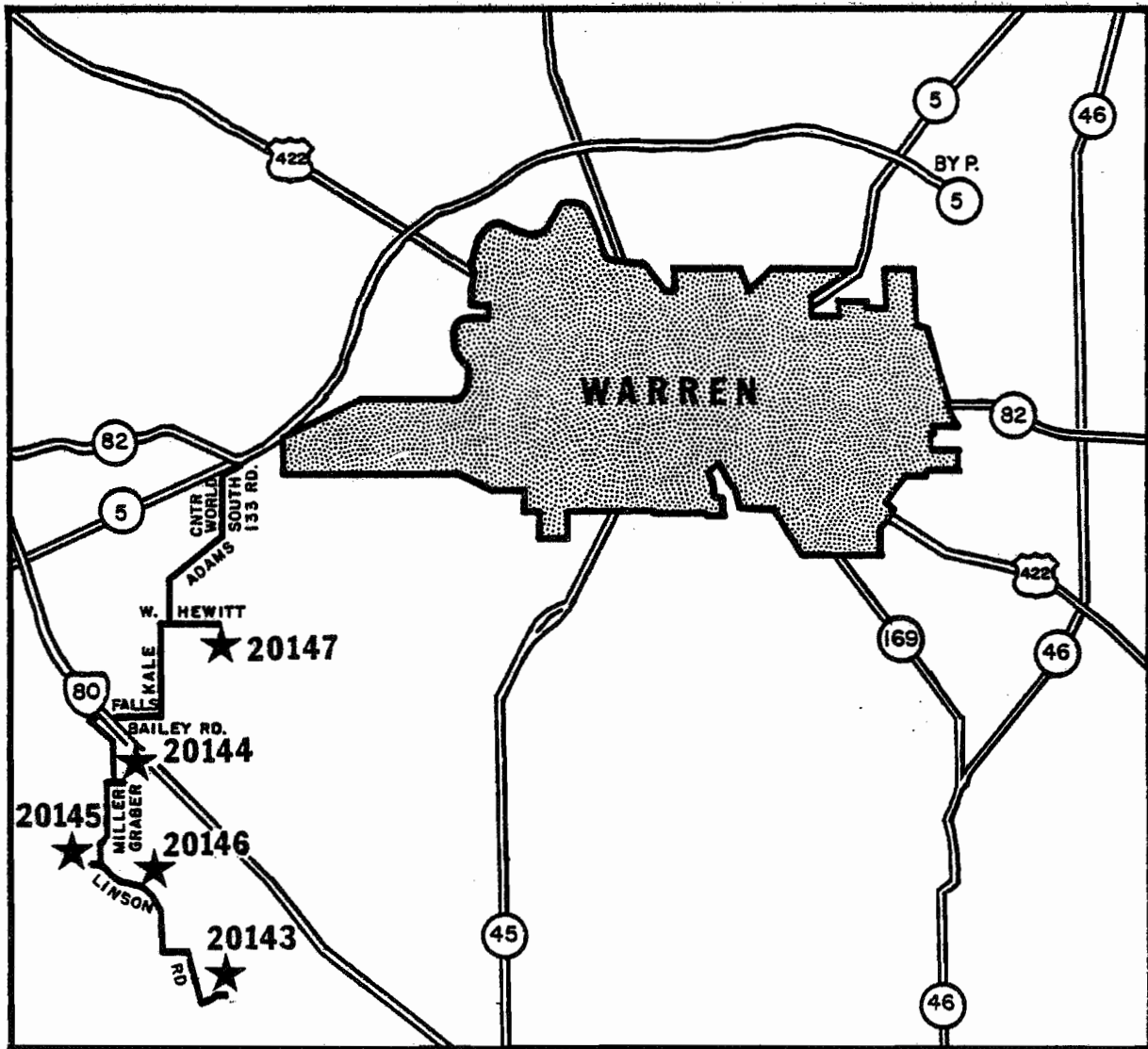
From six proposed locations, the program participants jointly agreed to fund research in Trumbull and Lorain Counties, Ohio (See Figures 1 and 2). Within these areas Columbia chose drilling sites in our leased acreage with ready access to operating pipelines.

The Devonian shale in Trumbull County attains a thickness of about 2400 feet at a total depth of 2700 feet (See Figure 3). About 100 feet of shale exhibit high radioactivity (greater than 230 API units in gamma radiation). Prior studies showed a low thermal maturity trend in this county and an absence of major structural features. Columbia's interest in the area stemmed from the frequency of reported gas shows in the shale section. Although these flows occurred at very shallow depths, and probably exhibited low pressures, we felt that other horizons could also have enhanced permeabilities.

The Devonian shale thickness in Lorain County averages 900 feet at total depth of 1300 feet. About 450 feet of this section exceeds 230 API units in gamma radiation. Previous studies showed the area had no major structural features and a low thermal maturity for the shale. Our interest in this area arose from the thickness of the radioactive shale and the shallow depth (which could allow for low cost gas production).



LOCATION MAP 10-WELL SHALE PROGRAM TRUMBULL CO., OHIO

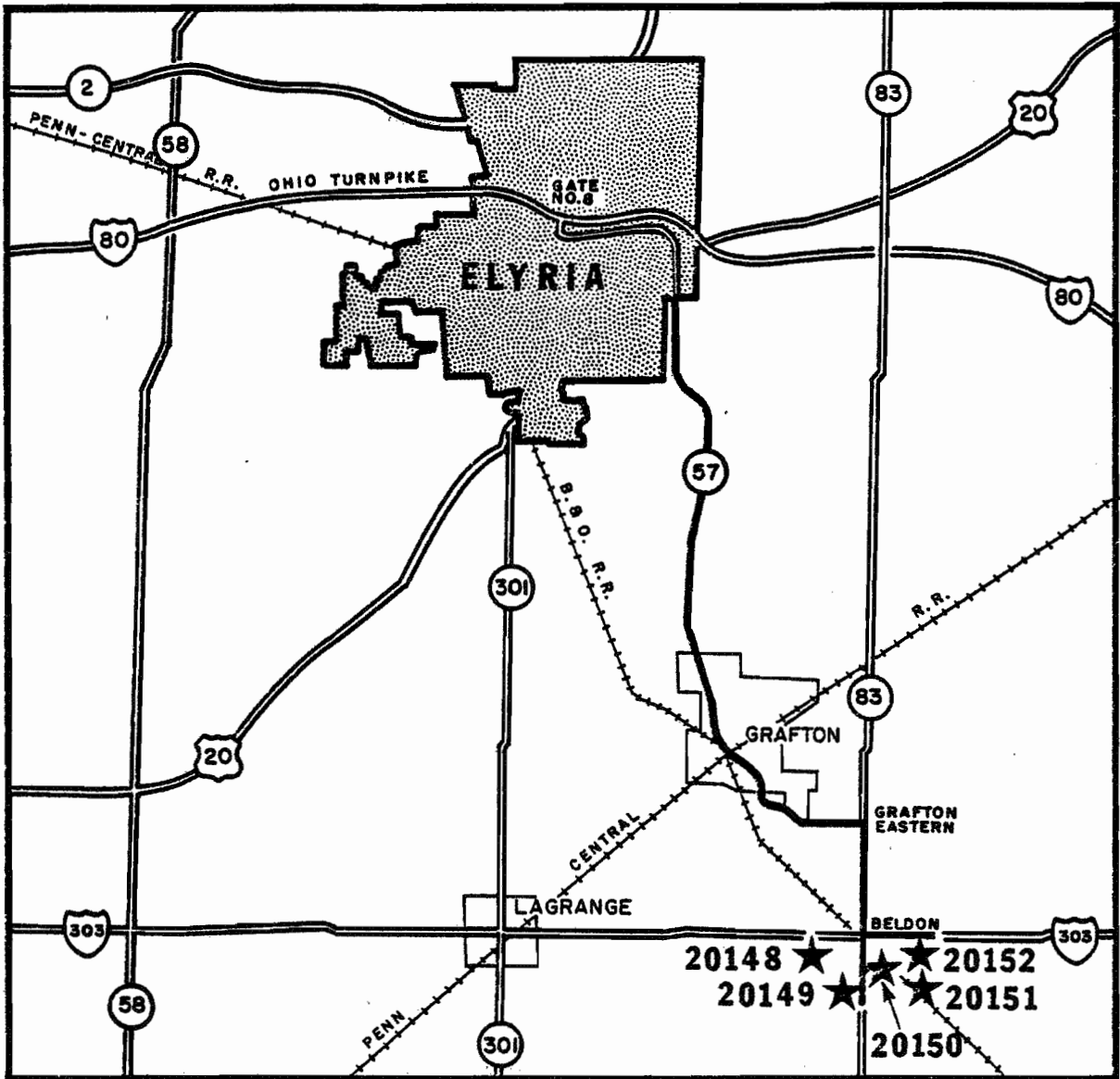


★ WELL SITES

FIGURE 1



LOCATION MAP 10-WELL SHALE PROGRAM LORAIN CO., OHIO

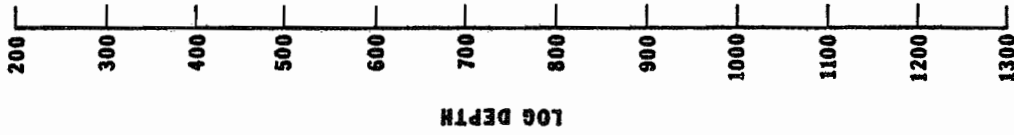
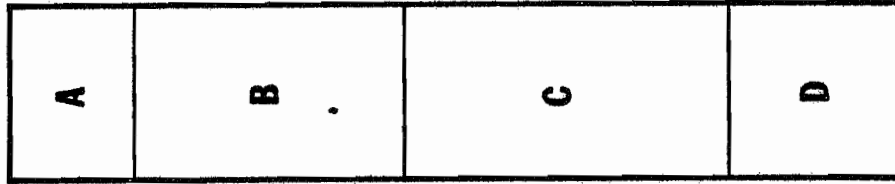


★ WELL SITES

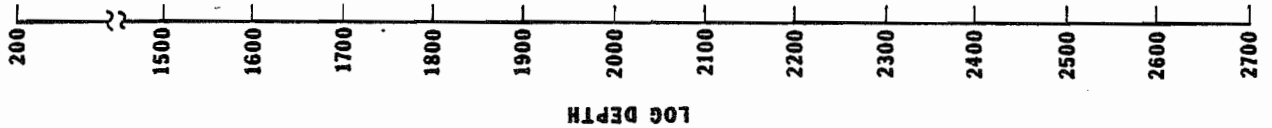
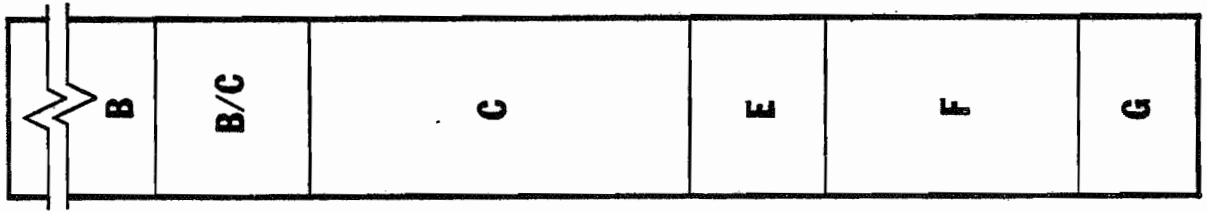
FIGURE 2

GEOLOGICAL SECTION IN OHIO TEST AREAS

WELL 20149
LORAIN CO.,
OHIO



WELL 20143
TRUMBULL CO.,
OHIO



SERIES	GROUP	FORMATION OR MEMBER	
UPPER DEVONIAN	CONEWANGO	A	CLEVELAND CHAGRIN
	CANADAWAY	B	
	JAVA	C	CHEMUNG
		E	HURON
MIDDLE DEVONIAN	WEST FALLS	D	UPPER OLENTANGY
	HAMILTON	F	PIPE CREEK
		G	RHINESTREET
			LOWER OLENTANGY

FIGURE 3

An analyses of available remotely-sensed imagery, made prior to the final site selection, revealed no evidence of natural fracture trends in either county. Both tracts have an extensive cover of glacial sediment which would obscure any surface expressions. In addition, agricultural activities have imposed obvious linear trends in northern Ohio. Field work failed to reveal any significant outcrops with measurable fracture trends in or near either region. Consequently, no credible information on natural fracture concentrations existed prior to drilling.

Personnel from the Lawrence Livermore Laboratory, Livermore, California, under the direction of Kerry O'Banion, reviewed the potential environmental impacts of this research program. On October 30, 1978, they published their report entitled, *"Environmental Report: Stimulation of Devonian Shale Formations in Ohio, New York, and Maryland"* (USID-17956). This report states, "None of the target areas present any environmental problems in general, . . .".

After Columbia selected the specific well sites, personnel from the Cleveland Museum of Natural History, Cleveland, Ohio, under the direction of David R. Bush, conducted archaeological surveys at each site. Their results concluded that the research operations probably would not disturb any cultural resources. Two separate reports entitled, *"Archaeological Resources for the Proposed Gas Well Drilling Sites in Lorain and Trumbull Counties, Ohio (dated January 17, 1979) and Archaeological Investigations of Three Additional Gas Well Drilling Sites in Trumbull and Lorain Counties, Ohio, (Dated August 17, 1979)"*, give the full details of these surveys.

After evaluating the environmental and archaeological reports, plus Columbia's site selection information, U.S. DOE verbally granted approval to proceed with the field work. By July 1979, the State of Ohio had issued the drilling permits.

DRILLING OPERATIONS

Drilling began on July 30, 1979, in Lorain County at well 20149 (McGuire). Delta Drilling Company drilled the well and the five Trumbull County wells with an air-rotary system. A cable tool rig operated by Fred Ingram Drilling performed the drilling and casing tasks on the remaining Lorain County sites. During the coring of 1187 feet of shale in Trumbull County and 879 feet in Lorain County, Christensen Diamond Products provided downhole equipment, orientation services, and supervision. Two reports by Cliffs Minerals, Inc. (included as appendices IV and V) describe the coring operations and core samples at length.

In Lorain County, the shale section averaged 1000 feet in thickness. All of the wells had measurable natural open flows with the exception of well 20151.

The Trumbull County wells had an average shale thickness of 2380 feet and only one reported gas show--from a very shallow and low pressured zone in well 20144. In addition, well 20147 had an open flow of 1 Mcfd before casing.

To provide a maximum volume of correlative data at a practical cost, we conducted comprehensive logging programs in the cored wells, and ran a rather practical suite for the other wells. By November 21, 1979, Columbia had drilled, logged, and cased the ten project wells. Tables I-V list the relevant drilling and completion information, and Figures 4-13 summarize the geological data.

TABLE I
SUMMARY OF DRILLING AND LOGGING INFORMATION

Well Number	County	Top of Shale	Base of Shale	Feet Cored	Temp./Stabil. Events at:	Gas Show at:	Open Flow
20143	Trumbull	263	2701	1187	--	trip gas 1616 Conn. gas 1792, 1906, 2198, 2256, 2316, 2434, 2552	TSTM*
20144	Trumbull	228	2593	--	614	Baroid 1913-2102 @1500 to 2000 units	Estimated at 90-100 MCF
20145	Trumbull	240	2610	--	--	--	TSTM
20146	Trumbull	229	2629	--	--	--	TSTM
20147	Trumbull	226	2593	--	--	--	1 MCF before logging
20148	Lorain	252	1246	--	345-347, 405-428, 514-525, 572-576, 610-624, 650-669, 1239-1286	398, 642, 656, 664, 980	4 MCF
20149	Lorain	293	1273	879	465-475, 538-543, 558-628, 729-732, 756-758, 790-797, 1274-1290, 1302- 1308	--	8 MCF
20150	Lorain	230	1253	--	650-745, 1092- 1124	503-653	38 MCF
20151	Lorain	247	1292	--	1200, 1270, 1224	--	TSTM
20152	Lorain	296	1277	--	300-400, 476, 648-652	527, 760	35 MCF

* too small to measure

TABLE II

DRILLING AND CASING SUMMARY
FOR LORAIN COUNTY WELLS

Well Number	20148	20149	20150	20151	20152
Elevation (feet)	863	878	867	900	899
Conductor Pipe: length (feet) diameter (inches)	60 11	32 13-3/8	41 11	41 11	21 13-3/8
Surface Casing: length (feet) diameter (inches) hole size (inches) sacks of cement cement type	266 8-5/8 10 150 Thixotropic	293 8-5/8 12-1/4 200 Thixotropic	262 8-5/8 10 100 Thixotropic	285 8-5/8 10 75 Thixotropic	295 8-5/8 10 300 Thixotropic
Production Casing: length (feet) diameter (inches) hole size (inches) sacks of cement cement type Staging Tool Depth	1284 4-1/2 8 300 Pozmix -	1340 4-1/2 7-7/8 325 Pozmix 685	1334 4-1/2 8 395 Pozmix/common 801	1327 4-1/2 8 400 Pozmix -	1309 4-1/2 8 300 Pozmix -
Breakdown Pressure (psi) Average Treatment Pressure (psf) Breakdown fluid (gallons): 15% HCl 7-1/2% HCl 2% KCl-water Mud Acid	1200/1700 2050/1400 500/5264 2500	1600 1800 500 3500	1500/1900 2300/2300 3000/500 5860/2500	1400/1800 2300/1900 500/0 0/500 2500/2100	2000 2500 600 2500
Total Depth (feet)	1288	1340	1351	1327	1309

TABLE III

DRILLING AND CASING SUMMARY
FOR TRUMBULL COUNTY WELLS

Well Number	20143	20144	20145	20146	20147
Elevation (feet)	951	913	930	921	929
Conductor Pipe: length (feet)		31	33	42	49
diameter (inches)		13-3/8	13-3/8	13-3/8	13-3/8
Surface Casing: length (feet)	485	311	296	305	355
diameter (inches)	8-5/8	8-5/8	8-5/8	8-5/8	8-5/8
hole size (inches)	12-1/4	12-1/4	12-1/4	12-1/4	12-1/4
sacks of cement	300	300	200	200	200
cement type	Thixotropic	Thixotropic	Thixotropic	Thixotropic	Thixotropic
Production Casing: length (feet)	2750	2621	2670	2665	2622
diameter (inches)	4-1/2	4-1/2	4-1/2	4-1/2	4-1/2
hole size (inches)	7-7/8	7-7/8	7-7/8	7-7/8	7-7/8
sacks of cement	750	710	600	675	710
cement type	Pozmix	Pozmix	Pozmix	Pozmix	Pozmix
Staging Tool Depth	1450	1318	1350	1459	1290
Breakdown Pressures (psi)	1900/2200	2400	1800/1600	2400	2350
Average Treatment Pressure (psi)	1700/2100	2200	2400/2800	1200	2200
Breakdown fluid (gallons):					
15% HCl	2500/2000	2000	600/0	5200	2000
7-1/2% HCl	-		2500/2000		
KCl-water	0/500			500	250
Mud Acid					
Total Depth (feet)	2762	2650	2670	2682	2660

TABLE IV

WELLBORE SURVEYS FOR TRUMBULL COUNTY WELLS

	Well Number -				
	<u>20143</u>	<u>20144</u>	<u>20145</u>	<u>20146</u>	<u>20147</u>
<u>SCHLUMBERGER</u>					
Borehole Compensated Sonic	x	x		x	x
Dual Laterolog	x				
Compensated Neutron	x			x	
Formation Density	x	x	x	x	x
Gamma Ray	x	x	x	x	x
Temperature		x	x	x	x
Audio		x	x	x	x
Fracture Identification		x	x	x	x
Dual Induction				x	
Spherically Focussed				x	
Differential Audio					
Synergetic Mechanical Properties	x				
Synergetic Coriband-Kerogen	x				
<u>BIRDWELL</u>					
Wellbore Sibilation	x				
Gamma Ray	x				
Differential Temperature	x				
3-D Velocity	x				
Density Borehole Compensated Caliper					
<u>BAROID</u>					
Litholog	x	x		x	x
<u>BASIN SURVEY</u>					
Cement Quality					
<u>MCCULLOUGH</u>					
Gamma Ray	x	x	x	x	x
Bond Cement	x	x	x	x	x
Casing Collar Locator	x		x	x	
Static Tracer Log	x		x		
Radioactive Tracer Log	x		x		
Caliper				x	

TABLE V

WELLBORE SURVEYS FOR LORAIN COUNTY WELLS

	<u>Well Number</u>				
	<u>20148</u>	<u>20149</u>	<u>20150</u>	<u>20151</u>	<u>20152</u>
<u>SCHLUMBERGER</u>					
Borehole Compensated Sonic		X			
Dual Laterolog					
Compensated Neutron		X			
Formation Density		X	X	X	X
Gamma Ray		X	X	X	X
Temperature			X	X	X
Audio		X	X	X	X
Fracture Identification		X			
Dual Induction		X			
Spherically Focussed		X			
Differential Audio		X			
Synergetic Mechanical Properties		X			
Synergetic Coriband-Kerogen		X			
<u>BIRDWELL</u>					
Wellbore Sibilation	X	X			
Gamma Ray	X	X			
Differential Temperature	X	X			
3-D Velocity	X	X			
Density Borehole Compensated	X				
Caliper	X				
<u>BAROID</u>					
Litholog		X			
<u>BASIN SURVEY</u>					
Cement Quality					X
<u>MCCULLOUGH</u>					
Gamma Ray	X	X	X	X	X
Bond Cement	X	X	X	X	X
Casing Collar Locator	X	X	X	X	X
Static Tracer Log					
Radioactive Tracer Log	X	X	X	X	X
Caliper					

DATA SUMMARY FOR WELL NO. 20143 TRUMBULL CO., OHIO

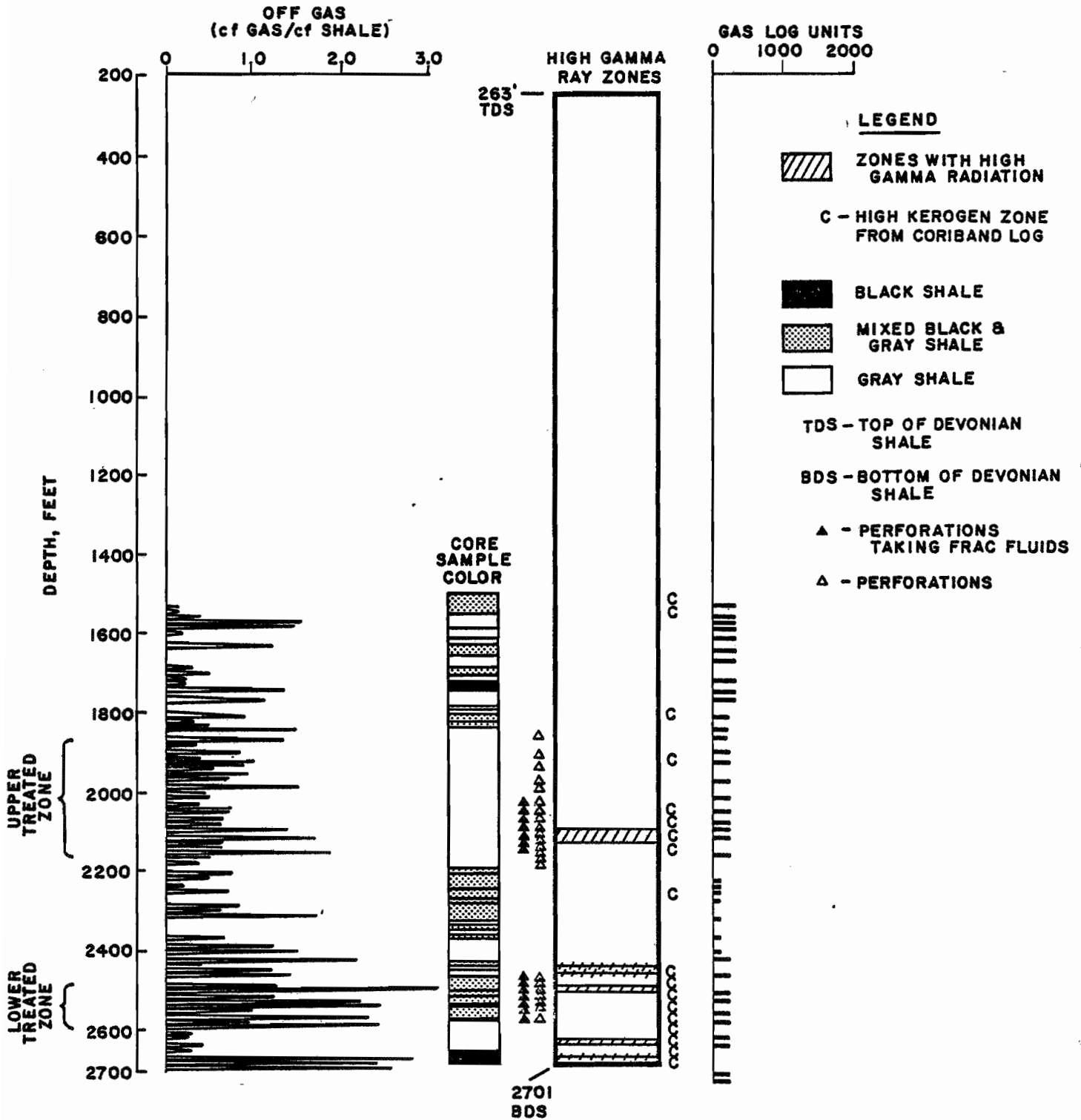


FIGURE 4

DATA SUMMARY FOR WELL NO. 20144 TRUMBULL CO., OHIO

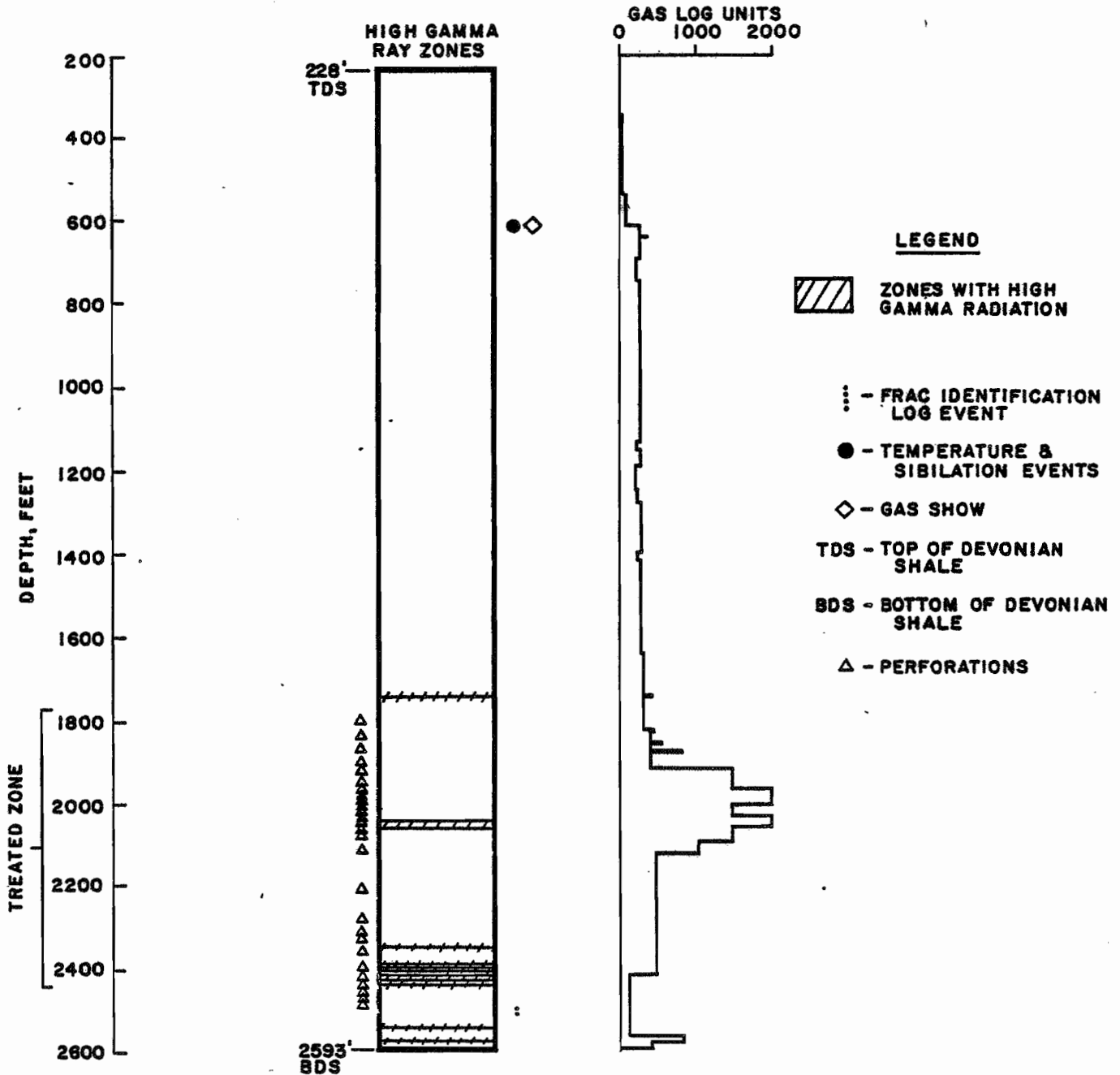


FIGURE 5

DATA SUMMARY FOR WELL NO. 20145 TRUMBULL CO., OHIO

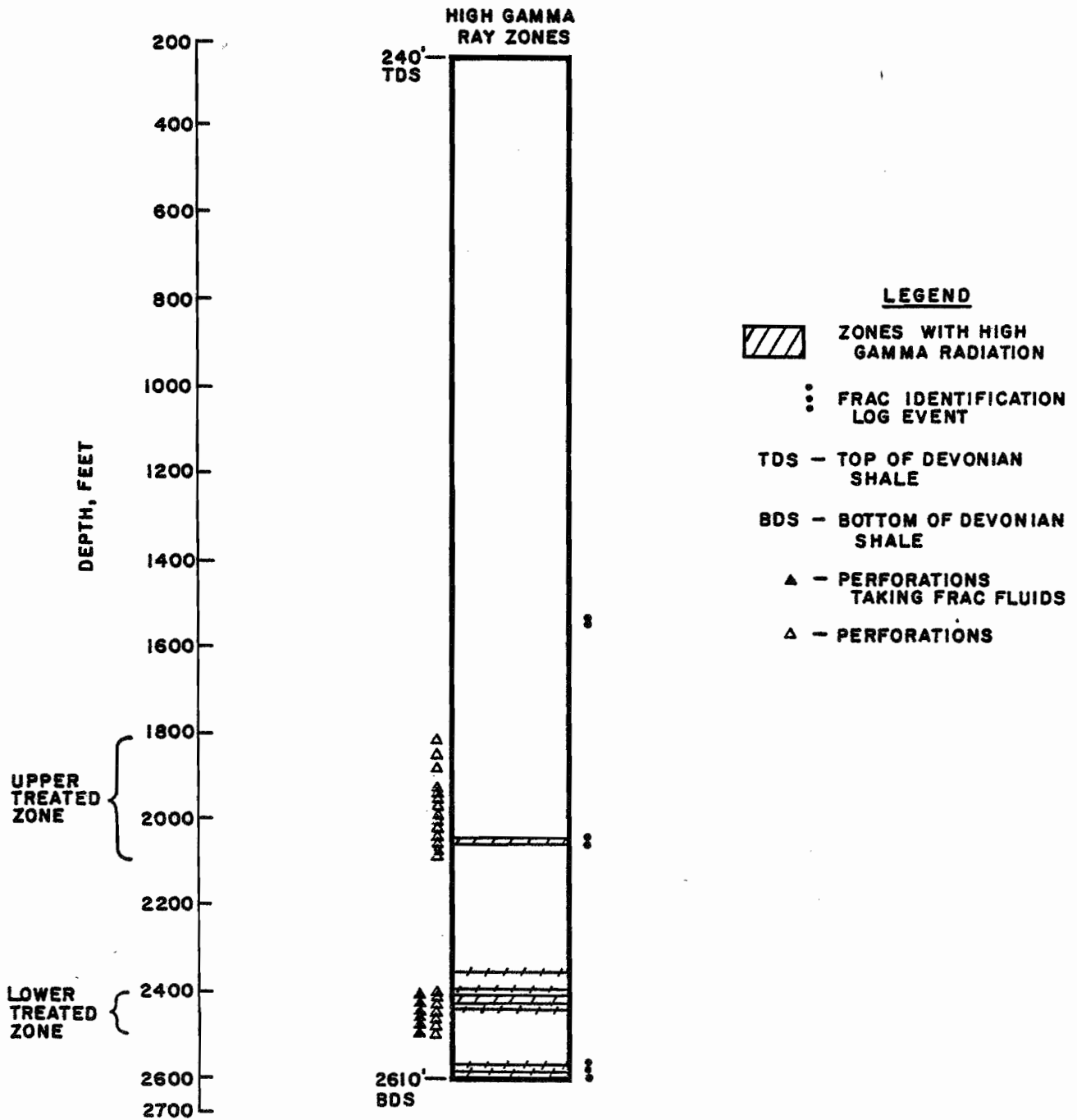


FIGURE 6

DATA SUMMARY FOR WELL NO. 20146 TRUMBULL CO., OHIO

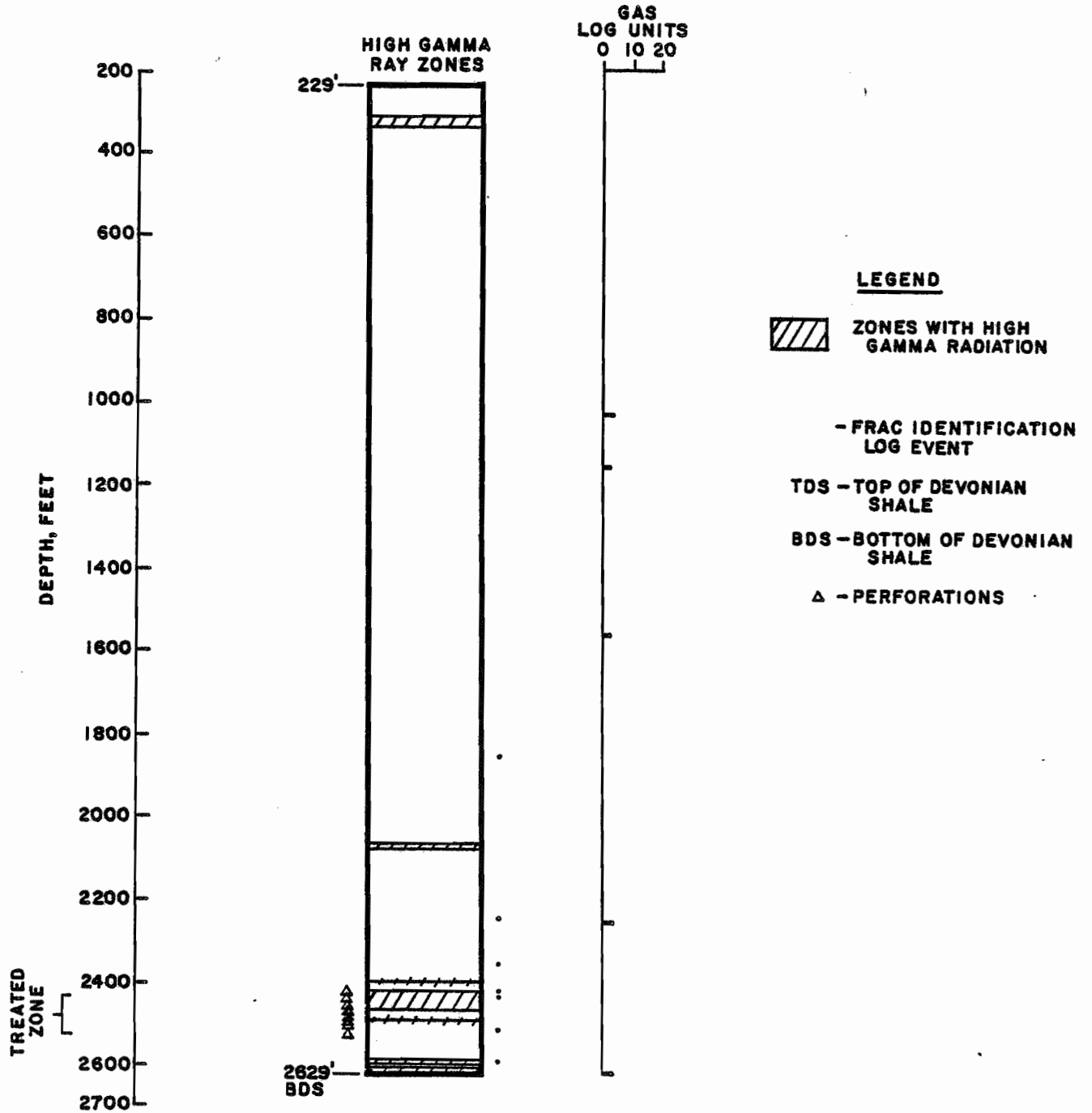


FIGURE 7

DATA SUMMARY FOR WELL NO. 20147 TRUMBULL CO., OHIO

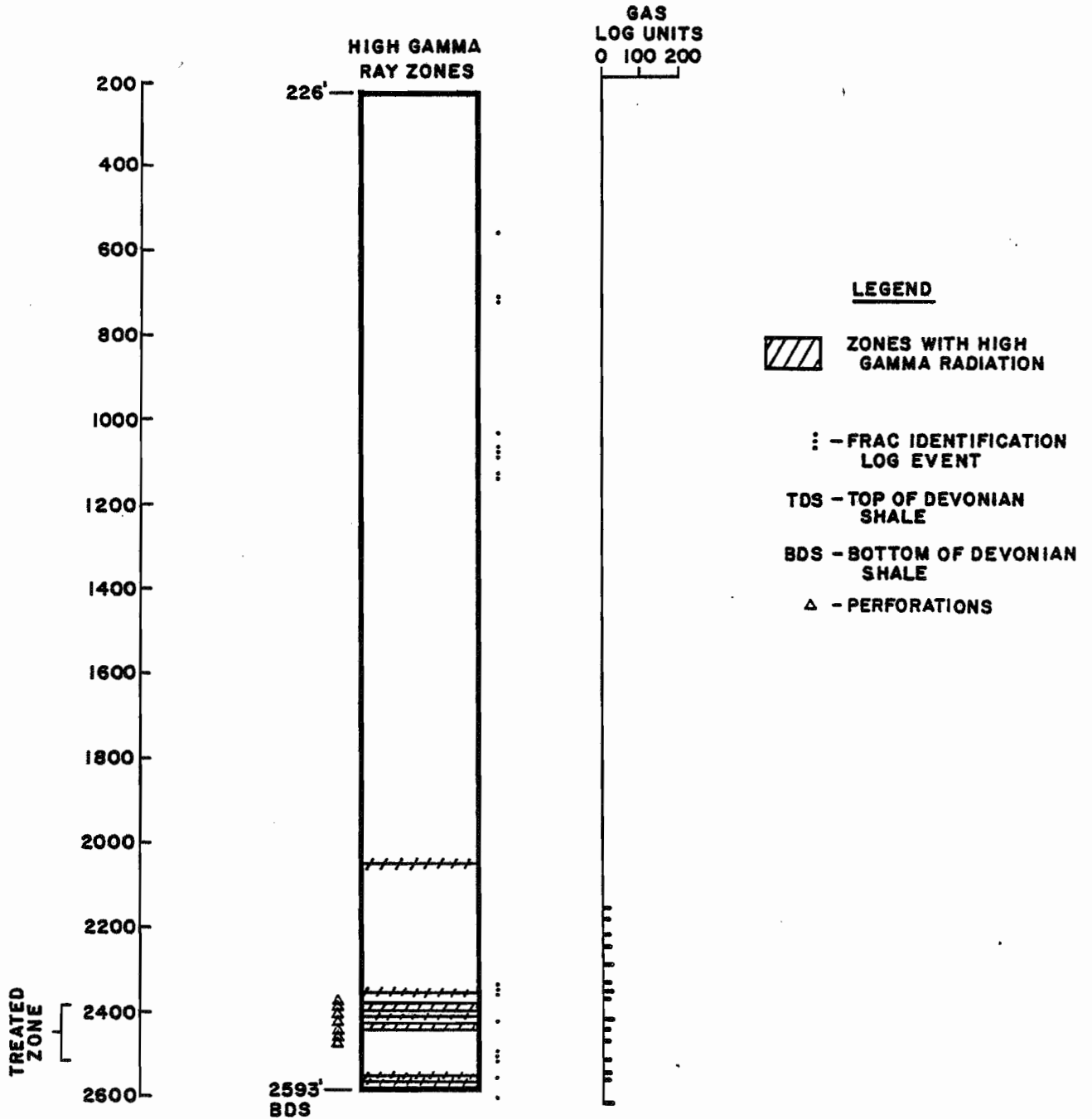


FIGURE 8

DATA SUMMARY FOR WELL NO. 20148 LORAIN CO., OHIO

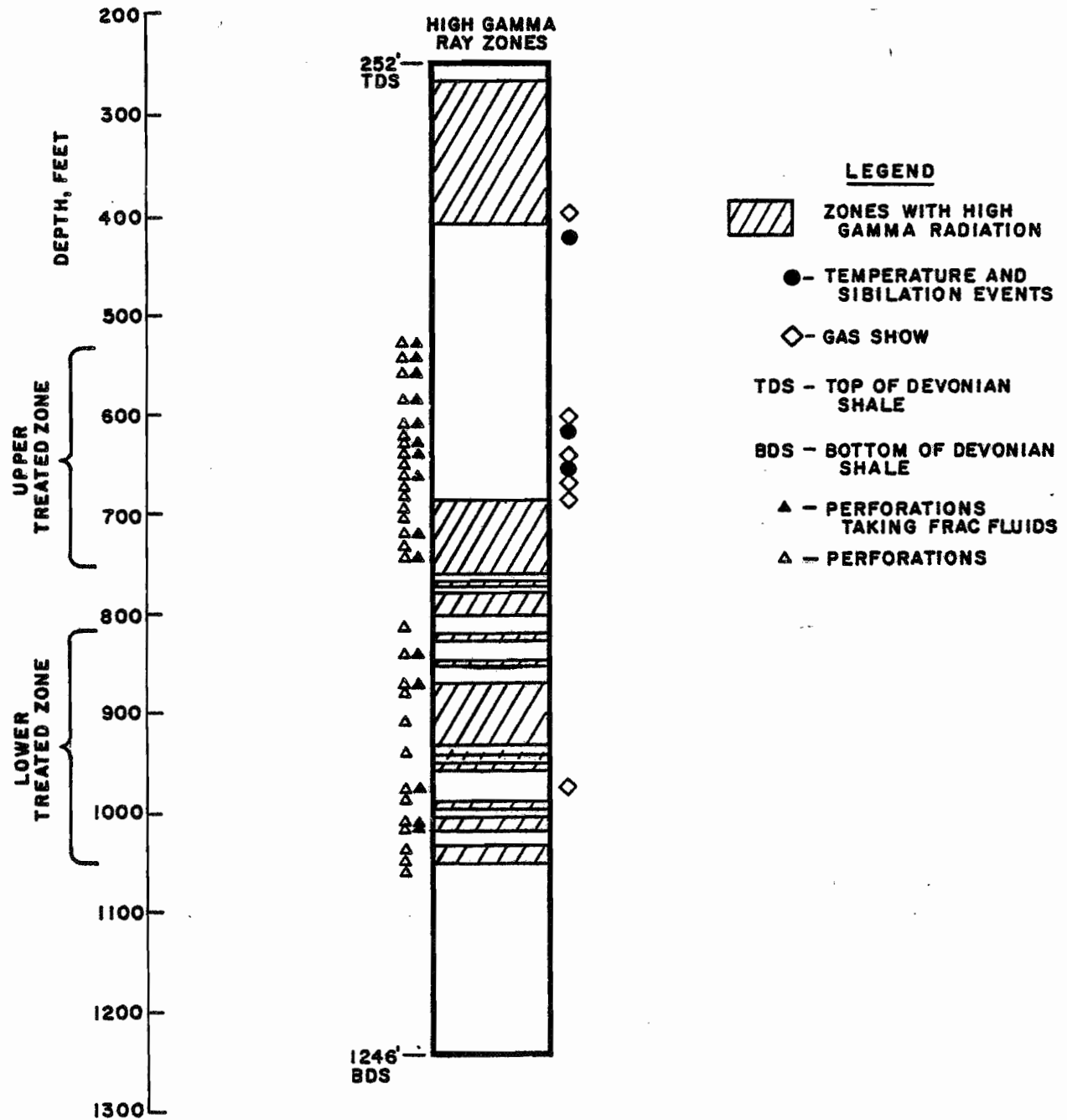


FIGURE 9

DATA SUMMARY FOR WELL NO. 20149 LORAIN CO., OHIO

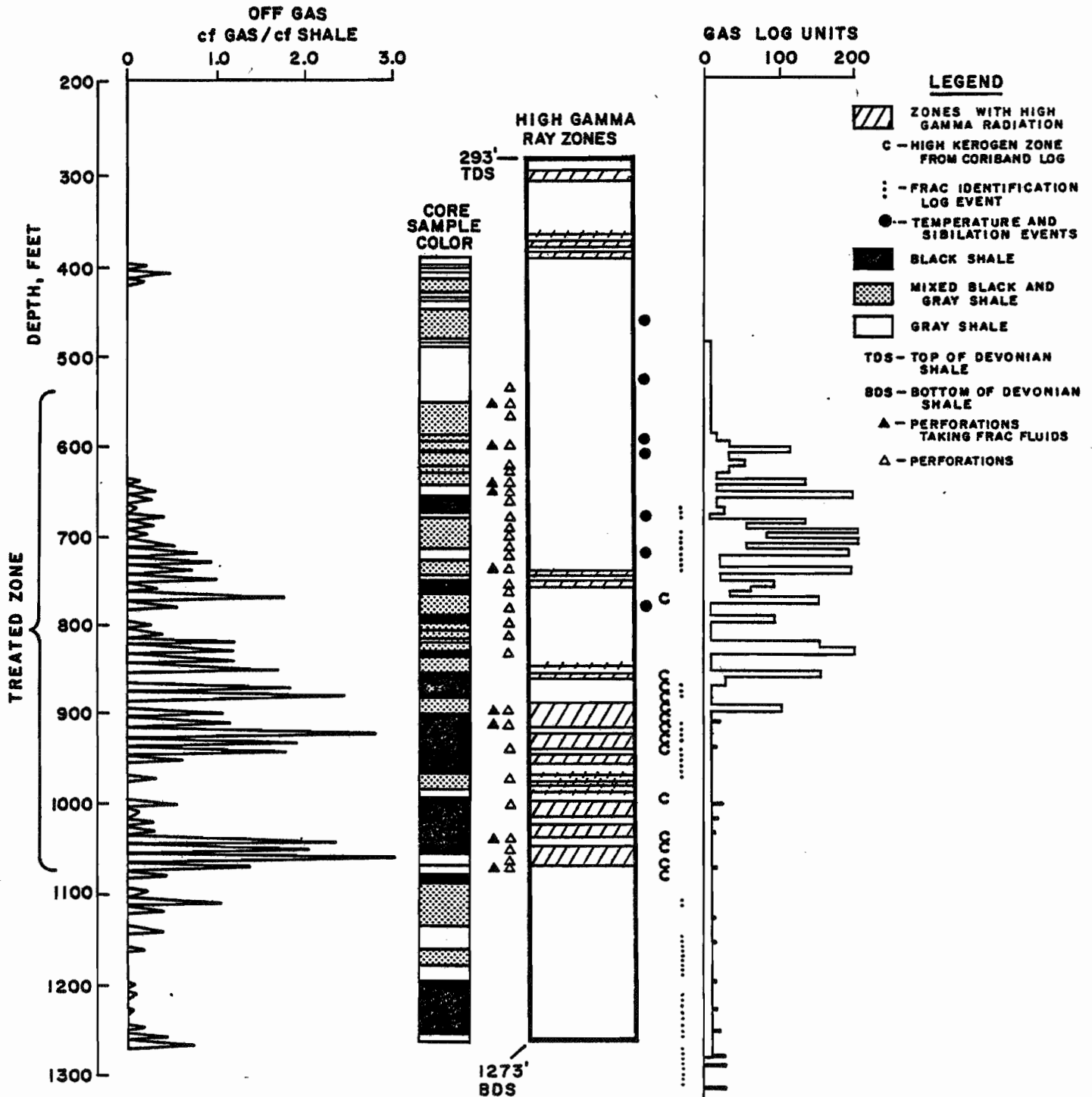


FIGURE 10

DATA SUMMARY FOR WELL NO. 20150 LORAIN CO., OHIO

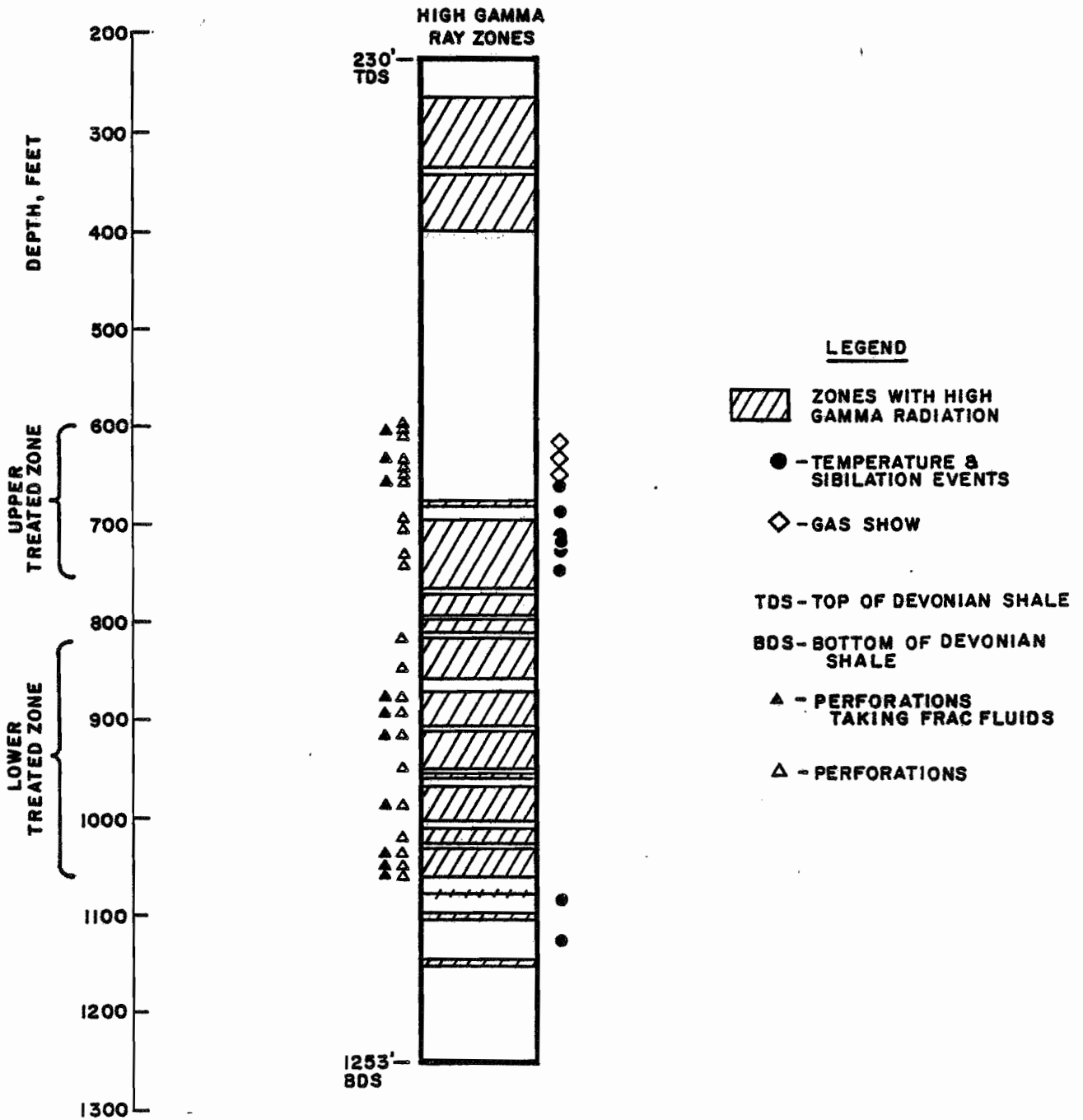


FIGURE 11

DATA SUMMARY FOR WELL NO. 20151 LORAIN CO., OHIO

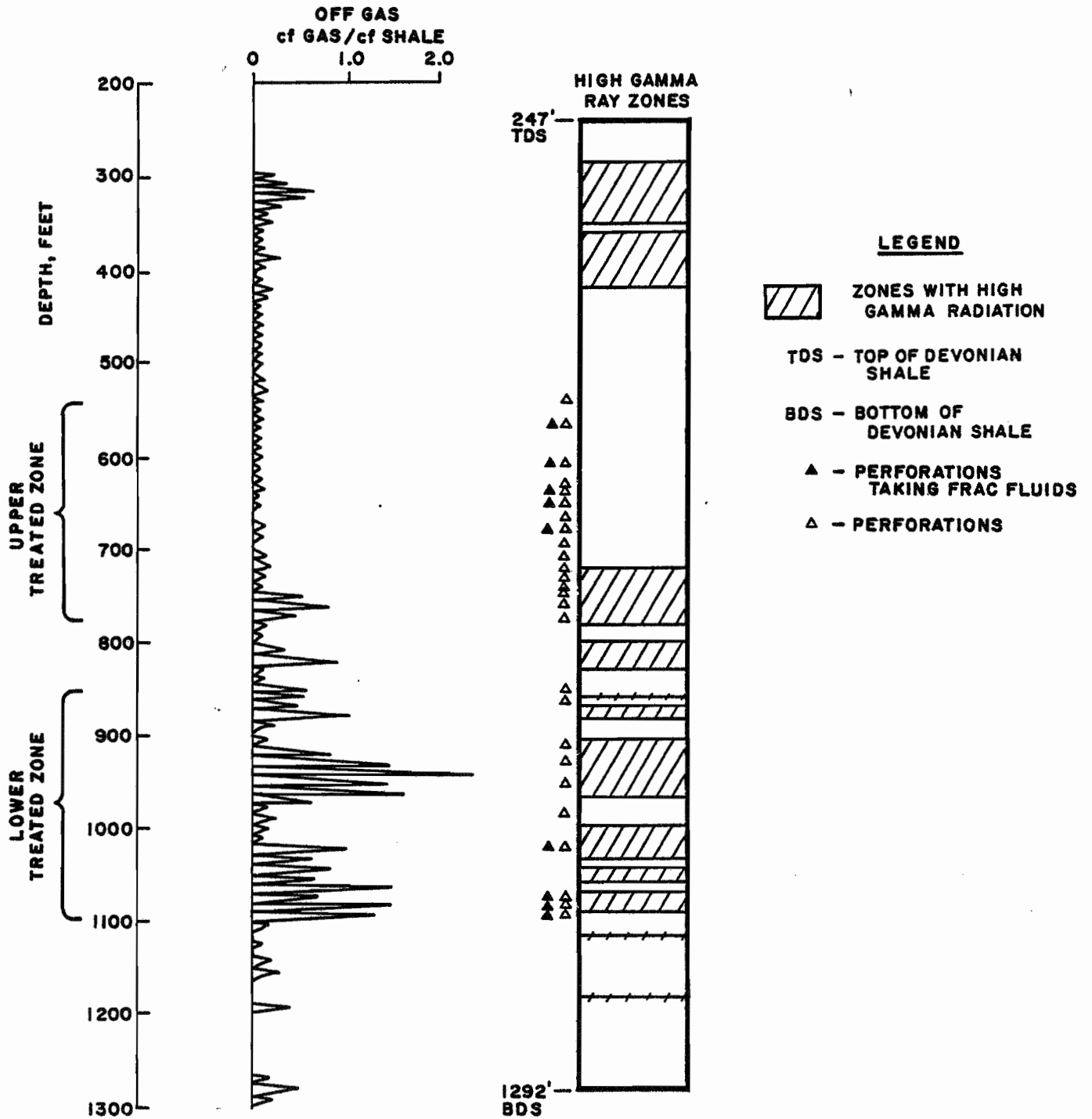


FIGURE 12

DATA SUMMARY FOR WELL NO. 20152 LORAIN CO., OHIO

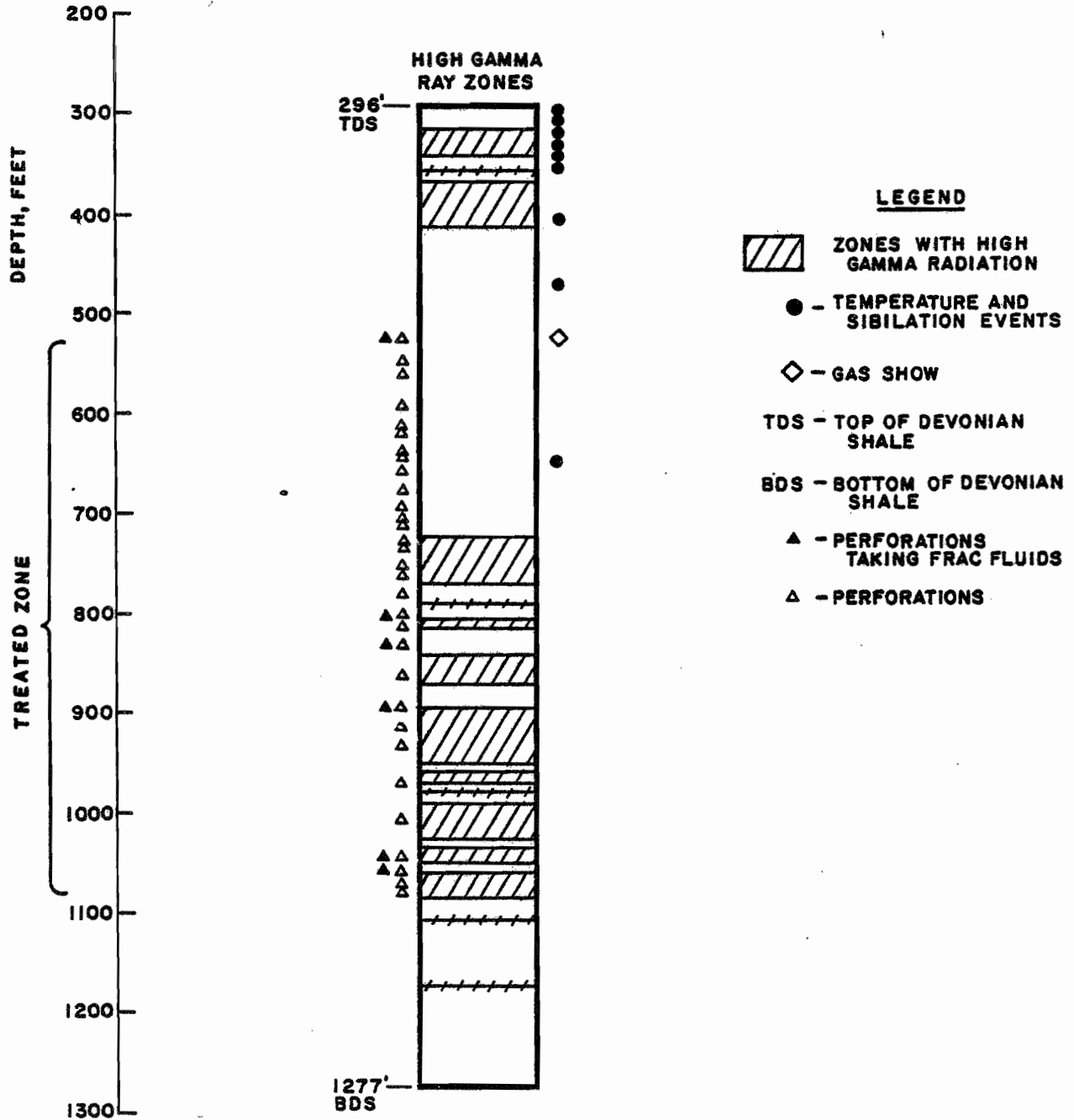


FIGURE 13

COMPLETION OPERATIONS

During and immediately after drilling and logging the project wells, Columbia reviewed the drilling and logging data to finalize each well completion. A uniform evaluation of the shale's potential across the Appalachian Basin requires the use of one standard fracturing type. However, the program objectives also called for replicate tests of at least two methods, because we cannot predict the best techniques for new areas. Foam seemed the most suitable technique of the hydraulic methods. Consequently, we decided to compare cryogenic and displaced explosive techniques with "standard" foam treatments in Lorain and Trumbull Counties, respectively.

Previous shale research has suggested that one stimulation and cleanup per well should provide the most efficient and economical treatment. However, the final decision to conduct two stimulations in five of the wells added the possibility of an assessment of the effects of varying treatment size (increased lateral penetration), and a comparison of distinct portions of the shale section.

The depth intervals slated for perforation and completion included all indications of high matrix gas content and natural gas shows within a 700 feet maximum practical treatment interval, and up to a minimum depth of 500 feet from the surface. Observed gas shows, temperature and "noise" log events, and preliminary high core off gas volumes comprised the basis for choosing the perforation depths. In the absence of any substantial natural flow, the location of high matrix gas concentrations

determined the perforation depths in both the Trumbull County wells and lower portions of the Lorain County wells. However, we perforated all of the observed gas shows in the upper shale section below 500 feet in Lorain County.

We also attempted to methodically compare the stimulation effects by completing identical zones in each county, based on a comparison of gamma ray and density logs. In other words, if one well had perforations corresponding to gas shows, the other four wells had perforations at the same stratigraphic horizon. However, the cost of explosives limited the targeted completion intervals to about 90 feet in the two wells designated for explosive fracturing.

The scheduled completion tasks consisted of:

- A. Drilling out the cement stage tools where present
- B. Running cement bond and perforation logs
- C. Perforating
- D. Breaking down the completion intervals with 7 1/2% hydrochloric acid and using excess ball sealers
- E. Recovering the breakdown fluid
- F. Pre-frac testing
- G. Conducting the stimulations
- H. Cleaning up after the treatment
- I. Post-frac testing

These activities began in January 1980. They halted in February after two breakdowns, and started again in July after the restructuring of the stimulation program. By March 1981 Columbia had completed all of the scheduled field work on this project.

After reviewing the cement bond logs, three of the ten wells appeared to have unsatisfactory bonding over part of the treated zone. In spite of this, pumping tests and further bond logging under pressure did not reveal any cement problems. Because our field engineer did not detect any operational problems during cementing, a microannular gap probably existed between the casing and cement in these wells. Pressurizing the casing (as during the breakdowns and stimulations) eliminated this problem. Consequently, all cement jobs proved functionally sound.

Initially, an acid treatment consisting of 2000 gallons of 7 1/2% hydrochloric acid was used to break down the wells. After the first acid treatment in well 20148, the well flowed back a large volume of unspent acid which created a potential work hazard. Consequently, after breaking down all of the Trumbull County wells, and the lower zone of well 20148, we reduced the acid volume to 500 gallons followed by a 2% potassium chloride solution.

The pre- and post-stimulation testing plans included a 48-hour pressure test and 24-hour open flow measurements for all wells. In addition, we intended to perform long-term transient reservoir tests, both before and after treatment, on the well in each area with the largest flow capacity. However, none of the wells had sufficient gas flows to justify this detailed testing.

The Dowell Division of Dow Chemical performed all of the hydraulic stimulations under this contract. Wells 20143, 20145, 20150, and 20151 each received two foam treatments, and well 20144 received a single foam treatment. They treated wells 20149 and 20152 with single cryogenic stimulations, and well 20148 with two cryogenic stimulations. GOEX Inc. attempted displaced

liquid explosive fractures on wells 20146 and 20147. By design, all of the hydraulic fractures used about 1500 barrels of total displaced fluid. The volume of fluid actually displaced varied somewhat due to equipment problems during the operations. With the exceptions of wells 20144, 20146, and 20147, McCullough injected a radioactive tracer in with the regular proppant to help indicate which perforations had accepted fluid. Ball sealers helped to effect a more even distribution of fracturing fluid in the perforations.

The Gas Research Institute employed Sandia Laboratories and M. D. Wood, Inc. to monitor the lower zone breakdown and stimulation of well 20148 in Lorain County, and to map the induced fracture growth. These two companies analyzed data from surface electrical potential probes and tiltmeter arrays plus borehole seismic devices to detect and measure the fracture orientation and height. Sandia also used surface geophones to determine the amount of GOEX explosives that detonated during the first displaced explosive completion. The appendix contains the available reports on the above tasks.

By prior agreement with our program partners, the results of the first cryogenic and liquid explosive treatments were used to determine whether subsequent treatments with these processes would be conducted. Although the first cryogenic treatment proved successful, the GOEX completion experienced surface hardware malfunctions and resulted in serious well damage. Columbia felt that it had not properly tested the method due to the malfunction at the surface equipment. Therefore, we obtained agreement from the other partners for a second trial. Despite attempted improvements in the equipment, the second treatment was also unsatisfactory, and an unexpected detonation occurred.

Columbia monitored the fluid volumes recovered after each hydraulic fracture by flowing or swabbing the water into pits. Field personnel measured the fluid volume while they pumped it into tank trucks for transport and disposal. Figures 14 through 21 show the clean up records for each completion.

CLEANUP SUMMARY

WELL NO. 20143

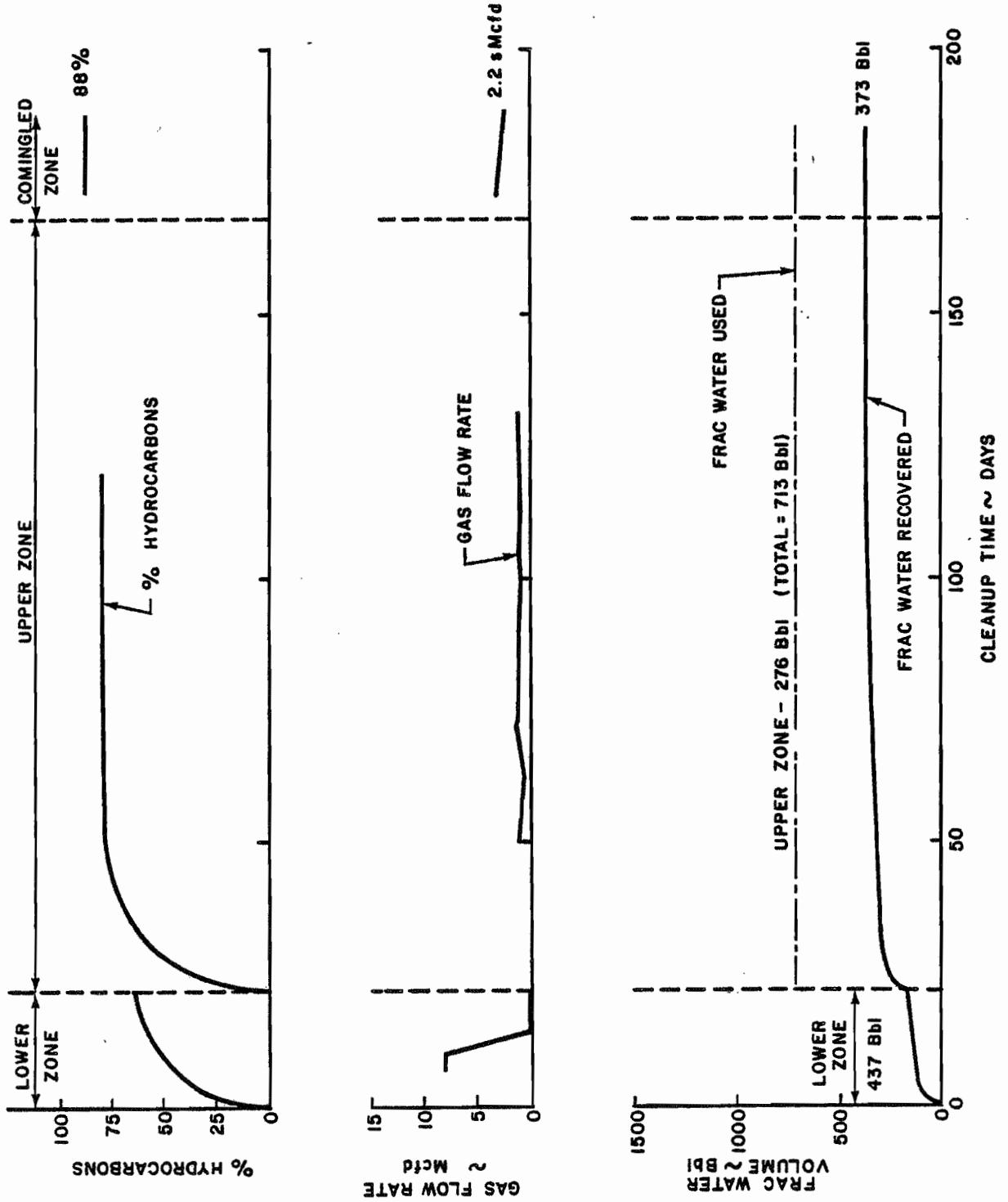


FIGURE 14

**CLEANUP SUMMARY
WELL NO. 20144**

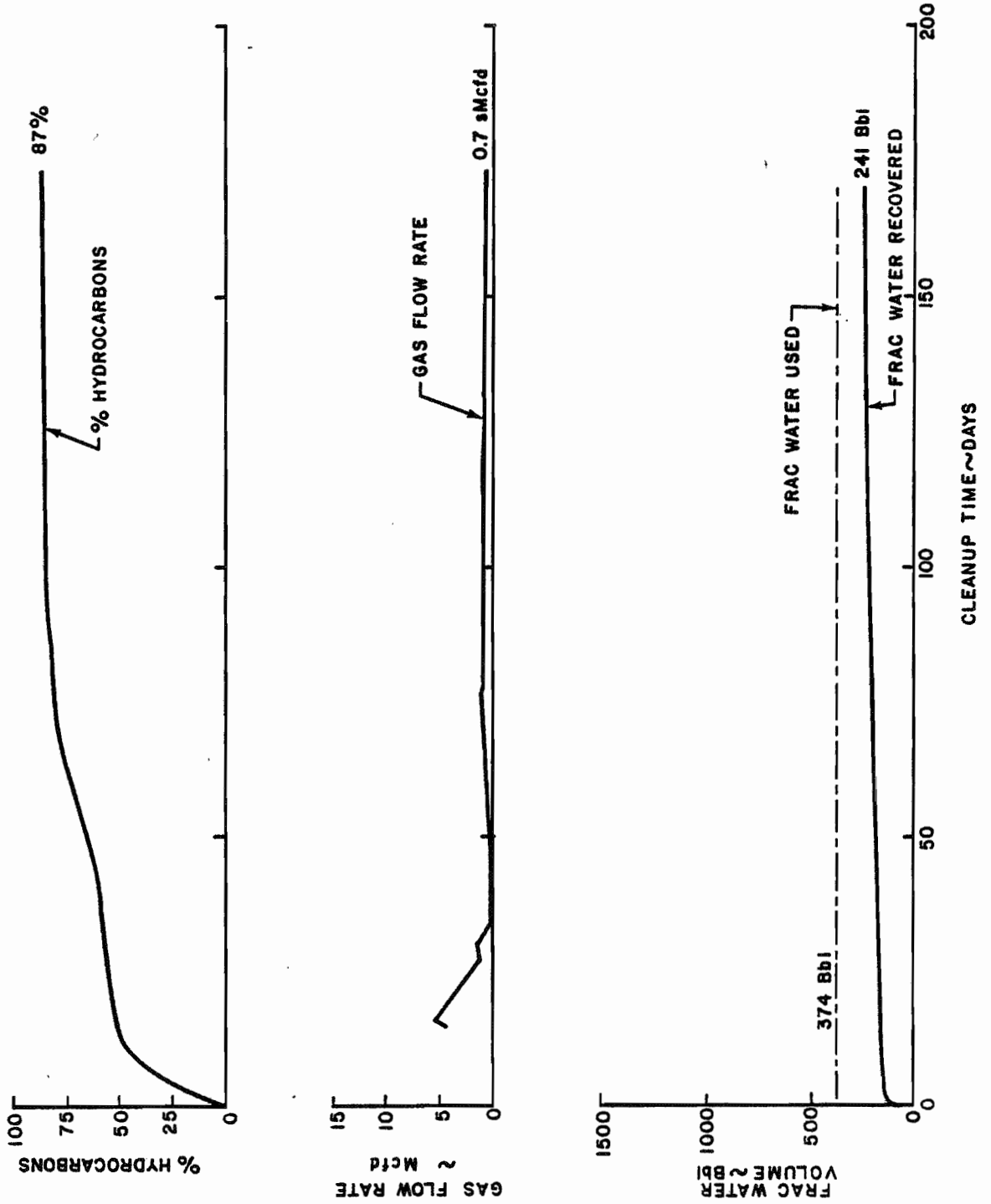


FIGURE 15

CLEANUP SUMMARY WELL NO. 20145

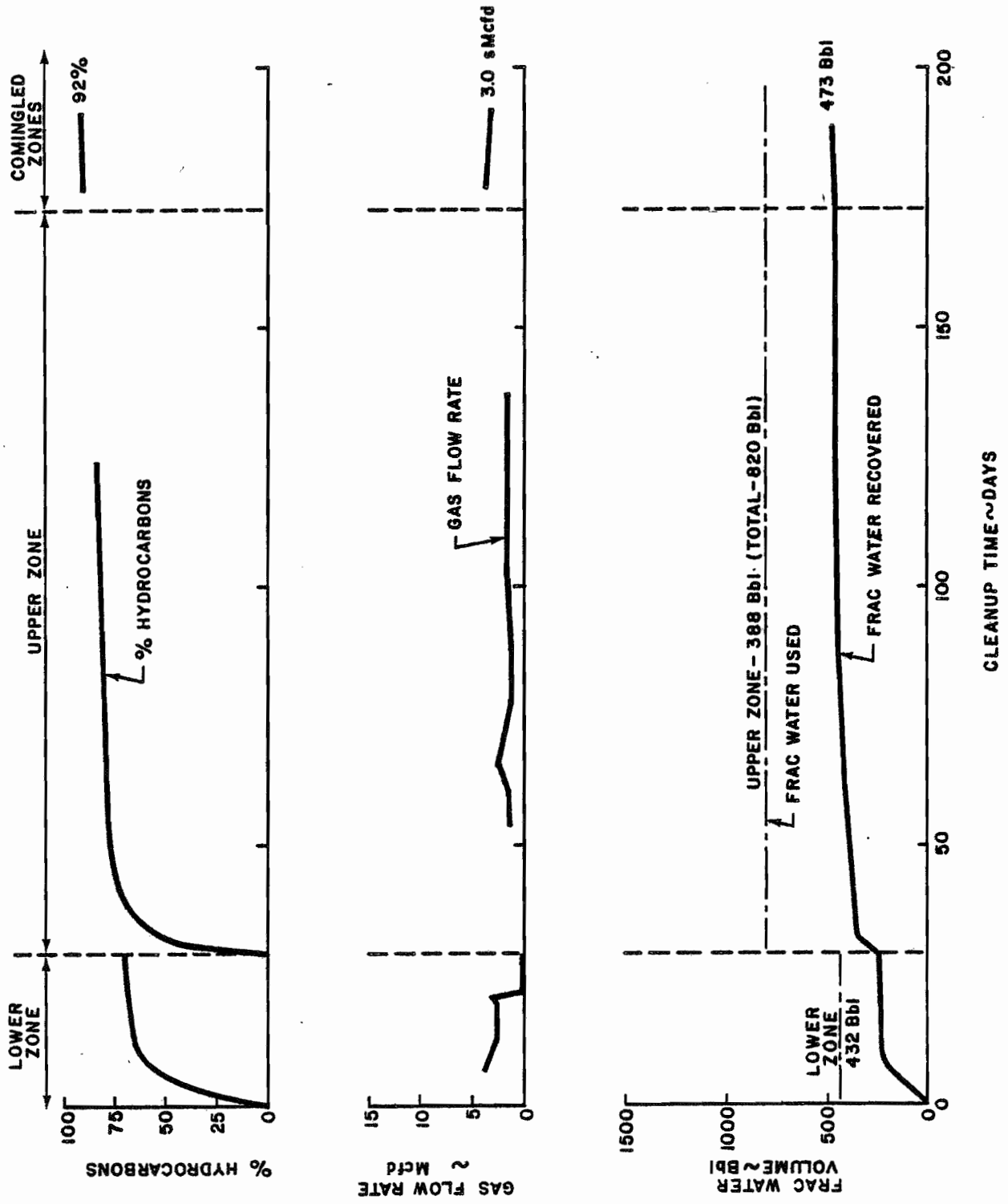


FIGURE 16

CLEANUP SUMMARY WELL NO. 20148

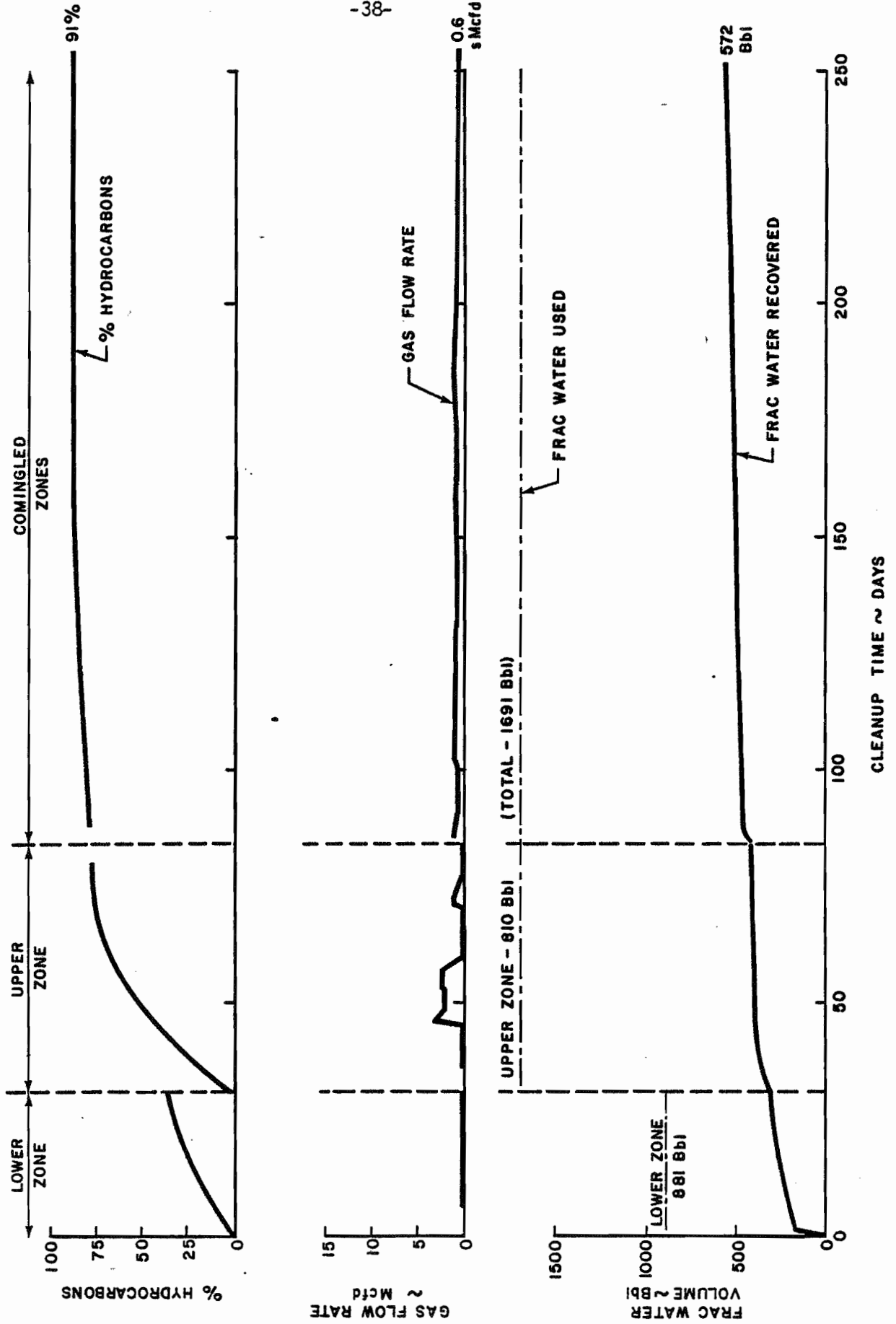


FIGURE 17

**CLEANUP SUMMARY
WELL NO. 20149**

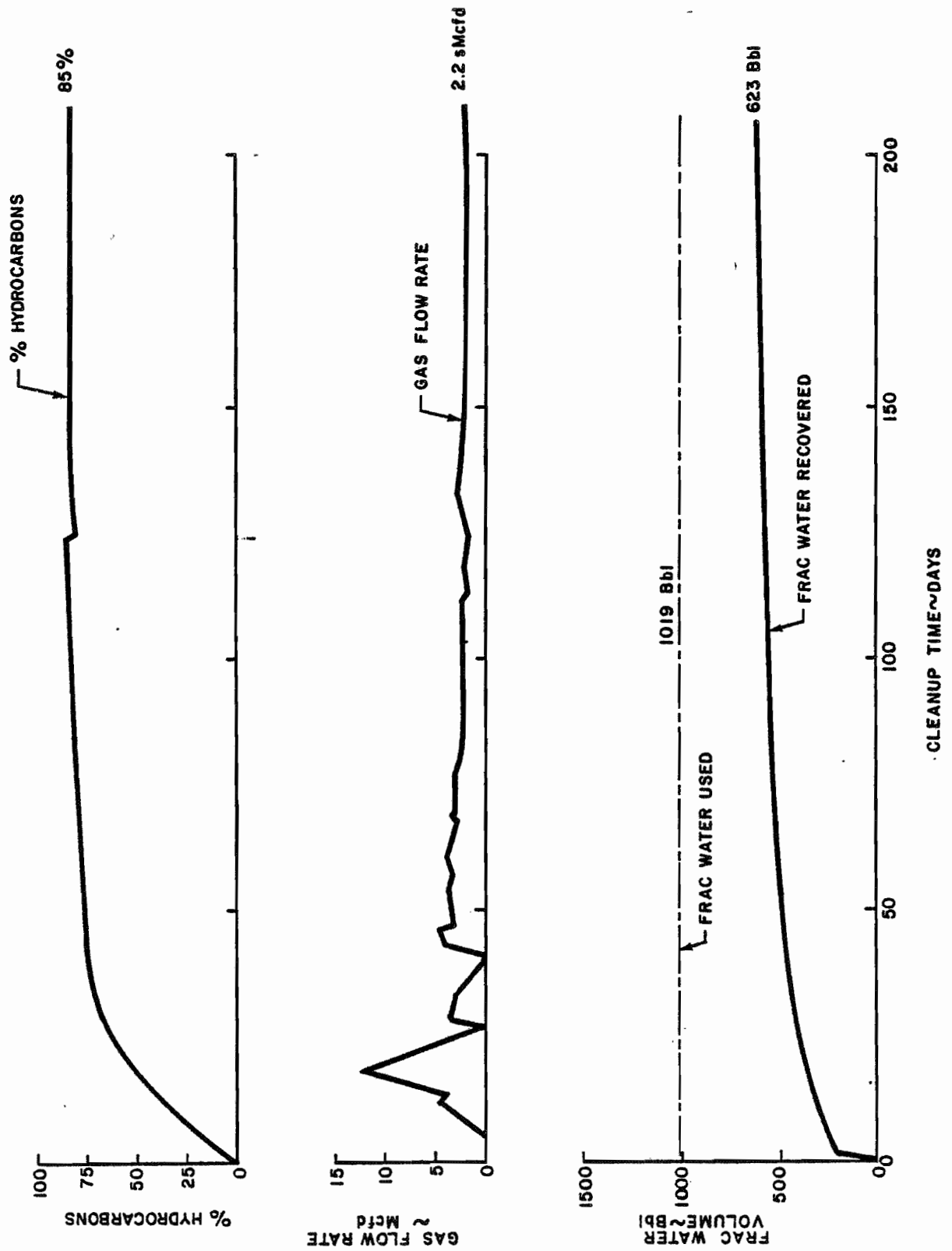


FIGURE 18

**CLEANUP SUMMARY
WELL NO. 20150**

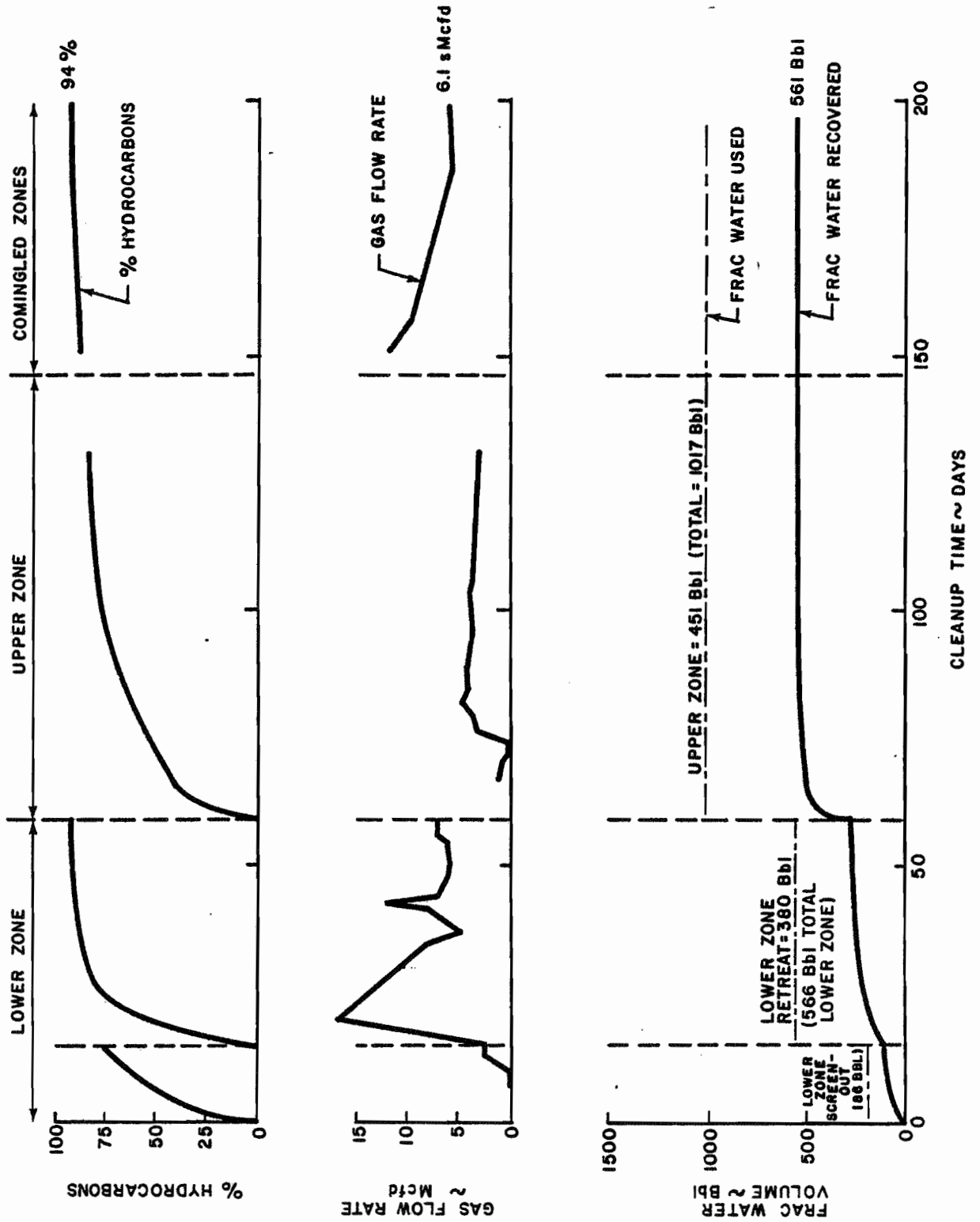


FIGURE 19

**CLEANUP SUMMARY
WELL NO. 20151**

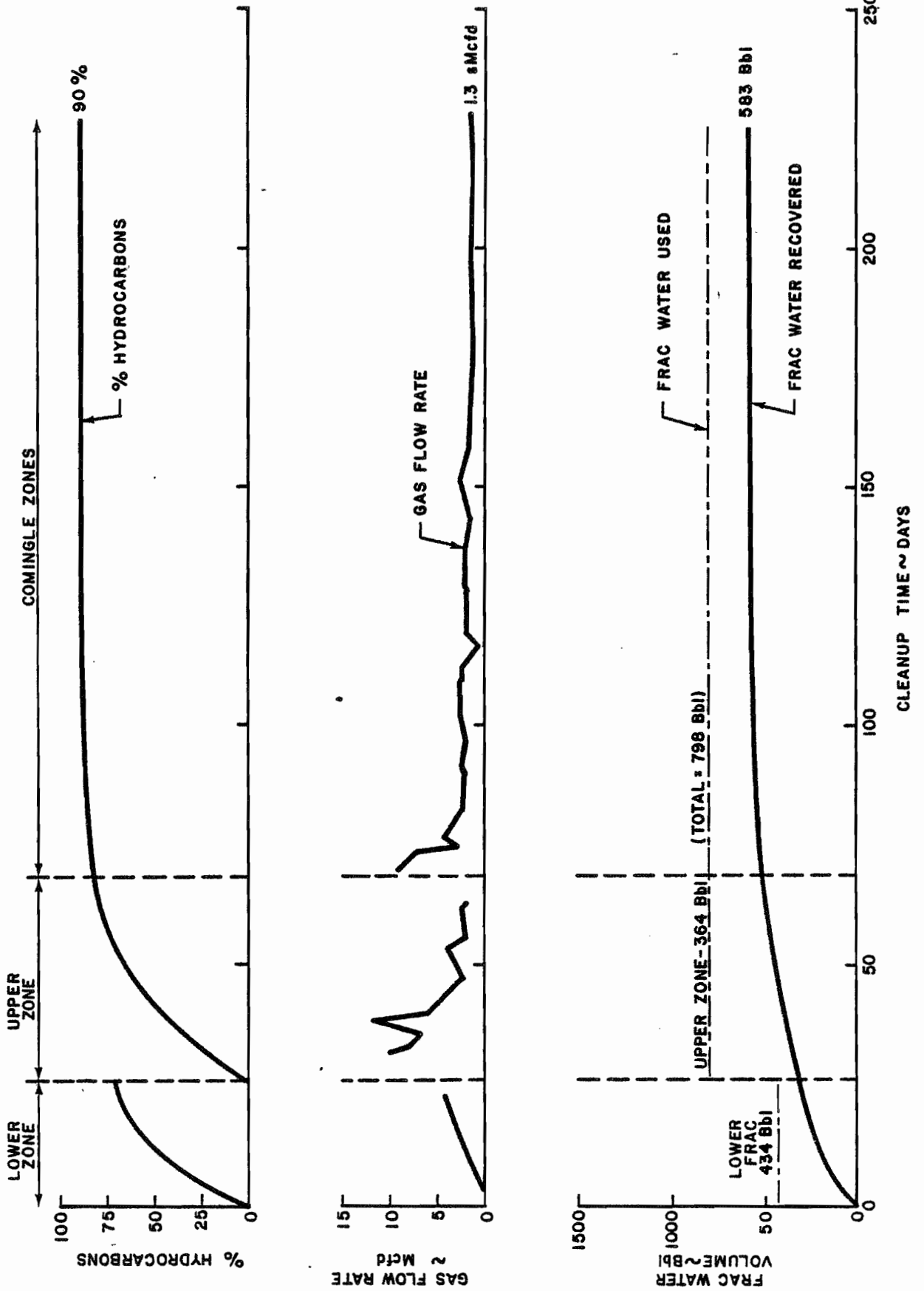


FIGURE 20

**CLEANUP SUMMARY
WELL NO. 20152**

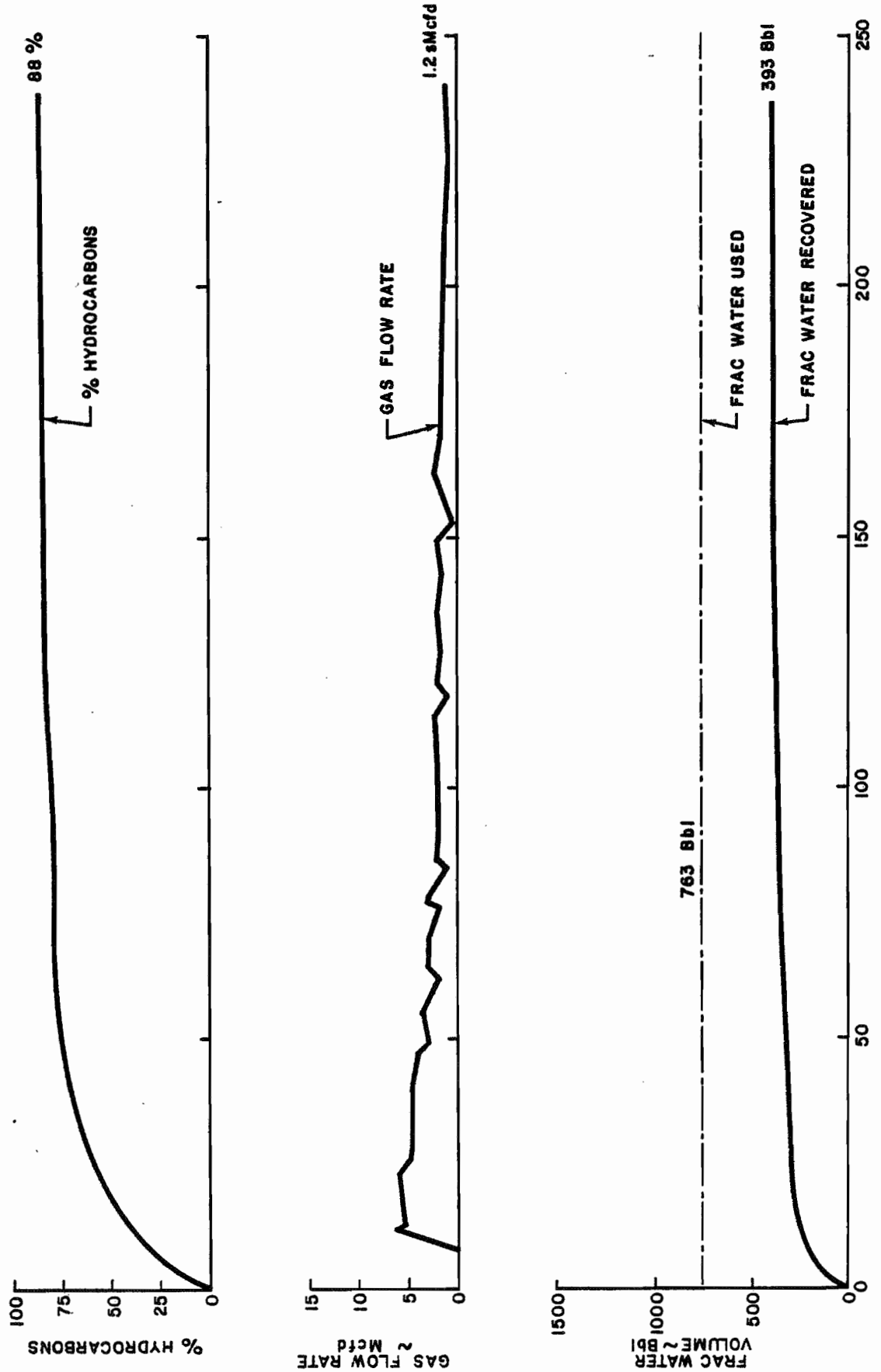


FIGURE 21

GEOLOGICAL CHARACTERIZATION

Devonian shale underlies about 110,000 square miles of the Appalachian Basin, and ranges in thickness to 12,000 feet. The shale consists primarily of two facies, one having a high content of organic material with high gamma radioactivity and generally dark gray to black in color, and a second having a low organic matter content with low radioactivity and gray to olive gray in color. Deposition of both shale types occurred within a warm, algae-filled sea at depth of about 500-2500 feet. A large river system to the east provided the major sediment source.

Organic-rich shales originated in the deeper, anoxic parts of seas. In the western half of the basin the black shales locally reach a thickness of over 350 feet. Organic material gives them their large hydrocarbon generating potential.

The organically-lean, gray shales contain sediments which intermittently accumulated and moved downslope along the river system's delta. In the eastern portion of the basin silt and sand increased in abundance as the turbidite sediments grade into delta deposits.

The present project test areas lie on the northern flank of the Appalachian Basin, about midway along its northeast trending axis. No major structural features occur near our sites. An analysis of remotely sensed imagery over the areas suggested a low natural fracture potential. However, both Lorain and Trumbull Counties have experienced heavy glaciation. Thus, glacial deposits could mask any existing indications of fracturing. A gamma ray log from Lorain County indicated as much as 480 feet of shale with potential for a high matrix gas concentration. In comparison, the

Trumbull County logs showed about 80 feet of promising shale. However, the drilling records mentioned several previous shale gas shows in both counties.

Lorain County's Devonian shale section has a total thickness of about 1000 feet compared to 2400 feet for Trumbull County. Immediately above the shale in Trumbull County lies a 15-foot Berea sandstone horizon underlain by 1250 feet of Chagrin shale, 600 feet of Huron shale, and 560 feet of Olentangy-equivalent shale overlying the Onondaga limestone. Lorain County has a 110-foot development of Berea sand and shale layers followed downward by 35 feet of Bedford shale, 130 feet of Cleveland shale, 310 feet of Chagrin shale, 350 of Huron shale, 190 feet of Olentangy shale and the Onondaga again underlies the shale section.

The Devonian shale may be accurately described as gray to black, shaly to silty mudstones. Siltstones and silty zones occur through much of the shale column in both areas. The lower 125 feet in Trumbull County are especially calcareous.

Cliffs Minerals, Inc. reported 26 natural fractures in the core from Trumbull County well 20143. This included three mineralized joints, six shear zones, and 16 microfaults (fractures which do not extend beyond the core sample, usually associated with concretions and pyrite nodules). The microfaults all have vertical or near vertical dips and strike north-westerly, with the exception of one northeast striking joint. Two joints and five of the faults occur within a siltstone bed at depths between 1587 and 1593 feet. The remaining fault and joint occur at 2534 and 2549, respectively. Virtually all of the coring-induced fractures had northeast strikes, and had vertical or inclined dips. They reported fewer induced fractures in the darker colored shale horizons.

Cliffs Minerals personnel found only two natural fractures in the core from the Lorain County well 20149. Both were microfaults. They did not report the orientation of the several core-induced fractures. Again, as in Trumbull County, the darker colored shale has generally fewer induced fractures.

Battelle Columbus Laboratories¹ tested several core samples from well 20149 and noted the effects of fluid contact on permeability. All water-based fluids reduced the shale's permeability. They believe that the fluids tend to block the matrix pore network. Their report shows large differences between individual samples. Battelle's results generally confirm previous studies by Chenevert & Associates² and Terra Tek³.

Hydrocarbon Content of the Shale

Core samples from well 20143, in Trumbull County, and well 20149, Lorain County, and cable tool cuttings from well 20151, Lorain County, provided data on the off gas (mobile matrix gas) content of the shale sections. Columbia personnel measured the matrix gas concentration in over three hundred sealed shale samples. Plots of cumulative released gas volume versus the log of time, projected back to the time of drilling determined the gas lost before canning the sample. This gas loss amounted to 5 to 10 percent of the total measured off gas volume.

¹Boyer, J. P. et al; Final Report on the Effect of Fracture Fluids in Tight Gas Formations to Gas Research Institute, 1980, 53 pp.

²Chenevert, M. E.; Devonian Shale-Fracturing Fluids Studies; Chenevert & Associates, Inc., Final Report, 1977, 24 p.

³Jones, A. H. et al; Rock Mechanics Studies Related to Massive Hydraulic Fracturing of Eastern United States Devonian Shales, Rept. No. TR 77-16, 1977, 24 pp.

Tables VI and VII list the average matrix gas contents for analyzed core and cuttings samples. Appendices I, II, and III contain the individual analyses. As with other shale research investigations, we found that black shale contains much higher gas concentrations than the gray shale intervals. Similarly, the zones with high gamma radiation have higher gas contents. The gas content derives from and is sorbed on the contained organic matter. High organic concentrations give the shale its dark color. Because organic debris selectively sorbs uranium, the organic rich shales also exhibit high gamma radiation. Thus, we find a general correlation between high radiation, gas content, and organic levels with black shales.

Table VI
 AVERAGE MATRIX GAS CONTENTS
 IN CORE AND CUTTINGS SAMPLES
 FROM LORAIN AND TRUMBULL COUNTIES, OHIO

Shale Member	(CORE)	(CORE)	(Cuttings)
	20143	20149	20151
	Trumbull Co., OH	Lorain Co., OH	Lorain Co., OH
	(cf gas/cf shale)	(cf gas/cf shale)	(cf gas/cf shale)
Cleveland	-	.28	.13
Chagrin	.09	.13	.05
Huron	.62	.97	.70
Olentangy	.87	.21	.08
Black	1.16	.83	.47
Gray	.36	.08	.05
High gamma	1.90	1.30	.57
Low gamma	.59	.29	.07
Overall	.66	.50	.30

Table VII

AVERAGE MATRIX GAS CONTENTS IN
CORE FROM PRIOR SHALE PROGRAMS

<u>Shale Member</u>	(CORE) 20403 <u>Lincoln Co., WV (cf gas/cf shale)</u>	(CORE) 20336 <u>Martin Co., KY (cf gas/cf shale)</u>	(CORE) 20338 <u>Wise Co., VA (cf gas/cf shale)</u>
Cleveland	-	-	2.54
Chagrin	.03	.18	.25
Huron	.26	.39	2.58
Olentangy	.48	.18	-
Black	.70	.41	2.14
Gray	.10	.10	.97
High gamma	.70	.47	2.73
Low gamma	.10	.07	.53
Overall	.26	.22	1.76

In Trumbull County, the Huron and Olentangy formations both have substantial matrix gas volumes. In contrast, only the Huron has a high gas content in Lorain County.

The present northern Ohio cores contained more gas than samples from historic producing areas in Lincoln County, West Virginia and Martin County, Kentucky, as shown in Table III, but less than the Wise County, Virginia shale. However, even the gray shale in Trumbull County contains a rather high gas level. In fact, this gray shale contains nearly as much gas as the black shale in Martin County. The only higher gray shale average occurred in a higher thermal maturity area of Wise County, Virginia. In summary, both Ohio test areas have Devonian shale sections with high matrix gas concentrations.

Table VI also lists the average gas contents of cable tool cuttings from well 20151 (located about one mile from the cored well 20149). These cuttings samples yielded about half as much as the cores. Most of the difference probably relates to higher release rates from the smaller

size of the cuttings particles rather than any geological differences in the shale sections. One can see that the off gas results of cuttings and core samples parallel each other. Apparently, cuttings off-gassing may serve to indicate gaseous shale zones, but does not quantitatively reflect matrix gas.

Columbia analyzed 100 matrix gas samples for light hydrocarbons to determine their chemical composition. Table VIII gives the mean composition of gas in cores from several locations. The gas from both Northern Ohio cores contained a smaller fraction of heavy hydrocarbons than the samples from the producing areas in West Virginia and Kentucky.

Table VIII

COMPOSITION OF MATRIX GAS
FROM COLUMBIA SHALE CORES

	<u>Methane</u>	<u>Ethane</u>	<u>Propane</u>
Lorain Co., Ohio	87.4%	6.0%	2.4%
Trumbull Co., Ohio	70.4%	14.5%	7.9%
Lincoln Co., WV	64.6%	17.7%	9.8%
Martin Co., KY	61.2%	18.5%	9.5%
Wise Co., VA	88.7%	9.6%	1.1%

Columbia also pyrolyzed about 40 core samples to measure the residual hydrocarbon generating capacity of the shale. Present technology does not enable us to economically produce the pyrolysis products. However, the data may assist us in evaluating well logs, indicating target zones for shale gas exploitation, and understanding the mode of gas occurrence.

We heated three grams of crushed shale at 700°C at a rate of 10°C per minute. The gas released between 400° and 500°C comes primarily from the breakdown of the Kerogen Fraction (KF). That released between 200° and 300°C

should represent pre-existing low-mobility hydrocarbons (LMH) driven off by the relative temperature increase. A steady flow of helium carries the produced gases to a thermal conductivity detector, and a chart recorder plots its response. We then calculated the volume of released combustible gas as methane-equivalent products by integrating the areas under the observed peaks. Some liquids condensed along the flow system; the method did not measure non-gaseous substances released by the heating. Therefore, this technique does not account for the total oil and gas potential of the shale.

Table IX lists the average LMH and KF gas concentrations from our pyrolysis analyses. Both of the present Ohio test areas have rather low residual gas generating potential. The Lorain and Trumbull County results compare closely to those from Wise County, Virginia and contrast sharply with the Lincoln and Martin County values. Lorain and Trumbull Counties' low LMH and KF values coupled with their high off gas volumes and gas composition suggest that natural processes have already converted most of the original organic matter in the shale to gas. This is also the case in Wise County where all lines of evidence (vitrinite reflectance, conodont color, and carbon isotopes analyses) defined a high thermal maturity in the shale. However, Mound Monsanto Quarterly Report MLM-EGSP-TPR-Q-015 reports that the shale in these areas of northern Ohio has a slight to moderate thermal maturity. While Mound's findings accord with the thermal maturity trends mapped in U.S.G.S. Professional Paper 995, it does appear that the shale in Trumbull and Lorain Counties has little potential for generating additional gas and oil. It is also interesting to note that the LMH values from the two producing areas (Lincoln and Martin County)

distinctly higher than for the remaining areas. Whether this is a feature characteristic of producing areas cannot be demonstrated at this time.

Table IX

AVERAGE GAS CONTENT OF PYROLYSIS PRODUCTS

	<u>Low Mobility Hydrocarbons:</u>		
	<u>Black Shale</u>	<u>Gray Shale</u>	<u>All Shale</u>
Lorain Co., OH	0.6	0.1	0.3
Trumbull Co., OH	0.3	0.1	0.2
Lincoln Co., WV	4.8	1.1	1.8
Martin Co., KY	3.3	0.6	1.7
Wise Co., VA	0.5	0.1	0.4

	<u>Gas from Kerogen Breakdown:</u>		
	<u>Black Shale</u>	<u>Gray Shale</u>	<u>All Shale</u>
Lorain Co., OH	1.1	0.3	0.7
Trumbull Co., OH	0.6	0.4	0.5
Lincoln Co., WV	14.6	4.5	6.6
Martin Co., KY	10.4	1.6	5.1
Wise Co., VA	0.9	0.3	0.7

Well Logging Program

From prior Devonian shale studies, Columbia found that a log suite consisting of gamma, density, temperature and noise/Sibilation devices provided optimum information. Additional logs and computer processing failed to provide further reliable information. However, we wanted to test two additional potential fracture locators - a gamma ray spectrometry log and the Fracture Identification Log. We also wanted further data on the use of the 3-D Velocity log as a fracture-finder and the Coriband-Kerogen log as a hydrocarbon-locator. A comparison of the present core analyses and well logs support our belief that a gamma-density-temperature-noise suite provides the most efficient and reliable information.

Both the density and gamma logs closely parallel the off gas trends, but the density log describes the trends most closely. The Coriband/Kerogen and hydrocarbon curves also reflect these trends, but lack some of the detail shown by the density plot. Resistivity logs also respond to some of the higher off gas horizons. However, only in Trumbull County did we find a fair Sonic log response to the gaseous shales.

Very few fractures occurred in any of the core samples. This complicated our evaluation of the fracture-finder logs, but we did conclude that:

- (1) The 3-D Velocity Log failed to respond to the very limited fracture concentrations in the Trumbull County core.
- (2) The Fracture Identification Log gave false indications of fracturing in Lorain County.
- (3) The Sonic log gave no clear response to the Trumbull County fractures and the Coriband secondary porosity seems to misinterpret matrix density changes as porosity.

Thus, the fracture logs appear unreliable for use in determining critical shale properties.

Both the temperature and "noise" logs indicated gas entry at various depths in the project wells. They did not indicate gas near the natural fractures in the Trumbull County cored well. However, the gas shows may correspond to permeable silty streaks in the shale.

Baroid analyzed the circulating air and gases during drilling. Their analyzer showed a gas increase over most, but not all of the high off gas shale section in Lorain County. In Trumbull County, Baroid showed highs which spanned two fractured zones, but also included other unfractured horizons.

For each cored well Schlumberger generated their Coriband Mechanical Properties logs. The resulting data which includes elastic moduli can be of use in designing hydraulic fracturing treatments. In both areas, we obtained straight-line plots of the various mechanical rock properties. These high fracture gradient values indicate that we would tend to create horizontal fractures by hydraulically fracturing the wells in northern Ohio.

During early 1980, Bendix Corp. logged two of our project wells with a gamma ray spectroscopy device. The U.S. DOE sponsored this work under a separate contract. This tool has the capability of determining the fractions of the total gamma radiation due to uranium, thorium, and potassium. Some surveys of this type have detected fracture planes along which uranium salts precipitated from flowing formation water. However, the present logs merely showed the relatively high uranium concentration level of the organic shale layers.

STIMULATION DESIGN AND EXECUTION

Columbia designed the Trumbull and Lorain County stimulations with the purpose of (1) evaluating the areas' hydrocarbon potential; (2) comparing the effects of foam, cryogenic, and displaced explosive fracturing; (3) comparing the importance of natural shows and high matrix gas content, and (4) studying the effects of increasing the treatment volume. We considered a practical limit of 700 feet for the maximum height of the treated (perforated) interval. To reduce the chances of extending a fracture to the surface, we perforated up to a minimum depth of 500 feet. In general, the Trumbull County well stimulations, and the lower zone treatments in the Lorain County wells tested high matrix gas concentrations. Several gauged shows, and temperature/noise log events occurred in the upper zones in Lorain County. The completion procedures included perforating in a fluid-filled wellbore, breaking down with acid using ball sealers, stimulating, recovering the fracturing fluid, and testing.

Table X and XI summarize the treatment parameters and hydraulic fracturing results in both Lorain and Trumbull Counties. Water recoveries ranged from 14% to 64% of the volume used in the treatments with clean up periods spanning up to 128 days. This ignores the reported 107% recovery from well 20144, based on rather crude estimates of the early recoveries which we regard as unreliable. We have observed stabilized gas flows of 1 to 7 Mcfd containing up to 90% hydrocarbons. The remaining 10% consisted of nitrogen or carbon dioxide. Post-fracturing pressures in both areas measured at the wellhead have ranged to 214 psi for 48 hour shut-in periods. However, long term shut-in tests (over several months) in the Trumbull County wells have shown

TABLE X

SUMMARY OF TREATMENT PARAMETERS

Well	Frac Type	Frac Date	Water Barrels	Sand Pounds	Gas million scf	Average Treatment Pressure psi	ISIP psi	Treated Interval
20143	Foam upper	9/24/80	276	55,000	1.20 N ₂	3000	1850	1865-2147
	Foam lower	8/19/80	437	88,000	1.32 N ₂	2800	1900	2488-2589
20144	Foam	7/30/80	374	88,000	1.20 N ₂	3000	1750	1793-2483
20145	Foam upper	9/26/80	388	88,000	1.38 N ₂	3127	1900	1873-2081
	Foam lower	8/13/80	432	86,000	1.32 N ₂	3400	2175	2407-2496
20146	GOEX	9/4/80	1150 gallons of explosive GOI-4					2423-2517
20147	GOEX	10/16/80	1100 gallons of explosive GOI-4					2394-2479
20148	Cryo upper	11/20/80	810	58,000	80 tons CO ₂	2200	550	527-748
	Cryo lower	10/7/80	881	55,000	84 tons CO ₂	2700	780	816-1050
20149	Cryo	10/23/80	1019	78,000	71 tons CO ₂	1500	600	541-1076
20150	Foam upper	2/18/81	451	130,000	0.61 N ₂	2000	480	601-747
	Foam lower	12/17/80	380	88,000	0.70 N ₂	2200	1000	820-1058
20151	Foam upper	12/10/80	364	79,000	0.62 N ₂	1800	1100	539-779
	Foam lower	11/3/80	434	60,000	0.52 N ₂	1750	1100	851-1096
20152	Cryo	11/12/80	769	120,000	79 tons CO ₂	2500	850	527-1081
20144	Gelled Water w Nitrogen	8/19/81	512	60,000	0.050 N ₂	2190	1700	610-620

TABLE XI

TEST DATA SUMMARY - .10 WELL NORTHERN OHIO SHALE PROGRAM

County	Well	Initial Open Flow (smcfd)		Initial Rock Pressure (psig)	
		Drilling	After Breakdown	After Breakdown	After Frac
Trumbull	20143 Lower zone	TSTM (Both zones)	TSTM	5 (48 hr)	23 (48 hr)
	20143 Upper zone		TSTM	2 (48 hr)	108 (48 hr)
	20143 Comingled				150 (48 hr)
Trumbull	20144 Main Zone	TSTM	TSTM	17 (48hr)/330(75day)	66 (48hr)
	Upper Silty Layer	Est. at 90-100	TSTM	TSTM (48 hr)	TSTM (48hr)
Trumbull	20145 Lower zone	TSTM (Both zones)	TSTM	83 (48 hr)	214 (48 hr)
	20145 Upper zone		TSTM	10 (48 hr)	125 (48 hr)
	20145 Comingled				107 (48 hr)
Trumbull	20146	TSTM	TSTM	12 (48 hr)	12 (48 hr)
Trumbull	20147	1	TSTM	29 (48 hr)/100 (8day)	No measurement ⁵⁷
Lorain	20148 Lower zone	4 (Both zones)	TSTM	562 (67 hr)	65 (48 hr)
	20148 Upper zone		TSTM	150 (48 hr)	196 (48 hr)
	20148 Comingled				157 (48 hr)
Lorain	20149	8	4	2 (15% CO ₂)	220 (48 hr)
Lorain	20150 Lower zone (1st frac)	38 (Both zones)	TSTM	106 (48 hr)	167 (48 hr)
	20150 Lower zone (2nd frac)		TSTM	167 (48 hr)	126 (48 hr)
	20150 Upper zone				29 (48 hr)
Lorain	20150 Comingled				51 (48 hr)
	20151 Lower zone	TSTM (Both zones)	TSTM	44 (48 hr)	No measurement
	20151 Upper zone		TSTM	45 (48 hr)	71 (48 hr)
Lorain	20151 Comingled				189 (48 hr)
	20152	35	2	1 (12% CO ₂)	261 (48 hr)

pressures up to 1300 psi. This indicates the presence of matrix gas, but suggests an absence of effective permeable paths, even after stimulation.

Either of two general reasons could account for the extremely low gas flows in both areas: (1) the areas have inadequate potential for production or (2) the completion methods and/or designs were ineffective.

We believe that both areas have a sufficient gas source for potential production, because the core samples contained higher gas concentrations than in some producing areas (see Tables VI and VII). Our fracturing targets included all gas shows and high off gas horizons in all wells (except for the very shallow show in well 20144). Moreover, the tracer logs indicated that about half of the perforations opposite the observed shows accepted fracturing fluid. The tracer also evidenced an adequate treatment influx in the high off gas zones. Therefore, we should have generated some significant gas flow unless: (1) the area has insufficient natural permeability (silt or fracture networks), (2) the treatment narrowly missed the target depths by fracturing out of the zone of interest or by narrowly missing the zone and paralleling the target via horizontal fracture extension, (3) the proppant is not properly distributed in the induced fractures, or (4) the fracturing fluid has blocked flow from the matrix or along the fractures.

Insufficient natural permeability remains a real possibility, but to prove this would require borehole shooting in additional wells to ensure some contact with the entire section. We should also consider the possibilities of formation damage or of our not having contacted the shows with our perforations, especially in the Lorain County wells which had no sustained flows after perforating, acidizing, or stimulation which equalled the natural flow. Because the gas shows in Lorain County appears to correlate with silty horizons in the upper shale section, the horizontally trending hydraulic fractures could have paralleled their bedding planes and failed to access any productive layers.

Proppant distribution could pose a serious problem in either area. This problem could be more serious in Trumbull County if the induced fractures extended horizontally, because we designed our treatments for a vertical orientation. In addition, one can usually expect some water blockage and matrix pore plugging by induced fluids.

After conducting the scheduled stimulations in the ten project wells, Columbia ran post-fracturing logging surveys (gamma ray-temperature-noise) and interference tests in both areas to determine which perforations had effectively contacted the formation, and to suggest limits to the induced vertical fracture growth.

RESULTS OF CRYOGENIC AND FOAM FRACTURING TREATMENTS OF THE
DEVONIAN SHALE IN LORAIN COUNTY

The initial pre-treatment of the formation involved the displacement of large acid volumes into the shale. However, after treating the lower zone of well 20148 with 5264 gallons of 7 1/2% hydrochloric acid, we found that the back-flowing unspent acid created a serious safety problem. Thereafter, we generally used 500 gallons of acid followed by 2100 to 3500 gallons of 2% KCl. However, we used a total of 3000 gallons of 7 1/2% acid and 5860 gallons in two separate acid treatments on well 20150, because it appeared that the first acid job did not break down all of the perforations. After the second breakdown, the pressure chart indicated that at least seven of the eleven perforations had accepted acid, but the impressions found on the used ball-sealers suggested that from 9 to 11 could have opened. A temperature survey run just after the second acid treatment failed to provide any further evidence of which perforations were open. Breakdown pressures ranged from 1200 to 2000 psi with average treating pressures between 1400 and 2500 psi as measured at the surface. All of the breakdowns used ball sealers, but we observed a complete ball-out only on the lower zone of well 20150.

Natural open flows occurred in all of the Lorain County wells, except for 20151. However, the core from well 20149 contained no natural microfractures. In order of descending depth, perforations number 1, 4-16, 22, and 24 all correspond to horizons with gauged or logged evidence of gas flow in at least one well (Table XII). Only high matrix gas concentrations occurred at the remaining perforated depths. In designing the stimulations, we expected that we would induce primarily horizontal fractures at these depths.

TABLE XII

PERFORATED DEPTHS (IN FEET) FOR
WELLS IN LORAIN COUNTY

<u>Well Number</u>				
<u>20148</u>	<u>20149</u>	<u>20150</u>	<u>20151</u>	<u>20152</u>
527	541	601	539	527
548	562	607	568	556
558	571	612	578	566
587	604	634	611	599
610	626	641	629	616
616	635	651	636	626
625	645	657	654	644
635	654	694	664	651
642	667	709	680	666
660	682	730	694	683
674	696	747	709	695
685	706	-	720	705
697	718	820	731	714
708	727	849	742	728
720	740	878	749	736
736	757	894	769	754
748	767	919	779	765
-	784	951	-	783
816	801	987	851	801
844	813	1021	866	812
874	839	1036	912	837
888	868	1049	931	864
913	899	1058	955	899
946	913	-	987	915
980	940	-	1023	936
1015	972	-	1062	972
1028	1004	-	1074	1009
1040	1041	-	1086	1047
1050	1054	-	1096	1059
-	1066	-	-	1071
-	1076	-	-	1081

Perforation Tools: Casing Gun for upper zone of 20150, otherwise,
Glass Jet Charges

By mutual agreement with all of the partners in this program, the Lorain County fracturing program called for:

two - 1500 barrel cryogenic treatments in well 20148 (Wakefield)

one - 1500 barrel cryogenic treatment in well 20149 (McGuire)

two - 1500 barrel foam treatments in well 20150 (Grecko)

two - 1500 barrel foam treatments in well 20151 (Mezurek)

one - 1500 barrel cryogenic treatment in well 20152 (Gest)

These hydraulic fractures all treated virtually the same stratigraphic horizons--either in one, or two stages. Wells 20149 and 20152 received single stage cryogenic treatments; wells 20150 and 20151 received dual-staged foam treatments; and well 20148 received a dual-staged cryogenic treatment. The limited success of previous stimulations prompted us to redesign the final treatment on the upper zone of well 20150. Consequently, we altered the last stimulation to focus on actual shows and increase the size of the job.

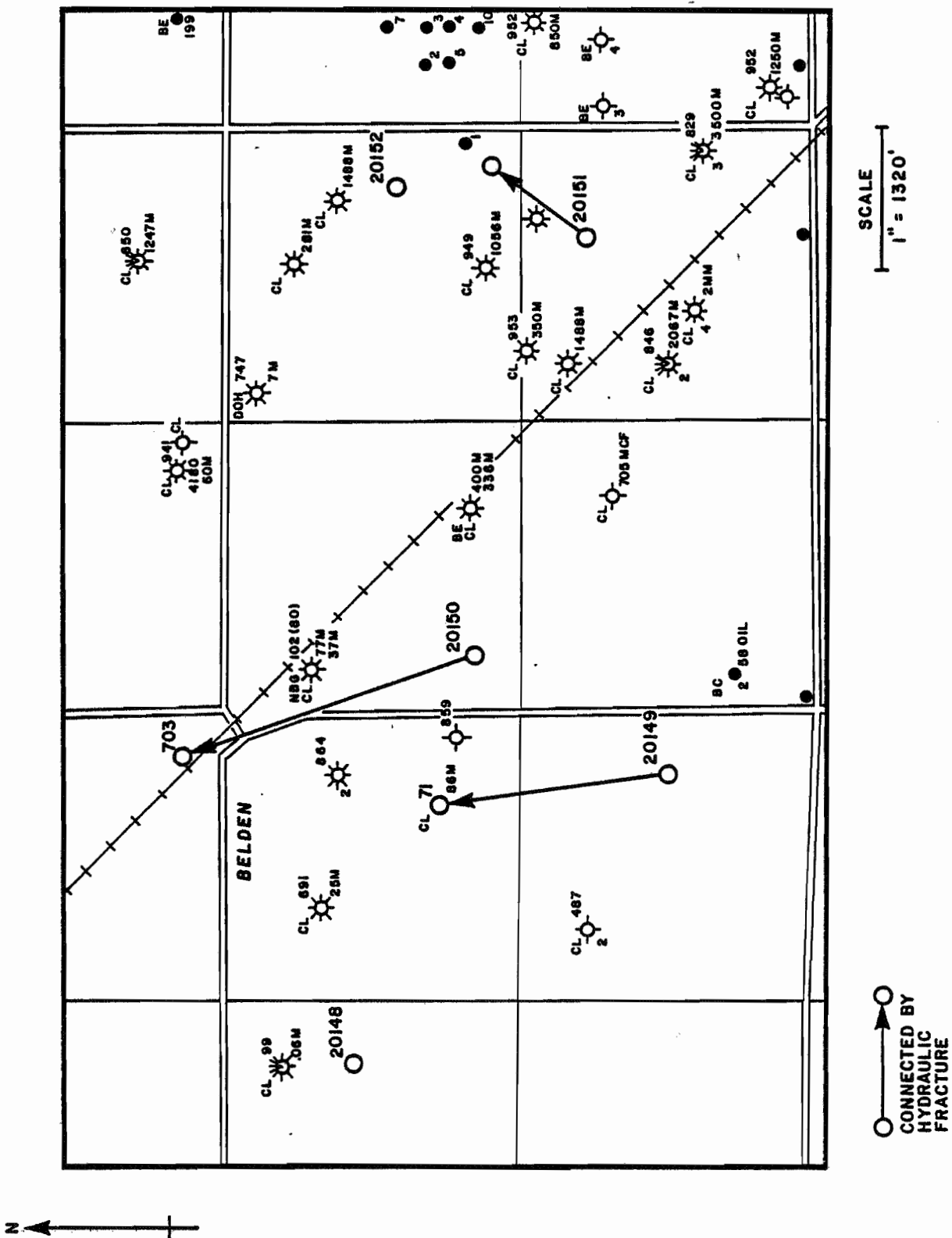
The hydraulic fracture designs for our Lorain County wells called for 1500 barrel treatments at a rate of 40 barrels per minute using either a 75 quality foam or 35% carbon dioxide cryogenic fracturing fluid. However, the foam quality obtained varied between 50 and 70, with pumping rates ranging from 50 to 10 barrels per minute for the foam and 14 to 35 barrels per minute for the cryogenic treatments. Average treatment pressures ranged from 1500 to 2700 psi, and the instantaneous shut-in pressures varied from 550 to 110 psi as measured at the surface. These stimulations used from 60,000 to 130,000 pounds of 20/40 mesh sand as proppant. As in Trumbull County, we injected balls according to our design and as the treatment pressure permitted, but did not ball-out on any stimulation. Consequently,

not all perforations accepted the fracturing fluid. Tracer log results indicated that individual fracturing treatments contacted between 13 and 64 percent of the perforations (as shown on Figures 3 through 12). This suggests that our stimulations only partially contacted the target zones. Malfunctions in Dowell's blender truck during the fracturing of the lower zone of well 20151 caused the sand concentration to vary abruptly. Due to an incomplete delivery of carbon dioxide to the wellsite, Dowell had to complete the treatment of well 20149 using only water. Other more serious mechanical problems included a screen-out on the upper zone of well 20151, which temporarily halted the treatment, and a total screen-out near the beginning of the lower zone treatment of well 20150. The 20150 screen-out required a major cleanup effort. Dowell successfully treated the zone three weeks later.

During the upper zone treatments in wells 20150 and 20151, and the single stage stimulation of well 20149, we achieved direct communication with nearby wells. In each case, the adjacent wells began flowing CO₂ or N₂ at high flow rates and two of the wells sprayed an observable oil mist which contained a low percentage of combustible gas. The treatment in well 20151 connected with an abandoned, unidentified well located 700 feet in a North 65° East direction. The treatment in well 20149 connected with the annulus of a Columbia Clinton well (permit #71) 2100 feet in a North 5° West direction to the uncased shale section of well 703. (See Figure 22)

Our modest treatment volumes can only create a limited total fracture volume. Consequently, the fracture length required for these well-to-well communications imply that the induced fractures extended from only one or few perforations. Furthermore, the lack of communication with closer

WELL SITES IN GRAFTON TOWNSHIP, LORAIN COUNTY



surrounding wells points to a strong directional fracture preference. Post-stimulation radioactive tracer results also support this claim. Each of the fracture jobs in Lorain County contained a radioactive tracer which should mark those perforations which received fracture fluid. After the treatments, we detected tracer material at 13% to 64% of the perforated depths as shown in Table XIII. In the most extreme cases, only 4 of the 31 perforations apparently accepted fluid. Some perforations which took fluid might appear to be untreated if the tracer beads did not remain close to the wellbore. However, the evidence suggests that most of the fracturing fluid of the induced fractures probably extended for considerable horizontal distances through several perforations.

Table XIII

RESULTS OF RADIOACTIVE
TRACER SURVEYS IN LORAIN COUNTY WELLS

<u>Well/Zone</u>	<u>Perforations</u>	<u>Perforations Accepting Tracer</u>
20148 upper zone	17	10 (59%)
lower zone	11	5 (45%)
20149 combined zone	31	9 (29%)
20150 upper zone	11	3 (27%)
lower zone	11	7 (64%)
20151 upper zone	17	5 (45%)
lower zone	11	4 (36%)
20152 combined zone	31	6 (19%)

M. D. Wood, Inc. and Sandia Laboratories furnished interpretations of their tiltmeter and borehole seismic data collected while monitoring the lower zone treatment in well 20148. Both surveys indicated a vertical fracture extension at the beginning of the stimulation. The seismic results

favor a northeast-striking fracture which initiated at a depth of 933 feet, split into multiple planes and may have terminated in a horizontal plane. Data from the tiltmeter array suggest a rapid vertical fracture growth up to a 70-160 feet depth, followed by the formation of a horizontal separation with a shut-in radius of 350-500 feet.

On June 3, 1981, we conducted post-treatment differential temperature and sibilation surveys in well 20150 to determine which perforations had detectable flow. Birdwell logged this well during a shut-in period, and with the flow controlled at 20 Mcfd, 30 Mcfd, 100 Mcfd, and finally during open flow conditions. Although the temperature log provided no useful information, the Sibilation log gave some evidence of gas entry during the open flow at the following perforations: 607, 613, 640, 647, 656, 752, 899, and 924. In addition, we could hear gas leakage through the following collar positions: 414, 502, 533, 593, and 806. The rising fluid level in the well did not allow us to test the lower six perforations. Because of the continued water recoveries, and low gas flows in the Lorain County well, plus the low quality log responses from well 20150, we decided against any further logging attempts.

Gulf Research and Development Company sponsored a final survey of well 20150. This involved a borehole television survey run by Deep Venture Diving Service. The results showed a substantial water flow from one or both of the lowest perforations. (We could not actually view the lowest due to the fluid level in the well.) The camera also showed sporadic fluid entry through the perforations at 901, 926, and 957 feet below ground level.

Landowner problems caused us to cancel an interference test in well 20150. A review of the post-treatment logging and testing did not suggest that additional completion work would improve the production of our wells. Therefore, because of the very low rates, Columbia decided to abandon all of the project wells.

RESULTS OF DISPLACED EXPLOSIVE AND FOAM STIMULATION OF THE
DEVONIAN SHALE IN TRUMBULL COUNTY

Of the five area test wells in Trumbull County, only well 20144 encountered a significant natural show of gas. This show occurred far above the main target horizons which had a high projected matrix gas content. Although we did not initially schedule a completion at this depth (640'), we did feel that a thorough evaluation of the area's shale section should include a test of this shallow silty shale.

The core from well 20143 contained only two microfractures within the target interval (one shear at 2534', and a joint at 2549'). We found no indication of gas influx at either horizon. In the absence of gas show evidence, high matrix gas (off gas) concentrations formed the basis of our completion program. We designed stimulations to treat a 90-foot zone of concentrated high gas content shale in all five wells as indicated by the perforations listed in Table XIV. This zone occurred at depths between 2400 and 2600 feet.

Three of the wells also received hydraulic stimulations over an upper interval which extends from about 1800 to 2200 feet. This zone contained several stratigraphic horizons with high matrix gas.

Our Trumbull County fracturing program consisted of:

two - 1500 barrel foam treatments in well 20143 (Meleski)

one - 1500 barrel foam treatment in well 20144 (Ware)

two - 1500 barrel foam treatments in well 20145 (Gordon)

one - 1500 gallon displaced explosive trial in well 20146 (Allman)

one - 1100 gallon displaced explosive trial in well 20147 (Church)

All of the hydraulic fracture treatment designs assumed that the formation in this area should tend to fracture vertically.

TABLE XIV

PERFORATED DEPTHS (IN FEET) FOR
WELLS IN TRUMBULL COUNTY

<u>Well Number</u>				
<u>20143</u>	<u>20144</u>	<u>20145</u>	<u>20146</u>	<u>20147</u>
1865	1793	1813	2423(x2)	2394
1905	1833	1852	2433(x2)	2400
1936	1860	1880	2452(x2)	2419
1978	1902	1920	2466(x2)	2433
1994	1919	1939	2475(x2)	2442
2030	1952	1973	2495(x2)	2459
2045	1970	1989	2517(x2)	2479
2062	1984	2004		
2074	1998	2018		
2086	2009	2028		
2102	2021	2043		
2114	2032	2051		
2131	2041	2061		
2136	2051	2072		
2147	2062	2081		
-	-	-		
2488	2127	2407		
2500	2217	2417		
2520	2289	2435		
2534	2306	2448		
2544	2329	2458		
2566	2368	2476		
2589	2400	2496		
	2416			
	2430			
	2448			
	2458			
	2470			
	2483			

Results of Displaced Explosive Treatments: The displaced explosive concept involves a hydraulic fracture of the shale using liquid explosives followed by the detonation of the explosives. By design, this combined hydraulic and explosive approach would have a greater effect than a wellbore shot. The advantages of this type of treatment are a short clean up period, and no significant fluid-formation interaction problems after the treatment.

Columbia scheduled well 20146 for the first displaced liquid explosive treatment to be performed by GOEX, Inc. After breaking down the formation to initiate hydraulic fractures, GOEX endeavored to pump their explosive slurry into the fractures, and detonate it to extend the fractures and shatter the shale near the fracture surfaces. Personnel from Sandia Laboratories monitored the first treatment with a geophone array to try to measure the amount of explosives which detonated.

Due to difficulties experienced in displacing fluid through the perforations, while acidizing, we had to conduct a second perforation and break down before attempting the stimulation.

Figure 23 shows the general wellbore configuration just prior to the GOEX treatments. A bridge plug was set at 2539 feet and was covered with twenty feet of sand. The treatment design required the use of cement cylinders in the well to reduce the amount of explosive in the wellbore during detonation. For this purpose, GOEX provided 24 cylinders, each 3 1/2 inches in diameter and 4 feet long. When emplaced in the well, these units extended over the target zone up to a depth of 2423 feet. On September 2, Halliburton displaced 600 gallons of Versagel into the formation with 2% KCl water to ensure they could achieve the proper pumping rate with the cylinders in place. Just above the treated zone, a wireline

WELLBORE CONFIGURATION FOR GOEX DISPLACED EXPLOSIVES TREATMENTS

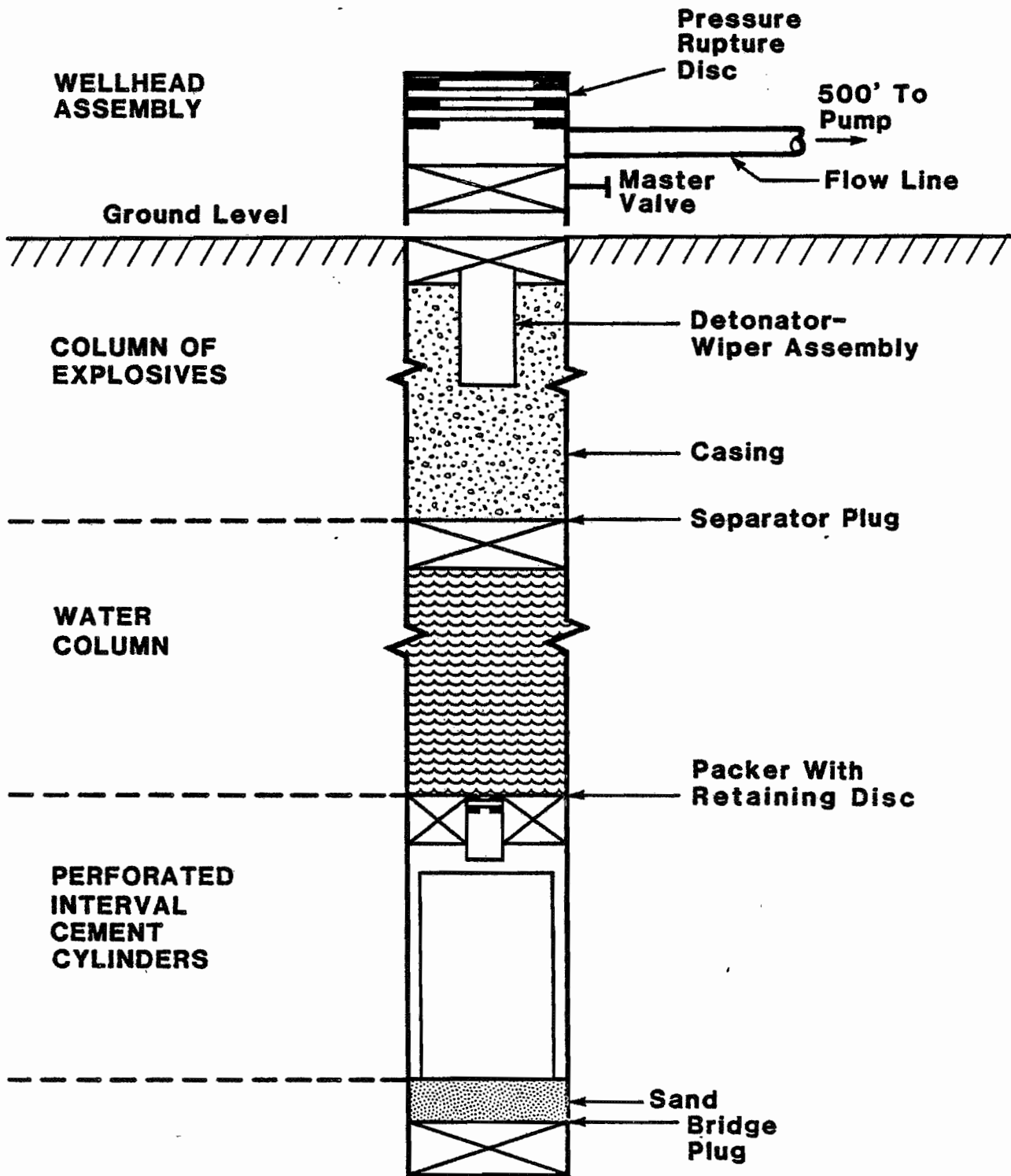


FIGURE 23

packer with 1/2 inch choke supported a column of fluid and explosives during the preparation for the treatment. With this packer set at 2408 feet, the pumping pressure would cause several shear pins in the packer to fail, releasing a disc in the packer and allowing displacement of the explosives.

At this point, the workover rig moved off the wellsite and GOEX personnel loaded 1150 gallons of GOI-4 explosives into the wellbore. Although the column of explosives did not quite extend to the surface, GOEX installed their pumpdown detonator, wiper plug, wellhead, and pressure-release disc before Halliburton connected their line to the wellhead and began pumping. The pressure disc failed three times at 1200 psi below the rated pressure during the explosive displacement. This apparently caused a large volume of explosives to surge past the detonator into the water column. GOEX observed a 500 psi pressure increase which they interpreted as a sign of detonation. However, it appeared from the Sandia geophone array that little or none of the explosives had detonated. To ensure that the detonator had seated in the packer, Halliburton pumped several more barrels of water.

We then ran a sinker bar in the wellbore to locate damaged casing or obstructions. Although this test showed no physical obstructions, we found that some unconsumed explosive remained in the water column. Apparently it had surged past the wiper plug when the discs failed. To avoid any possible danger in removing the explosive from the well, we arranged for a wireline service to detonate them in the well on September 5. After the shot, a 3-arm caliper survey showed that a section of the casing had contracted to two inches. The condition of casing below this point remains an unknown. No gas production resulted from the treatment.

In preparation for the second explosive treatment, GOEX, Inc. placed 1100 gallons of explosive into well 20147 (Church). On October 16, GOEX loaded the detonator in hole, installed the wellhead pressure discs, and attached the pump line. Halliburton started pumping displacement fluid on top of the detonator plug. After pumping about 1 barrel (Bbl) of fluid into the line at 1 Bbl/minute, the rupture discs on the wellhead yielded at their rated capacity of 4000 psi. One barrel equalled the unfilled capacity of the pump line and Halliburton felt that no fluid had been pumped downhole when the discs blew. The reason for the failure to displace the explosives into the wellbore at a reasonable pressure remains unknown.

GOEX then repaired the bottom sleeve of the detonator damaged during the first pump attempt and reloaded the detonator into the wellbore. Halliburton attached the pressure discs and pump line, and began pumping again. The wellhead pressurized to 2000 psi after displacing about 1 barrel of fluid. With the pumps shut down for five minutes, the pressure dropped approximately 100 psi. Halliburton considered this as the fillup capacity of the lines and a normal leakoff through the pumps. In their opinion, no fluid had been pumped downhole. After an increase in the pressure to 2500 psig for five minutes, they still could not displace the fluids. At 3200 psig, explosive detonation occurred, ejecting metal from the wellhead and stones followed by detonation gases.

Debris from the casing and wellhead landed up to 1/4 mile from the well; no injuries occurred. However, the roofs of nearby houses sustained damage, in addition to vehicles parked near the wells and across the road. A crater measuring 15 feet in diameter and 10 feet deep marked the former well site. Water rapidly filled the hole, and some gas bubbled up through

vents near the side. Columbia plugged and abandoned this well after obtaining the approval of our partners. Although GOEX had successfully performed 15 treatments prior to our tests, we must view the tests in our wells as operational failures.

Results of Hydraulic Stimulations in Trumbull County: The foam treatments in each well in Trumbull County treated the same stratigraphic zone. However, we fractured the target interval in well 20144 in one stage, whereas 20143 and 20145 received two-stage completions.

The hydraulic fracture designs for these Trumbull County wells called for 1500 barrel treatments with 75 quality foam and a displacement rate of 40 barrels per minute. During the treatments, actual foam qualities varied from 68% to 80%, and the pumping rate ranged from 5 to 10 barrels per minute. Dowell had to decrease their pumping rate from the designed rate to keep the treatment pressure within the working limits of the wellhead. Average treatment pressures ranged from 2800 to 3400 psi, with instantaneous shut in pressures from 1750 to 2175 psi. Dowell successfully emplaced 86,000 to 88,000 pounds of 20/40 mesh sand (proppant) in four of the five treatments. However, a leaking blender truck halted the stimulation of the upper zone in well 20143 after displacing only 55,000 pounds of sand.

According to current rock mechanics theory, one should expect vertically oriented hydraulic fractures at the depths of our treated zones. Consequently, we designed the above mentioned treatments assuming primarily vertical fracture growth.

High treatment pressures limited the number of ball sealers injected during the stimulations. This reduced the probability of displacing a similar fluid volume into all perforations. This in turn, could have reduced

the effect of the treatment. As shown in Table XV, post-fracture radioactive tracer logs indicated that all seven perforations in the lower zone of well 20143 accepted the treatment, compared to six of the fifteen in the upper zone. The tracer log results for well 20145 indicated fluid entry into six of the seven perforations in the lower zone, but only one definite entry point in the upper zone. The treatment in well 20144 did not contain a radioactive tracer. Although tracer logs can be misleading, this suggests that we contacted only a fraction of the upper zones in these wells.

Table XV
RESULTS OF RADIOACTIVE TRACER SURVEYS IN
TRUMBULL COUNTY WELLS

<u>Well/Zone</u>	<u>Total Perforations</u>	<u>Perforations Accepting Tracer</u>
20143 upper zone	15	7 (4.7%)
lower zone	7	7 (100%)
20145 upper zone	15	3 (20%)
lower zone	7	6 (86%)

To locate the depth zones with the most gas flow and determine whether the treatment generated vertical fracture growth as designed, we conducted a logging and testing program in well 20144 from May 13 to June 4, 1981. During this period, the well had a stabilized open flow of 1 Mcfd. Due to this low flow rate, we allowed the casing pressure to buildup for one day prior to conducting the temperature and sibilation survey. Birdwell then logged the well before, during, and after flowing the well at a rate of 15 Mcfd. Fluid entry prevented the effective use of the Sibilation log. However, the temperature log indicated gas influx across the six deepest perforations. We then

set a packer with tubing at a depth of 2449 feet to separate the three lowest perforations. The tubing and casing pressures showed a similar pressure buildup over a 14 1/2 day shut-in period. After flowing the well through tubing for 60 minutes, the casing pressure dropped to about 12 psi. These results lead us to believe that we could achieve at least 10 feet of vertical communication from perforations treated in this depth range.

Before retrieving the packer, we verified that it seated properly. For the second test we emplaced the packer and tubing at 2387 feet and permitted an eight day pressure buildup. This time the casing pressure continued to increase during the tubing flow period. The second interference test shows that any vertical fracture growth related to the lower perforations should not exceed 60 feet. It also shows comparable gas influx from the upper 21 and lower 7 perforations, in spite of the lack of temperature shows in the upper zone. Because our stimulation design assumed vertical fracture growth and the first test indicated some vertical communication, we felt that further stimulation efforts would not increase the gas production. Tables XVI and XVII list the pressure and flow data for both interference tests.

TABLE XVI

WELL 20144T - INTERFERENCE TEST #1 DATA
(PACKER AT 2449 FEET)

<u>Tubing/Casing Buildup (5/31/81-5/27/81)</u>			<u>Tubing Drawdown (5/27/81)</u>		
Δt (days)	Pressure ¹		Δt (min.)	Tubing Flow Rate ² (sMcf/d)	Casing ¹ Pressure (psig)
	Tubing (psig)	Casing (psig)			
0	0	0	0	-	108.5 DW
2	37	33	2	-	85.0 DW
3	59	53	3	-	80.0 DW
4	74	70	5	-	72.0 DW
5	84	83	6	-	70.0 DW
6	94	94	7	-	52.0 DW
7	100	99	8	-	50.0 DW
8	95	93	9	-	46.0 DW
9	95	92	10	-	40.0 DW
10	98	94	11	-	36.0 DW
11	99	96	12	-	32.0 DW
12	102	100	13	-	27.0 DW
13	105	104	18	-	19.0 DW
14	-	-	21	29.9	13.5 DW
14.5	106	104	24	22.1	-
	(109.0DW)	(106.7DW)	28	14.7	11.0 DW
			30	14.6	-
			45	8.4	11.5 DW
			60	7.5	12.0 DW

¹ Wellhead pressures measured with recording gauge unless noted otherwise
(DW=dead weight pressure)

² Flow rates measured with orifice well tester

TABLE XVII

WELL 20144T-INTERFERENCE TEST #2 DATA
(PACKER AT 2387 FEET)

Tubing/Casing Buildup (5/27/81 - 6/4/81)

Δt (days)	Pressure ¹	
	Tubing (psig)	Casing (psig)
0	0	0
2	76	35
3	88	50
4	96	67
5	87	83
6	94	97
7	99	109
7.8	105 (108.7DW)	117 (132.5DW)

Tubing/Casing Drawdown (6/4/81)

Δt (min.)	Flow Rate ²		Pressure ¹	
	Tubing (sMcf/d)	Casing (sMcf/d)	Tubing (psig)	Casing (psig)
<u>Tubing Drawdown</u>				
0	-	0	-	108.9 DW
2	1.82	0	-	108.9 DW
4	1.70	0	-	108.9 DW
6	1.00	0	-	108.9 DW
10	0.95	0	-	109.3 DW
15	0.63	0	-	109.4 DW
20	0.50	0	-	109.6 DW
30	0.35	0	-	109.8 DW
45	0.25	0	-	110.0 DW
60	0.19	0	-	110.3 DW
<u>Casing Drawdown</u>				
60	0.19	-	-	-
70	TSTM	14.1	-	-
90	TSTM	11.8	-	-
90	TSTM	10.6	-	-
150	TSTM	6.8	-	-
180	TSTM	5.6	-	-

¹Wellhead pressures measured with recording gauge unless noted otherwise
(DW=dead weight pressure)

²Flow rates measured with orifice well tester

SUMMARY

Core analyses showed that the shale matrix contained rather high gas concentrations in both test areas. Given a suitable combination of natural and stimulation-induced permeability, we would have expected commercial gas production from the project wells in both counties. In spite of this, no significant gas flows resulted from any of the fifteen hydraulic and explosive fracture treatments. In the case of wells 20146 and 20147, in Trumbull County, the damage sustained to the casings and wellbores, due to the failure of the displaced explosive treatments, virtually eliminated any chance of economic production. Both of these wells sustained damage to their casing to the degree that logging devices could not reach the treated interval.

In general, we recovered 30 to 70 percent of the water used in the hydraulic fracture treatment and observed stabilized gas flows ranging from 1000 to 6000 cubic feet of gas per day. Hydrocarbons comprised about 90 percent of this flow.

None of the project wells in Trumbull County had either gauged or logged gas shows within the stimulated zones. Core from well 20144 contained encouraging concentrations of matrix gas, but had no extensive natural fractures. The insignificant post-stimulation gas flows and sizeable wellhead pressures suggest that foam fracturing treatments of the size used in these wells cannot generate economic gas production in the absence of some minimum level of natural permeability (natural fractures or horizons of enhanced gas conductivity). However, if reservoir conditions did in fact exist in this area, the present completion techniques did not effectively contact them.

In Lorain County, we observed rather large gas shows in two project wells. The cored well (20149) had several shows in spite of its lack of natural fractures (except for a few micro-faults of little importance). Open flows from the shale sections of four wells ranged from 4-38 Mcfd. However, our perforating and breakdown efforts failed to contact the natural flow paths after the casing and cementing operations. Post-fracturing gas flows did not equal the natural gas flow rates.

The above results suggest three possible explanations:

1. The stimulations did not effectively treat the right shale horizons
2. Our completion and cementing methods damaged the formation or blocked existing permeability paths
3. Natural open flows came from a rather limited reservoir

In testing the Lorain County wells, the perforated and treated zones included all horizons with gas shows or high matrix gas (off gas) contents. Moreover, the tracer logs, borehole camera, and post-fracture Sibilation surveys suggest that more than half of our perforations did accept at least some of the treatment fluid. The possibility still remains that most of the induced fractures could have extended out of the target zone. This could have occurred if the target zone were more difficult to fracture than the surrounding rock. In this case, and given the tendency for induced fractures to extend horizontally, the fracture treatment could have paralleled a target silt layer without actually accessing it.

Fluids introduced during the breakdown, hydraulic fracturing, and cementing operations can and do reduce the permeability of the shale which

they directly contact. This may involve the plugging of rock zones with fluids, displaced mineral grains, or even gelatinous material produced by the reaction of breakdown acids with the cement or formation. Although we expect that the flow improvement due to the induced fractures outweighs the formation damage, we have no way of comparing their relative effects in-situ.

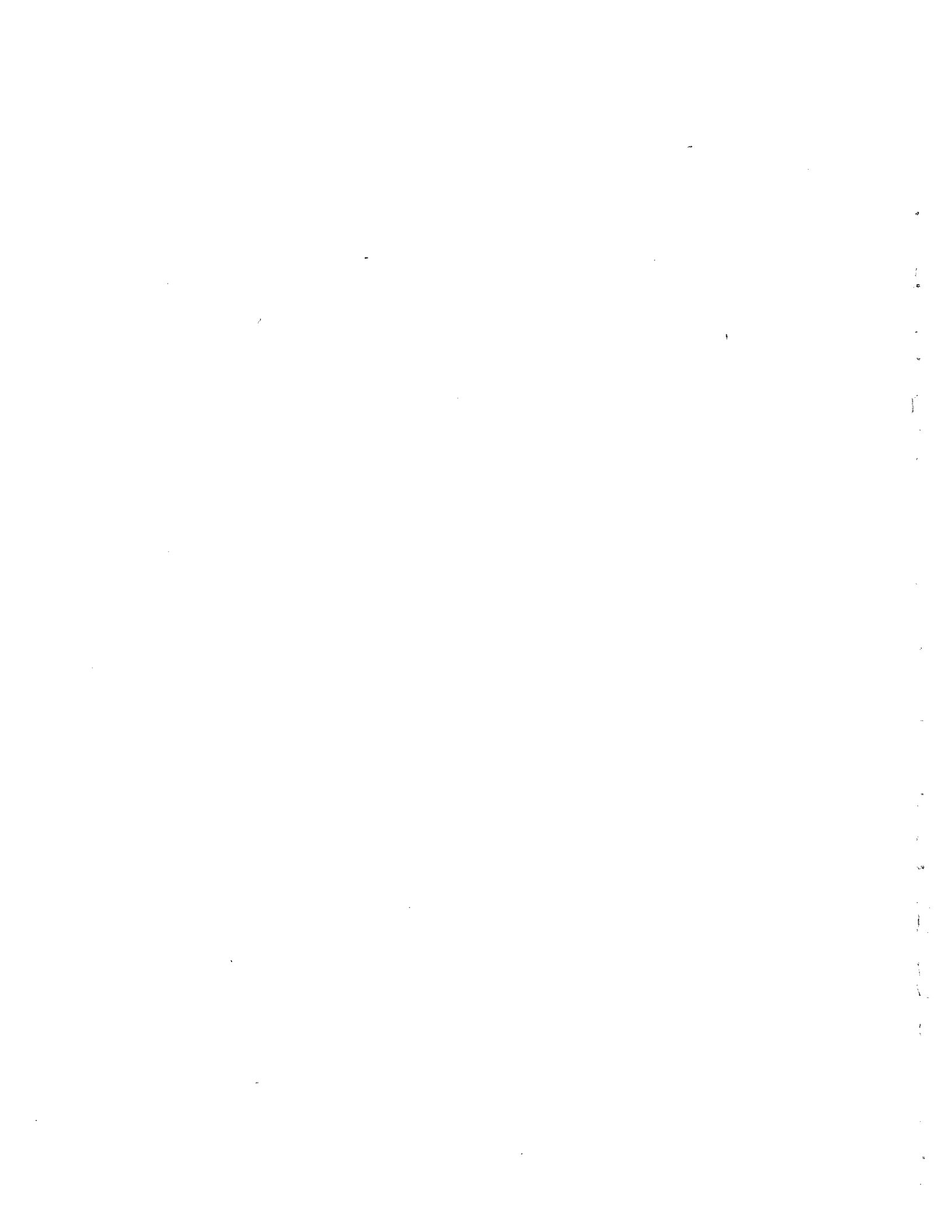
The lack of any measurable gas flow after casing could indicate that the natural flow completely drained some small gas pocket. However, our knowledge of shale wells suggests that such a pocket would have recharged during the months before we perforated the wells. Consequently, we should have measured some gas influx after breakdown if we actually contacted the flow network--small or not. While the lack of economic production in the shale sections of other nearby wells, in spite of reported shows, may support the occurrence of numerous insignificant gas pockets, it does not appear that our completion work successfully accessed the observed shows. Reported production in adjacent Eaton, Carlisle, Pittsfield, and Liverpool Townships may result from more extensive permeable silt layers.

In summary, it is fair to say that the present stimulation techniques did not prove effective in spite of high concentrations of gas within the matrix and sizeable natural shows.

1
2
3
4
5
6
7
8
9
10
11
12
13
14
15
16
17
18
19
20
21
22
23
24
25
26
27
28
29
30
31
32
33
34
35
36
37
38
39
40
41
42
43
44
45
46
47
48
49
50
51
52
53
54
55
56
57
58
59
60
61
62
63
64
65
66
67
68
69
70
71
72
73
74
75
76
77
78
79
80
81
82
83
84
85
86
87
88
89
90
91
92
93
94
95
96
97
98
99
100

APPENDIX A

Matrix Gas Contents of Core
Samples from Well #20143



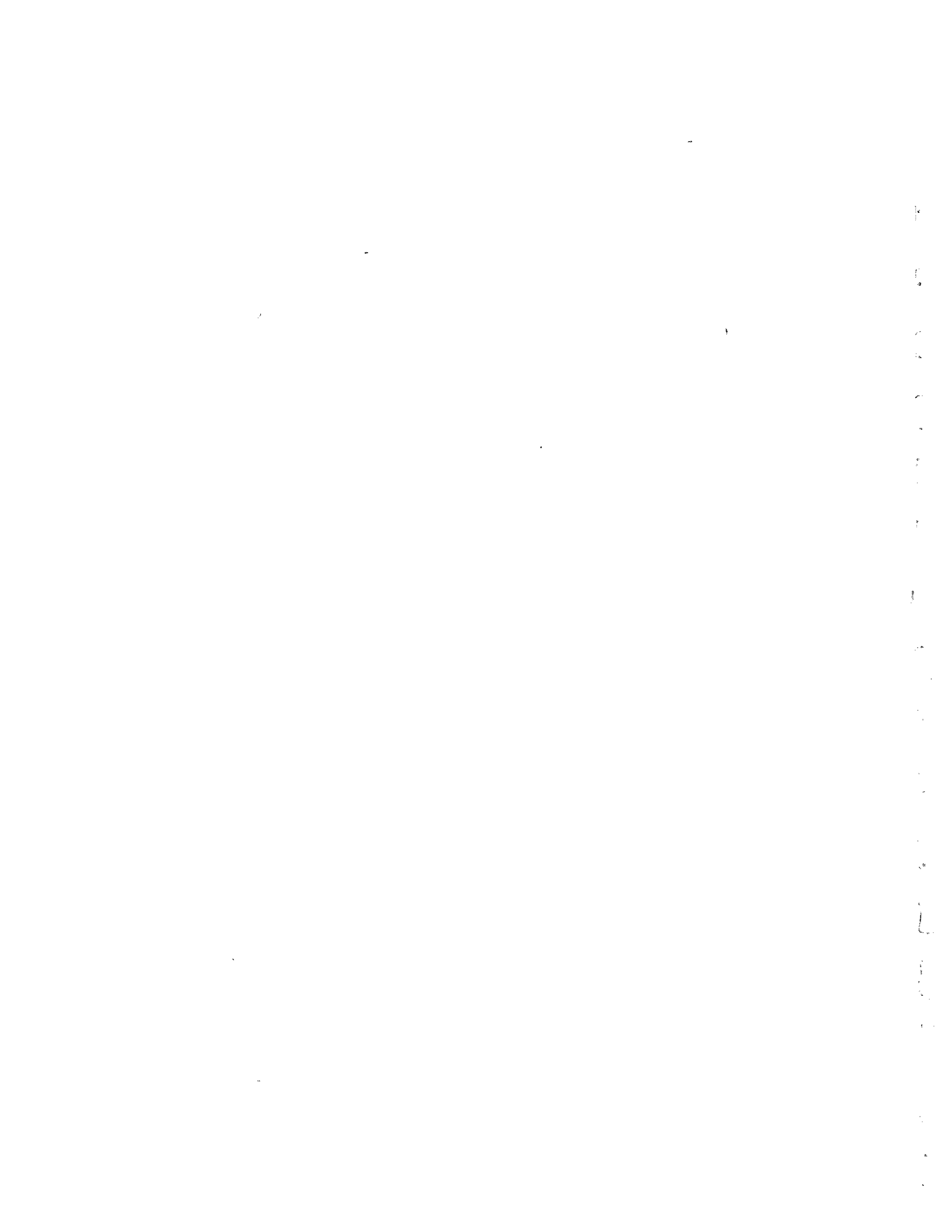
MATRIX GAS CONTENTS OF CORE SAMPLES
FROM WELL #20143

<u>Sample Depth</u>	<u>Off Gas (CF/CF)</u>	<u>Sample Depth</u>	<u>OffGas (CF/CF)</u>	<u>Sample Depth</u>	<u>Off Gas (CF/CF)</u>
1500	.00	1960	.94	2420	.00
1510	.00	1970	.75	2430	2.22
1520	.00	1980	.67	2440	.40
1530	.00	1990	1.50	2450	1.24
1540	.14	2000	.44	2460	1.46
1550	.13	2010	.50	2470	.17
1560	.36	2020	.00	2480	.00
1570	1.55	2030	.38	2490	1.25
1580	1.43	2040	.78	2500	3.14
1590	.00	2050	.78	2510	1.72
1600	.17	2060	.00	2520	1.26
1610	.00	2070	.65	2530	2.21
1620	.00	2080	.59	2540	2.41
1630	1.21	2090	1.37	2550	1.05
1640	.00	2100	.00	2560	1.30
1650	.00	2110	.41	2570	2.31
1660	.00	2120	1.71	2580	1.00
1670	.00	2130	.68	2590	2.42
1680	.28	2140	.61	2600	.00
1690	.51	2150	1.92	2610	.21
1700	.00	2160	.45	2620	.23
1710	.27	2170	.00	2630	.13
1720	.24	2180	.33	2640	.45
1730	.64	2190	.00	2650	.29
1740	1.35	2200	.00	2660	.38
1750	.00	2210	.77	2670	2.65
1760	.00	2220	.50	2680	2.86
1770	.00	2230	.00	2690	2.41
1780	1.18	2240	1.4	2700	2.43
1790	.00	2250	.65		
1800	.00	2260	.00		
1810	.92	2270	.00		
1820	.30	2280	.00		
1830	.51	2290	.88		
1840	1.49	2300	.66		
1850	.24	2310	1.74		
1860	.00	2320	.00		
1870	1.33	2330	.00		
1880	.35	2340	.00		
1890	.16	2350	.00		
1900	.86	2360	.00		
1910	.60	2370	.68		
1920	.38	2380	.00		
1930	1.05	2390	1.23		
1940	.90	2400	1.49		
1950	.56	2410	.00		

1
2
3
4
5
6
7
8
9
10
11
12
13
14
15
16
17
18
19
20
21
22
23
24
25
26
27
28
29
30
31
32
33
34
35
36
37
38
39
40
41
42
43
44
45
46
47
48
49
50
51
52
53
54
55
56
57
58
59
60
61
62
63
64
65
66
67
68
69
70
71
72
73
74
75
76
77
78
79
80
81
82
83
84
85
86
87
88
89
90
91
92
93
94
95
96
97
98
99
100

APPENDIX B

Matrix Gas Contents of Core
Samples from Well #20149



MATRIX GAS CONTENTS OF CORE SAMPLES
FROM WELL #20149

<u>Sample Depth</u>	<u>Gas (CF/CF)</u>	<u>Sample Depth</u>	<u>Gas (CF/CF)</u>
400	.21	850	1.65
410	.48	860	.00
420	.16	870	1.87
430	.00	880	2.49
440	.00	890	.00
450	.00	900	1.08
460	.00	910	1.17
470	.00	920	2.76
480	.00	930	1.96
490	.00	940	1.80
500	.00	950	.65
510	.00	960	.00
520	.00	970	.30
530	.00	980	.00
540	.00	990	.00
550	.00	1000	.55
560	.00	1010	.16
570	.00	1020	.30
580	.00	1030	.31
590	.00	1040	2.39
600	.00	1050	2.08
610	.00	1060	2.99
620	.00	1070	.135
630	.00	1080	.42
640	.14	1090	.00
650	.33	1100	.19
660	.31	1110	1.08
670	.10	1120	.40
680	.40	1130	.00
690	.30	1140	.41
700	.24	1150	.00
710	.56	1160	.19
720	.81	1170	.00
730	.97	1180	.00
740	.75	1190	.00
750	.99	1200	.09
760	.36	1220	.00
770	1.80	1230	.06
780	.58	1240	.00
790	.00	1250	.18
800	.20	1260	.46
810	.42	1270	.73
820	1.27		
830	1.15		
840	1.19		

1
2
3
4
5
6
7
8
9
10
11
12
13
14
15
16
17
18
19
20
21
22
23
24
25
26
27
28
29
30
31
32
33
34
35
36
37
38
39
40
41
42
43
44
45
46
47
48
49
50
51
52
53
54
55
56
57
58
59
60
61
62
63
64
65
66
67
68
69
70
71
72
73
74
75
76
77
78
79
80
81
82
83
84
85
86
87
88
89
90
91
92
93
94
95
96
97
98
99
100

APPENDIX C

Matrix Gas Contents in
Cuttings from Well #20151

<u>Sample Depth</u>	<u>Off Gas (CFG/CFS)</u>
298'-305'	.02
305'-311'	.36
311'-319'	.64
319'-325'	.57
325'-337'	.27
337'-345'	.14
355'-365'	.17
365'-375'	.07
375'-386'	.07
386'-396'	.22
396'-405'	.10
405'-415'	.04
415'-242'	.14
424'-435'	.10
435'-445'	.04
445'-455'	.05
455'-463'	.05
463'-473'	.05
473'-484'	.04
484'-494'	.02
494'-504'	.06
504'-514'	.04
514'-524'	.06
524'-532'	.06
533'-542'	.03
542'-550'	.02
550'-559'	.06
559'-570'	.03
570'-582'	.02
582'-591'	.05
591'-602'	.09
602'-614'	.03
614'-625'	.04
625'-635'	.10
635'-646'	.01
646'-656'	.02
656'-670'	---
670'-681'	.09
681'-692'	.05
692'-702'	.004
702'-712'	.12
712'-724'	.16
724'-733'	.08
733'-745'	.07

T A

1.0 INTR

2.0 SCOP

3.0 LABO

- 3.1
- 3.2
- 3.3
- 3.4
- 3.5
- 3.6
- 3.7

4.0 REPO

5.0 DISC

- 5.1
- 5.2
- 5.3
- 5.4

EAS
OHIO

PREL

A DETA

B SYMB
LOGG

C FRAC

BIBL
PLAT

1.0 INTRODUCTION

The U. S. Department of Energy is funding a research and development program entitled the Eastern Gas Shales Project designed to increase commercial production of natural gas in the eastern United States from Middle and Upper Devonian Shales. The program's objectives are as follows:

1. To evaluate recoverable reserves of gas contained in the shales.
2. To enhance recovery technology for production from shale gas reservoirs.
3. To stimulate interest among commercial gas suppliers in the concept of producing large quantities of gas from low-yield, shallow Devonian Shale wells.

During September and October of 1979 the Department of Energy and Columbia Gas Transmission Corporation funded the drilling/coring of the Anna V. Meleski #20143T well, hereafter referred to as EGSP-Ohio #7 in Trumbull County, Ohio. This report summarizes the procedures and results of core characterization work performed at the Eastern Gas Shales Project Core Laboratory on core retrieved from the Trumbull County well, designated EGSP-Ohio #7.

2.0 SCOPE OF WORK

The objective of work performed at the Eastern Gas Shales Project's Core Laboratory is to provide a detailed

characterization of the core recovered from the EGSP-Ohio #7 well. Data were acquired from several sources for analysis. At the well site, a suite of geophysical logs was run, which included the following:

<u>Dry Hole Logs</u>	<u>Wet Hole Logs</u>
Gamma Ray	Dual Laterolog
Compensated Formation Density	Bore Hole Compensated Sonic
Caliper	Compensated Neutron-Formation Density
Temperature	Gamma Ray
Sibilation	Caliper
3-D Velocity	

At the EGSP Core Laboratory, the EGSP-Ohio #7 core was laid out, washed, measured, oriented, and photographed prior to description and sampling. Characterization work performed includes photographic logs, detailed lithologic logs, fracture logs (both natural and induced types), core color variation, and stratigraphic interpretation of the cored intervals. In addition, physical property samples were prepared and are to be tested by Michigan Technological University under subcontract. Physical properties data obtained from specimen tests include:

- ° Directional Ultrasonic Velocity
- ° Directional Tensile Strength
- ° Strength in Point Load
- ° Trends of Microfractures
- ° Hydraulic Fracturing

3.0 LABORATORY PROCEDURES

3.1 Review of Geophysical Logs

During the initial stages of processing the EGSP-Ohio #7 core through the laboratory, dry hole geophysical logs from the well were examined and compared with published reference sections. Using the gamma ray and density logs a preliminary stratigraphic section was prepared for the cored interval. These two logs have proven to be the most useful correlation tools within the Devonian Shale sequence. Much of the development of existing formation nomenclature for the Devonian Shales is based on the recognition of characteristic features on these logs. Consequently, formation boundaries and thicknesses were, in some cases, more readily determined from gamma ray and density logs than from visual examination of the core itself.

Several other logs often provide information useful for core characterization. The fracture identification log and sonic log frequently indicate the occurrence of zones of structural discontinuity (joints, faults, concretions, zones of increased friability, etc.) within the core. The sibilation and temperature logs are useful for locating significant flows of gas into the well from isolated fractures or fracture systems.

The interpretation of prominent features on the geophysical logs in advance of core description is a means to assure that these features will receive adequate recognition.

3.2 Photographic Log

After the Ohio #7 core had been laid out, washed, and oriented on a group of laboratory tables, a series of photographs was taken to record the "as received" condition. A photographic log was then compiled for subsequent documentation. One copy of the log is to be forwarded to the Morgantown Energy Technology Center, under separate cover, together with this report.

3.3 Detailed Lithologic Log

After detailed visual examination the EGSP-Ohio #7 core was described in intervals which vary from about 5 feet to 10 feet in length. The first sentence of the description contains a brief summary of lithology, color, and sedimentary structure. Additional remarks were recorded to describe unique features observed within the interval. These remarks may concern any (or all) of the following:

1. Coarse clastic interbeds with scour surfaces, sole marks, cross-stratification, ripple lamination, etc.
2. Macroscopic fossils such as carbonaceous and pyritized vegetal constituents, conodonts, invertebrate shell fragments and casts, fish scales and teeth, etc.
3. Bioturbation, as discrete burrows or as mottled stratification, with emphasis on distribution and association with other rock fabric features.
4. Concretions, slump features, clasts and rip-up structures, gas pits, and other inorganic structures.

5. Modes of pyritization: as disseminated occurrences, nodules, coatings on shell fragments or plant tissue fragments; as accessory mineralization with concretions or clastic interbeds; and as primary irregular lenses or laminae in euxinic black shales.
6. Occurrence of fissility and friability.
7. Carbonate content.

Lithologic terminology applied to the shales is summarized in Figure 1. The classification scheme in use at the Core Laboratory for describing limestones is that of Dunham (1962), shown in Figure 2. Core colors were described using the Rock Color Chart published by the Geological Society of America (1948).

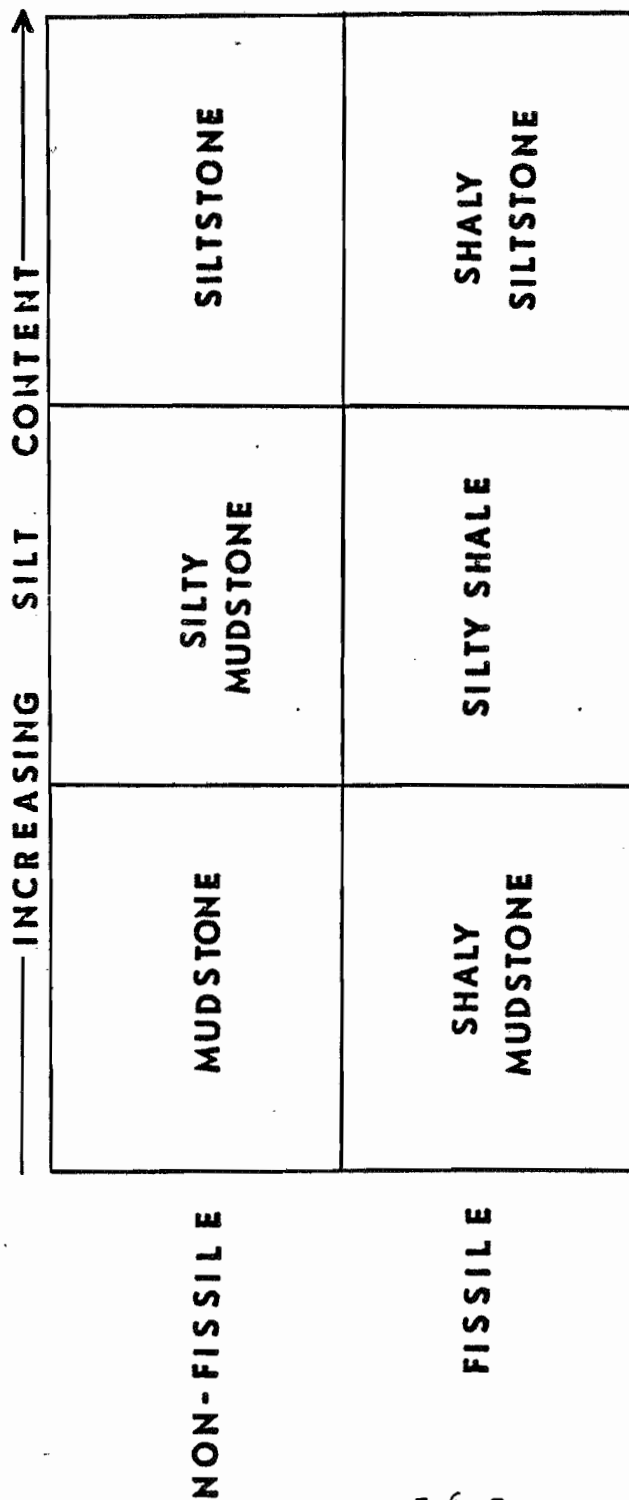


FIGURE 1

TEXTURAL CLASSIFICATION OF FINE CLASTIC SEDIMENTARY ROCKS

MUD SUPPORTED (Sand-size carbonate grains suspended in carbonate mud)		GRAIN SUPPORTED (Sand-size carbonate grains with interstitial carbonate mud)	
< 10% SAND-SIZE GRAINS	> 10% SAND-SIZE GRAINS	MUD PRESENT	NO MUD
Lime Mudstone	Wackestone	Packstone	Grainstone



BIOGENICALLY CEMENTED GRAINS: Boundstone
 NO RECOGNIZABLE TEXTURE: Crystalline Limestone

FIGURE 2
TEXTURAL CLASSIFICATION OF LIMESTONES

3.4 Stratigraphic Section

A stratigraphic section for the cored interval was prepared after the gamma ray and density logs were examined and the detailed lithologic log had been completed. Formation thicknesses were measured, contacts located as precisely as possible, and age relationships determined from published sources.

The locations of certain formation boundaries in the Devonian Shales are difficult to establish with precision. In some cases a contact between two units is gradational, or the nature of a contact may be problematical.

3.5 Color Histogram

A color histogram for the Ohio #7 core was compiled to provide a relative measure of the distribution of light and dark shales through the cored interval. Using the G.S.A. Rock Color Chart, the net length of each color present within each 5-foot segment of the core was recorded. Colors with values darker than dark gray (N3) were grouped together for each segment to determine the percentage of dark shale, and colors with values lighter than or equal to dark gray (N3) were combined to determine the percentage of light shale. Use of the term "value" refers to the Munsell system of color identification wherein a specific color is defined by a unique hue, value, and chroma designation.

3.6 Fracture Logs

Methods of fracture analysis employed at the EGSP Core Laboratory are similar to those described by Kulander et al. (1977). A standardized logging procedure has been developed by the Morgantown Energy Technology Center. Abbreviations and symbols used in conjunction with the EGSP Standard Core Fracture Logging Format are listed and defined in Appendix B.

Determination of the number, location, orientation, and character of natural fractures intercepted in the cored interval is of vital interest for the selection of appropriate well completion and stimulation techniques. Criteria applied to distinguish natural fractures from fractures induced during coring and handling are listed below (quoted from Evans, 1978):

CORING-INDUCED FRACTURES EXHIBIT THE FOLLOWING CHARACTERISTICS

1. Fracture origin within the core or on the core margin.
2. Hackle plumes diverging from the origin to intersect the core margin or preexisting fracture surface orthogonally.
3. Hackle marks becoming progressively coarser in the vicinity of the core margin or preexisting fracture surface.
4. Twist hackle originating near the core margin or preexisting fracture surface.
5. Hackle plumes diverging in a spiral pattern from the central part of the core on a subhorizontal fracture surface; indicative of torsional stress.

6. Closely spaced arrest lines on a vertical or near-vertical planar fracture; arrest lines are convex down-core and exhibit approximate bilateral symmetry.
7. Hackle marks on a vertical or near-vertical planar fracture diverging down-core from the center of the plane toward the margins.
8. An abrupt change in the direction of fracture propagation (hook) near the core margin or preexisting fracture surface.

NATURAL FRACTURES EXHIBIT THE FOLLOWING CHARACTERISTICS

1. Smooth, polished planar fracture faces, with or without slickensides.
2. Mineralization coating fracture surfaces or filling a closed fracture.
3. A smooth fracture extending across the core against which later fractures terminate.
4. Small conchoidal chips or hook features at the intersection of an inclined fracture plane and the core margin; the chips hook to meet the inclined fractures orthogonally.

Coring- and handling-induced fractures were logged in detail. This information provides additional documentation regarding the condition of the core as received from the field, and it is useful for assessing the effect of problems encountered during drilling. The frequency of disc fractures (generally the most prevalent and least diagnostic type of induced fracture) was recorded in the form of a histogram.

3.7 Measurement of Shore Hardness

The Shore hardness tests were deleted from core characterization work due to high equipment maintenance, questionable accuracy, and nonreproducible results. Substitute methods of hardness testing are being considered.

4.0 REPORTING OF RESULTS

A correlation chart has been compiled at a scale of 1 inch to 20 feet which provides a visual display of the following data recorded for the EGSP-Ohio #7 core.

1. Stratigraphic Column
2. Lithology
3. Color Histogram
4. Gamma Ray Log
5. Compensated Density Log
6. Temperature Log
7. Borehole Compensated Sonic Log
8. Orientation/Distribution of Natural Fractures
9. Frequency of Induced Fractures

The correlation chart accompanies this report as an enclosure.

Discussions of core stratigraphy, lithology, and the occurrence of fractures are provided in Section 5.0. Appendix A contains a detailed lithologic description of the core. Terminology applied in describing natural and induced fractures

is provided in Appendix B, and the fracture data are presented in Appendix C.

One copy of the photographic log was submitted as a separate document to the Morgantown Energy Technology Center. A second copy is available for inspection at the EGSP Core Laboratory.

When physical properties testing of samples from the EGSP-Ohio #7 core has been concluded, a final (Phase III) report will be issued containing an analysis of those data together with a summary of the information already compiled at the Core Laboratory.

After characterization was completed the core was sealed in a moisture barrier and packaged in 3-foot core boxes for temporary archiving at the EGSP Core Laboratory. Following a 90-day period the Ohio #7 core will be transferred to the Ohio Geological Survey.

5.0 DISCUSSION OF RESULTS

5.1 General

Coring of the EGSP-Ohio #7 well began on September 23, 1979. A conventional oil-field rotary rig equipped with a sixty-foot core barrel was used; the drilling medium was air and stiff foam with a KCl brine. The KCl brine was added to stabilize the clay fraction in the Devonian shales both in the borehole and the core. A continuous core was taken between 1,500' and 2,710'. Coring progressed very smoothly and no major problems were encountered.

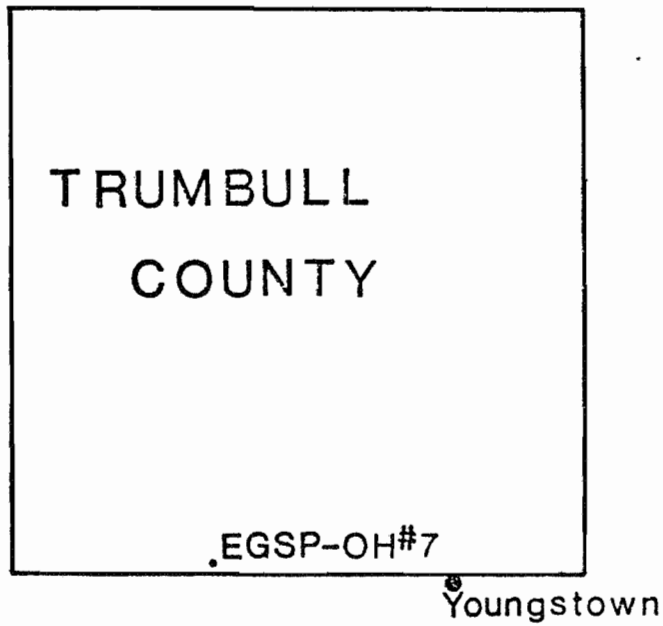


FIGURE 3

LOCATION OF THE EGSP-OHIO #7 WELL
TRUMBULL COUNTY, OHIO

5.2 Geologic Setting

The EGSP-Ohio #7 well is located approximately 12 miles west-northwest of Youngstown, Ohio (Figure 3). Drainage features to the southwest of the well site include Duck Creek, a tributary of the Mahoning River which feeds the Lake Milton-Berlin Reservoir. The local topography consists of a relatively flat-lying area with occasional gently rolling hills. The surface sediments are composed of Quaternary alluvium and lacustrine deposits and glacial outwash. Sandstones, limestones, shales and coals of the Pennsylvanian Pottsville Formation outcrop to the east of the well site.

5.3 Stratigraphy

A total of 1,210 feet of core was recovered from the EGSP-Ohio #7 well. The designated core point of 1,500' (depth from surface) is in the Chagrin Shale Member of the Ohio Shale. Coring was terminated at 2,710' in the Delaware Limestone of the Onondaga Group. Formations encountered and their thicknesses are summarized in Table 1. A summary description of each formation or member is provided below. A detailed lithologic description is provided in Appendix A. Stratigraphic nomenclature is patterned after that used by P. Potter, et al. (1980), and J. Schwietering (1979).

TABLE 1
FORMATION THICKNESSES

<u>Formation</u>	<u>Depth</u>	<u>Thickness</u>	<u>Depths Cored</u>
Ohio Shale:			
Chagrin Shale Memb.	CP-1,558'	---	1,500'-1,558'
Chagrin-Huron Shale Memb. (Intertongued)	1,558'-1,729'	171'	1,558'-1,729'
Huron Shale Memb.	1,729'-2,152'	423'	1,729'-2,152'
Java Formation:			
Hanover Shale Memb.	2,152'-2,284'	132'	2,152'-2,284'
Pipecreek Memb.	2,284'-2,298'	14'	2,284'-2,298'
West Falls Formation:			
Angola Shale Memb.	2,298'-2,490'	192'	2,298'-2,490'
Rhinestreet Shale Memb.	2,490'-2,584'	94'	2,490'-2,584'
Hamilton Group:			
Tichenor Limestone	2,584'-2,589'	5'	2,584'-2,589'
Mahantango Formation	2,589'-2,672'	83'	2,589'-2,672'
Marcellus Formation	2,672'-2,708'	36'	2,672'-2,708'
Onondaga Group:			
Delaware Limestone	2,708'-TD	---	2,708'-2,710'

Ohio Shale

In the EGSP-Ohio #7 well, the Ohio Shale is represented by two members; the Chagrin Shale Member and the Huron Shale Member. Approximately 652 feet of core was taken from these two members, even though the upper contact of the Chagrin Shale Member was not cored.

The Chagrin Shale Member is present from 1,500 feet to 1,558 feet, and the Huron Shale Member occurs from 1,729 feet to 2,152 feet. The interval between 1,558 feet and 1,729 feet is comprised of an intertonguing of the Chagrin and Huron Shale Members.

Chagrin Shale Member:

Total thickness of the Chagrin Shale Member could not be determined from well data obtained. At least, 558 feet (1,500' to 1,558') of the member is present in the EGSP-Ohio #7 core. Consequently, a detailed lithologic description was obtained for only part of the Chagrin Shale Member.

The Chagrin Shale Member (1,500' to 1,558') is mainly comprised of thinly laminated to thin-bedded dark greenish gray (5G 4/1 and 5GY 4/1) mudstones, olive black (5Y 2/1) and olive gray (5Y 4/1) silty mudstones, and light gray (N7) cross-stratified siltstones. The siltstones contain scour surfaces, load casts and occasionally are slightly calcareous. Moderate brown (5YR 4/4) to brownish gray (5YR 4/1) calcareous concretionary bands occur throughout the cored portion of the member. Occasional ash beds are present. Bioturbation is present in the form of mud-filled burrow structures. Fossil content is limited to occasional vitrinite fragments and pyritized and resinous spores (Tasmanites). Pyrite occurs in the lower 20 feet as lenses, nodules and disseminated crystals.

The contact (1,558') between the Chagrin Shale Member and the underlying Chagrin-Huron Shale Members (intertongued) appears on well logs as sharp increases in gamma radiation and decreases in bulk density and sonic velocity. The contact in the core is gradational (over = 10 feet); with Chagrin Shale Member being represented by green shales with multiple siltstone lenses, whereas the Huron Shale Member is typically brown shales absent in siltstone content.

Chagrin-Huron Shale Members (intertongued):

Core and well log analysis support the concept of the Chagrin Shale Member being intertongued with the Huron Shale Member. This concept was previously suggested by Schwietering (1979) and Potter, et al. (1980). This intertonguing occurs in the EGSP-Ohio #7 core between 1,558' and 1,729'

Intervals identified as the Chagrin Shale Member are typically dark greenish gray (5GY 4/1) to greenish gray (5G 4/1) mudstones, olive black (5Y 2/1) to olive gray (5Y 4/1) silty mudstones, and medium gray (N5) to very light gray (N8) siltstones, thinly laminated to thin-bedded. The siltstones are occasionally calcareous, cross-stratified and contain load casts. Calcareous concretionary bands, light olive gray (5Y 6/1) to pale olive brown (10YR 6/2) in color, are occasionally present. Ash beds tend to occur in the lighter, silty zones. Burrow structures, filled with pyrite and/or mudstone occur sparsely throughout; the lower 30 feet contain

mottled (bioturbation) zones. Fossil content consists primarily of pyritized and resinous spores (Tasmanites) and vitrinite fragments. Fish parts are present but rare in the upper 30 feet.

The intervals identified as Huron Shale Member consist of thickly laminated to thin bedded olive black (5Y 2/1) to olive gray (5Y 4/1), mudstones and silty mudstones. Calcareous zones occur where siltstone stringers are present in these darker mudstones. Disseminated mica occurs throughout the interval of intertonguing. Vitrinite and carbonaceous fragments (some partially pyritized) are also present throughout.

The contact (1,729') between the Chagrin-Huron Shale Members (intertongued) and the underlying Huron Shale Member is marked on well logs by a sharp increase in gamma radiation and moderate decreases in density and sonic velocities. The core is gradational between 1,725' and 1,730'.

Huron Shale Member:

The Huron Shale Member (1,729' to 2,152') is mainly composed of thick bedded, olive black (5Y 2/1) to olive gray (5Y 4/1) shaly mudstones and silty mudstones. Thin to thick laminae and thin beds of dark greenish gray (5G 4/1) to greenish gray (5G 6/1) occur throughout. Sparse siltstones, light gray (N7), thinly laminated and occasionally cross-stratified and scoured are also present. Greenish gray (5G 6/1) calcareous mudstones occur occasionally as thin beds. Calcareous zones occur throughout and often are associated with concre-

tionary bands ranging in color from light brownish gray (5YR 6/1) to brownish gray (5YR 4/1). Disseminated mica is present throughout, predominantly in the dark mudstones. A single silty, ash bed is present at 1,841.9'. Mottling and burrow structures filled with mud, silt or pyrite (commonly oxidized) are present throughout. Fossil content is limited to: pyritized and/or resinous spores (Tasmanites), carbonaceous and vitrinite fragments (some of which are partially pyritized), rare fish scales, inarticulate brachiopods and a single algal body (Foerstia, 1,846.3').

The contact (2,152') between the Huron Shale Member and the underlying Java Formation has been determined on well logs by a decrease in gamma radiation and subsequent increases in density and sonic velocities. The core contains a distinct color change at this contact from the dark olive black Huron shales to the consistently green shales of the Java Formation.

Java Formation:

The Java Formation, comprised of the Hanover Shale Member and the Pipecreek Member, occurs in the EGSP-Ohio #7 well between 2,152' and 2,298'. The entire Hanover Shale Member (132 feet thick) and underlying Pipecreek Member (14 feet thick) were cored.

Hanover Shale Member:

The Hanover Shale Member consists of thinly to thickly laminated and occasionally thin bedded (in the lower 1/2),

greenish gray (5GY 6/1 and 5G 6/1) silty mudstones and light olive gray (5Y 6/1) to dark gray (N3) mudstones. The dark greenish gray silty mudstones contain occasional calcareous zones and traces of glauconite. Concretionary bands, medium gray (N5) to yellowish gray (5Y 7/2) in color, are present, but sparse. Mottling (bioturbation) occurs in the upper 1/2, mud- and pyrite-filled burrow structures are present throughout. Pyrite occurs dominantly as disseminated grains; nodules, wave-form lenses, and pyritized spores (Tasmanites) are also present. Some of the pyritized spores have been partially oxidized. Resinous spores are present, but sparse. Vitrinite and carbonaceous fragments, some of which are partially to completely replaced by pyrite, occur throughout. Only two shell fragments are present, both unidentified.

The contact (2,284') between the Hanover Shale Member and the Pipecreek Member was selected in the EGSP Core Laboratory by J. Hosterman and J. Roen, U.S.G.S. (personal communication). Well logs display two sharp increases in gamma radiation, and equivalent decreases in density and sonic velocities, which outline the upper and lower boundaries of the Pipecreek Member.

Pipecreek Member:

The Pipecreek Member is composed of thinly and thickly laminated, dark greenish gray (5GY 4/1) silty mudstones and olive black (5Y 2/1) to dark gray (N3) mudstones. Zones within the Member are calcareous. Traces of glauconite occur in the dark greenish gray silty mudstones. A septarian nodule 5 cm in

diameter is present at 2,289.4'. Bioturbation (mud- and pyrite-filled burrows) is concentrated at the laminae contacts. Pyrite also occurs as disseminated grains, nodules and as coatings on spores (Tasmanites). Unidentified shell fragments and vitrinite fragments are present throughout.

The contact between the Pipecreek Member and the West Falls Formation is marked on well logs by a sharp increase in gamma radiation and equivalent sharp decreases in density and sonic velocities.

West Falls Formation:

The West Falls Formation consists of two members; the Angola Shale Member (192 feet thick) and the Rhinestreet Shale Member (94 feet thick). The entire formation was cored.

Angola Shale Member:

The Angola Shale Member is composed of thinly to thickly laminated, and occasionally thin bedded, dark greenish gray (5GY 4/1) to grayish olive green (5GY 5/2) silty mudstones and brownish black (5YR 2/1) to olive gray (5Y 4/1) mudstones. The interval contains calcareous zones. The lower 45 feet is dominantly brownish black (5YR 2/1) and olive black (5Y 2/1). Concretions present within the lower 2/3 contain pyrite, anhydrite, and/or calcite mineralization. Pyrite occurs in lenses throughout, and as nodules and disseminated grains in the lower 90 feet. Mottling (bioturbation) is occasionally present, whereas mud- and pyrite-filled burrow structure (some with calcite and/or anhydrite centers) occur through-

out. Fossils present within the interval include: vitrinite (some partially pyritized) and carbonaceous fragments, articulate brachiopods and cephalopods (lower 45'). A fossiliferous zone is present between 2,470' and 2,483'. Pyritized spore casts are present in the upper 10 feet; resinous spore bodies occur in the lower 10 feet.

The contact (2,490') between the Angola Shale Member and the Rhinestreet Shale Member is marked on well logs by a large increase in gamma radiation and a decrease in bulk density. The core grades from the green shales containing dark brown laminae of the Angola Shale to the dominantly olive brown shales of the Rhinestreet Shale Member.

Rhinestreet Shale Member:

The Rhinestreet Shale Member is comprised of thickly laminated and thin bedded, brownish black (5YR 2/1) to olive gray (5Y 4/1) silty mudstones and mudstones and occasionally thin laminations of light olive gray (5Y 5/2) siltstone. Zones within the interval are calcareous. The mudstones are dominate below 2,540'. Mottling (bioturbation) is present in the upper 40 feet, mud- and pyrite-filled burrow structures occur sparsely throughout. Fossil content includes: resinous and carbonaceous spores, conodonts, inarticulate and articulate brachiopods, cephalopods and sparse fish scales (between 2,520' and 2,555'), and carbonaceous and vitrinite fragments (some of which are partially pyritized).

The contact (2,584') between the Rhinestreet Shale Member and the underlying Hamilton Group is not readily discernible on the well logs. However, at this contact, the core shows a marked increase in carbonate content and gradually lightens in color.

Hamilton Group:

The Hamilton Group consists of the Tichenor Limestone (Schwietering, 1979) which is present between 2,584' and 2,589'; the Mahantango Formation between 2,589' and 2,672', and the Marcellus Formation between 2,672' and 2,708'. The entire interval was cored.

Tichenor Limestone:

The Tichenor Limestone consists of thickly laminated and thin bedded, olive black (5Y 4/1) to olive gray (5Y 2/1) mudstones and light olive gray (5Y 6/1) calcareous mudstone. The interval is calcareous throughout. Thin laminae of medium light gray (N6), carbonate cemented siltstone are interlaminated within the mudstones. Silt- and pyrite-filled burrow structures occur throughout. Fossils contained within the formation are limited to inarticulate and articulate brachiopods (poorly preserved) and a single vitrinite fragment.

In the core a sharp contact (2,589') exists between the Tichenor Limestone and the underlying Mahantango Formation. Well logs show decreased gamma radiation and increased density and sonic velocities at this contact.

Mahantango Formation:

The Mahantango Formation is comprised of thick to thin bedded, brownish black (5YR 2/1) to olive gray (5Y 3/2) shaly mudstones. The Formation is calcareous throughout. Pyrite occurs throughout as lenses and nodules, and occasionally as disseminated grains and mineralization in burrow structures. Fossils contained in the interval include: pyritized and carbonaceous spores (Tasmanites), inarticulate and articulate brachiopods, and a single pyritized cephalopod.

The contact between the Mahantango Formation and the underlying Marcellus Formation was determined from the well logs. At this contact gamma radiation is greatly increased, density and sonic velocities are decreased. The core becomes gradationally darker down core.

Marcellus Formation:

The Marcellus Formation is comprised of thick bedded, olive gray (5Y 3/2 and 5Y 4/1) to olive black (5Y 2/1) mudstones. The interval is moderately calcareous throughout. Disseminated mica and sand-sized biotite flakes occur in the lower 2 feet. Pyrite is present as lenses, nodules, and disseminated grains. Carbonaceous fragments, some of which are partially pyritized, and vitrinite fragments occur in the upper 20 feet. Fragments of inarticulate and articulate brachiopods, conodonts, pelecypods, cephalopods, and pyritized spores (Tasmanites) are sparse.

In the core the contact (2,708') between the Marcellus Formation and the Delaware Limestone of the Onondaga Group is marked by a sharp lithologic change from dark shales to medium gray limestone. Well logs display decreased gamma radiation and increased density and sonic velocities at this contact.

Onondaga Group:

The Onondaga Group is represented by the Delaware Limestone at the base of the Ohio #7 core.

Delaware Limestone:

The Delaware Limestone consists of thickly laminated and thin bedded, medium gray (N5) calcareous mudstone and brownish gray (5YR 4/1), wackestone (limestone). Lime-filled burrow structures and articulate brachiopods are present throughout. Coring was terminated at 2,710', 2 feet into the Delaware Limestone.

5.4 Fracture Analysis

Both natural and induced fractures present in the core were examined in detail. The resulting fracture logs are reproduced in Appendix C of this report. Terminology and abbreviations used in log compilation are summarized in Appendix B.

All natural fractures were analyzed to identify common structural trends in the core. Figure 4 is a graphic representation of the data (fracture strikes and dips) plotted in polar form on a Schmidt (Equal Area) Stereonet. The plotted data have been contoured to determine locations of maximum point density using the method described by Regan (1968).

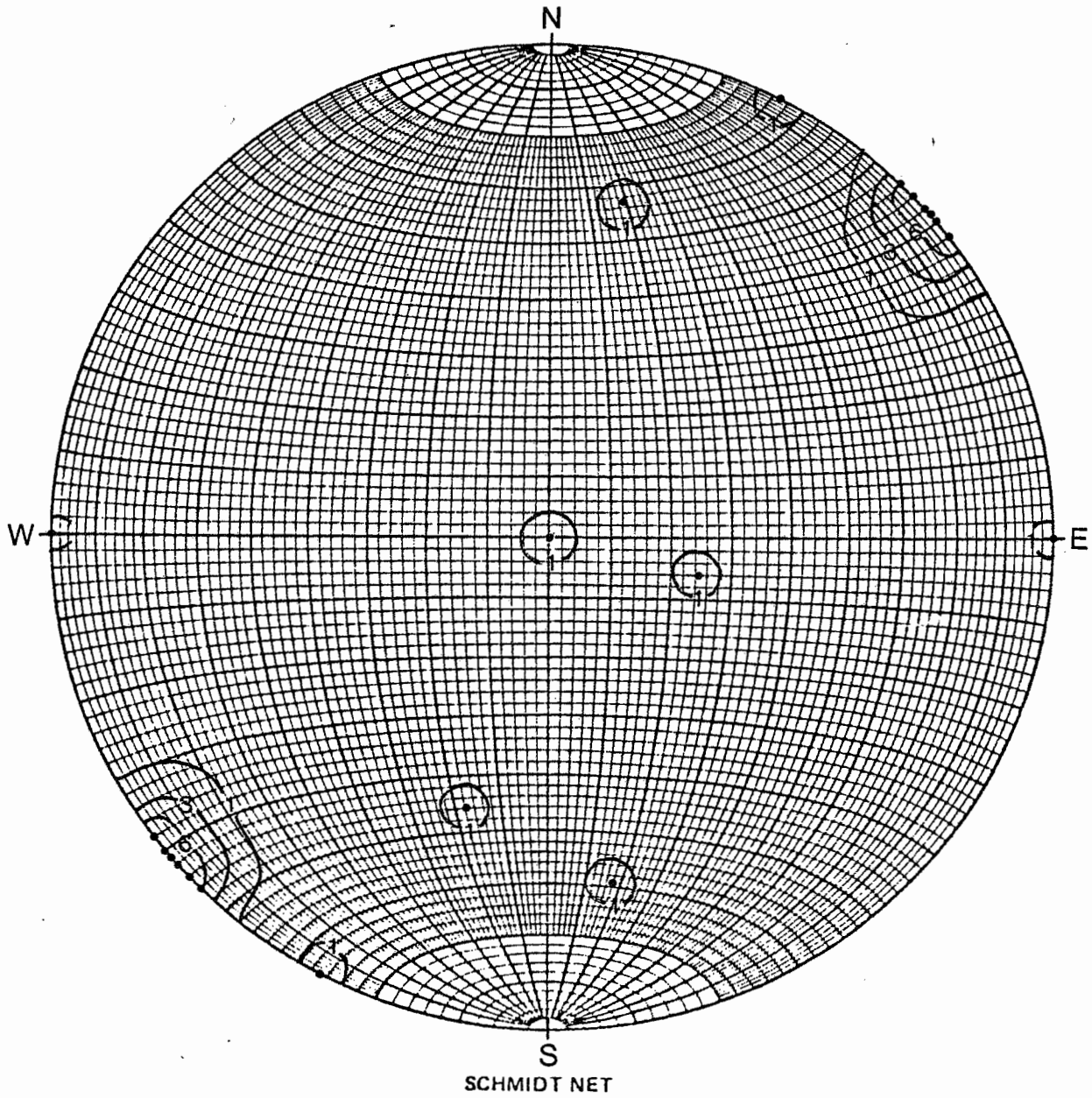
Approximately 26 natural fractures were observed in the core. Of this total, 3 are simple joints, 6 are faults, and 16 are microfaults. The distribution of natural fractures throughout the core is presented in Table 2.

Of the three simple joints present in the core, two are contained within a thin, unstratified siltstone bed, at 1,591.9', in the intertongued Chagrin-Huron Shale Member. These strike N44°W (near-vertical dip) and N78°W (60° dip) and are mineralized with gypsum-anhydrite (?). The third simple joint occurs at 2,549.4', in the Rhinestreet Shale Member, with a strike of N90°E (vertical dip) and is mineralized with calcite.

TABLE 2
DISTRIBUTION OF NATURAL FRACTURES

<u>Formation</u>	<u>Depth</u>	<u>Core Length</u>	<u>Number of Fractures</u>	<u>Frequency Per Foot</u>
Ohio Shale:				
Chagrin Shale Member	1,500'-1,558'	58'	0	0.00
Chagrin-Huron Shale Member (Intertongued)	1,558'-1,729'	171'	7	0.04
Huron Shale Member	1,729'-2,152'	423'	0	0.00
Java Formation:				
Hanover Shale Member	2,152'-2,284'	132'	0	0.00
Pipecreek Member	2,284'-2,298'	14'	0	0.00
West Falls Formation:				
Angola Shale Member	2,298'-2,490'	192'	0	0.00
Rhinestreet Shale Member	2,490'-2,584'	94'	2	0.02
Hamilton Group:				
Tichenor Limestone	2,584'-2,589'	5'	0	0.00
Mahantango Formation	2,589'-2,672'	83'	0	0.00
Marcellus Formation	2,672'-2,708'	36'	0	0.00
Onondaga Group:				
Delaware Limestone	2,708'-2,710'	2'	0	0.00

Of the six faults present in the core, five are contained in a set occurring between 1,587.0' and 1,593.0' in the Chagrin-Huron Shale Member. This fault set strikes between N38°W and N46°W. The dip angle on these faults is near vertical ($\approx 90^\circ$).



SCHMIDT NET

FIGURE 4

CONTOURED DIAGRAM OF POLES TO NATURAL FRACTURES

Fault movement is in a horizontal direction southeast-northwest. Mineralization (gypsum-anhydrite (?)) was present on the fracture plane prior to fault movement. A sixth unrelated fault occurs at 2,534.4', in the Rhinestreet Shale Member, striking N63°W with a 90° dip. Movement on this fault plane is also in a horizontal direction, southeast-northwest.

The two joints and the five faults, located between 1,587.0' and 1,593.0', appear to be associated with a siltstone bed. The two joints are located within the bed. Three of the faults extend down to and terminate at the upper boundary of the bed, two faults begin at the lower boundary of the bed and terminate downcore as dying hairline fractures. No movement is present within the siltstone bed, fractures above or below this bed display movement.

The 16 microfaults recorded, occur along the peripheral boundaries of concretions and pyrite nodules. These microfaults were not evaluated further (stereonet plots as they display random or indeterminate orientations.

Of the total number of fractures present in the core, more than 95% were interpreted to be coring- or handling-induced. Disc fractures are the most common type observed. Because these fractures are less diagnostic than other types of fractures, they are not logged individually. However, the disc fracture frequency does provide a rough measure of flexural rigidity of the core parallel to bedding, and those data are presented in Appendix C.

Petal fractures and hooks on disc fractures are not common features in the majority of cores examined from Devonian shale wells, although most cores do contain a few fractures of those types. Genetic implications of these fractures are poorly understood.

Petal fractures, hooks on disc fractures, and occasionally hooks on petal fractures occur in the EGSP-Ohio #7 core. All are confined to the Ohio Shale; hooks are confined to the core above 1,765.0' and petal fractures are restricted to the core above 1,910.0'. Distribution of these fractures is recorded in Tables 3 and 4. Separate stereonet projections have been prepared for petal fractures and hooks for analysis of trends (Figures 5 and 6).

Petal fracture strikes in the EGSP-Ohio #7 core range between $N26^{\circ}E$ and $N70^{\circ}E$ and dip at moderate angles (40° to 60°). Hook strikes range between $N30^{\circ}E$ and $N70^{\circ}E$ and usually have near-vertical dips ($\approx 90^{\circ}$).

TABLE 3
DISTRIBUTION OF PETAL FRACTURES

<u>Formation</u>	<u>Depth Cored</u>	<u>Core Length</u>	<u>Number of Fractures</u>	<u>Frequency Per Foot</u>
Ohio Shale:				
Chagrin Shale Member	1,500'-1,558'	58'	8	0.14
Chagrin-Huron Shale Member (Intertongued)	1,558'-1,729'	171'	14	0.08
Huron Shale Member	1,729'-2,152'	423'	1	0.002
Java Formation:				
Hanover Shale Member	2,152'-2,284'	132'	0	0.00
Pipecreek Member	2,284'-2,298'	14'	0	0.00
West Falls Formation:				
Angola Shale Member	2,298'-2,490'	192'	0	0.00
Rhinestreet Shale Member	2,490'-2,584'	94'	0	0.00
Hamilton Group:				
Tichenor Limestone	2,584'-2,589'	5'	0	0.00
Mahantango Formation	2,589'-2,672'	83'	0	0.00
Marcellus Formation	2,672'-2,708'	36'	0	0.00
Onondaga Group:				
Delaware Limestone	2,708'-2,710'	2'	0	0.00

TABLE 4
DISTRIBUTION OF HOOKS ON DISC FRACTURES

<u>Formation</u>	<u>Depth Cored</u>	<u>Core Length</u>	<u>Number of Hooks</u>	<u>Frequency Per Foot</u>
Ohio Shale:				
Chagrin Shale Member	1,500'-1,558'	58'	6	0.10
Chagrin-Huron Shale Member (Intertongued)	1,558'-1,729'	171'	12	0.07
Huron Shale Member	1,729'-2,152'	423'	1	0.002
Java Formation:				
Hanover Shale Member	2,152'-2,284'	132'	0	0.00
Pipecreek Member	2,284'-2,298'	14'	0	0.00
West Falls Formation:				
Angola Shale Member	2,298'-2,490'	192'	0	0.00
Rhinstreet Shale Member	2,490'-2,584'	94'	0	0.00
Hamilton Group:				
Tichenor Limestone	2,584'-2,589'	5'	0	0.00
Mahantango Formation	2,589'-2,672'	83'	0	0.00
Marcellus Formation	2,672'-2,708'	36'	0	0.00
Onondaga Group:				
Delaware Limestone	2,708'-2,710'	2'	0	0.00

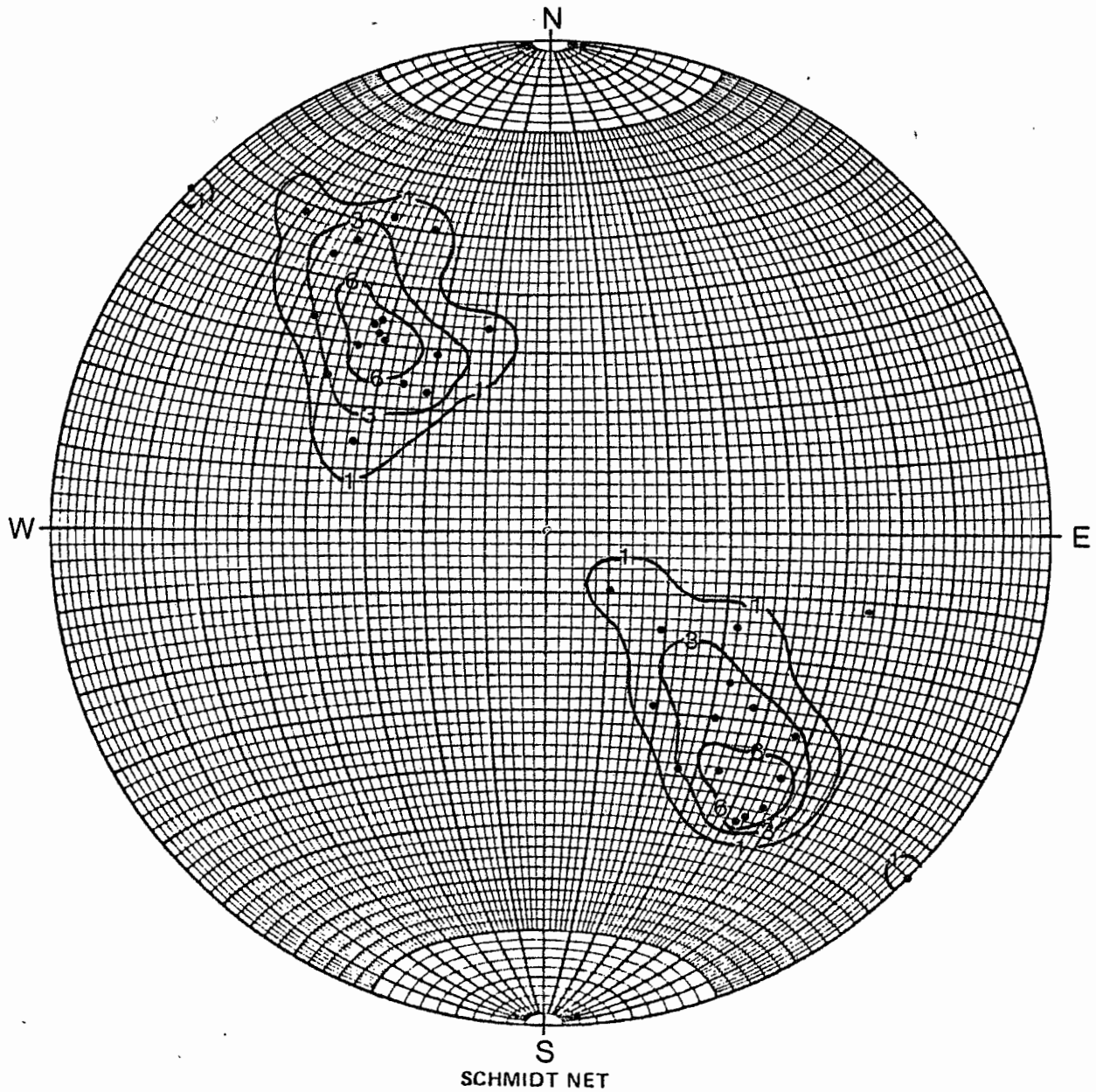


FIGURE 5

CONTOURED DIAGRAM OF POLES TO PETAL FRACTURES

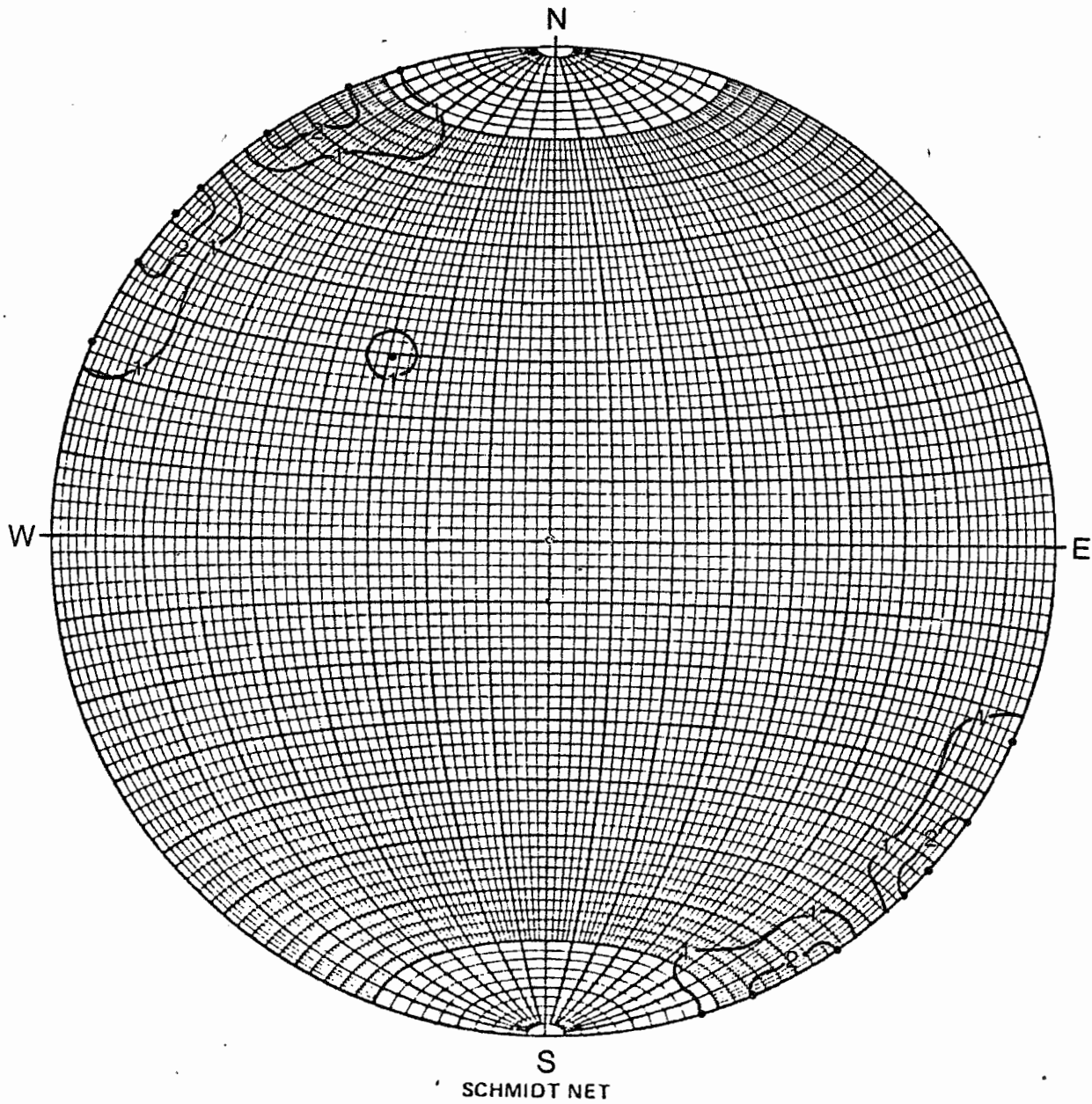
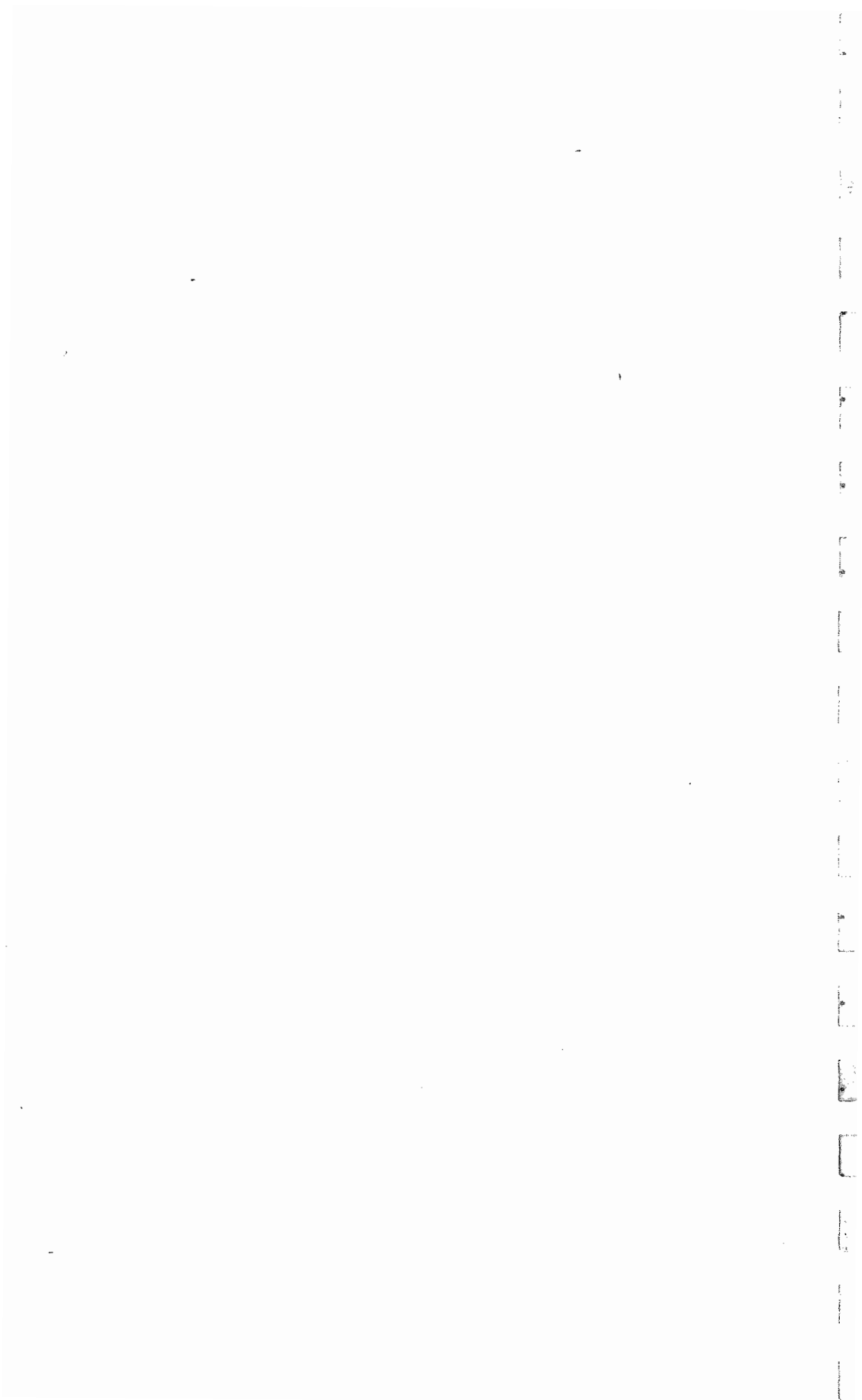


FIGURE 6

CONTOURED DIAGRAM OF POLES TO HOOKS ON DISC FRACTURES



A P P E N D I X A

DETAILED LITHOLOGIC DESCRIPTION

<u>INTERVAL</u>	<u>DESCRIPTION</u>
1,500.0' - 1,510.0' (10.0')	Mudstones, siltstones and silty mudstones, dark greenish gray (5GY 4/1), light gray (N7) to very light gray (N8), and olive black (5Y 2/1), thinly laminated to thin bedded. The siltstones are cross-laminated and contain load casts. Olive black mudstones occur in thick laminations with sharp upper and gradational lower boundaries. Sequences of siltstone or silty mudstone fining upward to mudstone are present throughout; scour surfaces are present at the bottom of most of these sequences. Ash beds occur in siltstone at 1,502.9' and 1,507.7'. The light mudstones contain pyritized spores. Moderate yellowish brown (10YR 5/4) concretionary bands, 4 cm thick, occur throughout and commonly rest on the olive black mudstones.
1,510.0' - 1,520.0' (10.0')	Mudstones, siltstones, and silty mudstones, greenish gray (5GY 6/1), light gray (N7), and olive black (5Y 2/1), thinly laminated to thin bedded. The siltstones are cross- to ripple-laminated and contain load casts and scour surfaces. The olive black mudstones are present as thick laminations with sharp upper and gradational lower boundaries. Sequences of siltstone or silty mudstone fining upward to mudstone are present throughout; scour surfaces are present at the bottom of each sequence. The light mudstones contain pyritized and resinous spores, and horizontal mud-filled burrows (≈ 2 mm diam.). A small (< 1 mm) vitrinite particle is present at 1,519.7'. Small, irregular concretions, moderate brown (5YR 4/4) in color are present throughout. A siltstone at 1,512.9' is calcareous.
1,520.0' - 1,530.0' (10.0')	Mudstones, siltstones, and silty mudstones, greenish gray (5G 5/1), light gray (N8), and olive black (5Y 2/1) to olive gray (5Y 4/1), thinly laminated to thin bedded. The siltstones are cross- to ripple-laminated and contain load casts. Olive black mudstone is present only as thick laminations. Sequences of siltstone or silty mudstone fining upward to mudstone are present throughout; scour surfaces often occur at the bases of these sequences. Occasional ash beds (?) are present in the siltstones. The light mudstones contain pyritized and resinous spores and horizontal mud-filled burrow structures (≈ 2 mm diam.). Moderate brown (5YR 4/4) concretionary bands, < 1 cm thick, occur throughout the interval.

<u>INTERVAL</u>	<u>DESCRIPTION</u>
1,530.0' - 1,537.7' (7.7')	Mudstones, siltstones, and silty mudstones, greenish gray (5GY 5/1), very light gray (N8), light gray (N7), and olive black (5Y 2/1), thinly laminated to thin bedded. The siltstones are cross-laminated and contain load casts and scour surfaces. An ash bed occurs at 1,534.6' in a siltstone. The light mudstones contain pyritized and resinous spores throughout; vitrinated wood at 1,534.3'. Iron staining (oxidation) often occurs around clusters of pyritized spores. Several small (<1 cm) moderate brown (5YR 4/4) concretionary bands are present throughout. The siltstone at 1,531.1' is calcareous.
1,537.7' - 1,547.0' (9.3')	Mudstones, siltstones, and silty mudstones, greenish gray (5GY 6/1), very light gray (N8), and olive black (5Y 2/1), thinly laminated to thin bedded. The siltstones are ripple-laminated and contain scour surfaces and load casts. Graded sequences of siltstone or silty mudstone fining upward to mudstone and usually <1 cm thick, are present throughout. Olive black mudstone occurs as thick laminae which often have sharp upper and gradational lower boundaries. The light mudstones contain pyritized and resinous spores and mud-filled burrows (horizontal, ≈2 mm thick) throughout, a vitrinated wood fragment at 1,540.9', and a mica bed (ash bed ?) at 1,544.6'. Mica beds (ash beds ?) are also present throughout the siltstones. A strongly calcareous, brownish gray (5YR 4/1) concretion is present at 1,543.0'. Several of the siltstones are slightly calcareous.
1,547.0' - 1,558.6' (11.6')	Mudstones, siltstones, and silty mudstones, greenish gray (5GY 6/1), olive black (5Y 2/1) to olive gray (5Y 4/1), and light gray (N7), thinly laminated to thin bedded. The mudstones contain definite light and dark thickly laminated to thin bedded zones; gradational color changes occur within these zones. The amount of olive black mudstone present increases in this interval. The siltstones are ripple-laminated and contain scour surfaces, load casts, and mica beds (ash beds ?). Several graded sequences are also present. The mudstones contain spore resin bodies and occasional small pyrite nodules. The light mudstones contain pyritized spores, and occasional small vitrinite fragments. Mica beds (ash beds ?) occur throughout the siltstones and at 1,533.6' between a light and dark mudstone. Several heavily calcareous, light olive brown (5Y 5/1) concretions are present at 1,547.7'. Occasionally, the siltstones are calcareous.

<u>INTERVAL</u>	<u>DESCRIPTION</u>
1,558.6' - 1,568.0' (9.4')	Mudstones, packstones, and siltstones, olive gray (5Y 4/1) to olive black (5Y 2/1), greenish gray (5GY 6/1), medium light gray (N6), and light olive gray (5Y 6/1), thinly laminated to thin bedded. Color changes within the mudstones are gradational. The packstones contain load casts and thin mudstone cross-laminations. Siltstone occurs as laminae, some of which are cross-laminated. The mudstones contain spore resin bodies. The dark mudstones also contain occasional pyrite nodules unidentified carbonaceous fragments, and mica flakes throughout, an ash bed (?) at 1,562.6', and a fish skin (?) imprint at 1,567.1'. The light mudstones contain pyritized spores throughout, and mud lumps with slickensides at 1,560.6'.
1,568.0' - 1,578.0' (10.0')	Mudstones, packstones, and siltstones, olive gray (5Y 4/1) to olive black (5Y 2/1), greenish gray (5GY 6/1), light olive gray (5Y 6/1), and very light gray (N8), thinly laminated to thin bedded. Color changes within the mudstones are gradational. The packstones contain load casts and thin mudstone cross-laminations. Siltstone occurs as laminae, some of which are cross-laminated. All of the mudstones contain spore resin bodies. The dark mudstones also contain abundant carbonaceous fragments (plant and unidentified fragments), fish (?) parts, small pyrite nodules and mica flakes throughout, vitrinite at 1,571.9', and biotite flakes (ash bed ?) at 1,576.1'. The light zones contain pyritized spores.
1,578.0' - 1,585.3' (7.3')	Mudstones, siltstones and silty mudstones, olive gray (5Y 4/1) to olive black (5Y 2/1), greenish gray (5GY 6/1) and light gray (N7), thinly laminated to thin bedded. Greenish gray mudstone and siltstone content increases down core. Color changes within the mudstones are gradational. The siltstones are ripple-laminated and contain load casts. Several sequences of siltstone or silty mudstone fining upward to mudstone are present; scour surfaces rest at the base of some of the sequences. All of the mudstones contain spore resin bodies and pyritized spores. The dark mudstones contain mica, carbonaceous plant fragments, mud lumps, and pyrite throughout, and a fish skin (?) at 1,581.6'. Pyrite occurs as flat laminae, waveform laminae, nodules, and in mineralized burrows. The light mudstones contain pyritized structures (4 - 10 mm in diam., sub-vertical).

<u>INTERVAL</u>	<u>DESCRIPTION</u>
1,585.3' - 1,587.5' (2.2')	Siltstones and mudstones, greenish gray (5GY 6/1), medium gray (N5), and light gray (N7), thinly laminated to thin bedded. The top 1/4 and bottom 1/4 of the interval are cross-laminated; the top 1/4 contains many load casts. The middle of the interval is composed of a massive siltstone. The siltstones contain disseminated pyrite and mica flakes. A mudstone at 1,587.1' contains pyritized spores, some of which are partially oxidized. Calcareous stringers are present near the middle of the interval. A light olive gray (5Y 6/1) concretionary band is present at 1,587.2'.
1,587.5' - 1,591.7' (4.2')	Mudstones and siltstones, greenish gray (5GY 6/1), olive gray (5Y 4/1), medium light gray (N6), and very light gray (N8), thinly laminated to thin bedded. The olive gray mudstones occur in several thick laminae. The siltstones are ripple- to cross-laminated and often contain load casts. The mudstones contain pyritized and resinous spores. A single partially pyritized woody fragment is present at 1,590.0' in a light mudstone.
1,591.7' - 1,592.9' (1.2')	Siltstones and mudstones, greenish gray (5GY 6/1) to 5GY 5/1), thinly laminated to thin bedded. A siltstone occurring from 1,592.0' to 1,592.1' is ripple laminated. Below 1,592.1', the siltstones are nonstratified. Mudstone occurs as lenses and fragmented bedding from 1,591.7' to 1,591.9'. The interval is calcareous below 1,592.0'.
1,592.9' - 1,605.0' (12.1')	Mudstones, siltstones, and silty mudstones, greenish gray (5GY 5/1), yellowish gray (5Y 8/1), olive gray (5Y 4/1), olive black (5Y 2/1), and medium light gray (N6), thinly laminated to thin bedded. Siltstone and mudstone content is approximately equal. The siltstones occur as ripple-laminated zones and in thin beds. The ripple-laminated siltstones also contain load casts and scour surfaces. Several sequences of siltstone or silty mudstone fining upward to mudstone are present; scour surfaces occur at the base of some of these sequences. The siltstones and dark mudstones contain zones of mica. A pyritized wood fragment containing sulfur (?) and vitrinite occurs at 1,604.6' in a light mudstone. The siltstones in the lower 1/2 of the interval are zonally calcareous.

<u>INTERVAL</u>	<u>DESCRIPTION</u>
1,605.0' - 1,606.1' (1.1')	Siltstones and mudstones, olive gray (5Y 4/1), olive black (5Y 2/1), and light gray (N7), thinly laminated to thin bedded. Fragmented inclusions of olive black mudstone and light gray siltstone are present from 1,605.0' to 1,605.3' in the olive gray siltstone. Below 1,605.3' the siltstones are non-stratified. Abundant mica flakes are present within the siltstones.
1,606.1' - 1,616.0' (9.9')	Siltstones, mudstones, and silty mudstones, medium light gray (N6) to very light gray (N8), greenish gray (5GY 5/1) to dark greenish gray (5GY 4/1), and olive black (5Y 2/1), thinly laminated to thin bedded. Approximately 1/2 of the siltstones are cross-laminated and contain load casts and scour surfaces. The olive black mudstones occur as thick laminae. Sequences of siltstone or silty mudstone fining upward to mudstone occur throughout; scour surfaces are present at the base of many of these sequences. The siltstones contain abundant zones of mica. The mudstones contain resinous and pyritized spores. The light mudstones contain mud-filled burrow structures (horizontal, 2 mm diam.) and partially oxidized pyritic spores throughout; pyritized organism trails (?) at 1,608.8'. A light olive gray (5Y 6/1) concretionary band occurs at 1,606.2'. The siltstones at 1,607.5' and 1,613.3' are calcareous.
1,616.0' - 1,626.0' (10.0')	Mudstones, siltstones, and silty mudstones, olive gray (5Y 4/1), medium light gray (N6) to light gray (N8), and olive black (5Y 2/1), thinly laminated to thin bedded. Approximately 1/2 of the siltstones are cross-laminated and contain load casts and scour surfaces. Several sequences of siltstone or silty mudstone fining upward to mudstone are present; scour surfaces occur at the base of some of these sequences. The olive black mudstone content increases in this interval. An olive gray siltstone occurs between 1,616.9' and 1,617.4'. Fragmented olive black mudstone and light gray siltstone inclusions are present within this lithology at 1,617.0'. The mudstones contain spore resin bodies. The light mudstones contain pyritized spores throughout; iron stains occur around some of the spore clusters. Also present in the light mudstones are mud-filled burrow structures (horizontal, \leq 2 mm diam.), a mica bed at 1,618.5', and vitrified wood with pyritic veins and sulfur at 1,620.2'. The dark mudstones contain occasional irregular pyrite laminations. The siltstones in the upper 1/2 of the interval are calcareous.

<u>INTERVAL</u>	<u>DESCRIPTION</u>
1,626.0' - 1,632.0' (6.0')	Mudstones, siltstones, and silty mudstones, olive gray (5Y 4/1), greenish gray (5GY 6/1), and light greenish gray (5GY 8/1), thinly laminated to thin bedded. The siltstones are ripple-laminated and contain load casts and scour surfaces. Several graded beds of siltstone or silty mudstone fining upward to mudstone are present; scour features often occur at the base of these sequences. The dark mudstones contain mica flakes throughout, anhydrite (?) surrounded by marcasite at 1,627.6' and a vitrified stem at 1,629.5'. The light mudstones rarely contain spore casts. A siltstone at 1,629.0' is calcareous.
1,632.0' - 1,642.0' (10.0')	Mudstones, siltstones, and silty mudstones, greenish gray (5GY 5/1), light olive gray (5Y 6/1), olive black (5Y 2/1) to olive gray (5Y 4/1), thinly laminated to thin bedded. The siltstones are ripple- to cross-laminated and contain load casts and scour surfaces. Abundant sequences of siltstone or silty mudstone fining upward to mudstone are present; scour surfaces frequently occur at the base of these sequences. All of the mudstones contain spore resin bodies. The light mudstones contain abundant pyritic spores (some oxidized) and an unidentified metallic mineral at 1,641.5'. The dark mudstones are mica-ceous. A slickensided surface is noted at 1,641.2' at the base of a calacereous siltstone.
1,642.0' - 1,649.0' (7.0')	Mudstones, siltstones, and silty mudstones, greenish gray (5GY 6/1), light greenish gray (5GY 8/1), and olive gray (5Y 4/1), thinly laminated to thin bedded. The color changes between the greenish gray and light greenish gray mudstones are gradational. The siltstones are ripple-laminated and contain scour surfaces and load casts. Several sequences of siltstone or silty mudstone fining upward to mudstone are present. The light mudstones contain pyritic spores (oxidized at 1,645.5') throughout, and a pyritic wood fragment at 1,644.8'. The dark mudstones contain spore resin bodies and mica flakes. A siltstone at 1,648.3' is calcareous.

<u>INTERVAL</u>	<u>DESCRIPTION</u>
1,649.0' - 1,656.2' (7.2')	Mudstones, siltstones, and silty mudstones, greenish gray (5GY 5/1), olive gray (5Y 4/1) to olive black (5Y 5/1), and light greenish gray (5GY 8/1), thinly laminated to thin bedded. The siltstones are ripple- to cross-laminated and contain load casts and scour surfaces. Several sequences of siltstone or silty mudstone fining upward to mudstone are present; scour surfaces often occur at the base of these sequences. All of the mudstones contain spore resin bodies. The light mudstones contain pyritic spores, some of which are oxidized, and carbonaceous woody fragments throughout and a partially vitrified and pyritized wood fragment with sulfur powder (?) at 1,651.8'. The dark mudstones are micaceous. Occasionally, the siltstones are calcareous.
1,656.2' - 1,657.9' (1.7')	Siltstones and mudstones, light olive gray (5Y 6/1), dark gray (N3), and yellowish gray (5Y 8/1). Thinly to thickly laminated stone occurs as thin to thick laminae. The interval is ripple-laminated at 1,656.4' and at 1,657.4'; the remainder of the interval is non-stratified. The siltstones are slightly calcareous.
1,657.9' - 1,668.0' (10.1')	Mudstones, siltstones, and silty mudstones, greenish gray (5GY 6/1), light greenish gray (5GY 8/1), and olive black (5Y 2/1) to olive gray (5Y 4/1) thickly laminated to thin bedded. Color changes are gradational between the olive gray and light olive gray mudstones. The olive black to olive gray mudstones usually occur as thick laminae with sharp upper, and gradational lower boundaries. The siltstones occur most commonly near the middle of the interval, are cross- to ripple-laminated and contain load casts and scour surfaces. Several sequences of siltstone or silty mudstone fining upward to mudstone are present; some of these sequences contain basal scour surfaces. The light mudstones contain occasional carbonaceous wood fragments and pyritic spores, some of which are occasionally oxidized. Spore resin bodies occur in dark mudstones, usually at the tops of these zones. Mud-filled burrows (horizontal, ≈4 mm in diam.) are present at 1,661.1' in a siltstone. Occasionally, the siltstones are slightly calcareous.

<u>INTERVAL</u>	<u>DESCRIPTION</u>
1,668.0' - 1,678.0' (10.0')	Mudstones, siltstones, and silty mudstones, greenish gray (5GY 6/1), light greenish gray (5GY 8/1) and olive black (5Y 2/1), thinly laminated to thin bedded. Most of the siltstones are ripple- to cross-laminated and contain load casts and scour surfaces. Several sequences of siltstone or silty mudstone fining upward to mudstone are present throughout. The light mudstones contain occasional oxidized plant fragments, pyritic spores and oxidized spores (?). The dark mudstones contain spore resin bodies. An ash bed (?) is present at the bottom of a siltstone at 1,668.0'. Occasionally, the siltstones are slightly calcareous.
1,678.0' - 1,688.0' (10.0')	Mudstones, siltstones, and silty mudstones, greenish gray (5GY 6/1), light greenish gray (5GY 8/1) and olive gray (5Y 4/1), thinly laminated to thin bedded. The siltstones are ripple- to cross-laminated and contain load casts and scour surfaces. Sequences of siltstone or silty mudstone fining upward to mudstone are occasionally present. The olive gray mudstones are thickly laminated and usually have sharp upper and gradational lower boundaries. The light mudstones contain pyritic spores (some oxidized) and occasional vitrified wood fragments with pyritized veins. The dark mudstones contain spore resin bodies. The siltstones contain occasional mud-filled burrow structures (horizontal, ≈4 mm). A pale yellowish brown (10YR 6/2), calcareous concretion is present at 1,685.0'. Most of the siltstones are calcareous.
1,688.0' - 1,698.0' (10.0')	Mudstones, siltstones, and silty mudstones, greenish gray (5GY 6/1), light greenish gray (5GY 8/1), and olive gray (5Y 2/1), thinly laminated to thin bedded. The siltstones are ripple- to cross-laminated and often contain load casts and scour surfaces. Several graded sequences are present; scour surfaces occur at the base of most of these sequences. A zone of soft sediment deformation occurs between 1,694.8' and 1,695.1' in a mudstone. The light mudstones contain pyritic spores (occasionally oxidized), and powdered sulfur (?). The dark mudstones contain spore resin bodies throughout, and a vitrinite fragment at 1,694.5'. A siltstone at 1,693.7' is slightly calcareous.

<u>INTERVAL</u>	<u>DESCRIPTION</u>
1,698.0' - 1,707.0' (9.0')	Mudstones, siltstones, silty mudstones, and calcareous mudstones, greenish gray (5GY 6/1), olive black (5Y 2/1) and yellowish gray (5Y 8/1), thinly laminated to thin bedded. The olive black zones increase in abundance down-core. The siltstones are ripple-laminated and contain scour surfaces and load casts. Sequences of siltstone or silty mudstone fining upward to mudstone are present. Yellowish gray calcareous mudstone is present at 1,704.9' and 1,705.1'. Heavily mottled zones (bioturbation) occur within the mudstones. Occasional mud-filled burrow structures (horizontal, ≈4 mm in diam.) are present in the siltstones. Both light and dark mudstones contain spore resin bodies. The light mudstones also contain oxidized plant stems and pyritized spores (occasionally oxidized) throughout; pyritized woody fragments at 1,704.2'. A vitrinite fragment is present at 1,704.3' in a dark mudstone. Occasionally, the siltstones are calcareous.
1,707.0' - 1,713.2' (6.2')	Mudstones, siltstones, and silty mudstones, olive black (5Y 2/1), greenish gray (5GY 6/1) and light greenish gray (5GY 8/1), thinly laminated to thin bedded. The siltstones are ripple-laminated and often contain scour surfaces. Several graded sequences of siltstone or silty mudstone fining upward to mudstone occur in the interval. The dark mudstones contain spore resin bodies throughout and a vitrinite fragment at 1,707.7'. The light mudstones contain pyritized spores and oxidized pyritic plant fragments. A heavily mottled zone (bioturbation) occurs in a mudstone at 1,712.5'. The siltstones contained in the interval are slightly calcareous.
1,713.2' - 1,721.0' (7.8')	Silty mudstones, siltstones, and mudstones, greenish gray (5GY 6/1), light greenish gray (5GY 8/1) and olive gray (5Y 4/1) to olive black (5Y 2/1), thinly laminated to thin bedded. The siltstones are ripple- to cross-laminated and often contain scour features and load casts. Several sequences of siltstone or silty mudstone fining upward to mudstone are present; the lower boundaries are often truncated by scour surfaces. A heavily bioturbated zone occurs at 1,719.1' in a mudstone. The mudstones and silty mudstones contain pyritized spores and spore resin bodies. The light silty mudstones also contain oxidized plant fragments (oxide stains encircle some of these fragments) and an organism trail at 1,719.3'. The siltstones are calcareous.

<u>INTERVAL</u>	<u>DESCRIPTION</u>
1,721.0' - 1,729.0' (8.0')	Silty mudstones, mudstones, siltstones, and packstones, light greenish gray (5GY 8/1), olive black (5Y 2/1), and yellowish gray (5Y 8/1), thinly laminated to thin bedded. The siltstones are ripple-laminated. The packstones are disrupted by load casts and scour surfaces. The light mudstones and silty mudstones contain oxidized plant fragments and pyrite nodules. Several heavily mottled zones (bioturbated) are present within the mudstones. The silty mudstones in the upper 1/2 are calcareous.
1,729.0' - 1,742.0' (13.0')	Mudstones and calcareous mudstones, olive gray (5Y 4/1) to olive black (5Y 2/1), light olive gray (5Y 6/1) and dusky yellow (5Y 6/4), thinly laminated to thin bedded. Color changes within the mudstones are gradational. The interval is predominantly thin bedded dark mudstone. Calcareous mudstones are present at 1,737.2' and at 1,737.3' as thin to thick laminations. The dark mudstones contain infrequent carbonaceous fragments throughout and pyritized spores in the lower 1/4.
1,742.0' - 1,752.0' (10.0')	Silty mudstones, mudstones, siltstones, and packstones, greenish gray (5GY 8/1), olive gray (5Y 4/1) to olive black (5Y 2/1), medium light gray (N6) and yellowish gray (5Y 8/1), thinly laminated to thin bedded. The siltstones are occasionally ripple-laminated and frequently contain load casts and scour surfaces. Several graded sequences of siltstone or silty mudstone fining upward to mudstone are present; these sequences rest on scour surfaces. Several heavily mottled zones (bioturbation) are present in the mudstones. The light silty mudstones and mudstones contain oxidized plant fragments and pyritic spores. Pyrite also occurs as nodules in the upper 1/2. The dark mudstones contain a few carbonaceous fragments. The silty mudstones in the upper 1/2 are calcareous.
1,752.0' - 1,760.0' (8.0')	Mudstones, silty mudstones, and siltstones, greenish gray (5GY 5/1), olive black (5Y 2/1), and light greenish gray (5GY 8/1), thinly laminated to thin bedded. The siltstones are ripple-laminated, infrequently present and contain scour surfaces. Several sequences of silty mudstone fining upward to mudstone are present; these sequences contain basal scour surfaces. Several heavily mottled zones (bioturbated) are present within the mudstones. Crushed, horizontal, pyritized burrow structures (?) occur within these mottled zones. The light mudstones contain oxidized plant fragments, iron stains, and pyritized spores. These features usually occur at the tops of the light mudstones. A single vitrified wood fragment occurs at 1,755.5' in a dark mudstone.

<u>INTERVAL</u>	<u>DESCRIPTION</u>
1,760.0' - 1,770.0' (10.0')	Silty mudstones, mudstones, and siltstones, greenish gray (5GY 6/1), olive black (5Y 2/1) and light greenish gray (5GY 8/1), thickly laminated to thin bedded. The siltstones are ripple-laminated, infrequently present and occasionally contain scour surfaces and load casts. Several heavily mottled zones (bioturbation) are present. Abundant, pyritized, sub-horizontal burrow structures (3-5 mm in diam.) are present in the light silty mudstones. These light zones also contain oxidized plant fragments. The dark mudstones contain occasional carbonaceous fragments. Several light brown (10 YR 5/6) concretionary bands occur in the lower 1/2; a highly calcareous, olive gray (5Y 4/1) concretion occurs at 1,766.3'. The siltstones and silty mudstones are zonally calcareous.
1,770.0' - 1,775.0' (5.0')	Mudstones, siltstones, and silty mudstones, greenish gray (5GY 6/1), light greenish gray (5GY 8/1) and olive black (5Y 2/1), thinly laminated to thin bedded. The siltstones are ripple-laminated. A single mottled zone occurs at 1,773.1'. Pyritized, horizontal, burrow structures (≈3 mm in diam.) occur throughout the light mudstones and silty mudstones. The light mudstones also contain oxidized plant fragments and iron stains. Light brown (5YR 5/6) calcareous concretions and concretionary bands occur in the lower 1/4. The top 1/2 of the interval is calcareous.
1,775.0' - 1,782.6' (7.6')	Mudstones, olive black (5Y 2/1) and greenish gray (5GY 6/1), thickly laminated to thin bedded. A single zone of bioturbation is present at 1,778.5'. The mudstones contain spore resin bodies. These bodies are somewhat concentrated in the darker mudstones which also contain occasional carbonaceous fragments throughout, and a slickensided, vitrinitized surface at 1,781.8'. The light mudstones contain pyritized spores throughout, and a pyrite nodule at 1,778.5'.
1,782.7' - 1,790.6' (7.9')	Mudstones, olive black (5Y 2/1) and dark greenish gray (5GY 4/1), thin bedded to thickly laminated. Siltstone, greenish gray (5G 6/1) in color, is present as a thin lamination (1,783.0') and a pinched-out thin lamination (1,784.2'). The dark greenish gray mudstone occurs as thin beds and thick laminations with sharp upper and lower contacts. The olive black mudstones contain disseminated mica. Resinous spores occur throughout. Partially pyritized burrow traces occur in the lower 1/4. A vitrinite/pyrite mineralized woody fragment is present at 1,783.1'. A faintly pyritized cellular (?) structure (6 mm x 100 mm) occurs at 1,789.1'.

<u>INTERVAL</u>	<u>DESCRIPTION</u>
1,790.6' - 1,799.8' (9.8')	Mudstones, dark greenish gray (5G 4/1) and olive black (5Y 2/1), thick bedded and thickly laminated to thin bedded. Occasional thin laminations of siltstone, greenish gray (5G 4/1) to light gray (N7) are iron stained on the core surface. The dark greenish gray mudstone is occasionally slightly calcareous. Mottling (bioturbation) occurs where dark greenish gray mudstones overlay olive black mudstones. Pyritized spore casts, partially-pyritized burrow traces (some oxidized) and disseminated pyrite occur throughout. Disseminated mica is present in the olive black mudstones. Sparce carbonaceous fragments occur throughout.
1,799.8' - 1,809.8' (10.0')	Mudstones, greenish gray (5G 6/1) and olive black (5Y 2/1), thick bedded to thickly laminated and thin bedded. Siltstone, light gray (N7) in color is present in large bioturbation features and as thick laminations (with iron staining) in the upper 1/2. Mottling occurs in the lower 1/2 of the interval where greenish gray mudstone overlies olive black mudstone. The greenish gray mudstone is slightly calcareous. Pyritized spore casts (occasionally in concentrations), partially pyritized burrow structures (some oxidized) and disseminated pyrite occur in the olive black mudstones. A single fish scale is present at 1,807.8'.
1,809.8' - 1,817.6' (7.8')	Mudstones, olive black (5Y 2/1) and dark greenish gray (5G 4/1), thick bedded and thickly laminated to thin bedded. Disseminated mica occurs in the olive black mudstones at the lower 1/2. Pyrite is present as nodules, spore casts, burrow structures, isolated crystals, and in disseminated form throughout. Resinous spore bodies are present throughout. A single vitrinite fragment (~1 mm thick) occurs on the core edge at 1,811.65'.
1,817.6' - 1,827.6' (10.0')	Mudstones, dark greenish gray (5G 4/1) and olive black (5Y 2/1), thin bedded and thickly laminated to thin bedded, shaly in the lower 1/2. A slightly calcareous, thin siltstone bed, light gray (N7) in color occurs at 1,817.9'. Disseminated mica occurs in the olive black mudstones. Resinous spore bodies are present throughout. Pyrite occurs as disseminated grains and as mineralized spore bodies. An unidentified fossil fragment is present at 1,818.3' (bone or tooth?). A large pyritized burrow structure (1 cm thick) has a slickenlined circumference. A single carbonaceous fragment (2 mm x 6 mm) occurs at 1,821.9'.

<u>INTERVAL</u>	<u>DESCRIPTION</u>
1,827.6' - 1,834.9' (7.3')	Mudstones, olive black (5Y 2/1) and dark greenish gray (5G 4/1), thick bedded and thickly laminated to thin bedded. The dark greenish gray mudstones are thickly laminated to thin bedded in the upper 1/3; with some gradational contacts. The lower 2/3 is dominantly thick bedded olive black mudstone having sharp boundary contacts with the dark greenish gray mudstones. The olive black mudstones contain disseminated mica. Mottling (bioturbation) occasionally occurs where dark greenish gray mudstone overlies the olive black mudstone. Some of the gradational contacts contain disseminated pyrite. Pyrite is also present throughout as nodules (\approx 2-3 mm diam.), pyritized burrow structures, and spores. Resinous spore bodies (up to 1 mm diam.) are also present throughout. A vitrinite fragment (5 cm x core diam.) is present at 1,830.9' and contains subvertical, dolomite-filled fractures (1 mm wide x up to 8 mm long). Another vitrinite fragment (1 cm x core diam.) occurs at 1,832.2'. A calcareous zone (\approx 5 mm thick) occurs at 1,834.6' within a dark greenish gray mudstone lamination.
1,834.9' - 1,844.7' (9.8')	Mudstones, olive black (5Y 2/1), and dark greenish gray (5G 4/1), thick bedded and thickly laminated to thin bedded, shaly in the lower 1/3. The olive black mudstone is thick bedded and dominant in the upper 1/2. Thickly laminated to thin bedded dark greenish gray mudstones are dominant in the lower 1/2. Mottling (bioturbation) occasionally occurs where dark greenish gray mudstone overlies olive black mudstone. The olive black mudstone contains disseminated mica. Pyritized burrow structures and pyrite lenses are present in the olive black mudstone of the upper 1/2. Pyrite nodules appear in the mid-section. Vitrinite fragments are present at 1,835.8' (3 cm x core diam.) and 1,838.1' (1 cm x 6 cm). A silty ash (?) bed occurs at 1,841.9'.
1,844.9' - 1,853.1' (8.2')	Mudstones and argillaceous limestones, olive black (5Y 2/1), dark greenish gray (5G 4/1) and greenish gray (5G 6/1), thick bedded and thickly laminated to thin bedded, shaly in the upper 1/2. The olive black mudstone is thick bedded and contains dark greenish gray thick laminations in the upper 1/2, and dark greenish gray thick laminations and thin beds in the lower 1/2. A calcareous siltstone nodule, light gray (N7) in color and encased in pyrite, occurs at 1,838.5'. Disseminated mica and pyrite, and pyritized and resinous spore bodies occur throughout the olive black mudstone. Pyritized burrow structures (up to 15 mm diam.) occur in the lower 1/3; pyrite nodules are present throughout. A small pyrite lens at 1,846.1' contains slickenlines. A single <u>Foerstia</u> (5 mm diam.) occurs at 1,846.3'.

<u>INTERVAL</u>	<u>DESCRIPTION</u>
1,853.1' - 1,861.6' (8.5')	Mudstones and siltstones, dark greenish gray (5G 4/1), olive black (5Y 2/1) and light gray (N7), thickly laminated to thin bedded, shaly. The siltstone laminations and beds are cross-stratified and calcareous. One bed at 1,860.9' contains a concretionary growth. Erosion surfaces are present at 1,855.4' and 1,857.0' (siltstone bed overlying olive black mudstone) and at 1,860.9' (olive black mudstone overlying siltstone). Disseminated mica and pyrite nodules (some with slickenlined circumferences) occur throughout the olive black mudstones. Pyritized spores are present in the lower 1/3. Pyritized burrow structures are present in the lower 1/2. Vitrinite fragments occur at 1,856.3' (4 mm x 10 mm-woody?), 1,860.0' (1.5 cm x 7 cm, bark?), and 1,860.2' (2 cm x core diam, plant?).
1,861.6' - 1,870.6' (9.0')	Mudstones, calcareous mudstones and siltstones, olive black (5Y 2/1), dark greenish gray (5G 4/1), greenish gray (5G 6/1) and light gray (N7), thin bedded to thickly laminated, shaly. Disseminated mica occurs in the olive black mudstone. The calcareous mudstones occur as thin beds. The dark greenish gray mudstones are laminated and bedded within the olive black mudstones. Bioturbation occurs at these contacts in the upper 1/3 and in the thin greenish gray calcareous mudstone beds. A large (2 cm thick) pyritized bioturbation feature occurs at 1,862.5'. A sandy concretionary nodule, containing disseminated pyrite and isolated pyrite crystals and outlined by slickenlines is present at 1,867.7'. Pyritized burrow structures, and resinous and pyritized spores occur throughout.
1,870.6' - 1,879.4' (8.8')	Mudstones, olive black (5Y 2/1) and dark greenish gray (5G 4/1), thick bedded and thickly laminated. A single thin bed of siltstone, greenish gray (5G 6/1) in color is present at 1,870.9'. Mottling (bioturbation) occasionally occurs where dark greenish gray mudstone is laminated with the olive black mudstone. Disseminated mica occurs in the olive black mudstones. Resinous and pyritized spores and a sparse amount of carbonaceous fragments occur throughout. A vitrinite fragment (3 mm x 8 mm) occurs at 1,875.7'.

<u>INTERVAL</u>	<u>DESCRIPTION</u>
1,879.4' - 1,887.2' (7.8')	Mudstones and siltstones, olive black (5Y 2/1), dark greenish gray (5G 4/1) and light gray (N7), thick bedded and thickly laminated to thin bedded. The siltstone laminations and one thin bed of dark greenish gray mudstone are calcareous. Thick laminations and thin beds of dark greenish gray mudstone are confined to the mid-section. A large (6 cm diam.) mud lump occurs at 1,885.3'. Pyritized spore bodies are sparse throughout. Vitrinite fragments are present at 1,885.9' (4 mm x 8 mm) and 1,886.7' (2 cm x core diam.). Occasional pyrite nodules occur throughout.
1,887.2' - 1,894.5' (7.3')	Mudstones and calcareous mudstones, olive black (5Y 2/1) and greenish gray (5G 6/1), thick bedded and thickly laminated to thin bedded, shaly in the lower 1/2. Thin beds of greenish gray calcareous mudstone in the upper 1/2 become thick laminations in the lower 1/2. Mottling (bioturbation) is present at the lamination and bed boundaries where olive black mudstone is basal. The lower 1/2 contains pyrite nodules (≈5 mm diam.) and pyritized burrow structures.
1,894.5' - 1,902.2' (7.7')	Mudstones and siltstones, olive black (5Y 2/1), dark greenish gray (5G 4/1) and light greenish gray (5G 8/1), thick bedded and thickly laminated to thin bedded, shaly. Minor amounts of disseminated mica are present in the olive black mudstones. Pyritized spores occur at the olive black mudstone basal contacts.
1,902.2' - 1,911.9' (9.7')	Mudstones and siltstones, dark greenish gray (5G 4/1), olive black (5Y 2/1) and light gray (N7), thin bedded and thickly laminated. Thin siltstone laminations overlay the olive black mudstones. The olive black mudstones contain minor amounts of disseminated mica in the upper 2/3, and disseminated pyrite and pyritized burrow structures in or near each basal boundary. Pyritized spore bodies (some oxidized) occur throughout in lenses, and as lag deposits (currents ? at 1,904.1').
1,911.9' - 1,922.4' (10.5')	Mudstones and siltstones, olive black (5Y 2/1), dark greenish gray (5G 4/1) and light gray (N7), thin bedded and thickly laminated. A thin bed of calcareous mudstone, greenish gray (5G 6/1) in color is present between 1,920.5' and 1,921.2'. Mottling (bioturbation) occurs in the occasional siltstone laminations and at the dark greenish gray olive black mudstone contacts. Pyritized burrow structures and spores and gypsum-anhydrite (?) crystals occur throughout. A vitrinite fragment (4 cm x core diam.) is present at 1,914.5'.

<u>INTERVAL</u>	<u>DESCRIPTION</u>
1,922.4' - 1,931.6' (9.2')	Mudstones and calcareous mudstones, olive black (5Y 2/1) and greenish gray (5G 6/1), thick and thin bedded. The calcareous mudstone bed contains a sandy nodule-shaped inclusion, light gray (N7) in color. Disseminated mica and pyritized spores are present in the olive black mudstones. A single irregular pyrite nodule occurs at 1,927.4'. A single fish scale occurs at 1,927.5'.
1,931.6' - 1,940.6' (9.0')	Mudstones, calcareous-silty mudstones and siltstone, olive black (5Y 2/1), dark greenish gray (5G 4/1), greenish gray (5G 6/1) and light gray (N7), thin bedded and thickly laminated to thinly laminated. The only thin siltstone bed (1,939.3') is cross-stratified and calcareous. The dark greenish gray mudstone is laminated into the olive black mudstone. The calcareous-silty mudstone bed (1,937.6') contains a septarian nodule (8 cm diam.) with calcareous cemented fractures. Pyrite is present throughout as nodules, burrow-structure fillings and mineralized spore bodies. An inarticulate brachiopod cast occurs at 1,939.4'.
1,940.6' - 1,950.6' (10.0')	Mudstones and siltstones, olive black (5Y 2/1), dark greenish gray (5G 4/1) and light gray (N7), thick to thin bedded and thickly to thinly laminated, shaly. The olive black mudstones are thick bedded in the lower 1/2 and contain disseminated mica throughout. Mottling (bioturbation) between the dark greenish gray and olive black mudstone laminations and thin beds occurs in the upper and lower 1/4. These zones are slightly calcareous. Pyrite nodules (≈5 mm diam.) and resinous spore bodies are present throughout. A vitrinite lens (1 mm thick) is visible on the core edge at 1,944.3'.
1,950.6' - 1,958.0' (7.4')	Mudstones, silty mudstones and siltstones, olive black (5Y 2/1), dark greenish gray (5G 4/1) and light gray (N7), thick bedded, thickly laminated and thinly laminated, shaly. The upper 1/3 of the interval is olive black mudstone; the lower 2/3 is laminated dark greenish gray and olive black silty mudstone and light gray siltstone. A siltstone lamination at 1,953.0' is bioturbated. Mottling (bioturbation) occurs at the dark greenish gray-olive black contacts. Disseminated mica occurs throughout the olive black zones. Resinous spore bodies are present throughout. Pyritized burrow structures are confined to the lower 1/3. Vitrinite fragments occur at 1,953.3' (15 mm x 3 cm) and 1,953.9' (5 mm diam.).

<u>INTERVAL</u>	<u>DESCRIPTION</u>
1,958.0' - 1,967.0' (9.0')	Silty mudstones and mudstones, dark greenish gray (5G 4/1) and olive black (5Y 2/1), thick bedded and thickly laminated. The olive black mudstones contain disseminated mica. Mottling occurs in the dark greenish gray mudstones at its upper boundary in contact with olive black mudstone. Resinous spore bodies occur throughout.
1,967.0' - 1,975.6' (8.6')	Mudstones and siltstones, olive black (5Y 2/1), dark greenish gray (5G 4/1), and light gray (N7), thin bedded to thinly laminated. The thin siltstone laminations are calcareous. The dark greenish gray mudstones are thickly laminated in the upper 1/2 and thin bedded in the lower 1/2. Disseminated mica occurs in the olive black mudstone. Mottling at the dark greenish-gray and olive black (basal) contacts occurs in the upper 1/2. Pyrite nodules (5 to 10 mm diam.) with associated slickelined circumferences occur at 1,972.7' and 1,973.1'. Resinous spore bodies are present throughout.
1,975.6' - 1,984.1' (8.5')	Mudstones, olive black (5Y 2/1), thick bedded, shaly. Thin laminations of siltstone, light gray (N7) in color, occur in the lowest 1'. Disseminated mica is present within the mudstones throughout the interval. Resinous spore bodies occur throughout.
1,984.1' - 1,988.8' (4.7')	Calcareous mudstones and mudstones, greenish gray (5G 6/1) and olive black (5Y 2/1), thick bedded and thin bedded to thickly laminated. Mottling and oxidized pyrite burrow traces, primarily in the greenish gray calcareous mudstones, occur throughout. Pyritized burrow structures occur in the lowest 0.2'.
1,988.8' - 1,994.7' (5.9')	Mudstones, olive black (5Y 2/1), thick bedded, shaly. Thin siltstone laminations, light gray (N7) in color, occur at 1,990.7' and are calcareous. Disseminated mica occurs throughout the olive black mudstones. Minor amounts of resinous spore bodies are present throughout. A single vitrinite fragment (5 mm x 6 cm) occurs at 1,994.4'.
1,994.7' - 2,004.7' (10.0')	Mudstones, olive black (5Y 2/1) and dark greenish gray (5G 4/1), thick bedded and thickly laminated, shaly. Mottling is associated with the thick laminations of the dark greenish gray mudstone in the lower 1/2. Disseminated mica occurs throughout the olive black mudstones. Small pyritized burrow structures (1 mm diam.) occur throughout the olive black mudstones. Occasional pyrite nodules are present throughout. Minute vitrinite fragments and carbonaceous plant fragments occur throughout; some are coated with oxidized pyrite and contain calcite; some have a resinous appearance.

<u>INTERVAL</u>	<u>DESCRIPTION</u>
2,004.7' - 2,011.9' (7.2')	Mudstones, olive black (5Y 2/1), thick bedded, shaly. Thick laminations of dark greenish gray (5G 4/1) mudstone occur in the lower 1/2 and are calcareous and highly mottled. The olive black mudstones contain disseminated mica. Resinous spore bodies are present throughout. A vitrinite fragment (4 cm x core diam.) is present at 2,007.8'.
2,011.9' - 2,020.6' (8.7')	Calcareous mudstones and mudstones, greenish gray (5G 6/1) and olive black (5Y 2/1), thick to thin bedded. At 2,015.8' a thin bed of light greenish gray (5G 8/1) silty mudstone is present. Thin laminations of olive black mudstone occur in the upper 1/2. The interval is strongly mottled, providing gradational contacts throughout.
2,020.6' - 2,029.0' (8.4')	Mudstones, olive black (5Y 2/1) and dark greenish gray (5G 4/1), thin bedded to thickly laminated. Disseminated mica occurs in the olive black mudstones. Mottling occurs where dark greenish gray mudstone overlies olive black. Contacts are gradational in the upper and lower 1/4's. A single, distinct dark greenish gray thin bed occurs at 2,205.8'. A calcareous, sandy nodule is present at 2,021.2'. Resinous spore bodies are present in the lower 1/2. Pyrite nodules (≈3 mm diam.) encasing gypsum-anhydrite (?) occur at 2,201.0'. A layer of pyritized spore bodies is present at 2,024.6'; a possible pyritized fecal pellet occurs at 2,026.9'. Gypsum-anhydrite (?) is present at 2,025.9'.
2,029.0' - 2,039.8' (10.8')	Mudstones, olive black (5Y 2/1) and dark greenish gray (5G 4/1), thin bedded to thickly laminated, shaly. Mottling provides gradational contacts between alternating thin beds and thick laminations; occasional, fragmented thin laminations of olive black mudstone are present in the mottled zones. A sandy nodule (2 cm diam.) occurs at 2,037.6'. Pyritized burrow structures are present throughout. Resinous spore bodies occur in the lower 2/3. A single fish scale occurs at 2,032.4'; a single fish tooth at 2,030.9'. A vitrinite fragment (8 mm x 25 mm) is present at 2,029.8'. An inarticulate brachiopod, <u>Lingula</u> , is present at 2,038.9'.

<u>INTERVAL</u>	<u>DESCRIPTION</u>
2,039.8' - 2,049.9' (10.1')	Mudstones, olive black (5Y 2/1) and dark greenish gray (5G 4/1), thick bedded and thickly laminated. A thick slightly calcareous, highly mottled (bioturbation) dark greenish gray bed with olive black laminations occurs in the upper 1/2; this is reversed to a thick olive black bed with dark greenish gray laminations having sharp contacts in the lower 1/2. The lower instance is slightly mottled. An inarticulate brachiopod, <i>Lingula</i> , occurs at 2,040.1', 2,043.1', 2,045.4' and 2,048.2'. Disseminated mica occurs in the olive black zones. Vitrinite fragments occur throughout.
2,049.9' - 2,059.5' (9.6')	Mudstones, olive black (5Y 2/1) and dark greenish gray (5G 4/1), thin bedded to thickly laminated, shaly. Two thin laminations of siltstone and light gray (N7) in color, are calcareous. Thin beds of mottled dark greenish gray mudstone with gradational contacts and occasional fragments laminations of olive black are present in the upper 2/3. The olive black mudstones contain disseminated mica. Pyrite nodules (up to 15 mm diam.) and pyritized burrow structures (oxidized) are present in the upper 2/3.
2,059.5' - 2,063.9' (4.4')	Mudstones, olive black (5Y 2/1) and dark greenish gray (5G 4/1), thickly laminated and thin bedded, shaly. A thick lamination of siltstone, light gray (N7) in color, calcareous and iron-stained at its upper and lower contacts occurs in this interval. The dark greenish gray mudstone is highly mottled and contains fragmented laminations of olive black in the upper 1/2; sharp contacts dominate the lower 1/2. The olive black mudstones contain disseminated mica. A single pyrite nodule (5 mm x 2 cm) and a layer of pyritized spore bodies occur in the lower 2'.
2,064.0' - 2,075.0' (11.0')	Silty mudstones, mudstones, and siltstone, olive black (5Y 2/1), olive gray (5Y 4/1) and light olive gray (5Y 5/2) thinly laminated to thin bedded. The interval is predominantly olive black in color; numerous irregularly spaced gray bands, up to 0.6' thick are also present. The contacts are sharp with no evidence of scouring or deformation. Several siltstone laminae are present between 2,072.1' and 2,072.3'. Carbonaceous fragments and small pyrite nodules are very sparse throughout.

<u>INTERVAL</u>	<u>DESCRIPTION</u>
2,075.0' - 2,081.5' (6.5')	Silty mudstones and mudstones, olive black (5Y 2/1), olive gray (5Y 4/1) and greenish gray (5GY 6/1), thinly laminated to thin bedded. The core is comprised of alternate olive gray, greenish gray and olive black bands, varying in thickness up to 1.0'. The contacts are sharp with little or no evidence of burrowing or deformation. Pyrite occurs as sparse nodules and coatings on spore bodies in the black silty mudstones. One small vitrinite fragment is present at 2,039.5'.
2,081.5' - 2,091.3' (9.8')	Silty mudstones and mudstones, brownish black (5YR 2/1), olive gray (5Y 4/1) and greenish gray (5GY 6/1), thinly laminated to thin bedded. The interval is composed of alternate brownish black and olive gray laminae with numerous greenish gray laminae present in the upper and lower 2.0'. A greenish gray band also occurs between 2,087.8' and 2,087.9'. Pyrite is sparsely present as small waveform laminae and mineralized spore bodies (<u>Tasmanites</u> sp.). A <u>Lingula</u> sp. (2,083.6') and a possible carbonaceous fish scale (2,088.4') occur within the interval. A vitrinite fragment is present at 2,085.2'.
2,091.3' - 2,100.0' (8.7')	Silty mudstones and mudstones, brownish black (5YR 2/1), greenish gray (5GY 6/1), light olive gray (5Y 6/1) and dark gray (N3), thinly laminated to thin bedded. The core is comprised of irregularly spaced and alternately colored bands varying in thickness and up to 1.0' in length. A few contacts are sharp, the rest are indistinct, partially due to bioturbation and/or deformation. Both mud- and pyrite-filled burrows occur throughout. Pyrite is also present as waveform laminae, small nodules and mineralized spore bodies. Small carbonaceous plant fragments occur throughout, but are rare. Slightly calcareous zones up to 1.0' thick are present throughout.
2,100.0' - 2,110.0' (10.0')	Silty mudstones and mudstones, olive black (5Y 2/1), and greenish gray (5GY 6/1), thinly laminated to thin bedded. The upper 3.8' is predominantly greenish gray; olive black silty mudstone content increases in the lower 6.2'. Two thin greenish gray bands appear at 2,104.2' and 2,109.2'. Sparse pyrite nodules and laminae occur in the lower 6.2'. A zone containing resinous spore bodies (<u>Tasmanites</u> sp.) is present between 2,108.0' and 2,110.0'.

<u>INTERVAL</u>	<u>DESCRIPTION</u>
2,110.0' - 2,120.0' (10.0')	Silty mudstones and mudstones, olive black (5Y 2/1), brownish black (5YR 2/1) and greenish gray (5GY 6/1), thinly laminated to thin bedded. The core is comprised of alternate black and gray bands up to ~1.9' thick. Some of the color change contacts are sharp, with only sparse mud-filled burrows present. Carbonaceous plant fragments (throughout), a single fish scale (2,114.6') and a large vitrinite fragment (2,119.1') occur within the interval. Resinous spore bodies are present in the upper 5.0'. Pyrite occurs as isolated, mineralized spore bodies.
2,120.0' - 2,130.0' (10.0')	Silty mudstones, mudstones and siltstones, olive black (5Y 2/1), medium light gray (N6) and light olive gray (5Y 6/1) thinly laminated to thin bedded. The interval is composed of irregularly spaced, alternating black and gray zones, <0.1' thick. A light olive gray band, containing a few olive black laminae is present between 2,129.0' and 2,129.5'. A carbonaceous plant fragment occurs at 2,126.0'. Resinous spore bodies occur throughout the interval. Two small pyrite nodules are present at 2,120.2'. Numerous calcareous laminae occur throughout.
2,130.0' - 2,140.0' (10.0')	Silty mudstones, olive black (5Y 2/1) brownish black (5YR 2/1) and olive gray (5Y 4/1), thinly laminated to thin bedded. Both carbonaceous and vitrinitized plant fragments are found throughout. Pyrite occurs as waveform laminae, crystallized masses, nodules and as coatings on sparse spore bodies (<u>Tasmanites</u> sp.).
2,140.0' - 2,150.0' (10.0')	Silty mudstones and mudstones, brownish black (5YR 2/1), olive black (5Y 2/1) and olive gray (5Y 4/1), thinly to thickly laminated. The interval is comprised of distinct alternate black and gray bands of varying thickness. The contacts between these bands are occasionally mottled. Resinous spore bodies are found throughout the interval. Pyrite occurs as both horizontal and vertical burrow fillings, mineralized spore bodies, small nodules, thick waveform laminae, and laminae of disseminated grains. Isolated crystals of a moderate reddish orange (10R 6/6) mineral (stained gypsum?) are present at 2,140.2' and appear to be associated with a pyrite laminae. Both carbonaceous and vitrinitized fragments occur throughout the interval. A large (3 mm diam.) mud-filled burrow is present at 2,147.6'. Slightly calcareous zones, up to 1.0' thick, are present within the gray mudstones.

<u>INTERVAL</u>	<u>DESCRIPTION</u>
2,150.0' - 2,160.0' (10.0')	Silty mudstones and mudstones, light olive gray (5Y 5/2 and 5Y 6/1) olive gray (5Y 4/1) and brownish black (5YR 2/1), thinly laminated to thin bedded. The interval is comprised of irregularly spaced olive gray and brownish black bands occurring in the predominantly light olive gray silty mudstones and mudstones. The core is slightly mottled by bioturbation. The upper 2.0' contain brownish black zones. Two thin light olive gray calcareous bands (<10 cm) are present at 2,155.4' and 2,159.6'. Pyrite occurs as laminae of disseminated grains, mineralized spore bodies, and burrow fillings. Carbonaceous fragments are present, but rare. Calcareous silty mudstone bands, up to 1.0' thick, occur within the interval.
2,160.0' - 2,170.0' (10.0')	Silty mudstones and mudstones, greenish gray (5GY 6/1 and 5G 6/1), olive gray (5Y 4/1) and olive black (5Y 2/1), thinly laminated to thin bedded. The core contains irregularly spaced olive gray and brownish black laminae in the greenish gray silty mudstones and mudstones. Some of the color changes are gradational due to bioturbation. A few light olive gray (5Y 6/1) calcareous concretionary bands occur throughout the interval. Pyrite occurs primarily as a burrow filling or in sparse laminae of disseminated grains. Slightly calcareous zones, up to 1.0' thick, occur in several of the silty mudstones.
2,170.0' - 2,180.0' (10.0')	Silty mudstones and mudstones, greenish gray (5GY 6/1 and 5G 6/1), olive gray (5Y 4/1) and olive black (5Y 2/1), thinly to thickly laminated. The core is mottled and contains indistinct olive black laminae. A few calcareous concretionary bands occur within the interval. Pyrite occurs as burrow fillings, in laminae of disseminated grains and as a plant fragment replacement. Numerous mud-filled burrows are also present. Several of the silty mudstone laminae are slightly calcareous.
2,180.0' - 2,190.0' (10.0')	Silty mudstones, greenish gray (5GY 6/1 and 5G 6/1), light olive gray (5Y 6/1) and medium dark gray (N4), thinly laminated to thin bedded. The interval contains numerous medium dark gray laminae in the greenish gray silty mudstones within the upper 7.0'; the remainder of the interval is mottled. Pyrite is present as a burrow filling and as a plant fragment replacement. A single unidentified shell fragment occurs at 2,186.4'. Mud-filled burrows occur throughout. Sparse silty mudstone laminae are slightly calcareous in the lower 1/2.

<u>INTERVAL</u>	<u>DESCRIPTION</u>
2,190.0' - 2,200.0' (10.0')	Silty mudstones and mudstones, greenish gray (5GY 6/1 and 5G 6/1), medium dark gray (N4) and olive gray (5Y 4/1), thinly to thickly laminated. The interval is composed of greenish and olive gray silty mudstones and mudstones containing irregularly spaced medium dark gray laminae. The contacts between these color changes are indistinct, probably due to bioturbation. Both pyrite- and mud-filled burrows are present, the latter being more common. Iron staining (oxidized pyrite ?) surrounds some of the burrows.
2,200.0' - 2,210.0' (10.0')	Silty mudstones and mudstones, greenish gray (5GY 6/1 and 5G 6/1), light olive gray (5Y 4/1) and olive black (5Y 2/1), thinly laminated to thin bedded. The interval is comprised of greenish gray silty mudstones and mudstones within irregularly spaced olive black laminae dispersed throughout. These olive black laminae are more concentrated in the lower 1/2. Bioturbation and burrow structures occur throughout the interval. Pyrite is present in isolated laminae containing disseminated grains and as a burrow filling and plant fragment replacement. Thick silty mudstone laminae within the upper half are calcareous.
2,210.0' - 2,220.0' (10.0')	Silty mudstones, greenish gray (5GY 6/1 and 5G 6/1) and olive black (5Y 2/1), thinly to thickly laminated. The interval is predominantly greenish gray, with irregularly spaced olive black laminae throughout. Contacts are mottled due to bioturbation and burrowing. Numerous vitrinite fragments are present below 2,215.0'. Pyrite is present in the form of burrow fillings, plant fragment replacements and in sparse laminae of disseminated grains.
2,220.0' - 2,230.0' (10.0')	Silty mudstones and mudstones, greenish gray (5GY 6/1 and 5G 6/1) dark greenish gray (5GY 4/1) and olive black (5Y 2/1), thinly to thickly laminated and thin bedded. The upper half of the core is composed of alternating greenish gray and olive black laminae and bands, up to 0.4' in thickness. The upper half is mottled in appearance and mud-filled burrows are apparent. The lower half is a uniform dark greenish gray color with sparse olive black laminae occurring near the bottom. Pyrite is present as coatings on spore bodies (<i>Tasmanites</i> sp.) and burrow fillings, small nodules and some mineralized fragments are also present. Resinous spore bodies are present, but rare in the olive black zone. Slightly calcareous silty mudstone laminae occur in the lower 1/2.

<u>INTERVAL</u>	<u>DESCRIPTION</u>
2,230.0' - 2,240.0' (10.0')	Silty mudstones and mudstones, greenish gray (5GY 6/1 and 5G 6/1) dark greenish gray (5GY 4/1) and olive black (5Y 2/1), thinly to thickly laminated and thin bedded. The interval is comprised of irregularly spaced, greenish gray, dark greenish gray and olive black bands up to 0.8' thick. Some of the contacts are sharp, the remainder are mottled and indistinct. Pyrite occurs as a fragment replacement and as a coating on spore bodies. Some of these spores have been oxidized (2,235.5'); unoxidized resinous spores are also present. Calcareous silty mudstone laminae occur in zones up to 1.0' thick, throughout.
2,240.0' - 2,250.0' (10.0')	Silty mudstones and mudstones, dark greenish gray (5GY 4/1 and 5G 4/1), greenish gray (5GY 6/1 and 5G 6/1) and dark gray (N3), thinly laminated to thin bedded. The interval is composed of dark greenish and greenish gray silty mudstones and mudstones containing irregularly spaced dark gray laminae. A thin concentration of these laminae is present between 2,244.9' and 2,245.3'. Very sparse carbonaceous fragments are present throughout. Pyrite occurs as both a coating on spore bodies (<i>Tasmanites</i> sp.) and as mineralized fragments and burrow fillings. Several of the silty mudstones and mudstones are calcareous.
2,250.0' - 2,260.0' (10.0')	Silty mudstones and mudstones, dark greenish gray (5GY 4/1 and 5G 4/1) and dark gray (N3), thinly to thickly laminated and thin bedded. The core is comprised of greenish gray silty mudstones and mudstones with dark gray irregularly spaced laminae. A thin (<0.1') dark yellowish orange band (10YR 6/6) is also present at 2,254.0'. Burrows and bioturbation are present throughout, but occur primarily near the dark gray laminae. Pyrite is found as small nodules, burrow fillings, waveform laminae, mineralized plant fragments, and as a coating on spore bodies (some of which are oxidized). A carbonaceous wood fragment is present at 2,252.2'. Glauconite (?) traces occur within the interval, but are sparse. Numerous zones containing slightly calcareous silty mudstone laminae and up to 1.0' thick occur throughout.

<u>INTERVAL</u>	<u>DESCRIPTION</u>
2,260.0' - 2,270.0' (10.0')	Silty mudstones and mudstones, dark greenish gray (5GY 4/1 and 5G 4/1) and dark gray (N3), thinly laminated to thin bedded. The interval is composed of dark greenish gray silty mudstones and mudstones containing laminae of irregularly spaced dark gray silty mudstone. The contacts are indistinct due to burrowing. A thin, medium light gray (N6) calcareous concretionary band is present between 2,260.1' and 2,260.3'. Pyrite occurs as mineralization on oxidized spore bodies and plant fragments. A carbonaceous plant fragment, with dolomitized veins, occurs at 2,267.7'. The silty mudstone laminae contained within the interval are moderately calcareous.
2,270.0' - 2,280.0' (10.0')	Silty mudstones and mudstones, greenish gray (5G 6/1 and 5GY 6/1), dark gray (N3) and dark greenish gray (5GY 4/1), thinly to thickly laminated and thin bedded. The silty mudstones occur in irregularly spaced zones up to 1.0' thick. Color change contacts are indistinct, primarily due to burrowing and bioturbation. Pyrite occurs as burrow fillings, laminae of disseminated grains, sparse nodules and as a coating on spore bodies (<i>Tasmanites</i> sp.). Some resinous spore bodies are also present. Carbonaceous plant fragments are present, but rare. A vitrinite plant fragment, with dolomitic veins is present at 2,271.5'. Calcareous silty mudstone laminae occur throughout the interval.
2,280.0' - 2,290.0' (10.0')	Silty mudstones, mudstones and siltstones, dark greenish gray (5GY 4/1 and 5G 4/1), dark gray (N3) and brownish black (5Y 2/1), thin bedded to thickly laminated. The dark gray and brownish black mudstones occur as bands (<1.0' thick) and thinner laminae in the dark greenish gray silty mudstone. The color change contacts are relatively sharp, however heavy burrowing and bioturbation is found at some of the color interfaces. A calcite mineralized septarian concretion is present between 2,289.4' and 2,289.7'. Pyrite occurs as nodules, laminae of disseminated grains and as mineralized spore bodies and burrow fillings. Traces of glauconite (?) are predominantly present in the dark greenish gray mudstones. Slightly calcareous silty mudstone laminae occur within zones up to 1.0' thick, throughout.

<u>INTERVAL</u>	<u>DESCRIPTION</u>
2,290.0' - 2,300.0' (10.0')	Silty mudstones and mudstones, dark greenish gray (5GY 4/1 and 5G 4/1), brownish black (5YR 2/1) and light olive gray (5Y 5/2), thinly laminated to thin bedded. The interval is comprised of alternating dark greenish gray, brownish black and light olive gray bands. Color change contacts are relatively sharp, with some slight bioturbation present at the color interfaces. A yellowish gray (5Y 7/2) calcareous silty mudstone concretionary band is present from 2,299.3' to 2,299.5'. Burrows occur throughout the interval, the mud-filled burrows are mineralized with pyrite and anhydrite (?). Sparse unidentified fossils occur between 2,294.4' and 2,298.3'. A large (≈0.1') vitrinite plant fragment occurs at 2,291.6'. The silty mudstone laminae which occur in bands, <1.0' thick, are very slightly calcareous.
2,300.0' - 2,310.0' (10.0')	Silty mudstones and mudstones, greenish gray (5GY 6/1 and 5G 6/1), dark greenish gray (5GY 4/1) and dark gray (N3), thin bedded to thickly laminated. The dark gray silty mudstones occur as thin bands and are contained within the greenish and dark greenish gray silty mudstones and mudstones. The bands are up to 1.0' thick and approximately half of the color change contacts are indistinct due to slight bioturbation. Pyrite occurs as a burrow filling, in sparse laminae and as mineralized and oxidized spore bodies (<i>Tasmanites</i> sp.). Numerous mud-filled burrows are also present. The interval is slightly calcareous in zones (<1.0' thick) which contain predominantly silty mudstone.
2,310.0' - 2,320.0' (10.0')	Silty mudstones and mudstones, dark greenish gray (5G 4/1), greenish gray (5GY 6/1), olive gray (5Y 4/1) and dark gray (N3), thinly to thickly laminated and thick bedded. The interval is composed of irregularly spaced dark gray and olive gray bands (<2.0' thick) in the greenish and dark greenish gray silty mudstones and mudstones. The majority of the contacts between color changes are indistinct and mottled (bioturbation). Pyrite occurs as mineralized, very sparse spore bodies, burrow fillings and mineralization of plant fragments. Glauconite (?) is found as disseminated grains and burrow coatings. A pyrite mineralized vitrinite fragment is present at 2,310.8'. A few of the silty mudstone laminae are slightly calcareous.

<u>INTERVAL</u>	<u>DESCRIPTION</u>
2,320.0' - 2,334.4' (14.4')	Silty mudstones and mudstones, dark greenish gray (5GY 4/1 and 5G 4/1), greenish gray (5GY 6/1) and dark gray (N3), thinly laminated to thin bedded. The interval is comprised of irregularly spaced dark gray laminae in the greenish and dark greenish gray silty mudstones and mudstones. Contacts between color changes are relatively sharp, with a minor amount of bioturbation creating a slight mottled appearance. Glauconite- and pyrite-mineralized burrows and disseminated grains are present throughout. The thin silty mudstone laminae are weakly calcareous.
2,334.4' - 2,346.0' (11.6')	Silty mudstones and mudstones, grayish olive green (5GY 3/2), olive black (5Y 2/1) and dusky yellow green (5GY 5/2), thinly laminated to thin bedded. The grayish olive green and olive black mudstones occur as alternating colored laminae and bands (<.01' to 1.0' thick) with gradational contacts. The dusky yellow green mudstones are restricted to the upper 1.0'. Occasional horizontal mud-filled burrows (1 mm to 9 cm in length) are present in the light mudstones. A 1 cm thick zone of anhydrite-filled (?) burrows occurs at 2,343.7'. Slightly calcareous zones occur from 2,338.0' to 2,339.0' and from 2,342.0' to 2,344.0'.
2,346.0' - 2,357.0' (11.0')	Silty mudstones and mudstones, dark greenish gray (5GY 4/1), grayish olive green (5GY 3/2) and olive black (5Y 2/1), thinly laminated to thin bedded. The interval consists of alternating colored laminae and bands (<.01' to 1.5' thick) with a concentration of olive black laminae occurring from 2,351.0' to 2,352.6'. Contacts between colors are gradational due to slight bioturbation in the olive black zones. Numerous mud-filled burrows are present in the light zones. Pyrite occurs as a small lens at 2,348.6', and as burrow fillings in the lower 4.0'. The core is slightly to moderately calcareous from 2,347.5' to 2,349.3', and from 2,352.7' to 2,355.0'.

<u>INTERVAL</u>	<u>DESCRIPTION</u>
2,357.0' - 2,370.7' (13.7')	Silty mudstones and mudstones, dusky yellow green (5GY 5/2), olive black (5Y 2/1) and grayish olive green (5GY 3/2), thinly laminated to thin bedded. The interval is composed of alternating colored laminae and bands (<.01' to 1.5' thick) with gradational contacts. Occasional pyrite-filled burrows occur in the olive black zones. The light zones contain mud-, calcite-, and pyrite-filled burrows, and are occasionally iron-stained. A large vitrinite fragment (≈0.1' x core diam.) is present at 2,363.8'. Zones from 2,358.0' to 2,360.0' and from 2,364.2' to 2,367.0' are moderately calcareous.
2,370.7' - 2,380.1' (9.4')	Silty mudstones and mudstones, dusky yellow green (5GY 5/2), grayish olive green (5GY 3/2) and olive black (5Y 2/1), thinly laminated to thin bedded. The core is comprised of alternating colored laminae and bands (<.01' to 1.8' thick) with gradational contacts. Vertical and horizontal burrows (0.1 cm to 0.5 cm diam by 8 cm) occur throughout the interval. Pyrite is found in several forms: as burrow fillings, lenses, and as horizontal stringers. Calcite is found both as a concretion (<0.1' diam.) at 2,372.2' and as mineralization in a layer (<0.1' thick) of concentrated burrows at 2,373.1'. Traces of glauconite (?) are found between 2,376.0' and 2,377.0'. The interval is slightly calcareous.
2,380.1' - 2,391.1' (11.0')	Silty mudstones and mudstones, olive black (5Y 2/1), grayish olive green (5GY 3/2) and dusky yellow green (5GY 5/2), thinly laminated to thin bedded. The mudstones occur as alternating colored laminae and bands (<.01' to 1.1' thick) with gradational contacts. The gradational nature of the contacts is partially due to bioturbation. The near-vertical and horizontal burrows (3 mm to 5 mm diam. by 5 cm) which are present are both mud- and pyrite-filled; an anhydrite (?) filling occurs at 2,391.1'. Pyrite is also commonly present as lenses, nodules, and waveform laminae (2,388.8'). Occasional carbonaceous fossils occur throughout the interval. A carbonaceous woody plant fragment (8 mm diam by 1 cm) is found at 2,384.5'. Two large vitrinite fragments (2 cm diam. by 6 cm) and (25 mm diam. by 85 mm) occur at 2,385.0' and 2,386.4', respectively. The green zones from 2,382.6' to 2,383.6' and from 2,389.9' to 2,389.7' are slightly calcareous.

<u>INTERVAL</u>	<u>DESCRIPTION</u>
2,391.1' - 2,402.3' (11.2')	Silty mudstones and mudstones, grayish olive green (5GY 3/2), dusky yellow green (5GY 5/2) and olive black (5Y 2/1), thinly laminated to thin bedded. Alternating colored laminae and bands (<.01' to 2' thick) with gradational contacts (bioturbation) comprise this interval. A 3 cm thick pale olive (10Y 6/2) band also occurs within the interval at 2,392.3'. Vertical and horizontal burrows (2 mm to 5 mm diam. by 8 cm) containing mud, pyrite, and anhydrite (?) are common throughout. Pyrite also occurs as horizontal stringers, lenses, and nodules. Stringers of calcite are found at 2,392.7'. Two anhydrite-filled (?) concretions (7 mm diam. by 1 cm) occur at 2,396.5'. Numerous yellowish gray (5Y 7/2) calcareous concretionary lenses (avg. 1 cm diam by 4 cm) are found at 2,343.3'. The interval also contains two carbonaceous fossils at 2,398.0' and 2,400.4' and a rill mark (?) at 2,398.7'. One foot thick zones begin at 2,392.0', 2,396.0' and 2,401.0' and are slightly calcareous.
2,402.3' - 2,416.5' (14.2')	Silty mudstones and mudstones, grayish olive green (5GY 3/2), dusky yellow green (5GY 5/2) and olive black (5Y 2/1), thinly laminated to thin bedded. The interval consists of alternating colored zones (<.01' to 1.5' thick) with gradational contacts. The gradational nature of the contacts is partially due to bioturbation; only a few sharp contacts are present. Pyrite occurs commonly throughout the interval in various forms: as nodules, lenses, burrow fillings, and as laminae of disseminated grains. Near-vertical and horizontal mud- and anhydrite-(?) filled burrows are common throughout. A 1 cm thick dark yellowish orange (10YR 6/6) concretionary band is present at 2,408.6'. Sparse traces of glauconite (?) are found throughout this interval, but occur predominantly in the upper 7'. One foot zones at 2,406.7', 2,410.2' and 2,413.0', as well as a zone from 2,403.5' to 2,406.0' are slightly calcareous.

<u>INTERVAL</u>	<u>DESCRIPTION</u>
2,416.5' - 2,425.3' (8.8')	Silty mudstones, mudstones and siltstones, grayish olive green (5GY 3/2), dusky yellow green (5GY 5/2) and olive black (5Y 2/1), thinly laminated to thin bedded. The mudstones occur as alternating colored zones (<.01' to 1.7' thick). A dusky yellow green fine-grained siltstone bed extends from 2,417.5' to 2,419.3'. Contacts throughout the core are gradational, partially due to bioturbation. Numerous vertical and horizontal burrows (1 mm to 5 mm diam. by 3 cm) are present. These are predominantly mud- and pyrite-filled and are occasionally anhydrite-(?) filled; some iron staining is also present. Pyrite is also contained within the core as nodules and disseminated grains. Two carbonaceous plant fragments are present at 2,424.5'. A siltstone bed and the bottom 2 1/2' of the interval are slightly calcareous.
2,425.3' - 2,434.1' (8.8')	Silty mudstones and mudstones, dusky yellow green (5GY 5/2), grayish olive green (5GY 3/2) and brownish black (5YR 2/1), thinly laminated to thin bedded. The core is composed of alternating colored laminae and bands (<.01' to 1.5' thick) with a predominance of gradational contacts. A yellowish gray (5Y 8/1) band (5 cm thick) and concretion (3 cm diam. by 8 cm) occur at 2,431.6' and 2,427.3', respectively. A series of thick to thin dark yellowish orange (10YR 6/6) laminations are present from 2,428.4' to 2,428.7'. The numerous vertical and horizontal burrows (1 mm to 5 mm diam by 9 cm) found throughout this interval are commonly pyrite- and mud-filled and occasionally are anhydrite-filled (?). Pyrite. occurs in many forms: as horizontal stringers and disseminated grains throughout, and as waveform laminae at 2,429.2'. Vitrinized fossil fragments are present at 2,425.9' and 2,428.0'. Slightly to moderately calcareous zones extend from 2,426.5' to 2,428.0' and from 2,430' to 2,434.0'.

<u>INTERVAL</u>	<u>DESCRIPTION</u>
2,434.1' - 2,446.7' (12.6')	Silty mudstones and mudstones, grayish olive green (5GY 3/2) and olive black (5Y 2/1), thinly laminated to thin bedded. The interval is composed of alternating colored laminae and bands (<.01' to 1.5' thick) exhibiting gradational contacts, due in part to bioturbation. A highly calcareous light olive gray (5Y 6/1) concretion (6 cm diam. by 8 cm) extends from 2,438.4' to 2,438.7'; disturbed laminae from 2,438.2' to 2,439.0' encompass this concretion. Numerous vertical and horizontal burrows found throughout the interval are both mud- and pyrite-filled and are occasionally iron-stained (oxidized pyrite). Pyrite occurs in many forms: as lenses, nodules, disseminated grains, and as waveform laminae (2,438.5'). Pyritized shells of the cephalopod genus <u>Bactrites</u> (?) are present at 2,440.0' and 2,443.5'. Unidentified carbonaceous fossil fragments occur at 2,442.8' and 2,446.2'. A cast of an articulate brachiopod is present at 2,443.7'. This interval also contains vitrified plant fragments (5 mm diam. by 4 cm) at 2,440.7' and at 2,446.4'. The upper 6' of the interval, as well as a 2' zone 2,443.0' to 2,445.0', are slightly to moderately calcareous.
2,446.7' - 2,460.3' (13.6')	Mudstones, silty mudstones and siltstones, olive gray (5Y 4/1) and brownish black (5YR 2/1), thinly laminated to thin bedded. The mudstones occur as alternating colored laminae and bands (<.01' to 0.8' thick) with gradational contacts. Light olive gray (5Y 6/1), fine-grained siltstone occurs in a 0.1' thick bed at 2,454.4', and as a concretion (25 mm diam. by 55 mm) at 2,448.5'. A few small (≪0.1' diam.) siltstone concretions rimmed by pyrite and containing occasional anhydrite (?) crystals are found in a zone from 2,458.6' to 2,459.1'. Mud- and pyrite-filled sub-horizontal burrows (<1 mm to 4 mm diam. by 6 cm), occur throughout. Occasional iron-staining (oxidized pyrite ?) occurs around the burrows and the numerous pyritized plant fragments. Several carbonaceous plant fragments are found between 2,450.6' and 2,454.0'. A large vitrinite plant fragment with stained veins of anhydrite-dolomite (?) is located at 2,452.4'. Pyrite occurs in many forms: as nodules, lenses, disseminated grains, horizontal stringers (throughout) and as waveform laminae (2,454.8'). A pyritized cast of a coiled cephalopod occurs at 2,458.7'; a partially-pyritized shell of the cephalopod genus <u>Bactrites</u> (?) is present at 2,459.7'. A few articulate brachiopod casts are found within the bottom 3' of this interval. Except for the zone from 2,450' to 2,452', the entire interval is calcareous.

<u>INTERVAL</u>	<u>DESCRIPTION</u>
2,460.3' - 2,470.2' (9.9')	Silty mudstones, mudstones and siltstones, olive gray (5Y 4/1), brownish black (5YR 2/1) and grayish olive green (5GY 3/2), thinly laminated to thin bedded. This interval is composed of alternating colored laminae and bands (<.01' to 1.6' thick) with a predominance of sharp contacts. A 2 cm thick bed of light olive gray (5Y 6/1) siltstone is found at 2,463.6'. Disturbed laminae encompass a 15 mm diameter pyritic concretion, with anhydrite (?) crystals at its center (2,465.9'). Burrows are scarce, pyrite-filled and occasionally contain anhydrite (?) crystals. Pyrite also occurs as laminae of disseminated grains, waveform laminae, and nodules; these nodules are prevalent in the bottom 1' of the interval. A pyritized shell of the cephalopod genus <u>Bactrites</u> (?) is found at 2,461.9'. Numerous pyritized cephalopod casts (<0.4 cm diam.) of several different genera are found throughout this interval. A large cast (3 cm diam. by 4 cm) of the cephalopod genus <u>Tornoceras</u> (?) is present at 2,468.3'. Several articulate brachiopod casts, some of which are carbonaceous, are contained within this interval. A carbonaceous woody plant fragment occurs at 2,461.2'; pyritized plant fragments occur throughout. The zone from 2,463.3' to 2,464.5' and the bottom 2' of the interval are slightly calcareous.
2,470.2' - 2,483.2' (13.0')	Mudstones and siltstones, olive gray (5Y 4/1), brownish black (5YR 2/1) and light olive gray (5Y 6/1), thinly laminated to thin bedded. The mudstones occur as alternating colored laminae and bands. Sharp contacts occur between the thick (>0.4') bands, gradational contacts occur between the laminae. A highly calcareous, 0.9' thick, light olive gray, fine-grained siltstone bed is located from 2,475.4' to 2,476.3'. A series of dark yellowish orange (10YR 6/6) noncalcareous laminae, some of which are waveform and/or lenticular, occur between 2,478.2' and 2,482.0'. Occasional horizontal pyrite-filled burrows (2 mm to 5 mm diam. by 5 cm) occur throughout. Pyrite also occurs rarely as nodules, laminae, lenses, and disseminated grains. Numerous pyritized wood fragments and pyritized casts of coiled and straight cephalopod are present throughout. Numerous articulate brachiopods casts (<3 mm diam.) also occur throughout, the mold of a single large (15 mm diam. by 35 mm) articulate brachiopod is present at 2,473.9'. Slightly to moderately calcareous zones occur in the upper 2' of the interval and from 2,474.1' to 2,480.0'.

<u>INTERVAL</u>	<u>DESCRIPTION</u>
2,483.2' - 2,494.0' (10.8')	Mudstones and silty mudstones, olive gray (5Y 4/1) and brownish black (5YR 2/1), thinly laminated to thin bedded. The core is comprised of alternating colored laminae and bands (<.01' to 5.5' thick) with gradational contacts. Disturbed laminae encompass a siltstone concretion (65 mm diam.) at 2,491.0'. The outer edge of this concretion is composed of disseminated pyrite grains. Near-vertical to sub-horizontal pyritized burrows occur throughout, but are abundant only at the midsection. Waveform and/or lenticular pyrite laminae and disseminated pyrite grains also occur throughout. A single carbonaceous leaf (2 cm diam. by 35 mm) is present at 2,486.1'. Resin spore bodies are contained within the interval at 2,485.8'. The upper 6' of this interval are slightly to moderately calcareous.
2,494.0' - 2,502.0' (8.0')	Silty mudstones and mudstones, olive gray (5Y 4/1) and brownish black (5YR 2/1), thinly laminated to thin bedded. The mudstones occur as alternating colored laminae and bands (<.01' to 0.4' thick) with gradational contacts. Slight bioturbation and horizontal pyrite-filled burrows (3 mm diam. to 1 cm) occur throughout. Occasional pyritized, plant fragments and coiled cephalopods are also present. Pyrite is also present as disseminated grains, laminae and as a nodule (1 cm diam. by 3 cm in length) at 2,501.9'. The core between 2,495.0' and 2,498.9' is moderately calcareous.
2,502.0' - 2,513.2' (11.2')	Silty mudstones, mudstones and siltstones, brown black (5YR 2/1) and olive gray (5Y 4/1), thinly laminated to thin bedded. This interval is comprised of alternating colored laminae and bands (<.01' to 1.3' thick) with a predominance of sharp contacts. A highly calcareous septarian siltstone concretion (12 cm diam.) is located between 2,506.6' and 2,507.1' and is flanked by disturbed laminae. Pyrite is scattered throughout and occurs as laminae, disseminated grains, and nodules. A few carbonaceous fragments are found in the bottom 1/2 of the interval. A large vitrinite plant fragment with stained veins of anhydrite-dolomite (?) occurs at 2,512.3'.

<u>INTERVAL</u>	<u>DESCRIPTION</u>
2,513.2' - 2,520.8' (7.6')	Silty mudstones and mudstones, brownish black (5YR 2/1) and olive gray (5Y 4/1), thinly laminated to thin bedded. The mudstones occur as alternating colored bands and laminae (<.01' to 1.2' thick) with gradational contacts. Slight mottling is found within this interval. Mud- and pyrite-filled burrows are sparse. Pyrite occurs in several forms: as disseminated grains, a waveform laminae (3 mm thick) at 2,518.3', and as a lens with calcite veining at 2,515.4'. A few carbonaceous fragments are scattered throughout; spore resin bodies are found in the bottom 2'.
2,520.8' - 2,538.3' (17.5')	Silty mudstones, mudstones and siltstones, brownish black (5YR 2/1), olive gray (5Y 4/1) and light olive gray (5Y 5/2), thinly laminated to thin bedded. The brownish black and olive gray mudstones occur as bands and laminae (<.01' to 1.7' thick) with gradational contacts. A light olive gray, fine-grained siltstone concretion occurs between 2,533.2' and 2,534.0'; disturbed laminae, including calcite lenses encompass this concretion. Mottling is sparse, occasional horizontal pyritized burrows and carbonaceous fragments occur mainly within the bottom 2/3 of the interval. Pyrite also occurs as nodules and disseminated grains. A slightly calcareous mud clast (?) (1 cm diam.) is contained within the core at 2,531.8'. Fish scales are found at 2,537.0'.
2,539.8' - 2,545.2' (5.4')	Mudstones, brownish black (5YR 2/1) and olive black (5Y 2/1), thickly laminated to thin bedded. Pyrite is common throughout, occurring as nodules, lenses, and disseminated fine crystals. The pyrite nodules range in size from 2 to 10 mm; a 5 mm-thick laminae rich in pyrite occurs at 2,545.0'. Fossils are moderately abundant in this interval, carbonization is the primary mode of preservation. Several fish scales occur on a parting at 2,540.12'. A poorly preserved pelecypod (?) shell, 5 mm across, is present at 2,540.75'. A large carbonaceous plant fragment (1 cm x 8 cm) occurs at 2,541.7'. Small (2 to 3 mm wide) inarticulate brachiopod casts are distributed sparsely throughout.

<u>INTERVAL</u>	<u>DESCRIPTION</u>
2,545.2' - 2,553.9' (8.7')	Mudstones with a few thin siltstone laminae, olive black (5Y 2/1), brownish black (5YR 2/1) and dusky yellowish brown (10YR 2/1), thinly laminated to thin bedded. A thin lamina of micaceous ash (?) occurs at 2,547.3'; a clayey (bentonite ?) ash bed (?) light olive gray (5Y 5/2) in color, is present between 2,551.77' and 2,551.92'. Several thin laminae of the same material also occur directly above and below this bed. Minor amounts of pyrite are present in the interval, mainly as disseminated fine crystals and occasional 3 to 5 mm diam. nodules. A few pyrite lenses occur on a bedding plane at 2,555.3'. The interval is moderately fossiliferous. Casts of coiled cephalopods are present in the upper 1/2; a 1 cm wide individual occurs at 2,545.72'; a 25 mm wide individual is present at 2,546.2'. A single, 1 cm long pyritized inarticulate brachiopod shell (<u>Lingula</u> sp.) occurs at 2,545.5'. Two vitrinite fragments (25 mm x 9 cm) are present at 2,549.52'. A pyrite-coated vitrinite fragment (6 cm x 7 cm) occurs at 2,546.83'. Finely divided carbonaceous plant material is distributed sparsely throughout.
2,553.9' - 2,560.6' (6.7')	Mudstones, with a few thin siltstone laminae in the lower 1/2, brownish black (5YR 2/1), olive black (5Y 2/1) and olive gray (5Y 3/2), thinly laminated to thin bedded. Several subhorizontal, pyrite-filled burrow structures, 3 to 5 mm in diam. and about 2 cm in length occur throughout the lower 1/2. Vitrinitized fragments containing concentric ring structures (ridges) are present throughout. A 2 x 5 cm vitrinite fragment occurs at 2,558.72'; smaller fragments are present at 2,559.75' and 2,555.6'. A pyrite-coated vitrinite fragment, 3 mm x 4 cm occurs at 2,560.0'. A 2 mm thick lamina, rich in pyrite, is present at the base of the interval.
2,560.6' - 2,565.1' (4.5')	Mudstones, with a few thin siltstone laminae, olive black (5Y 2/1), olive gray (5Y 3/2) and light olive gray (5Y 5/2), thinly laminated to thin bedded. Pyrite is common throughout, occurring as thin laminae, occasional 3 to 5 mm diam. nodules, and irregular concentrations of 5 mm diam. nodules, and irregular concentrations of fine crystals. Subhorizontal, pyrite-filled burrow structures, 2 to 4 mm in diam. and extending the width of the core, are distributed sparsely throughout the darker zones. A pyrite-coated vitrinite fragment (5 cm x 6 cm) occurs at 2,561.17'. Smaller vitrinite fragments (1 to 3 cm across) containing concentric ring structures (ridges) are common throughout. A parting at 2,563.41' contains a concentration of these fragments, along with 1 to 4 mm long, permineralized inarticulate brachiopods (<u>Lingula</u> sp.) and a permineralized conodont (?).

<u>INTERVAL</u>	<u>DESCRIPTION</u>
2,565.1' - 2,569.0' (3.9')	Mudstones and argillaceous lime mudstone, olive black (5Y 2/1), olive gray (5Y 3/2, 5Y 4/1) and greenish gray (5GY 6/1), thinly laminated to thin bedded. A few irregular, discontinuous thin siltstone laminae are present throughout. Pyrite is common in this interval, occurring as lenses, nodules (3 to 6 mm in diam.) and irregular concentrations of fine crystals. Subhorizontal, pyrite-filled burrow structures, 2 to 5 mm in diam. and several cm long, occur throughout. The calcareous zones contain locally abundant, large subhorizontal burrow structures filled with dark mudstone. These burrow structures are approximately 1 cm in diam. and extend across the core. Fossils in this interval are limited to a few small carbonaceous plant fragments.
2,569.0' - 2,577.6' (8.6')	Mudstones, with a few siltstone laminae, olive black (5Y 2/1), dusky yellowish brown (10YR 2/1) and olive gray (5Y 3/2, 5Y 4/1), thinly laminated to thin bedded. The siltstone laminae are generally irregularly shaped and discontinuous across the core; several contain carbonate cement. A zone of moderate to strongly calcareous mudstone occurs from 2,571.0' to 2,572.0'. Irregular, laminae of pyrite are present throughout; pyrite also occurs as occasional 1 to 3 mm diam. nodules and as lens-shaped bodies within several of the siltstone laminae. A faint odor of kerogen is present on fresh surfaces throughout the interval. Subhorizontal, pyrite-filled burrow structures, 1 to 2 mm in diam. and 2 to 3 cm in length, are moderately abundant throughout the darker zones. Fossils are sparse in this interval and consist of a few 1 to 2 mm long inarticulate brachiopod casts (<u>Lingula</u> sp.), and carbonaceous spore bodies (<u>Tasmanites</u> sp.). The brachiopods occur sparsely throughout the lower 1/2; <u>Tasmanites</u> are present at 2,573.4' and 2,574.1'. A large vitrinite fragment occurs at 2,575.31'.

<u>INTERVAL</u>	<u>DESCRIPTION</u>
2,577.6' - 2,584.6' (7.0')	Mudstone with occasional siltstone laminae, olive black (5Y 2/1), olive gray (5Y 3/2, 5Y 4/1) and light olive gray (5Y 6/1), thinly laminated to thin bedded. The lighter zones are slightly to moderately calcareous; a few of the siltstone laminae contain carbonate cement. The light and dark mudstones are interbedded, giving the core a banded appearance; light mudstone predominates. Siltstone laminae are generally irregular and discontinuous across the core. Pyrite is common throughout, occurring as thin, wave-form laminae, disseminated fine crystals, and a few small nodules (1-3 mm diam.). A bed between 2,579.3' and 2,579.4' contains a concentration of small pyrite crystals. Subhorizontal, pyrite-filled burrow structures, less than 1 mm in diam. and several cm in length, occur infrequently throughout the darker zones. Fossils in this interval consist of a few thin (<1 mm) inarticulate brachiopod casts and moderately abundant carbonaceous plant fragments. Carbonaceous spores (<i>Tasmanites</i>) occur at 2,580.9'; a large vitrinite fragment coated with pyrite is present at 2,581.25'.
2,584.6' - 2,589.3' (4.7')	Mudstone, argillaceous lime wackestone, and siltstone, olive black (5Y 2/1), olive gray (5Y 4/1, 5Y 3/2), light olive gray (5Y 6/1) and medium light gray (N6), thinly laminated to thin bedded. The siltstone units are generally irregular and discontinuous across the core; most contain carbonate cement and fine laminae of darker mudstone. The lime wackestone is concentrated in thick laminae and thin beds in the lower 1/2, although most of the interval is moderately to strongly calcareous. Several subhorizontal, silt-filled burrow structures, 3 to 7 mm in diam. and several cm in length, occur in the mudstone units in the upper 1/2. Subhorizontal, pyrite-filled burrow structures, 1 to 2 mm in diam. and approximately 2 cm in length, are locally abundant throughout the darker mudstone units. Small, poorly preserved casts of inarticulate and articulate brachiopod casts occur sparsely throughout. A vitrinite fragment (5 mm x 20 mm) is present on a parting at 2,586.1'.

<u>INTERVAL</u>	<u>DESCRIPTION</u>
2,589.3' - 2,594.9' (5.6')	Mudstones, brownish black (5YR 2/1), thick bedded. Four thin, discontinuous siltstone laminae, olive gray (5Y 4/1) in color, are widely spaced throughout the interval. Pyrite commonly occurs as lenses, nodules (2 to 10 mm diam.) and disseminated fine crystals. Numerous small pyrite nodules, possibly fecal in origin, are present on partings at 2,591.85' and 2,593.72'. Resinous spore bodies (<i>Tasmanites</i>) are numerous throughout; a few carbonaceous plant fragments are also present.
2,594.9' - 2,602.9' (8.0')	Shaly mudstones, olive gray (5Y 3/2), thin bedded, moderately to strongly calcareous throughout. Although fissility is present throughout, it is much greater in the lower 1/2. Pyrite commonly occurs as nodules and irregular concentrations of fine crystals. Numerous pyrite nodules (=2 mm diam.) which are possibly fecal in origin are present on a parting at 2,595.77'. A large pyrite nodule (5 cm diam.) surrounded by slickensides occurs at 2,600.9'. Fossils are sparse throughout and consist of poorly preserved small articulate brachiopod casts, carbonaceous plant fragments and small (0.5 mm diam.) disc-shaped carbonaceous fragments, possibly a type of plant cyst. A vitrinite fragment coated with pyrite occurs at 2,600.1'.
2,602.9' - 2,608.8' (5.9')	Shaly mudstones, olive gray (5Y 3/2), thin bedded, moderately to strongly calcareous throughout. Pyrite is fairly common in the upper 1/2, occurring in lenses and as disseminated fine crystals. Pyrite is absent in the lower portion of the interval. Fossils occur sparsely throughout, and are generally restricted to isolated bedding planes. Calcite-permineralized, articulate brachiopod shell fragments occur on partings at 2,603.5' and 2,606.42'. A parting at 2,605.37' contains a hash of very finely divided, calcite-permineralized skeletal material. Carbonaceous plant fragments occur sparsely throughout. Unidentified, disc-shaped carbonaceous fragments, 0.5 mm in diam., are sparse throughout.

<u>INTERVAL</u>	<u>DESCRIPTION</u>
2,608.8' - 2,616.1' (7.3')	Shaly mudstones, olive gray (5Y 3/2), thin bedded, moderately to strongly calcareous. Subhorizontal, pyrite-filled burrow structures, less than 1 mm in diam. and about 1 cm in length, are distributed sparsely throughout. Disc-shaped carbonaceous fragments 0.5 mm in diam., are fairly common in the interval. A few carbonaceous plant fragments occur sparsely in the lower 1/2; one at 2,615.2' is coated with pyrite.
2,616.1' - 2,623.1' (7.0')	Shaly mudstones, olive gray (5Y 3/2), thin bedded, moderately to strongly calcareous. Pyrite-filled, subhorizontal burrow structures, less than 1 mm in diam. and about 1 cm in length, occur sparsely throughout. Occasional poorly preserved shell casts are present throughout; a large (3 cm) cast of an articulate brachiopod (?) occurs at 2,617.73'. Unidentified, disc-shaped carbonaceous objects, 0.5 mm in diam., are also present throughout. Pyrite-coated spores (<u>Tasmanites</u>) occur sparsely in the upper 1/2. Carbonaceous plant fragments, some coated with pyrite, are distributed sparsely throughout. Pyrite coated plant fragments occur at 2,620.63' and 2,620.90'.
2,623.1' - 2,629.6' (6.5')	Shaly mudstones, olive gray (5Y 3/2), thin bedded, moderately to strongly calcareous. Occasional, subhorizontal, pyrite-filled burrow structures, less than 1 mm in diam. and about 1 cm in length, occur throughout. A thin, wrinkled laminae of pyrite is present at 2,625.92'. Poorly preserved casts of unidentified shell fragments occur sparsely throughout. Plant fragments are fairly common in this interval. Casts of woody material occur at present at 2,627.7'. Carbonaceous disc-shaped fragments, 0.5 mm in diam., occur sparsely throughout, except in the lowest foot where they are locally abundant. Finely divided carbonaceous plant material is distributed sparsely throughout.
2,629.6' - 2,637.6' (8.0')	Shaly mudstones, olive gray (5Y 3/2), thin bedded, moderately to strongly calcareous throughout. Occasional pyrite nodules, 3 to 5 mm in diam. are present throughout the lower 1/2. A few small carbonaceous plant fragments and disc-shaped carbonaceous fragments, 0.5 mm in diam., are distributed sparsely throughout the interval.

<u>INTERVAL</u>	<u>DESCRIPTION</u>
2,637.6' - 2,644.8' (7.2')	Shaly mudstones, olive gray (5Y 3/2 and 5Y 4/1), thickly laminated to thin bedded. The interval is slightly to moderately calcareous. Pyrite occurs sparsely throughout as lenses, nodules (2 to 4 mm in diam.) and thin laminae; a prominent pyrite lamina is present at 2,644.17'. Spore bodies (<u>Tasmanites</u>) are moderately abundant throughout. Most of the spores are carbonaceous; a few are coated with pyrite. Disc-shaped carbonaceous fragments 0.5 mm in diameter, occur sparsely throughout. Pyritized shell and plant fragments are present in the lower 1/2; a pyritized coiled cephalopod shell occurs at 2,641.2'.
2,644.8' - 2,652.6' (7.8')	Shaly mudstones, olive gray (5Y 3/2) with a few thin bands of light olive gray (5Y 6/1). The interval is thickly laminated to thick bedded, strongly calcareous. A few pyrite lenses are present in the lower 1/2; occasional irregular concentrations of fine pyrite crystals occur throughout. Subhorizontal, pyrite-filled burrow structures, less than 1 mm in diam. and several cm in length, are distributed sparsely throughout. A few scattered carbonaceous plant fragments are present. Occasional, poorly preserved permineralized articulate brachiopods, less than 5 mm in size, occur sparsely throughout the lower 1/2. Carbonaceous spore bodies (<u>Tasmanites</u>) are locally abundant on a few partings.
2,652.6' - 2,658.7' (6.1')	Shaly mudstones, olive gray (5Y 3/2 and 5Y 4/1), thickly laminated to thin bedded. The interval is slightly to moderately calcareous. A few pyrite lenses are present in the upper 1/2; small pyrite nodules (<4 mm in diam.) are distributed sparsely throughout the lower 1/2. Occasional, subhorizontal, pyrite-filled burrow structures, less than 1 mm in diam. and several cm in length, are present throughout. Carbonaceous spore bodies (<u>Tasmanites</u>) occur throughout and are locally abundant on partings between 2,655.6' and 2,656.6'. Pyrite-coated <u>Tasmanites</u> are present at 2,657.4'. Disc-shaped carbonaceous fragments, 0.5 mm in diam., and carbonaceous plant fragments are distributed sparsely throughout.

<u>INTERVAL</u>	<u>DESCRIPTION</u>
2,658.7' - 2,665.0' (6.3')	Shaly mudstones, olive gray (5Y 3/2), thickly laminated to thin bedded. The interval is slightly to moderately calcareous. Pyrite occurs sparsely throughout. A pyrite nodule (1 cm diam.) with a coarsely crystalline dolomite center is present at 2,663.5'. Carbonaceous spore bodies (<u>Tasmanites</u>) are moderately abundant on several partings which are scattered throughout the interval. Disc-shaped carbonaceous bodies, 0.5 mm in diam., and poorly preserved casts of shell fragments occur sparsely in this interval. A cast of a plant fragment (2 mm x 5 cm) is present at 2,659.9'.
2,665.0' - 2,672.8' (7.8')	Shaly mudstones and mudstones, olive gray (5Y 3/2) darkening downcore to olive black (5Y 2/1), thickly laminated to thin bedded. The upper 1/2 is moderately to strongly calcareous; the lower 1/2 contains approximately equal numbers of calcareous and noncalcareous laminae. A few pyritic laminae occur throughout. Most of the fissility is present in the upper 1/2. Fossils are rare in the interval, consisting mainly of carbonaceous bodies, 0.5 mm in diam., which are moderately abundant on a few partings in the upper 1/2. Triangular, leaf-shaped carbonaceous fragments occur sparsely throughout; a large (1.5 cm x 2 cm) fragment of this type is present on a parting at 2,669.5'.
2,672.8' - 2,677.8' (5.0')	Mudstones, olive black (5Y 2/1), thick bedded, moderately calcareous throughout. A small amount of pyrite is present within the interval, occur as disseminated crystals and occasional small (<5 mm diam.) nodules. Fossils occur sparsely throughout and consist mainly of shell fragment casts and finely divided carbonaceous plant material. A few triangular, leaf-shaped carbonaceous objects, approximately 1 cm across, are present on several partings. Disc-shaped carbonaceous bodies, 0.5 mm in diam., occur infrequently in the interval. A deformed, poorly preserved pelecypod (?) cast displaying ribs, hinge line and a faint shell outline (5 cm x 5 cm) is present on a parting at 2,675.2'. A vitrinite fragment (2 cm x 6 cm) occurs at 2,676.75'.

<u>INTERVAL</u>	<u>DESCRIPTION</u>
2,677.8' - 2,683.1' (5.3')	Mudstones, olive black (5Y 2/1) lightening downcore to olive gray (5Y 3/2), thick bedded. The interval is noncalcareous in the upper 1/2, very slightly calcareous near the base. Pyrite is common throughout, occurring in lenses and as laminae and nodules. Numerous pyrite nodules, 1 to 5 mm in diam., are present on a parting at 2,677.82'; a large nodule (2 cm diam.) occurs at 2,678.0'. A slight to moderate kerogen odor is present on fresh surfaces throughout the interval. Fossils are rare, consisting of a few pyrite-coated carbonaceous plant fragment and unidentified, pyritized spine-shaped objects. The spine-like objects are generally less than 1 cm in length and occur on partings at 2,677.91' and 2,680.9'.
2,683.1' - 2,689.0' (5.9')	Mudstones, olive gray (5Y 3/2), thin bedded to thick bedded, moderately to strongly calcareous. A slight kerogen odor is present on fresh surfaces throughout. This interval is moderately fossiliferous, containing carbonaceous plant fragments and casts of shells. A faint cast of a 1 cm diam., coiled cephalopod occurs at 2,683.95'. Calcite permineralized spine-shaped objects, less than 1 cm in length, are abundant on a parting at 2,684.35'. A poorly preserved cast of a pelecypod (?) occurs at 2,684.97'; casts of inarticulate brachiopods (<u>Orbiouloidea</u> sp. ?) are present at 2,685.4'. Pyrite-coated spore bodies (<u>Tasmanites</u>) occur abundantly on a parting at 2,684.82'.
2,689.0' - 2,697.3' (8.3')	Mudstones with several thin beds of argillaceous lime mudstone, olive black (5Y 2/1) and olive gray (5Y 3/2, 5Y 4/1), thin to thick bedded. The interval is moderately to strongly calcareous. Argillaceous lime mudstone occurs at 2,689.0', 2,692.0', 2,692.4' and 2,696.0'. Occasional, thin pyritic laminae occur throughout; a few irregular concentrations of very fine pyrite crystals are distributed sparsely in the interval. A few pyritized spore bodies (<u>Tasmanites</u>) occur on a parting at 2,691.58'. A faint kerogen odor is present on fresh surfaces throughout.

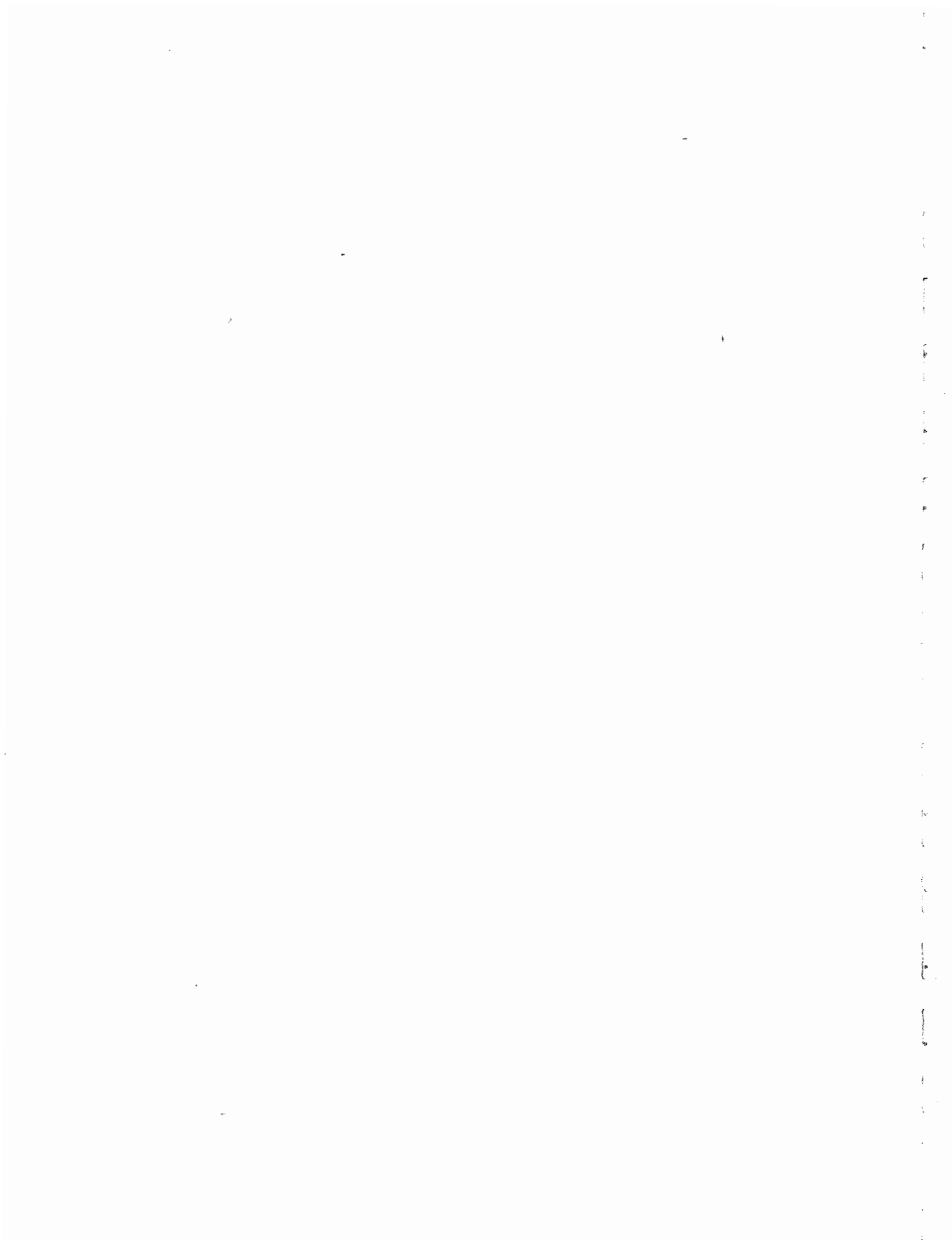
<u>INTERVAL</u>	<u>DESCRIPTION</u>
2,697.3' - 2,705.4' (8.1')	Mudstones, olive black (5Y 2/1), thick bedded. The interval is moderately calcareous at the top; carbonate content decreases down core. The portion of the interval below 2,703.5' is noncalcareous. A faint kerogen odor is present on fresh surfaces throughout. A pyrite nodule (1 cm diam.) occurs at 2,702.85'; a similar nodule (7 mm diam.) at 2,704.21' is surrounded by a halo of disseminated crystals. Very fine pyrite crystals occurring in irregular concentrations are distributed sparsely throughout. A parting at 2,705.3' contains very abundant permineralized conodonts; the remainder of the interval is barren of fossils.
2,705.4' - 2,707.1' (1.7')	Calcareous mudstone and argillaceous lime mudstone, olive black (5Y 2/1), olive gray (5Y 3/2) and medium dark gray (N4), thinly laminated to thin bedded. Pyrite laminae and lenses are common between 2,705.4' and 2,705.9'. Subhorizontal burrow structures, filled with pyrite or lime mudstone, occur between 2,705.8' and 2,706.1'. These burrow structures range in diameter from 5 mm to 10 mm and are several cm in length. A few calcite-permineralized shell fragments are present in a tightly cemented zone from 2,705.6' to 2,705.1', and are only visible edge-on. This interval comprises a transitional zone from the underlying limestone to the overlying shales and mudstones.
2,707.1' - 2,710.2' (3.1')	Lime mudstone and wackestone, medium gray (N5) and brownish gray (5YR 4/1), thickly laminated to thin bedded. The core between 2,707.1' and 2,707.6' is highly micaceous, containing numerous flakes of biotite. Pyrite lenses and nodules (≈5 mm diam.) are present in the upper 1/2 of the interval. Argillaceous laminae occur at 2,708.8' and 2,709.2'. Subhorizontal, lime-filled burrow structures, 2 mm to 5 mm in diameter and several cm long, are abundant throughout. Permineralized articulate brachiopod shells and unidentified shell fragments are common throughout.

A P P E N D I X B

SYMBOLS, TERMS, AND ABBREVIATIONS USED

IN FRACTURE LOGGING

EGSP-OHIO #7 WELL - TRUMBULL COUNTY



Appendix B

1. CHARACTER: Specifically, the character of the fracture plane.
 - (P): Planar
 - (CP): Curvilinear

2. FRACTURE TYPE: These terms are used to classify the different types of fractures into genetic groups.
 - (N): Natural
 - Spl. Jt. (Simple Joint): One discrete fracture plane, no displacement.
 - Cpd. Jt. (Compound Joint): Two or more parallel, closely spaced (approximately 1 cm or less) fracture planes, no displacement.
 - Flt. (Fault): A shear fracture with demonstrable displacement indicated by displaced primary features or slickensides.
 - Mcr. Flt. (Micro-Fault): A small-scale shear fracture, generally curvilinear; of the same order of size as the core diameter.
 - (CI): Coring Induced
 - PF (Petal Fracture): An oblique fracture, usually planar or slightly curvilinear, which originates at the core margin and terminates against bedding within the core.
 - PFC (Petal-Centerline Fracture): A fracture originating as a petal fracture which curves down-core and bisects the core as a vertical planar fracture. The strike of the vertical fracture and the petal fracture is identical. The face of the vertical fracture is characterized by regularly spaced arrest lines, convex down-core and symmetrical about the core axis.
 - DF (Disc Fracture): A subhorizontal fracture originating within the core and displaying hackle plumes radiating from the fracture origin to meet the core margin orthogonally.

TF	(Torsional Fracture): A spiraling or irregular fracture developed when a couple is applied to the core.
DCS	(Disc Fracture with Circular Slickensides): A feature induced by coupling of the inner and outer core barrels, causing core in the barrel to rotate against a stationary core stump.
KES	(Knife Edge Spall): A fracture, typically conchoidal, formed by scribe knives cutting orientation grooves into the core. This fracture type can be used to determine the down-core direction and the relative age of induced fractures.
CBS	(Core Bit Spall): A tiny conchoidal fracture caused by a diamond from the core bit plucking a chip off the edge of a preexisting fracture. When the face of the preexisting fracture is viewed with the core in normal position the spalls should appear along the right-hand margin. This fracture type is useful in inferring relative fracture chronology.

3. FRACTOGRAPHIC FEATURES:

Org.	(Fracture Origin): A discrete fracture surface irregularity from which hackles originate. Fractures may originate at the boundaries of fossils, concretions, preexisting fractures, etc.
Hkl.	(Hackle): A linear marking on a fracture face, similar to a striation, which trends in the direction of fracture propagation. Hackles radiate away from the origin, are perpendicular to arrest lines, and will curve to meet preexisting surfaces orthogonally.
Fn. Hkl. Plm.	(Fine Hackle Plume): A very fine, wispy plumose structure on an otherwise featureless fracture face.
Inc. Hkl.	(Inclusion Hackle): A hackle trailing an inclusion or obstacle on the fracture plane.
Cs. Tw. Hkl.	(Coarse Twist Hackle): A hackle composed of discrete steps generally appearing as a fringe near the edge of a fracture face.
Ar. Ln.	(Arrest Line): A crescentic feature with a cusp-like profile which marks the still stand of the fracture front. Two types are noted: Term. Ar. Ln.: Terminal Arrest Lines. Int. Ar. Ln.: Intermediate Arrest Lines.

Hk.

(Hook): The curving of a fracture plane to adjust to a change in the stress field orientation. Fractures hook to meet preexisting free surfaces orthogonally and in the vicinity of the neutral axis developed in bending.

4. TERMINATIONS: These terms are used to describe how a fracture terminates. The upper entry depicts the upper termination, the lower entry depicts the lower.

M:

The fracture exits the margin of the core.



A subhorizontal fracture that exits the margin of the core. This symbol is entered only once straddling the dividing line.



A fracture that terminates within the core as a dying hairline fracture.



The upper and lower extents of the fracture die out within the core. This symbol is drawn straddling the dividing line.

?:

Missing or disrupted core prohibits observation of the mode of termination.

?/M:

Same as above, but the fracture probably exits the core margin.

?/ (C):

Same as above, but the fracture probably terminates within the core margin.

BDG:

The fracture terminates along a conspicuous bedding plane indicating an abrupt change in lithology.

TAL:

The fracture terminates as a terminal arrest line which is visible only on the fracture face.



The fracture terminates in a terminal arrest line so that the fracture enters one side of the core but does not exit the other. This symbol is entered only once straddling the dividing line.

F22:

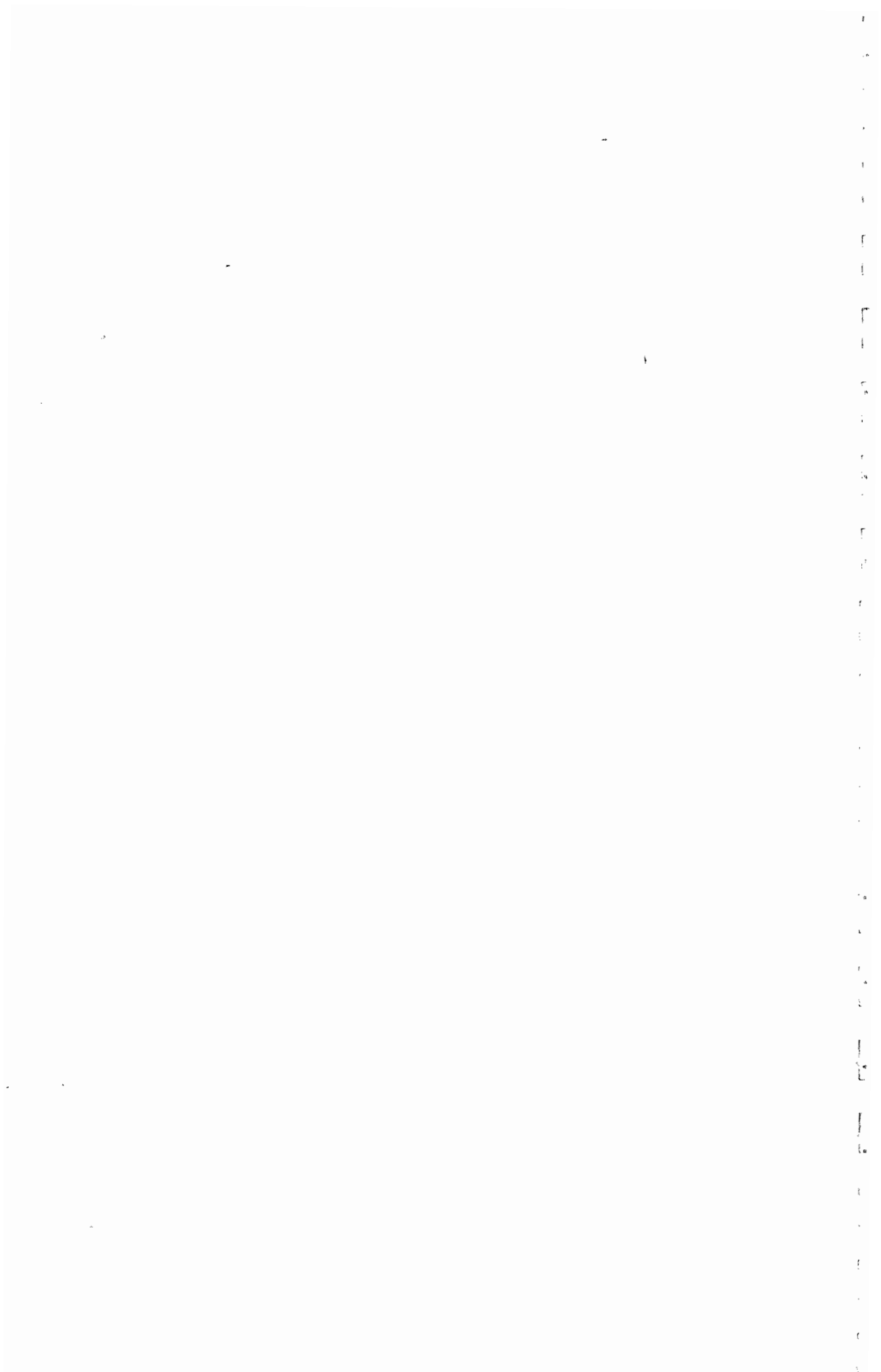
This symbol is used when one fracture terminates against another (i.e., fracture 23 terminates against fracture 22).

1
2
3
4
5
6
7
8
9
10
11
12
13
14
15
16
17
18
19
20
21
22
23
24
25
26
27
28
29
30
31
32
33
34
35
36
37
38
39
40
41
42
43
44
45
46
47
48
49
50
51
52
53
54
55
56
57
58
59
60
61
62
63
64
65
66
67
68
69
70
71
72
73
74
75
76
77
78
79
80
81
82
83
84
85
86
87
88
89
90
91
92
93
94
95
96
97
98
99
100

A P P E N D I X C

FRACTURE LOGS

EGSP-OHIO #7 WELL - TRUMBULL COUNTY



CORING DATE: <u>Sept. 1979</u>		EG.S.P. REVISED FRACTURE LOGGING FORMAT				PAGE <u>1</u> OF <u>2</u>		NATURAL FRACTURES			
LOG DATE: <u>June 1980</u>		WELL: <u>OH #7 Trumbull County</u>									
DEPTH NUMBER	EXTENT	LENGTH	LITHOLOGY	TERMINATIONS	CHARACTER	STRIKE DIP	FRACTURE TYPE	MINERALIZATION	SLICK- ENDSIDES	FRACTOGRAPHIC FEATURES	COMMENTS
1	1587.0 1589.6	2.6'	MDST. SLTST (5G-4H) (N7)	M BDG	P	N38°W ~90°	FILT	Gypsum- ANHYDRITE	PRESENT	FN.HKL.PLM., TAL, CS.TW.HKL.	OPEN; PROPAGATION: SE TO NW; MINERALIZATION IS SLICKENSIDED
2	1587.5 1591.1	3.6'		↗	P	N40°W ~90°	FILT		PRESENT	FN.HKL.PLM.	OPEN; PROPAGATION: SE TO NW
3	1587.0 1587.4	0.4'		↗	P	N42°W ~90°	FILT		PRESENT		CLOSED
4	1591.6 1592.2	0.6'	SLTY. MDST. (5G-4H) SLTST. BED. (N7)	M →	P	N44°W ~90°	SPLTJT			CS.TW.HKL., FN.HKL.PLM.	CLOSED
5	1591.9 1592.0	0.1'	SLTY. MDST. (5G-4H)	→	P	N78°W 60°SW	SPLTJT				CLOSED
6	1592.8 1593.7	0.9'		M →	P	N42°W ~90°	FILT		PRESENT	FN.HKL.PLM.	PROPAGATION: SE TO NW
7	1593.7 1594.5	0.8'		↗	P	N47°W ~90°	FILT		PRESENT	FN.HKL.PLM.	MINERALIZATION IS SLICKENSIDED
8	1592.9 1594.7	1.8'		↗	P	N42°W ~90°	FILT		PRESENT		CLOSED
9	1728.6 1728.7	0.1'		↗	CP	N73°W 48°NE	MCRELT		65° N77°E		SLICKS OCCUR IN BIOTURBATED AREA OF MDST.
10	1841.2		SLTST. (N7)	M →	CP	N59°E 18°NW	MCRELT		15° N38°W		
11	1818.3		MDST. (5G-4H)	↗	CP	N34°E 15°NW	MCRELT		17° N58°W		SLICKENLINES ASSOCIATED WITH PYRITTED BURROWS
12	1846.1		MDST. (5Y-2H)	M →	CP	—	MCRELT		PRESENT		FRACTURE ASSOCIATED WITH PYRITE NODULES
13	1849.6 1849.7	0.1'	LS. (5G-6H)	M →	CP	N15°E ~25°NW	FILT?		PRESENT SEE COMMENTS		FAULT HAS TWO TEND DIRECTIONS AT RIGHT ANGLES TO EACH OTHER: N77W & N25E
14	1867.7 1867.8	0.1'	MDST. (5Y-2H)	↗	CP	—	MCRELT		PRESENT		SLICKS ASSOC. W/ SAND NODULE
15	1892.1			↗	CP	—	MCRELT		PRESENT		SLICKS ASSOC. W/ PYRITE NODULES
16	1972.7			M →	CP	—	MCRELT		PRESENT		
17	1973.1			M →	CP	—	MCRELT		PRESENT		

CORING DATE: Sept. 1979		EGSP REVISED FRACTURE LOGGING FORMAT					PAGE 2 OF 2				
LOG DATE: June 1980		WELL: OH #7 Trumbull County									
		NATURAL FRACTURES									
NUMBER	DEPTH EXTENT	LENGTH	LITHOLOGY	TERMINATIONS	CHARACTER	STRIKE DIP	FRACTURE TYPE	MINERALIZATION	SLICKENSIDES	FRACTOGRAPHIC FEATURES	COMMENTS
18	2141.3		MDST., (SY ² /I)	M →	CP	---	MCREFT		PRESENT		
19	2289.4 2289.6	0.2'	L.S. CONCRETION, (56-6%)	↗	CP	---	MCREFT		PRESENT		SLICKENSIDES ASSOCIATED WITH L.S. SEPTARIAN CONCRETION
20	2419.2 2419.3	0.1'	LIMEY MDST., (56-6%)	↗	CP	---	MCREFT		PRESENT		SLICKENSIDES ASSOCIATED WITH PYRITE LENSES
21	2491.1 2491.2	0.1'	MDST., (SY ² /I)	M	CP	---	MCREFT		PRESENT		SLICKENSIDES ASSOCIATED WITH SAND NODULES
22	2506.7 2506.8	0.1'	SEPTARIAN NODULE	M →	CP	N80°E 60°NW	MCREFT		NBS'U PRESENT		SLICKENSIDES ASSOCIATED WITH SEPTARIAN CONCRETION
23	2510.9		MDST., (SY ² /I)	↗	CP	---	MCREFT		PRESENT		SLICKENSIDES ASSOCIATED WITH PYRITE NODULE
24	2531.8			↗	CP	---	MCREFT				
25	2534.4 2535.2	0.8'		↗	P	N63°U ~90°	FLT	CALCITE	0° N63°U		PROPAGATION: SE TO NW

CORING DATE: Sept. 1979										E.G.S.P. REVISED FRACTURE LOGGING FORMAT										PAGE 1 OF 5	
LOG DATE: June 1980										WELL: OH #7 Trumbull County										CORING INDUCED FRACTURES	
NUMBER	DEPTH EXTENT	LENGTH	LITHOLOGY	TERMINATIONS	CHARACTER	STRIKE DIP	FRACTURE TYPE	MINERALIZATION	SLICKENSIDES	FRACTOGRAPHIC FEATURES	COMMENTS										
1	1506.9 1507.0	0.1'	MDST. (5Y ^{3/2})	M BDG	CP	N48°E VARIABLE SE	HK														
2	1526.6 1526.7	0.1'	MDST. (56Y ^{5/6})	M BDG	CP	N48°E 41°NW	PF														
3	1526.6 1526.7	0.1'	↓	M BDG	CP	N50°E 44°SE	PF														
4	1529.1 1529.2	0.1'	↓	BDG M	CP	N65°E VARIABLE	HK														
5	1541.6 1541.8	0.2'	MDST. (5Y ^{3/2})	M BDG	CP	N46°E VARIABLE NW	HK														
6	1546.6 1546.8	0.2'	↓	M BDG	CP		HK														
7	1548.4 1548.5	0.1'	↓	M BDG	CP	N50°E 85°NW	HK														
8	1548.5 1548.6	0.1'	↓	M →	CP	N53°E 70°SE	PF														
9	1548.8 1548.9	0.1'	↓	M →	CP	N42°E 55°SE	PF														
10	1551.9 1552.1	0.2'	MDST. SLTST. (5G ^{4/1}) (N7)	M →	CP	N58°E 35°NW	PF														
11	1551.9 1552.1	0.2'	↓	M →	CP	N58°E 35°NW	PF														
12	1552.1 1552.2	0.1'	MDST. (5G ^{4/1})	BDG M	CP	N73°E 45°NW	HK														
13	1553.0 1553.1	0.1'	MDST. SLTST. (5G ^{4/1}) (N7)	BDG M	CP		TF														
14	1553.2 1553.3	0.1'	MDST. (5G ^{4/1})	M BDG	CP	N44°E 45°SE	PF														
15	1556.4 1556.5	0.1'	↓	M BDG	CP	N57°E 60°	PF														
16	1556.4 1556.5	0.1'	↓	M BDG	CP	N57°E 60°	PF														
17	1557.0 1557.1	0.1'	↓	↗	P	N43°E ~90°	SEE COMMENTS			ITAL., EN. HKL. PLM.	(PROPAGATION: NE TO SW) (CLOSED HALF OF HAIRLINE FRACTURE OF INDETERMINATE ORIGIN)										

EG.S.P REVISED FRACTURE LOGGING FORMAT

CORING DATE: Sept. 1979
 LOG DATE: June 1980

WELL: OH #7 Trumbull County

PAGE 2 OF 5
 CORING INDUCED FRACTURES

NUMBER	DEPTH EXTENT	LENGTH	LITHOLOGY	TERMINATIONS	CHARACTER	STRIKE DIP	FRACTURE TYPE	MINERALIZATION	SLICK-ENSIDES	FRACTOGRAPHIC FEATURES	COMMENTS
18	1557.0 1557.1	0.1'	MDST. (SG-4/1)	M F.17	CP	N43°E 15°NW	PF				
19	1558.4 1558.5 1558.4 1558.5	0.1'		↗	P	N40°E ~90°	SEE COMMENTS				CLOSED ; HAIRLINE FRACTURE- INDETERMINATE ORIGIN
20	1559.4 1559.5	0.1'		M BDG	CP	N40°E 16°NW	HK				
21	1559.5 1559.7	0.1'	MDST. SLTST. (SG-4/1) (N3)	M BDG	CP	N47°E 12°NW	HK				
22	1560.2 1560.3	0.1'	MDST. (SG-4/1)	M BDG	CP	N30°E 85°NW	HK				
23	1578.0 1578.2	0.2'		⊕	CP		KFS				
24	1581.7 1581.4	0.2'	MDST. (SG-4/1)	M BDG	CP	N40°E 16°NW	HK				
25	1581.3 1581.4	0.1'		M BDG	CP	N68°E 16°SE	HK				
26	1582.9 1583.1	0.2'	MDST. SLTST. (SG-4/1) (N3)	M →	CP	N76°E 35°	PF				
27	1582.9 1583.1	0.2'		M →	CP	N76°E 35°	PF				
28	1595.7 1595.9	0.2'	MDST. (SG-4/1)	BDG M	CP	N41°E ~90°	HK				
29	1596.4 1596.6	0.2'		BDG M	CP	N34°E ~90°	HK				
30	1597.5 1597.7	0.2'	MDST. SLTST. (SG-4/1) (N3)	⊕	CP		TF				
31	1598.8 1598.9	0.1'	MDST. (SG-4/1)	↗	CP	N38°E ~90°	SEE COMMENTS				HAIRLINE FRACTURE ; INDETERMINATE ORIGIN
32	1602.1 1602.2	0.1'		BDG →	CP	N58°E ~90°	SEE COMMENTS				
33	1615.3 1615.4	0.1'	MDST. (SG-4/1) (SY 2/1)	M BDG	CP	N52°E 10°SE	PF				
34	1615.3 1615.5	0.1'		M →	P	N54°E 50°	PF				

CORING DATE: Sept. 1979		E.G.S.P. REVISED FRACTURE LOGGING FORMAT										PAGE 3 OF 5	
LOG DATE: June 1980		WELL: OH #7 Trumbull County										CORING INDUCED FRACTURES	
W.P. #	DEPTH EXTENT	LENGTH	LITHOLOGY	TERMINATIONS	CHARACTER	STRIKE DIP	FRACTURE TYPE	MINERALIZATION	SLICKENSIDES	FRACTOGRAPHIC FEATURES	COMMENTS		
35	1619.4 1619.5	0.1'	MDSL. (56-4/1)	M BDG	CP	N65°E 60°SE	PF						
36	1619.4 1619.5	0.1'		M BDG	CP	N61°E 45°NW	PF						
37	1621.8 1622.0	0.2'	↓	M BDG	CP	N50°E 42°SE	PF						
38	1626.5 1626.6	0.1'	MDSL. (58-2/1)	M BDG	CP	N53°E 60°SE	PF						
39	1628.0 1628.1	0.1'	MDSL. SLIST. (56-4/1) (N3)	M BDG	CP	N34°E 45°SE	PF						
40	1628.0 1628.1	0.1'		M BDG	CP	N39°E 55°NW	PF						
41	1633.5 1633.7	0.2'		M BDG	CP	N50°E 40°SE	HK						
42	1633.5 1633.7	0.2'	↓	M BDG	CP	N13°E ~90°	HK						
43	1619.0 1619.3	0.3'	MDSL. (56-4/1)	BDG M	CP	N55°E ~90°	HK						
44	1649.3 1649.4	0.1'		M BDG	CP	N70°E 55°SE	PF						
45	1649.3 1649.4	0.1'		M BDG	CP	N146°E ~90°	HK						
46	1661.8 1661.9	0.1'		M BDG	CP	N41°E 25°NW	PF						
47	1661.8 1661.9	0.1'		M BDG	CP	N51°E 45°SE	PF						
48	1664.8 1664.9	0.1'		M BDG	CP	N55°E 60°NW	PF						
49	1664.8 1664.9	0.1'		M BDG	CP	N53°E 45°SE	PF						
50	1676.4			⊕ BDG	CP		DCS						
51	1677.7 1677.8	0.1'	↓	M BDG	CP	N45°E 35°SE	PF						

CORING DATE: <u>Sept. 1979</u>		EG.S.P. REVISED FRACTURE LOGGING FORMAT										PAGE <u>4</u> OF <u>5</u>	
LOG DATE: <u>June 1980</u>		WELL: <u>OH #7 Trumbull County</u>										CORING INDUCED FRACTURES	
WJ: #BER	DEPTH EXTENT	LENGTH	LITHOLOGY	TERMINATIONS	CHARACTER	STRIKE DIP	FRACTURE TYPE	MINERALIZATION	SLICK-ENSIDES	FRACTOGRAPHIC FEATURES	COMMENTS		
52	1677.7 1677.8	0.1'	MDST. (56 3/4')	M BDG	CP	N44°E ~90°	PF						
53	1692.0 1692.1	0.1'	MDST. (58 3/4')	M BDG	CP	N75°E 35°SE	PF						
54	1692.0 1692.1	0.1'		M BDG	CP	N72°E ~90°	HK						
55	1708.0 1708.1	0.1'		M BDG	CP	N40°E 40°NW	PF						
56	1708.0 1708.1	0.1'		M BDG	CP	N45°E ~90°	HK						
57	1710.0 1710.2	0.2'		M BDG	CP	N41°E 58°NW	PF						
58	1765.4 1835.8	0.2'		M BDG	CP	N69°E ~90°	HK						
59	1836.0 1906.5	0.2'		M M	CP		KES						
60	1910.2 1910.3	0.1'		M BDG	CP		DCS						
61	1910.2 1910.3	0.1'		M BDG	CP	N50°E 30°SE	PF						
62	1910.2 1910.3	0.1'		M BDG	CP	N40°E 45°NW	PF						
63	1938.4		SLTST. (N3)	M	CP		TF						
64	1945.6 1945.7	0.1'	MDST. SLTST. (58 3/4') (N3)	M BDG	CP		TF						
65	2005.0 2005.1	0.1'	MDST. (58 3/4')	M BDG	CP		KES						
66	2023.0			M	CP		DCS						
67	2023.2			M	CP		DCS						
68	2033.1 0.53	0.3	MDST. (56 3/4')	M	CP		KES						

EASTERN GAS SHALES PROJECTDISC FRACTURE FREQUENCY LOGOHIO #7 - TRUMBULL COUNTY

<u>Feet</u>	<u>Freq/ Foot</u>	<u>Feet</u>	<u>Freq/ Foot</u>	<u>Feet</u>	<u>Freq/ Foot</u>
1,500	7.2	1,730	3.2	1,960	2.6
1,505	10.6	1,735	6.0	1,965	3.2
1,510	9.2	1,740	6.2	1,970	2.8
1,515	7.8	1,745	5.6	1,975	3.4
1,520	6.0	1,750	5.2	1,980	2.8
1,525	8.0	1,755	7.2	1,985	2.8
1,530	7.8	1,760	4.4	1,990	6.0
1,535	8.0	1,765	4.2	1,995	7.6
1,540	6.8	1,770	6.0	2,000	4.8
1,545	7.8	1,775	5.2	2,005	5.6
1,550	5.4	1,780	4.4	2,010	4.0
1,555	5.4	1,785	5.2	2,015	5.4
1,560	3.2	1,790	5.4	2,020	6.0
1,565	3.2	1,795	4.0	2,025	6.2
1,570	5.6	1,800	2.0	2,030	4.6
1,575	3.8	1,805	3.2	2,035	4.0
1,580	3.8	1,810	3.6	2,040	5.6
1,585	3.4	1,815	5.0	2,045	7.4
1,590	2.8	1,820	3.8	2,050	6.2
1,595	4.6	1,825	4.0	2,055	6.0
1,600	5.2	1,830	2.8	2,060	6.2
1,605	4.4	1,835	2.8	2,065	7.0
1,610	4.6	1,840	3.2	2,070	7.8
1,615	6.2	1,845	2.8	2,075	6.4
1,620	6.0	1,850	3.0	2,080	5.2
1,625	4.4	1,855	4.6	2,085	5.0
1,630	5.6	1,860	2.6	2,090	4.8
1,635	6.0	1,865	5.2	2,095	6.4
1,640	5.6	1,870	4.6	2,100	4.4
1,645	4.8	1,875	4.6	2,105	5.0
1,650	3.8	1,880	3.8	2,110	2.6
1,655	3.2	1,885	4.2	2,115	5.6
1,660	6.6	1,890	4.0	2,120	4.4
1,665	5.8	1,895	5.0	2,125	3.2
1,670	7.0	1,900	4.4	2,130	3.4
1,675	6.4	1,905	5.6	2,135	3.0
1,680	5.8	1,910	3.4	2,140	2.8
1,685	6.0	1,915	3.2	2,145	4.2
1,690	4.4	1,920	1.8	2,150	2.2
1,695	6.4	1,925	3.8	2,155	2.0
1,700	5.4	1,930	4.0	2,160	2.4
1,705	5.6	1,935	3.2	2,165	2.8
1,710	6.0	1,940	2.6	2,170	1.8
1,715	3.6	1,945	3.6	2,175	3.0
1,720	3.6	1,950	2.6	2,180	2.6
1,725	2.0	1,955	2.8	2,185	2.8

<u>Feet</u>	<u>Freq/ Foot</u>	<u>Feet</u>	<u>Freq/ Foot</u>	<u>Feet</u>	<u>Freq/ Foot</u>
2,190	3.6	2,450	3.4	2,710	2.0
2,195	4.2	2,455	3.2		
2,200	3.6	2,460	2.2		
2,205	3.8	2,465	3.0		
2,210	2.4	2,470	3.2		
2,215	3.4	2,475	2.4		
2,220	2.2	2,480	3.2		
2,225	5.2	2,485	3.4		
2,230	5.2	2,490	2.4		
2,235	3.0	2,495	3.0		
2,240	5.2	2,500	1.8		
2,245	4.4	2,505	1.6		
2,250	6.2	2,510	1.6		
2,255	5.2	2,515	2.4		
2,260	6.0	2,520	2.2		
2,265	3.4	2,525	1.2		
2,270	4.0	2,530	1.4		
2,275	4.8	2,535	1.4		
2,280	3.0	2,540	3.8		
2,285	4.4	2,545	2.0		
2,290	2.2	2,550	3.4		
2,295	2.0	2,555	2.2		
2,300	2.6	2,560	2.6		
2,305	4.2	2,565	1.4		
2,310	6.8	2,570	2.6		
2,315	3.2	2,575	2.0		
2,320	3.0	2,580	2.0		
2,325	3.4	2,585	2.2		
2,330	4.4	2,590	3.0		
2,335	3.8	2,595	6.8		
2,340	3.2	2,600	7.0		
2,345	3.2	2,605	7.0		
2,350	3.6	2,610	8.0		
2,355	3.8	2,615	7.2		
2,360	4.0	2,620	6.6		
2,365	2.8	2,625	5.6		
2,370	3.4	2,630	6.6		
2,375	4.6	2,635	5.4		
2,380	3.4	2,640	5.8		
2,385	3.4	2,645	5.0		
2,390	3.0	2,650	3.6		
2,395	2.6	2,655	6.6		
2,400	4.2	2,660	6.8		
2,405	4.2	2,665	6.4		
2,410	2.0	2,670	5.8		
2,415	1.6	2,675	3.2		
2,420	2.2	2,680	2.8		
2,425	2.8	2,685	2.0		
2,430	2.2	2,690	2.0		
2,435	3.8	2,695	2.4		
2,440	3.4	2,700	2.2		
2,445	2.2	2,705	2.4		

BIBLIOGRAPHY

Bennison, A. P., 1978, Geological Highway Map of the Great Lakes Region: Map No. 11, AAPG, Tulsa, Oklahoma.

Dunham, R. J., 1962, Classification of Carbonate Rocks According to Depositional Texture: in W. E. Ham (Ed.), Classification of Carbonate Rocks, pp. 108-21, AAPG, Tulsa, Oklahoma.

Evans, M., 1979, Fracture Density and Orientation Study of the Reel Energy #3 D/K Core from Mason County, West Virginia: (Unpublished Contract Report, U. S. Department of Energy Contract No. DE-AC21-76MC05194, Morgantown, West Virginia).

Geological Society of America, 1948, Rock Color Chart: Geological Society of America, Boulder, Colorado.

Hosterman, J., and Roen, J., 1980, Personal Communication.

Kulander, B. R., et al., 1978, Stratigraphy and Gas Occurrence in the Devonian Organic Rich Shales of Pennsylvania: in G. L. Schoot, et al., (Ed.), Proceedings First Eastern Gas Shales Symposium, p. 127, U. S. Department of Energy, Morgantown, West Virginia.

Potter, P., et al., 1980, Final Report of Special Geological, Geochemical, and Petrological Studies of the Devonian Shales in the Appalachian Basin: U. S. Department of Energy, under Contract No. DE-AC21-76MC05201, Morgantown, West Virginia.

Ragan, D. M., 1973, Structural Geology, An Introduction to Geometrical Techniques: 2nd ed., John Wiley & Sons, New York, New York.

Schwietering, J. F., 1979, Devonian Shales of Ohio and their Eastern and Southern Equivalents: Prepared for West Virginia Geological and Economic Survey, under Contract No. EY-76-C-05-5199, Morgantown, West Virginia.

APPENDIX E

Cliffs Minerals, Inc.
Eastern Gas Shales Project
Ohio #5 Well - Lorain County

Phase II Report
Preliminary Laboratory Results
April 1980

CLIFFS MINERALS, INC.
EASTERN GAS SHALES PROJECT
OHIO #5 WELL - LORAIN COUNTY

PHASE II REPORT
PRELIMINARY LABORATORY RESULTS
APRIL 1980

T A B L E O F C O N T E N T S

	<u>PAGE NO.</u>
1.0 INTRODUCTION	1
2.0 SCOPE OF WORK	1
3.0 LABORATORY PROCEDURES	3
3.1 Review of Geophysical Logs	3
3.2 Photographic Log	3
3.3 Detailed Lithologic Log	3
3.4 Stratigraphic Section	7
3.5 Color Histogram	7
3.6 Fracture Logs	7
3.7 Measurement of Shore Hardness	9
4.0 REPORTING OF RESULTS	9
5.0 DISCUSSION OF RESULTS	11
5.1 Geologic Setting	11
5.2 Stratigraphy	11
5.3 Fracture Analysis	18

A P P E N D I C E S

- A DETAILED LITHOLOGIC DESCRIPTION
- B SYMBOLS, TERMS, AND ABBREVIATIONS USED IN FRACTURE LOGGING
- C FRACTURE LOGS

BIBLIOGRAPHY

PLATE IN POCKET

L I S T O F F I G U R E S

<u>FIGURE NO.</u>	<u>TITLE</u>	<u>PAGE NO.</u>
1	TEXTURAL CLASSIFICATION OF FINE CLASTIC SEDIMENTARY ROCKS	5
2	TEXTURAL CLASSIFICATION OF LIMESTONE	6
3	LOCATION OF THE EGSP-OHIO #5 WELL, LORAIN COUNTY, OHIO	12

L I S T O F T A B L E S

<u>FIGURE NO.</u>	<u>TITLE</u>	<u>PAGE NO.</u>
1	EGSP-OHIO #5 - FORMATION THICKNESSES	13
2	DISTRIBUTION OF NATURAL FRACTURES	19

1.0 INTRODUCTION

The U. S. Department of Energy is funding a research and development program entitled the Eastern Gas Shales Project designed to increase commercial production of natural gas in the eastern United States from Middle and Upper Devonian Shales. The program's objectives are as follows:

1. To evaluate recoverable reserves of gas contained in the shales.
2. To enhance recovery technology for production from shale gas reservoirs.
3. To stimulate interest among commercial gas suppliers in the concept of producing large quantities of gas from low-yield, shallow Devonian Shale wells.

The EGSP-Ohio #5 well was cored under a cooperative cost-sharing agreement between the Department of Energy (METC) and Columbia Gas Transmission Corporation. Overall, the coring of this well proceeded approximately as scheduled. Minor mechanical problems slowed the process somewhat but not excessively. Conventional coring (oriented) and drilling methods were used.

2.0 SCOPE OF WORK

The objective of work performed at the Eastern Gas Shales Project's Core Laboratory is to provide a detailed characterization of the core recovered from the EGSP-Ohio #5 well. Data are acquired from several sources for analysis. At the well site, suites of wet and dry hole geophysical logs were run, including the following:

Dry Hole Logs: Gamma Ray
Compensated Formation Density
Temperature
Sibilation

Wet Hole Logs: Compensated Formation Density
Gamma Ray
Dual Induction - SFL
Borehole Compensated Sonic
Fracture Identification
Noise

At the EGSP Core Laboratory, the core was laid out, washed, measured, oriented, and photographed prior to description and sampling. Characterization work performed includes photographic logs, detailed lithologic logs, fracture logs (both natural and induced types), measurements of core color variation, and stratigraphic interpretation of the cored intervals. In addition, physical property samples were selected and prepared for testing. The samples were tested by Michigan Technological University under subcontract. Physical properties data obtained from specimen tests include:

- Directional Ultrasonic Velocity
- Directional Tensile Strength
- Strength in Point Load
- Trends of Microfractures

3.0 LABORATORY PROCEDURES

3.1 Review of Geophysical Logs:

During the initial stages of processing the EGSP-Ohio #5 core through the laboratory, wet and dry hole geophysical logs from the well were examined and compared with published reference sections. Using the gamma ray and density logs a preliminary stratigraphic section was prepared for the cored interval. These two logs have proven to be the most useful correlation tools within the Devonian Shale sequence. Much of the development of existing formation nomenclature for the Devonian Shales is based on the recognition of characteristic features of these logs. Consequently, formation boundaries and thicknesses are, in some cases, more readily determined from gamma ray and density logs than from visual examination of the core itself.

Several other logs often provide information useful for core characterization. Both fracture identification and sonic logs frequently indicate the occurrence of zones of structural discontinuity (joints, faults, concretions, zones of increased friability, etc.) within the core. Sibilation and temperature logs are useful for locating significant flows of gas into the well from isolated fractures or fracture systems.

The interpretation of prominent features on the geophysical logs in advance of core description is a means of assuring that these features will receive adequate recognition.

3.2 Photographic Log:

After the EGSP-Ohio #5 core had been laid out, washed, and oriented on a laboratory table, a series of photographs was taken to record the "as-received" condition. A photographic log was then compiled for subsequent

documentation. One copy of the log is to be forwarded to the Morgantown Energy Technology Center, under separate cover, together with this report.

3.3 Detailed Lithologic Log:

After detailed visual examination the EGSP-Ohio #5 core was described in intervals which vary from about 5 feet to 10 feet in length. The first sentence of the description contains a brief summary of lithology, color, and sedimentary structure. Additional remarks were recorded to describe unique features observed within the interval. These remarks may concern any (or all) of the following:

1. Coarse clastic interbeds with scour surfaces, sole marks, cross-stratification, ripple lamination, etc.
2. Macroscopic fossils such as carbonaceous and pyritized vegetal constituents, conodonts, invertebrate shell fragments and casts, fish scales and teeth, etc.
3. Bioturbation, as discrete burrows or as mottled stratification, with emphasis on distribution and association with other rock fabric features.
4. Concretions, slump features, clasts and rip-up structures, gas pits, and other inorganic structures.
5. Modes of pyritization: as disseminated occurrences, nodules, coatings on shell fragments or plant tissue fragments; as accessory mineralization with concretions or clastic interbeds; and as primary irregular lenses or laminae in euxinic black shales.
6. Occurrence of fissility and friability.
7. Carbonate content.

Lithologic terminology applied to the shales is summarized in Figure

1. The classification scheme in use at the Core Laboratory for describing limestones is that of Dunham (1962), shown in Figure 2. Core colors were described using the Rock Color Chart published by the Geological Society of America (1948).

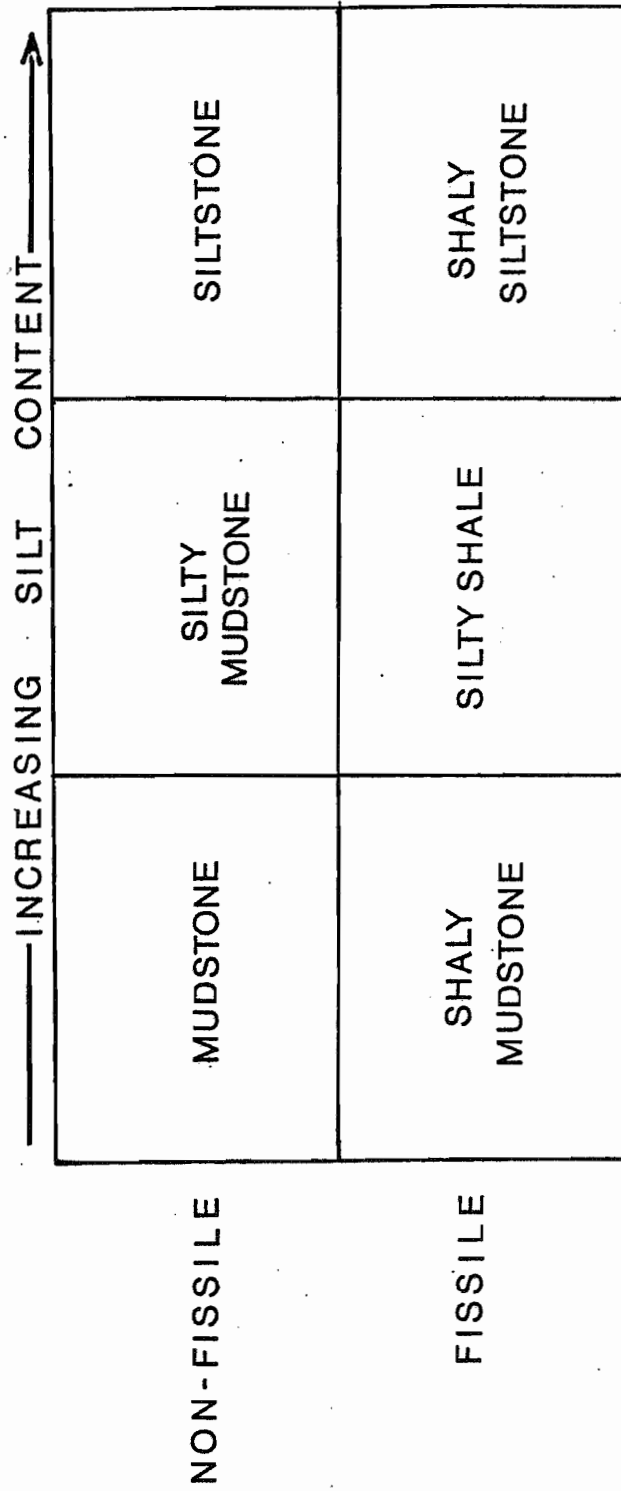
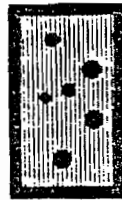


FIGURE 1

TEXTURAL CLASSIFICATION OF FINE CLASTIC SEDIMENTARY ROCKS

MUD SUPPORTED (Sand-size carbonate grains suspended in carbonate mud)		GRAIN SUPPORTED (Sand-size carbonate grains with interstitial carbonate mud)	
< 10% SAND-SIZE GRAINS	> 10% SAND-SIZE GRAINS	MUD PRESENT	NO MUD
Lime Mudstone	Wackestone	Packstone	Grainstone



BIOGENICALLY CEMENTED GRAINS: Boundstone
 NO RECOGNIZABLE TEXTURE: Crystalline Limestone

FIGURE 2

TEXTURAL CLASSIFICATION OF LIMESTONES

3.4 Stratigraphic Section:

A stratigraphic section for the cored interval was prepared after the gamma ray and density logs were examined and the detailed lithologic log had been completed. Formation thicknesses were measured, contacts located as precisely as possible, and age relationships determined from published sources.

The locations of certain formation boundaries in the Devonian Shales are difficult to establish with precision. In some cases a contact between two units is gradational, or the nature of a contact may be problematical.

3.5 Color Histogram:

A color histogram for the Ohio #5 core was compiled to provide a relative measure of the distribution of light and dark shales through the cored interval. Using the G.S.A. Rock Color Chart, the net length of each color present within each 5-foot segment of the core was recorded. Colors with values darker than N3 were grouped together for each segment to determine the percentage of dark shale, and colors with values lighter than or equal to N3 were combined to determine the percentage of light shale. Use of the term "value" refers to the Munsell system of color identification wherein a specific color is defined by a unique hue, value, and chroma designation.

3.6 Fracture Logs:

Methods of fracture analysis employed at the EGSP Core Laboratory are similar to those described by Kulander, et al (1977). A standardized logging procedure has been developed by the Morgantown Energy Technology Center. Abbreviations and symbols used in conjunction with the EGSP Standard Core Fracture Logging Format are listed and defined in Appendix B.

Determination of the number, location, orientation, and character of natural fractures intercepted in the cored interval is of vital interest for the selection of appropriate well completion and stimulation techniques. Criteria applied to distinguish natural fractures from fractures induced during coring and handling are listed below (quoted from Evans, 1978):

CORING-INDUCED FRACTURES EXHIBIT THE FOLLOWING CHARACTERISTICS

1. Fracture origin within the core or on the core margin.
2. Hackle plumes diverging from the origin to intersect the core margin or pre-existing fracture surface orthogonally.
3. Hackle marks becoming progressively coarser in the vicinity of the core margin or pre-existing fracture surface.
4. Twist hackle originating near the core margin or pre-existing fracture surface.
5. Hackle plumes diverging in a spiral pattern from the central part of the core on a subhorizontal fracture surface; indicative of torsional stress.
6. Closely spaced arrest lines on a vertical or near-vertical planar fracture; arrest lines are convex down-core and exhibit approximate bilateral symmetry.
7. Hackle marks on a vertical or near-vertical planar fracture diverging down-core from the center of the plane toward the margins.
8. An abrupt change in the direction of fracture propagation (hook) near the core margin or pre-existing fracture surface.

NATURAL FRACTURES EXHIBIT THE FOLLOWING CHARACTERISTICS

1. Smooth, polished planar fracture faces, with or without slickensides.
2. Mineralization coating fracture surfaces, or filling a closed fracture.

3. A smooth fracture extending across the core against which later fractures terminate.
4. Small conchoidal chips or hook features at the intersection of an inclined fracture plane and the core margin; the chips hook to meet the inclined fracture orthogonally.

Coring- and handling-induced fractures also are logged in detail. This information provides additional documentation regarding the condition of the core as received from the field, and it is useful for assessing the effects of problems encountered during drilling. The frequency of disc fractures (generally the most prevalent and least diagnostic type of induced fracture) is recorded in the form of a histogram.

3.7 Measurement of Shore Hardness:

The Shore Hardness tests were deleted from core characterization work due to high equipment maintenance requirements in addition to questionable accuracy and nonproducibility of results. Alternative testing methods are being considered for future core characterization work.

4.0 REPORTING OF RESULTS

A correlation chart has been compiled at a scale of 1 inch to 20 feet which provides a visual display of the following data recorded for the EGSP-Ohio #5 core:

1. Stratigraphic Column
2. Lithology
3. Color Histogram
4. Gamma Ray Log

5. Compensated Density Log
6. Sibilation Log
7. Orientation/Distribution of Natural Fractures
8. Frequency of Induced Fractures

The correlation chart accompanies this report as an enclosure.

Discussions of core stratigraphy, lithology, and the occurrence of fractures are provided in Section 5. Appendix B contains a detailed lithologic description of the core. Terminology applied in describing natural and induced fractures is provided in Appendix C and the fracture data are presented in Appendix D.

One copy of the photographic log was submitted as a separate document to the Morgantown Energy Technology Center. A second copy is available for inspection at the EGSP Core Laboratory.

When physical properties testing of samples from the EGSP-Ohio #5 core has been concluded, a final (Phase III) report will be issued containing an analysis of those data together with the information already compiled at the core laboratory.

After characterization was completed the core was sealed in a moisture barrier and packaged in 3-foot core boxes for temporary archiving at the EGSP core laboratory. Following a 90-day period the Ohio #5 core will be transferred to the Ohio Geological Survey.

5.0 DISCUSSION OF RESULTS

5.1 Geologic Setting:

The EGSP-Ohio #5 well site is located approximately 13 miles south-southeast of Elyria in Lorain County, Ohio (Figure 3). The topography in this area is gently rolling to near-level and is glacial in origin (Bennison, 1978). The major drainage features of the area include the East Branch of the Black River to the west, and the west branch of the Rocky River to the east. Both rivers flow into Lake Erie.

The site is located to the north of the Cincinnati Arch and east of the Findlay Arch in the western portion of the Appalachian Basin. The regional dip of the bedrock is gentle and to the east. Bedrock outcrops of the Waverly Group are present at the surface but are restricted to stream cuts.

5.2 Stratigraphy:

A total of 881 feet of core was recovered from the EGSP-Ohio #5 well. Core point was at 400 feet (depth below surface) in the lower part of the Cleveland Shale Member of the Ohio Shale. Coring was terminated 1 foot below the top of the Onondaga (?) Limestone. Formations encountered in this well are summarized in Table 1. Following the table, a summary description of each formation or member is provided.

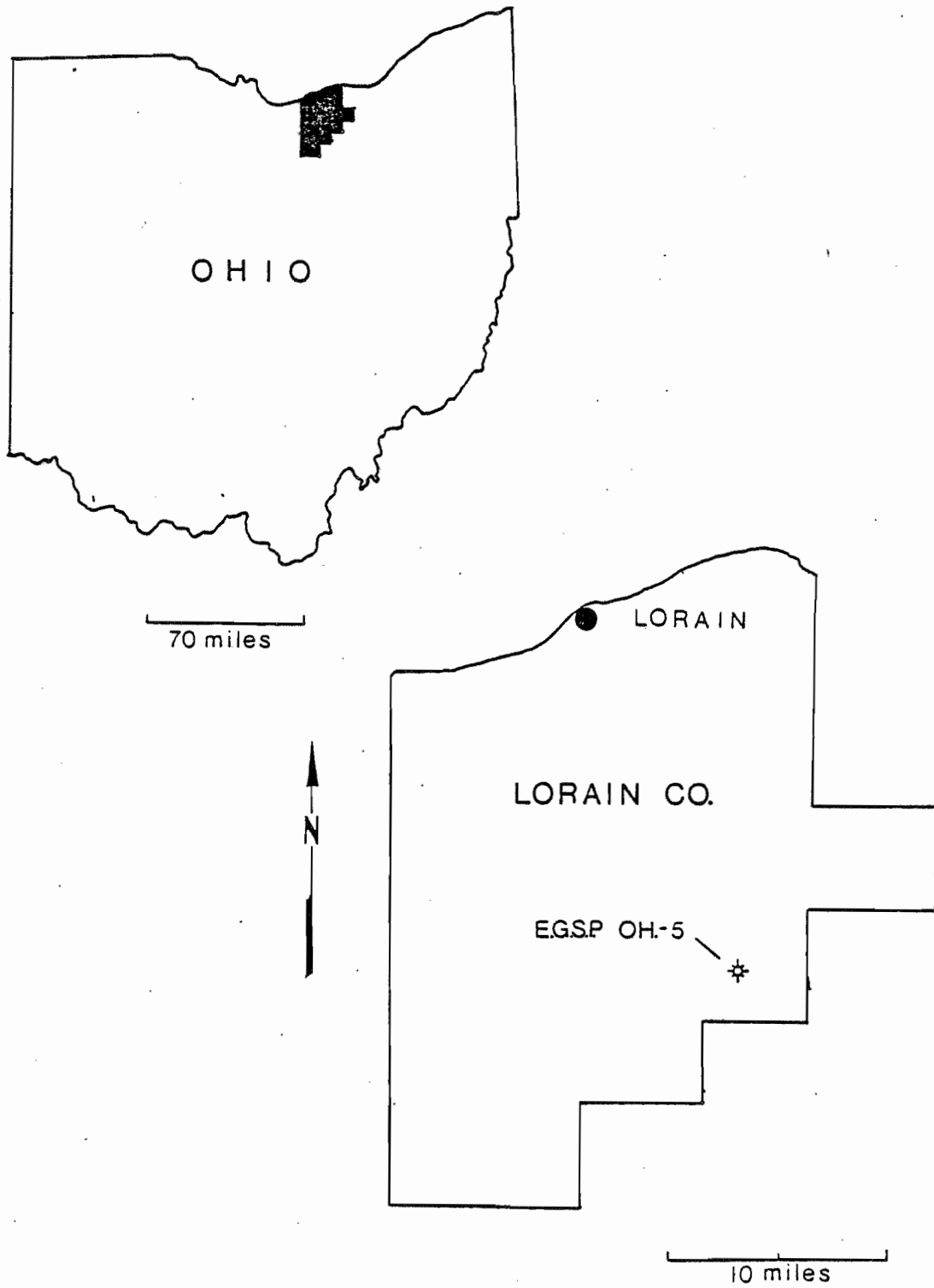


FIGURE 3

LOCATION OF THE EGSP-OHIO #5 WELL
LORAIN COUNTY, OHIO

TABLE 1

FORMATION THICKNESSES

<u>Formation</u>	<u>Depths</u>	<u>Formation Thickness</u>	<u>Depths Cored</u>
Ohio Shale:			
Cleveland Shale	299'-428'	129'	400'-428'
Chagrin Shale	428'-735'	307'	428'-735'
Huron Shale:			
Upper	735'-814'	79'	735'-814'
Middle	814'-901'	87'	814'-900'
Lower	901'-1,088'	187'	900'-1,088'
Olentangy Shale:			
Upper	1,088'-1,279'	191'	1,088'-1,279'
Onondaga Limestone:	1,279'- *		1,279'-1,281'

* Contact undetermined.

Ohio Shale (Cleveland, Chagrin, and Huron Shales):

The Ohio Shale consists of three members: the Cleveland Shale, Chagrin Shale, and Huron Shale. The lower 28 feet of the Cleveland Shale and the entire thickness of Chagrin and Huron Shales were cored (400 feet to 1,088 feet).

Cleveland Shale:

Only 28 feet of the base of the Cleveland Shale (400 feet to 428 feet) was cored. The cored interval is composed of thinly laminated to thick-bedded mudstone and siltstone. The predominant colors are olive gray (5Y 3/1), greenish gray (5GY 5/1), and medium light gray (N6). Fossils and biogenic structures contained in the mudstones include mud filled burrow structures, abundant spore casts and resin bodies, carbonaceous plant fragments, and occasional fish parts. Pyrite occurs occasionally throughout as lenses, nodules, and mineralized pellets. The siltstones are ripple laminated and contain infrequent soft-sediment deformation features. Micaceous laminations occur within the siltstones in the lower 1/4 of the interval.

Core examination reveals an increase in siltstone occurrence near the base of the Cleveland Shale but that the contact between it and the underlying Chagrin Shale is gradational. On the geophysical log the contact is indicated by a moderate decrease in the gamma ray count.

Chagrin Shale:

The Chagrin Shale (428 feet to 735 feet) consists of thinly laminated to thin-bedded mudstone, siltstone, and silty mudstone. The mudstone portion is dominantly greenish gray (5G 6/1) from 428 to 629 feet, and olive gray (5Y 4/1) from 629 to 735 feet. The siltstone and silty mudstone intervals are predominantly light gray (N7). Siltstone is dominant in the upper 30 feet. Numerous examples of graded bedding (silty mudstone fining upward to mudstone) occur from 428 to 629 feet. Also present within this interval are numerous concretionary bands, predominantly yellowish brown (10YR 5/4), and the siltstones that are ripple cross-laminated and disrupted by scour surfaces, sole marks, and soft-sediment deformation. The siltstones also contain micaceous laminations between 428 and 522 feet. Below 629 feet the amount of siltstone decreases sharply and fewer sedimentary structures are present. Biogenic features present in the mudstone include: mottling (bioturbation) between the light and dark mudstones from 587 to 597 feet, from 629 to 658 feet, and from 688 to 735 feet; and mud-filled burrow structures from 570 to 638 feet. Fossils present within the member include: spore cases and resin bodies which occur throughout, rare fish parts which occur in the lower half, a trilobite (Anchiopsis sp.?) at 578 feet, and an unidentified fossil fragment at 482 feet. Pyrite occurs in the lower half of the member as disseminated grains, lenses, mineralized pellets, and as coatings on woody fragments. Calcareous zones occur throughout the member except for a noncalcareous interval from 522 to 534 feet.

The contact between the Chagrin Shale and the Huron Shale is indicated by a slight increase in gamma ray count on the geophysical log. In the core the contact is expressed as a gradual color change from olive gray to olive black.

Huron Shale:

The total thickness of the Huron Shale, which is a member of the Ohio Shale, is present in the core between 735 and 1,088 feet. The Huron Shale is informally divided into three units: the Upper, Middle, and Lower Huron. These subdivisions are more easily distinguished from the geophysical logs than from core examination.

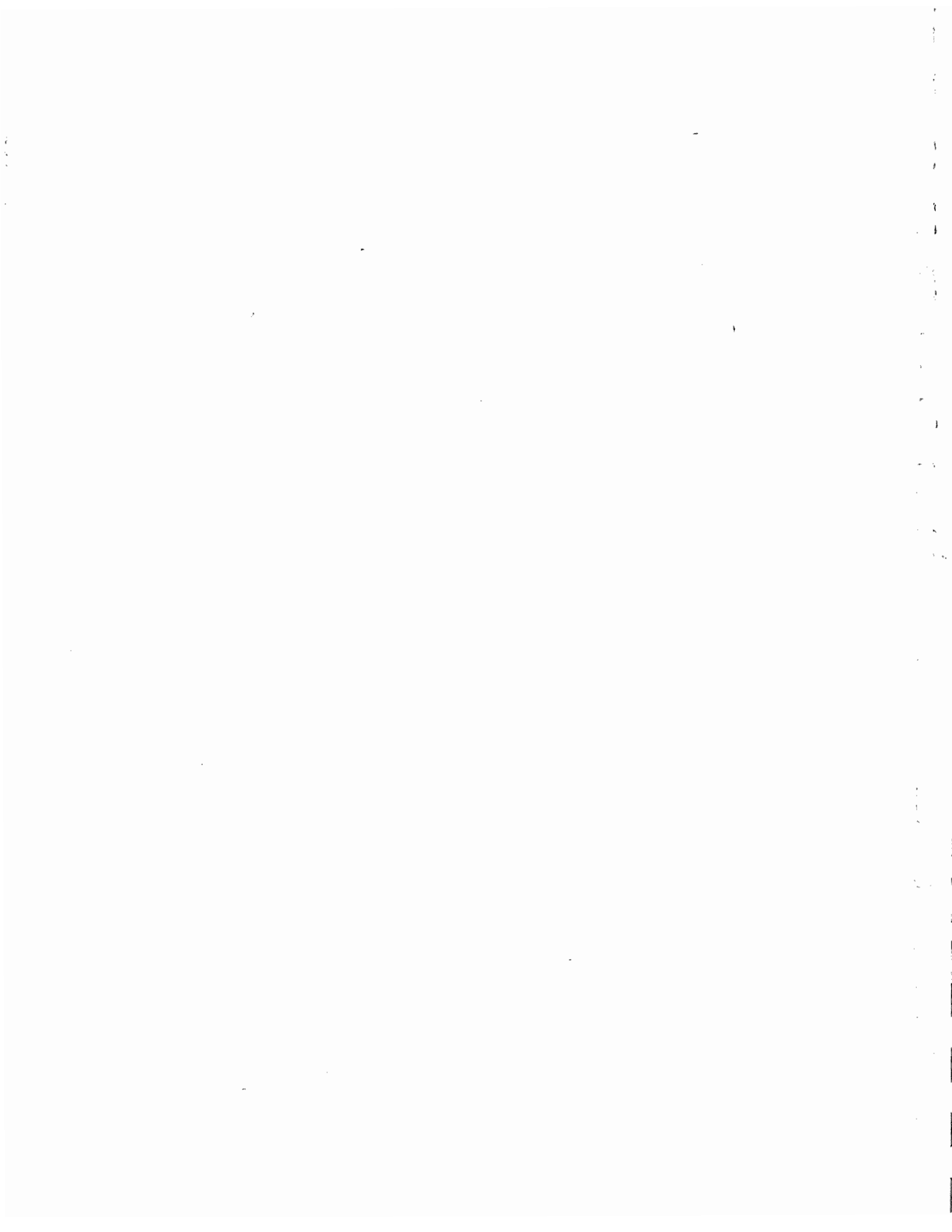
The Upper Huron (735 to 814 feet) consists of thinly laminated to thin-bedded mudstone and siltstone. Predominant colors are olive gray (5Y 4/1), olive black (5Y 2/1), greenish gray (5GY 6/1), and light gray (N7). Several olive gray lime mudstones are present at 737.1 feet, 737.2 feet, and 744.1 feet. Siltstone, thinly to thickly laminated and highly calcareous, occurs throughout the Upper Huron. Contacts between mudstone and siltstone are gradational except for occasional sharply defined greenish gray mudstone intervals. Most of these sharply defined zones are slightly mottled by bioturbation and occasionally contain mud-filled burrow structures. Siltstone occurrences at 810.9 feet contain scour surfaces and load casts. Fossils present throughout the interval include spore casts and resin bodies, carbonaceous fragments, and fish parts. Conodonts occur at 776.1, 779.9, and 804.4 feet. Vitrinite is present at 736.9 and 776.1 feet. Pyrite occurs throughout as nodules, pellets, lenses, and as coatings on wood fragments. Calcareous zones are present throughout the Upper Huron.

The contact between the Upper Huron and underlying Middle Huron was determined primarily from the geophysical logs, expressed as a slight decrease in the gamma ray count. Core examination revealed no apparent change in lithology or color.

The Middle Huron is present in the core from 814 to 901 feet. It consists of thinly laminated to thin-bedded mudstone, siltstone, and silty mudstone. The predominant colors are olive gray (5Y 4/1), greenish gray (5GY 6/1), and light olive gray (5Y 6/1). Contacts between the olive gray, olive black, and greenish gray mudstone are gradational except for several well-defined greenish gray zones. Many of these well-defined zones are mottled by bioturbation and occur throughout the Middle Huron except between 880 and 887 feet where they are absent. Spore cases and resin bodies, and fish parts are present throughout. Foerstia sp. fragments occur in several zones below 840 feet. Conodonts occur randomly throughout but are most common between 860 and 880 feet. Calcareous zones are present throughout as is pyrite which occurs as pellets, nodules, laminations, and as coatings on woody stems.

The contact between the Middle Huron and the underlying Lower Huron is indicated in the core by a distinct color change from greenish to olive gray and in the geophysical logs by a sharp increase in gamma ray count.

The Lower Huron consists of thinly laminated to thin-bedded mudstone, siltstone, and lime mudstone. Predominant colors are olive gray (5Y 4/1), olive black (5Y 2/1), greenish gray (5GY 6/1), and light olive gray (5Y 6/1). Lime mudstone occurs in single thin beds at 1,034.7 and at 1,078.2 feet. Contacts between mudstone and other rock types are gradational except for occasional well defined greenish gray zones. Zones containing mottling



<u>INTERVAL</u>	<u>DESCRIPTION</u>
400.0' - 409.0' (9.0')	Mudstones and siltstones, olive gray (5Y 4/1), greenish gray (5GY 5/1), and light gray (N7), thinly laminated to thin bedded. The siltstones are ripple-laminated. The olive gray mudstones contain fish teeth and jaws, a single fish-skin imprint at 403.5', and carbonaceous plant fragments throughout. Pyrite occurs in the olive gray mudstones as coatings on fecal pellets; these pellets are especially abundant between 402.0' and 403.0'. A burrow structure is present at 500.3' in greenish gray mudstone. <u>Tasmanites</u> spore cases are present at the base of each greenish gray mudstone interval and at 400.3' and 407.7' in olive gray mudstone.
409.0' - 421.0' (12.0')	Mudstones and siltstones, olive gray (5Y 3/1), greenish gray (5GY 5/1), and medium light gray (N6), thinly laminated to thick bedded. The siltstones are lightly to heavily ripple laminated and contain basal load casts. The siltstone at 414.5' is calcareous. The olive gray mudstones contain fish teeth, carbonaceous plant fragments, spore resin bodies, and a few pyritized fecal pellets throughout. <u>Tasmanites</u> spore cases are present throughout in the mudstones, occurring in dense collections between closely spaced siltstone zones. Light olive gray (5Y 6/1) concretionary bands are common.
421.0' - 428.5' (7.5')	Mudstones and siltstones, olive gray (5Y 3/1), greenish gray (5GY 5/1), and medium light gray (N6), thinly laminated to thin bedded. The siltstones are ripple-laminated and contain scour surfaces throughout; micaceous laminations (ash beds?) are common. A siltstone layer at 422.5' is calcareous. The olive gray mudstones contain spore resin bodies and carbonaceous plant fragments throughout and mud-filled burrows at 427.3'. The medium light gray mudstones contain occasional carbonaceous plant fragments and <u>Tasmanites</u> spore cases throughout and partially oxidized plant stems within the lower 2/3. Pyrite occurs in the olive gray mudstones as nodules and laminae between 426.8' and 427.3', and as coatings on spore cases. Light olive gray (5Y 6/1) concretionary bands occur frequently.
428.5' - 436.0' (7.5')	Siltstones, mudstones, and silty mudstones, light gray (N7), greenish gray (5G 6/1), and olive gray (5Y 3/1), thinly laminated to thin bedded. The siltstones are ripple-laminated and contain load casts and scour surfaces. Examples of silty mudstone fining upward to mudstone are present in the interval. The greenish gray mudstones contain partially oxidized plant fragments and <u>Tasmanites</u> spore cases, and the olive gray mudstones contain spore resin bodies throughout. Light olive gray (5Y 7/1) concretionary bands are present throughout the interval.

<u>INTERVAL</u>	<u>DESCRIPTION</u>
436.0' - 446.0' (10.0')	Siltstones, mudstones, and silty mudstones, medium light gray (N6), and greenish gray (5G 5/1), thinly laminated to thin bedded. The siltstones are ripple-laminated and often contain load casts and scour surfaces. Micaceous laminations (ash beds?) occur within the siltstones throughout the interval. Zones of silty mudstone fining upward to mudstone are present. The mudstones contain partially oxidized plant fragments and iron stains throughout, and spore casts and a single fish jaw at 439.8' and 444.0', respectively. Several light olive gray (5Y 5/1) concretionary bands are present. Siltstone occurrences are calcareous in the lower 1/2 of the interval.
446.0' - 456.0' (10.0')	Siltstones, mudstones, and silty mudstones, medium dark gray (N4) and greenish gray (5G 5/1), thinly laminated to thin bedded. The siltstones are cross- to ripple-laminated and are occasionally disrupted by load casts, slumps, basal groove casts, and scour surfaces. Micaceous laminations (ash beds?) rest on some of the scour surfaces. Several occurrences of silty mudstone fining upward to mudstone are present throughout. A vertical mud-filled crack cross cutting several siltstone and mudstone layers is present at 448.0'. The mudstones contain carbonaceous plant fragments, partially oxidized plant fragments, and <u>Tasmanites</u> spore cases. Several siltstone layers within the upper 1/2 of the interval are calcareous. Several moderate brown (5YR 4/4) concretionary bands are present.
456.0' - 465.0' (9.0')	Siltstones, mudstones, and silty mudstones, olive gray (5Y 5/1), medium dark gray (N4), greenish gray (5G 5/1), and olive gray (5Y 4/1), thinly laminated to thin bedded. The siltstones are cross- to ripple-laminated and contain slumps, load casts, sole marks, and scour surfaces. Zones of graded bedding (silty mudstone fining upward to mudstone) are present throughout. Micaceous laminations (ash beds?) occur in both mudstone and siltstone. Carbonaceous fragments, spore resin bodies, and <u>Tasmanites</u> spore cases occur in the mudstones. Organism trails and partially oxidized plant fragments were noted in the greenish gray mudstones. Siltstone occurrences in the lower 1/2 and at 457.7' are calcareous. Yellowish brown (10YR 5/4) concretionary bands are widespread.
465.0' - 472.4' (7.4')	Mudstones, siltstones, and silty mudstones, greenish gray (5G 6/1), olive gray (5Y 3/1), very light gray (N8), and medium gray (N5), thinly laminated to thin bedded. The siltstones are cross- to ripple-laminated and contain load casts and scour surfaces. Several zones of graded bedding (silty mudstone fining upward to mudstone) are present. Micaceous laminations (ash beds?) were observed throughout, occurring most frequently in siltstones. The greenish gray

<u>INTERVAL</u>	<u>DESCRIPTION</u>
465.0' - 472.4' (Continued)	mudstones contain partially oxidized plant fragments, whereas the olive gray mudstones contain carbonaceous fragments throughout. Pyrite occurs as coatings on spore cases and as disseminated grains in mudstones. Light brown (5YR 5/6) concretionary bands are common. Most of the siltstones in the lower 1/3 of the interval are calcareous.
472.4' - 480.2' (7.8')	Mudstones, siltstones, and silty mudstones, greenish gray (5G 5/1), olive gray (5Y 3/1), light greenish gray (5G 7/1), and medium dark gray (N4), thinly laminated to thin bedded. The siltstones are cross- to ripple-laminated and often contain scour surfaces, slump features, load casts, and sole markings. A single micaceous lamination was noted at 472.9'. Silty mudstone fining upward to mudstone is present at 472.6'. The olive gray mudstones contain occasional carbonaceous fragments. The greenish gray mudstones contain partially oxidized plant fragments throughout and several iron stains at 476.9'. The mudstones contain <u>Tasmanites</u> spore cases and resin bodies throughout. A single, dark yellowish brown (10YR 4/2) concretionary band occurs at 476.8'. The siltstones in the upper and lower 1 foot are calcareous; a single mudstone band at 473.7' is calcareous.
480.2' - 489.7' (9.5')	Siltstones, mudstones, and silty mudstones, light olive gray (5Y 6/1), greenish gray (5G 5/1), and olive gray (5Y 3/1), thinly laminated to thin bedded. Several zones of silty mudstone fining upward to mudstone are present. The siltstone occurrences are cross- to ripple-laminated and contain slumps, scour surfaces, and load casts. Micaceous laminations (ash beds?) were noted in siltstone. The mudstones contain partially oxidized plant fragments, <u>Tasmanites</u> spore cases and resin bodies throughout. An unidentified arthropod fossil was noted at 482.0' in greenish gray mudstone. Pyritized wood fragments are present at 483.2' in olive gray mudstone. Several light brown (5YR 6/4) concretionary bands occur in the upper 1/2 of the interval. Several siltstone layers are calcareous and occur throughout the interval.
489.7' - 497.0' (7.3')	Mudstones, siltstones, and silty mudstones, greenish gray (5G 5/1), olive gray (5Y 3/1), and light olive gray (5Y 6/1), thinly laminated to thin bedded. The siltstones are cross- to ripple-laminated and often disrupted by scour surfaces, slumps, load casts, and sole marks. Several layers of silty mudstone fining upward into mudstone occur throughout the interval. The greenish gray mudstones contain partially oxidized plant fragments, and olive gray mudstones contain carbonaceous fragments. <u>Tasmanites</u> spore cases and resin bodies occur in mudstone throughout the interval. Light brown (5YR 6/4) concretionary bands occur at 494.5' and 495.4'. Several widespread siltstone layers are calcareous; several micaceous laminations (ash beds?) appear within siltstone intervals.

<u>INTERVAL</u>	<u>DESCRIPTION</u>
497.0' - 502.0' (5.0')	Mudstones, siltstones, and silty mudstones, greenish gray (5G 6/1), olive gray (5Y 3/1), and light gray (N7), thinly laminated to thin bedded. The siltstones are cross- to ripple-laminated and occasionally contain load casts, sole marks, and scour surfaces. Several zones of silty mudstone fining upward to mudstone are present throughout. Micaceous laminations (ash beds?) rest on top of several of the siltstones. The greenish gray mudstones contain partially oxidized plant fragments throughout and a pyritized wood fragment at 499.0'. The olive gray mudstones contain biotite, mica, and anhydrite. <u>Tasmanites</u> spore cases and resin bodies occur throughout the mudstones, with dense clusters at the top of greenish gray mudstones.
502.0' - 510.0' (8.0')	Siltstones, mudstones, and silty mudstones, light olive gray (5Y 7/1), greenish gray (5G 6/1), and olive gray (5Y 3/1), thinly laminated to thin bedded. The siltstones are cross- to ripple-laminated and often contain load casts, scour surfaces and sole marks. Zones of silty mudstone fining upward to mudstone are present throughout. Micaceous laminations (ash beds?) rest at the top of several of the siltstones. The olive gray mudstones contain spore resin bodies and anhydrite throughout. <u>Tasmanites</u> spore cases occur at the bases of the olive gray mudstones. Several moderate yellowish brown (10YR 4/2) concretionary bands are present. Occasionally the siltstones are calcareous.
510.0' - 515.0' (5.0')	Mudstones, siltstones, and silty mudstones, greenish gray (5G 6/1), olive gray (5Y 3/1), and light olive gray (5Y 7/1), thinly laminated to thin bedded. The occurrence of siltstone increases down core. The siltstones are cross- to ripple-laminated and contain scour features, load casts, and slumps. Sequences of silty mudstone fining upward into mudstone are present within the interval. The greenish gray mudstones occasionally contain partially oxidized plant fragments. The olive gray mudstones contain abundant anhydrite, carbonaceous fragments, and <u>Tasmanites</u> spore cases and resin bodies throughout. A pale yellowish brown (10YR 6/2) concretionary band was noted at 513.9'. Several of the siltstones in the lower 1/3 of the interval are calcareous.
515.0' - 522.0' (7.0')	Mudstones, siltstones, and silty mudstones, greenish gray (5G 6/1), olive gray (5Y 3/1) and light olive gray (5Y 7/1), thinly laminated to thin bedded. The siltstones are cross- to ripple-laminated and contain scour surfaces, slumps, and load casts. Several sequences of silty mudstone fining upward to mudstone occur within the interval. The greenish gray mudstones contain partially oxidized plant fragments. The olive gray mudstones contain carbonaceous fragments, biotite, and anhydrite throughout, and an ash bed (?) at 518.7'.

<u>INTERVAL</u>	<u>DESCRIPTION</u>
515.0' - 522.0' (Continued)	<u>Tasmanites</u> spore cases and spore resin bodies occur throughout within the mudstones. Several pale yellowish brown (10YR 6/2) concretionary bands were also observed. Several of the siltstone laminae are calcareous.
522.0' - 530.0' (8.0')	Mudstones, siltstones, and silty mudstones, greenish gray (5G 5/1), olive gray (5Y 3/1), and light greenish gray (5G 7/1), thinly laminated to thin bedded. The siltstones are cross-to ripple-laminated and contain occasional load casts and scour surfaces. Several graded beds (silty mudstone fining upward to mudstone) occur within the interval. At 521.8' a micaceous, rippled lamination is present. The mica flakes are aligned parallel to the ripple faces. A micaceous lamination rests on top of a siltstone at 529.6'. Greenish gray mudstones containing partially oxidized plant fragments occur throughout. The olive gray mudstones contain abundant biotite and anhydrite, and occasional carbonaceous fragments. Several concretionary bands, light moderate brown (5YR 5/6), occur within the interval. Siltstones occurring between 522.0' and 525.0' are calcareous.
530.0' - 534.6' (4.6')	Mudstones, siltstones, and silty mudstones, greenish gray (5G 6/1), olive gray (5Y 3/1), and light gray (N7), thinly laminated to thin bedded. The siltstones generally occur in laminations less than 1 cm thick. Rippled laminations and load casts are restricted to a single siltstone layer at 532.7'. Several sequences of silty mudstone fining upward to mudstone are present within the interval. The greenish gray mudstones contain partially oxidized plant fragments throughout. The olive gray mudstones contain abundant biotite, anhydrite, and occasional carbonaceous fragments. <u>Tasmanites</u> spore cases and resin bodies are present throughout the mudstones.
534.6' - 547.0' (12.4')	Mudstones, siltstones, and silty mudstones, greenish gray (5G 5/1), olive gray (5Y 3/1), and light gray (N7), thinly laminated to thin bedded. The siltstones are cross-to ripple-laminated and contain load casts and slumps throughout; sole marks at 542.7'. Sequences of silty mudstone fining upward to mudstone are present. The greenish gray mudstones contain partially oxidized plant fragments. The olive gray mudstones contain carbonaceous fragments, anhydrite, and occasional flakes of biotite. Abundant <u>Tasmanites</u> spore cases and spore resin bodies were observed throughout the mudstones and are concentrated at the tops of greenish gray zones. Disseminated euhedral pyrite grains were observed at 544.8' in a greenish gray mudstone. Several concretionary bands, moderate yellowish brown (10YR 5/4), occur throughout the interval.

<u>INTERVAL</u>	<u>DESCRIPTION</u>
547.0' - 555.0' (8.0')	Mudstones, siltstones, and silty mudstones, greenish gray (5G 5/1), olive gray (5Y 3/1), and light gray (N7), thinly laminated to thin bedded. The siltstones are cross- to ripple-laminated and contain slumps, load casts, and scour features. Sequences of silty mudstone fining upward to mudstone are present throughout. The greenish gray mudstones contain partially oxidized plant fragments. The olive gray mudstones contain occasional carbonaceous fragments and anhydrite. <u>Tasmanites</u> spore cases and spore resin bodies are present in the mudstone zones. Dense concentrations of anhydrite and <u>Tasmanites</u> spore cases occur at 548.4' and 548.9', at the bases of two olive gray mudstones. Several moderate brown (5YR 4/4) concretionary bands occur within the interval.
555.0' - 560.0' (5.0')	Mudstones, siltstones, and silty mudstones, greenish gray (5G 6/1), olive gray (5Y 3/1), and light gray (N7), thinly laminated to thin bedded. The siltstones are cross- to ripple-laminated and contain slumps, load casts, scour surfaces, and sole marks. Zones of silty mudstone fining upward to mudstone occur throughout the interval. The greenish gray mudstones contain partially oxidized plant fragments. The olive gray mudstones contain occasional carbonaceous fragments. Dense concentrations of anhydrite crystals are present at the bottom of several olive gray mudstones. Pyrite was observed as coatings on <u>Tasmanites</u> spore cases in mudstones throughout the interval. Several moderate yellowish brown (10YR 5/4) concretionary bands are present within the interval.
560.0' - 570.0' (10.0')	Mudstones, siltstones, and silty mudstones, greenish gray (5G 6/1), olive gray (5Y 3/1), and light gray (N7), thinly laminated to thin bedded. Greenish gray mudstone is the dominant lithology. Mud-filled burrows are present in the mudstone zones. The siltstones are cross- to ripple-laminated and occasionally are disrupted by slumps, load casts, scour surfaces, and sole marks. Zones of silty mudstone fining upward to mudstone occur throughout. The greenish gray mudstones contain occasional partially oxidized plant fragments and ferruginous stains. The olive gray mudstones occasionally contain carbonaceous fragments and concentrations of anhydrite crystals. Abundant <u>Tasmanites</u> spore cases and spore resin bodies are present in the mudstone zones. Several slightly calcareous concretionary bands, light brown (5YR 5/6), are contained within the interval.

<u>INTERVAL</u>	<u>DESCRIPTION</u>
570.0' - 575.6' (5.6')	Mudstones, siltstones, and silty mudstones, greenish gray (5G 6/1), olive gray (5Y 3/1), and very light gray (N8), thinly laminated to thin bedded. The occurrence of siltstone laminae increases down core. These siltstones are cross- to ripple-laminated and contain load casts, slumps, scour surfaces, and sole marks. Several zones of silty mudstone fining upward to mudstone are present. The greenish gray mudstones occasionally contain partially oxidized plant fragments. The olive gray mudstones contain carbonaceous fragments throughout. <u>Tasmanites</u> spore cases, mica, and anhydrite occur in the olive gray mudstones, with dense collections at the bases of these strata. Several slightly calcareous concretionary bands, moderate yellowish brown (10YR 5/4), occur throughout the interval.
575.6' - 587.0' (11.4')	Mudstones, siltstones, and silty mudstones, greenish gray (5G 6/1), olive gray (5Y 3/1), and light gray (N7), thinly laminated to thin bedded. The siltstones are cross- to ripple-laminated and are disrupted by slumps, load casts, scour surfaces, and sole marks. Several zones of silty mudstone fining upward to mudstone are present within the interval. Mud-filled burrow structures are noted at the tops of several greenish gray strata. The greenish gray mudstones also contain partially oxidized plant fragments and occasional ferruginous stains throughout; a single unidentified fossil arthropod at 578.0'; and pyrite lenses at 578.2'. The olive gray mudstones contain mica, anhydrite, and carbonaceous fragments. <u>Tasmanites</u> spore cases and spore resin bodies occur frequently throughout in the mudstones with dense concentrations at the base of the olive gray zones. Occasional moderate yellowish brown (10YR 5/4) concretionary bands and nodules, which are slightly to strongly calcareous, are present in the lower 2/3 of the interval.
587.0' - 597.0' (10.0')	Mudstones, siltstones, and silty mudstones, greenish gray (5G 6/1), olive gray (5Y 3/1), and light gray (N7), thinly laminated to thin bedded. The siltstones are cross- to ripple-laminated and contain slumps and load casts. Several zones of silty mudstone fining upward to mudstone are present. The tops of the greenish gray mudstones occasionally are mottled by bioturbation and contain mud-filled burrow structures. The greenish gray mudstones also contain partially oxidized plant fragments and ferruginous stains. The olive gray mudstones contain mica, anhydrite, and carbonaceous fragments. <u>Tasmanites</u> spore cases and spore resin bodies are present throughout in the mudstones with dense concentrations present at the bases of the olive gray mudstones. Disseminated, euhedral pyrite grains are present at 587.1'. Several moderate yellowish brown (10YR 5/4), slightly calcareous, concretionary bands occur within the interval.

<u>INTERVAL</u>	<u>DESCRIPTION</u>
597.0' - 603.0' (6.0')	Mudstones, siltstones, and silty mudstones, greenish gray (5G 5/1), olive gray (5Y 3/1), and light gray (N7), thinly laminated to thin bedded. The siltstones are cross- to ripple-laminated and are heavily disrupted by slumps, load casts, and scour surfaces in the upper 1/3 of the interval. In the lower 2/3, the siltstones occur as individual laminations, ~2 mm thick. Several zones of silty mudstone fining upward to mudstone are present. Mud-filled burrows occasionally are present at the top of the greenish gray mudstones. The greenish gray mudstones occasionally contain oxidized plant fragments and ferruginous stains. The olive gray mudstones contain mica, anhydrite, and carbonaceous fragments. <u>Tasmanites</u> spore cases and spore resin bodies occur throughout in the mudstones, with dense concentrations present at the base of dark units. Several moderate yellowish brown (10YR 5/4), slightly calcareous concretionary bands occur within the interval. Occasional calcareous zones (<1 cm) are noted throughout in the mudstones.
603.0' - 610.0' (7.0')	Mudstones, siltstones, and silty mudstones, greenish gray (5Y 3/1), thickly laminated to thin bedded. The siltstones are cross- to ripple-laminated and occasionally contain slumps, load casts, and scour surfaces. Zones of silty mudstone fining upward to mudstone are abundant throughout. The tops of the greenish gray mudstones often contain mud-filled burrow structures. Oxidized plant fragments and ferruginous stains are also present throughout in the greenish gray mudstones. Within the olive gray mudstones, carbonaceous fragments and abundant mica and anhydrite flakes occur throughout, a single fish scale occurs at 619.5'.
610.0' - 620.0' (10.0')	Mudstones, siltstones, and silty mudstones, greenish gray (5GY 6/1), olive gray (5Y 3/1), and light gray (N7), thinly laminated to thin bedded. The siltstones are cross- to ripple-laminated and often contain slumps, load casts, and scour surfaces. Abundant zones of silty mudstones fining upward to mudstone are present throughout. Mud-filled burrow structures occur at the top of many of the greenish gray mudstones. The greenish gray mudstones also occasionally contain partially oxidized plant fragments and iron stains. The olive gray mudstones contain carbonaceous fragments, abundant anhydrite crystals and mica flakes throughout; and a fish scale at 619.5'. <u>Tasmanites</u> spore cases and spore resin bodies are present in the mudstones but are concentrated at the base of the olive gray strata. Several moderate yellowish brown (10YR 5/4), calcareous concretionary bands and several calcareous siltstone units occur throughout the interval. <u>Tasmanites</u> spore cases and resin bodies are present in dense concentrations at the base of olive gray mudstones. Occasional silty laminations (calcareous) occur throughout.

<u>INTERVAL</u>	<u>DESCRIPTION</u>
620.0' - 629.3' (9.3')	Mudstones, siltstones, and silty mudstones; greenish gray (5G 6/1), olive gray (5Y 3/1), and light gray (N7), thinly laminated to thin bedded. Mudstone is the dominant lithology. Several graded beds, silty mudstone fining upward to mudstone, are present throughout. The ripple-laminated siltstones are disrupted by slumps, load casts, and scour surfaces. Mud-filled burrow structures are present at the tops of the greenish gray mudstones. The greenish gray mudstones also contain partially oxidized plant fragments and ferruginous stains. The olive gray mudstones contain carbonaceous plant fragments, mica and anhydrite throughout; a woody stem at 628.5' and fish scales at 628.9'. <u>Tasmanites</u> spore cases and resin bodies are distributed throughout the mudstones with dense concentrations present at the contacts between the light and dark zones. A slightly calcareous concretionary band and a noncalcareous concretionary nodule, moderate yellowish brown (10YR 5/4), occur at 625.3' and 622.1', respectively. Occasional calcareous laminations occur throughout the mudstones.
629.3' - 637.9' (8.6')	Mudstones and siltstone, olive gray (5Y 3/1), greenish gray (5GY 6/1), and light gray (N7), thinly laminated to thin bedded. Mudstone is the dominant lithology in the interval, with the upper 1/3 predominantly light colored and the lower 2/3 predominantly dark colored. The greenish gray mudstones contain mud-filled burrow structures and groove casts. The light mudstones occasionally contain oxidized plant fragments and ferruginous stains; disseminated pyrite grains at 629.9'. The olive gray mudstones contain carbonaceous and partially oxidized plant fragments, anhydrite, and abundant mica. <u>Tasmanites</u> spore cases and resin bodies are distributed throughout the mudstones, with dense concentrations present at the contact between the light and dark zones. A single ripple laminated siltstone bed is present at 630.0' and is slightly calcareous.
637.9' - 648.0' (10.1')	Mudstones and siltstones, olive gray (5Y 4/1) to olive black (5Y 2/1), greenish gray (5G 6/1), and light gray (N7), thinly laminated to thin bedded. Mudstone is the dominant lithology. The siltstones are ripple-laminated and slightly disrupted by slumps and load casts. The top of the greenish gray mudstones are slightly mottled by bioturbation in the top 1/2 of the interval. The greenish gray mudstones also contain occasional partially oxidized plant fragments. The dark mudstones contain carbonaceous fragments, partially pyritized wood stems, anhydrite, and mica throughout; fish scales at 645.2'. <u>Tasmanites</u> spore cases and resin bodies occur throughout the mudstones with dense concentrations present at the contact between the light and dark zones. Pyrite occurs as disseminated grains and laminations in the lower 1/2 within the dark mudstones. The lower 1/2 of the interval is slightly calcareous in zones and around pyrite laminations.

INTERVAL	DESCRIPTION
648.0' - 658.0' (10.0')	Mudstones and siltstones, olive gray (5Y 4/1) to olive black (5Y 2/1), greenish gray (5GY 6/1), and light gray (N7), thinly laminated to thin bedded. Olive gray to olive black mudstone is the dominant lithology. The siltstones are ripple-laminated. The tops of the greenish gray mudstones occasionally are slightly mottled by mud-filled burrow structures and bioturbation. The dark mudstones contain carbonaceous fragments, anhydrite, abundant mica, and <u>Tasmanites</u> spore cases and resin bodies throughout; a single fish jaw at 650.0' and a fish scale at 654.1'. The siltstones between 653.0' and 655.0' are highly calcareous.
658.0' - 668.0' (10.0')	Mudstones and siltstones, olive gray (5Y 4/1) to olive black (5Y 2/1), greenish gray (5GY 6/1), and light gray (N7), thinly laminated to thin bedded. Color changes between the olive gray and olive black mudstones are gradational. Occasional ripple-laminated siltstones occur throughout. Mud-filled burrow structures are present in the mudstone zones within the lower 1/2. The greenish gray mudstones contain several ferruginous stains. The dark mudstones contain carbonaceous fragments, pyritized stems, occasional fish jaws and scales, abundant anhydrite and mica, and several pyritized fecal pellets. Pyrite is also present as a coating on <u>Tasmanites</u> spore cases which occur at the bases of the dark mudstones. Spore resin bodies were noted throughout in the mudstones. The siltstones are slightly calcareous.
668.0' - 673.0' (5.0')	Mudstones and siltstones, olive gray (5Y 4/1) to olive black (5Y 2/1), greenish gray (5GY 6/1), and light gray (N7), thinly laminated to thin bedded. Olive gray mudstone is the predominant lithology. Abundant thin laminations of siltstone are distributed throughout. A single thick siltstone lamination at 677.0' contains load casts. The dark mudstones contain carbonaceous fragments, pyritized woody fragments, spore resin bodies, abundant anhydrite, and mica. Pyrite is present as coatings on fecal pellets between 673.0' and 674.5', and on <u>Tasmanites</u> spore cases which are concentrated in laminations throughout the mudstones. The siltstones are very calcareous between 668.0' and 670.0'.
673.0' - 678.0' (5.0')	Mudstones and siltstones, olive gray (5Y 4/1) to olive black (5Y 2/1), greenish gray (5GY 6/1), and light gray (N7), thinly laminated to very thin bedded. Olive gray mudstone is the dominant lithology. Abundant thin laminations of siltstone are distributed throughout. The dark mudstones contain carbonaceous fragments, pyritized wood fragments, spore resin bodies, abundant anhydrite, and mica throughout,

<u>INTERVAL</u>	<u>DESCRIPTION</u>
673.0' - 678.0' (Continued)	and pyritized fecal pellets in the upper 1/2. Pyrite also occurs as coatings on <u>Tasmanites</u> spore cases which are concentrated in laminations throughout in the mudstones. The siltstones are very calcareous between 675.0' and 676.0'.
678.0' - 688.0' (10.0')	Mudstones and siltstones, olive gray (5Y 4/1) to olive black (5Y 2/1), greenish gray (5GY 6/1), and light gray (N7), thinly to thickly laminated. Bedding contacts vary from gradational between the olive gray and olive black mudstones, to sharp throughout the remainder of the interval. The siltstones occur in thin laminations. Occasional ripple laminations are present within the mudstones. The greenish gray mudstones contain ferruginous stains in the upper 1/4. The dark mudstones contain carbonaceous plant (?) fragments, pyritized woody stems, spore resin bodies, anhydrite, and abundant mica throughout; concentrated fish parts at 686.0'; a highly calcareous pyritic lens at 683.4'. Pyrite is also present in the mudstones as coatings on <u>Tasmanites</u> spore cases which occur throughout. The interval is noncalcareous except for the siltstones between 681.0' and 684.0'.
688.0' - 698.0' (10.0')	Mudstones and siltstones, olive gray (5Y 4/1) to olive black (5Y 2/1), greenish gray (5GY 6/1), and light gray (N7), thinly to thickly laminated. Olive gray to olive black mudstone is the dominant lithology. Color changes are gradational within this lithology. Siltstone usually occurs as thin laminations, however, a single thick lamination also is present at 691.5' and does contain slumps. Features present in the mudstones include: ripple laminations, a mud-filled burrow structure at 687.7', and bioturbation (mottling) at 695.0'. The dark mudstones contain pyritized woody stems, abundant spore resin bodies, anhydrite, and abundant mica; a pyritized fecal pellet at 610.1'. Pyrite was also observed as a coating on <u>Tasmanites</u> spore cases at 693.9', which occur at the base of a light mudstone. Several siltstones at 695.5' are highly calcareous.
698.0' - 708.0' (10.0')	Mudstones and siltstones, olive gray (5Y 4/1) to olive black (5Y 2/1), greenish gray (5GY 6/1), and light gray (N7), thinly to thickly laminated. The contacts between the olive gray, olive black, and greenish gray mudstones are gradational except for several greenish gray zones which have sharp basal contacts. Siltstone is present as thin laminations. Features contained in the mudstones include ripple laminations, mud-filled burrow structures, and bioturbation (mottling). Carbonaceous fragments, pyritized woody stems, spore resin bodies, anhydrite, and mica are present in the dark mudstones. Pyrite was observed as lenses at 701.2' in a dark zone, and as mineralized <u>Tasmanites</u> spore cases at the tops of several greenish gray mudstones. The siltstones in the lower 2/3 are slightly calcareous.

<u>INTERVAL</u>	<u>DESCRIPTION</u>
708.0' - 715.0' (7.0')	Mudstones and siltstones, olive gray (5Y 4/1) to olive black (5Y 2/1), greenish gray (5GY 6/1), and light olive gray (5Y 6/1), thinly to thickly laminated. Contacts between the olive gray, olive black, and greenish gray mudstones are gradational. The tops of several of the light mudstones are slightly mottled by bioturbation. Light olive gray, calcareous siltstone laminations occur between 708.0' and 708.8', and from 712.0' to 713.0'. The dark mudstones contain spore resin bodies, mica, pyrite, and occasionally anhydrite. Pyrite is present as disseminated grains throughout, as mineralized fecal pellets at 714.3' and 718.8', and as <u>Tasmanites</u> spore cases at 714.3'.
715.0' - 725.0' (10.0')	Mudstones and siltstones, olive gray (5Y 4/1) to olive black (5Y 2/1), greenish gray (5GY 6/1), and light olive gray (5Y 6/1), thinly to thickly laminated. Mudstone is the predominant lithology. Contacts between the olive gray, olive black, and greenish gray mudstones are gradational, except for several light zones which have sharp basal contacts. Some of these light zones are slightly mottled by bioturbation. Light olive gray, calcareous siltstone laminations occur between 721.5' and 722.2'. The dark zones contain spore resin bodies, carbonaceous plant (?) fragments, mica, pyrite, and occasionally anhydrite. Pyrite is present as fecal pellets between 718.4' and 718.6' and as partially pyritized stems in the dark zones.
725.0' - 735.0' (10.0')	Mudstones and siltstones, olive gray (5Y 4/1) to olive black (5Y 2/1), greenish gray (5GY 6/1), and light olive gray (5Y 6/1), thinly to thickly laminated. The contacts between the olive gray, olive black, and greenish gray mudstones are gradational, except for several greenish gray zones which have sharp contacts. A few of these sharply defined light zones are slightly mottled by bioturbation. Light olive gray, calcareous siltstone laminations are present at 726.1' and 726.2'. The dark mudstones contain spore resin bodies, carbonaceous plant (?) fragments, anhydrite, mica, and pyrite throughout. Pyrite occurs as disseminated grains and as coatings on <u>Tasmanites</u> spore cases at 728.4'.
735.0' - 740.0' (5.0')	Mudstones and siltstones, olive black (5Y 2/1) to olive gray (5Y 4/1), greenish gray (5GY 6/1), and light olive gray (5Y 6/1), thinly to thickly laminated. The contacts between the olive black, olive gray, and greenish gray mudstones are gradational except for several greenish gray zones which have sharp contacts. Several of these sharply defined zones are slightly mottled by bioturbation. Light olive gray, very calcareous siltstone laminations occur between 735.0' and 738.0'. Two olive gray limey mudstones occur between 737.1'

<u>INTERVAL</u>	<u>DESCRIPTION</u>
735.0' - 740.0' (Continued)	and 737.2' with inclusions of fragmented siltstone laminae, pyrite nodules (?), and noncalcareous mudstone laminations. The dark mudstones contain spore resin bodies, anhydrite, mica, and carbonaceous fragments throughout; fish scales at 736.2' and 737.4', and vitrinite at 736.9'.
740.0' - 745.0' (5.0')	Mudstones and siltstones, olive black (5Y 2/1) to olive gray (5Y 4/1), greenish gray (5GY 6/1), and light olive gray (5Y 6/1), thinly to thickly laminated. Contacts between the olive black, olive gray, and greenish gray mudstones are gradational except for the greenish gray zones which occasionally have sharp contacts. Several of these sharply defined zones are slightly mottled by bioturbation. Light olive gray, highly calcareous siltstone laminations occur between 742.0' and 743.0'. A single olive gray limy mudstone is present at 744.1', and contains abundant pyrite lenses and nodules. The dark mudstones contain spore resin bodies, anhydrite, mica, and carbonaceous fragments. Pyrite is present as nodules at 740.8' and 741.8' in dark mudstones, and as mineralized <u>Tasmanites</u> spore cases at 743.7' in a light mudstone. The edges of the pyrite nodules in this interval are calcareous.
745.0' - 755.0' (10.0')	Mudstones, olive black (5Y 2/1) to olive gray (5Y 4/1), and greenish gray (5GY 6/1), thinly to thickly laminated. The contacts between the olive black, olive gray, and greenish gray mudstones are gradational. The interval occasionally is slightly mottled by bioturbation. The mudstones contain carbonaceous plant (?) fragments, spore resin bodies, mica, and anhydrite. Pyrite is present throughout as calcareous lenses and nodules which are calcareous around the perimeters. Calcareous, silty (?) laminations are distributed throughout the interval.
755.0' - 765.0' (10.0')	Mudstones and siltstones, olive gray (5Y 4/1) to olive black (5Y 2/1), greenish gray (5GY 6/1), and light olive gray (5Y 6/1), thinly to thickly laminated. Contacts are gradational between the olive gray, olive black, and greenish gray mudstones, except for a few greenish gray zones with sharp contacts. Some of these sharply defined zones are slightly mottled by bioturbation. Occasionally rippled laminations are present in the mudstones. Light olive gray, calcareous siltstone laminations are present throughout, but are more concentrated in the upper 1/2, and are abundant at 757.2' and 763.0'. The dark mudstones contain carbonaceous plant (?) fragments, spore resin bodies, mica, anhydrite, and occasionally fish jaws and scales throughout; a fish-skin imprint at 756.2'. Pyrite is present in the dark mudstones as a pyritized woody stem at 759.3', and as a coating on fecal pellets at 758.3'; as a nodule at 763.9'. <u>Tasmanites</u> spore cases were noted at 756.3' in a light mudstone. A calcareous concretion occurs at 763.9'.

<u>INTERVAL</u>	<u>DESCRIPTION</u>
765.0' - 773.4' (8.4')	Mudstones, olive black (5Y 2/1) to olive gray (5Y 4/1), thinly to thickly laminated. Contacts between the mudstones are gradational. The interval is slightly mottled by bioturbation. Frequent spore resin bodies, carbonaceous plant (?) fragments, mica, and occasional fish jaws and teeth are present throughout. Pyrite occurs as nodules and fecal pellets. Silty, calcareous laminations are distributed throughout the interval.
773.4' - 784.0' (10.6')	Mudstones, olive gray (5Y 4/1) to olive black (5Y 2/1), and greenish gray (5GY 6/1), thinly laminated to thin bedded. Contacts between the olive gray, olive black, and greenish gray zones are gradational except for several sharply defined greenish gray zones. Some of these sharply defined zones are slightly mottled by bioturbation. A single rippled lamination was noted at 773.8' at the base of a light mudstone. The dark mudstones contain carbonaceous plant (?) fragments, fish scales, spore resin bodies, anhydrite, and mica throughout; conodonts at 779.9' and 776.1', and vitrinite with pyrite veins at 776.1'. Pyrite also occurs in the dark mudstones as lenses and coatings on occasional fecal pellets. The light mudstones contain pyritized <u>Tasmanites</u> spore cases. Several silty laminations in the lower 1/2 of the interval are calcareous.
784.0' - 794.0' (10.0')	Mudstones, olive black (5Y 2/1) to olive gray (5Y 4/1), and greenish gray (5GY 6/1), thinly to thickly laminated. Contacts between the olive black, olive gray, and greenish gray mudstones are gradational except for several sharply defined greenish gray zones. Some of these sharply defined light zones are slightly mottled by bioturbation. A rippled mudstone lamination is present at 784.3'. The dark mudstones also contain abundant spore resin bodies, carbonaceous plant fragments, and mica throughout, and a single fish scale at 793.2. Pyrite occasionally occurs in the dark mudstones as mineralized fecal pellets; in the light mudstones as a calcareous lamination at 791.0', as several burrows (?) at 792.3', and as coatings on <u>Tasmanites</u> spore cases. Silty calcareous laminations are present throughout the interval.
794.0' - 800.0' (6.0')	Mudstones, olive black (5Y 2/1) to olive gray (5Y 4/1), greenish gray (5GY 6/1), thinly to thickly laminated. The contacts between the olive black, olive gray, and greenish gray mudstones are gradational except for a few sharply defined greenish gray zones. The dark mudstones contain abundant spore resin bodies, carbonaceous plant fragments, anhydrite, and mica. Several fish scales were noted at 795.8' in a dark mudstone. Occasional calcareous, silty (?) laminations occur throughout.

<u>INTERVAL</u>	<u>DESCRIPTION</u>
800.0' - 807.0' (7.0')	Mudstones and siltstones, greenish gray (5GY 6/1), olive black (5Y 2/1) to olive gray (5Y 4/1), and light gray (N7), thinly laminated to thin bedded. Bedding contacts within the mudstones vary from sharp between the light and dark zones to gradational throughout the remainder of the interval. Several of the light mudstones are mottled by bioturbation. Siltstones occur throughout and are predominantly located at the base of several of the light zones. These siltstones are ripple-laminated and contain scour surfaces and sole marks. The light mudstones contain mica, <u>Tasmanites</u> spore cases, and ferruginous stains. Pyrite occurs in the light mudstones as coatings on spore cases throughout and on a stem at 801.9'. The dark mudstones contain spore resin bodies, carbonaceous plant fragments, anhydrite, and mica. A single conodont was noted at 804.4' in a dark mudstone. Occasionally the siltstones are calcareous.
807.0' - 815.0' (8.0')	Mudstones and siltstones, olive gray (5Y 4/1) to olive black (5Y 2/1), greenish gray (5GY 6/1), and light gray (N7), thinly to thickly laminated. The bedding contacts between the olive gray, olive black, and greenish gray mudstones are gradational except for several sharply defined greenish gray zones. Some of these sharply defined zones are mottled by bioturbation. The siltstones occur as laminations throughout but are more concentrated in the upper 1/2 of the interval. The thicker laminations are ripple-laminated and contain load casts. The mudstones are occasionally ripple-laminated. The dark mudstones contain carbonaceous woody fragments, fish jaws, and mica. Pyrite occurs as coatings on fecal pellets in dark mudstones, and on <u>Tasmanites</u> spore cases in light mudstones. The siltstones are calcareous.
815.0' - 822.0' (7.0')	Mudstones and siltstones, olive black (5Y 2/1) to olive gray (5Y 4/1), greenish gray (5GY 6/1), and light olive gray (5Y 6/1), thinly to thickly laminated. The contacts between the olive black, olive gray, and greenish gray mudstones are gradational except for a few sharply defined greenish gray zones. Several of these sharply defined zones are slightly mottled by bioturbation. Light olive gray, calcareous siltstone laminations occur throughout the interval. The dark mudstones contain fish jaws and teeth, carbonaceous fragments, and spore resin bodies throughout; vitrinite at 818.0'; a single conodont at 821.7'. Pyrite is more common in the dark mudstones and occurs as coatings on fecal pellets at 815.9' and 819.6', and as pyritized wood fragments at 819.6'.

<u>INTERVAL</u>	<u>DESCRIPTION</u>
822.0' - 830.0' (8.0')	Mudstones and silty mudstones, olive black (5Y 2/1) to olive gray (5Y 4/1), and greenish gray (5GY 6/1), to light greenish gray (5GY 8/1), thinly laminated to thin bedded. The contacts between the olive black, olive gray, and greenish gray mudstones are gradational except for several greenish gray zones which have sharp contacts. Some of these sharply defined light zones are mottled by bioturbation. Zones of light greenish gray silty mudstone fining upward into greenish gray mudstone are present at 822.5', 826.5', and 829.2'. A single rippled lamination was noted at 824.2' in a mudstone. The dark mudstones also contain carbonaceous woody fragments, fish jaws, spore resin bodies, and mica. The light mudstones contain several iron stains throughout, and fluorite (?) at 822.4'. Pyritized fecal pellets occur throughout. The silty mudstones are slightly calcareous. Highly calcareous, silty laminations are present throughout.
830.0' - 840.0' (10.0')	Mudstones, siltstones, and silty mudstones, olive gray (5Y 4/1) to olive black (5Y 2/1), greenish gray (5GY 6/1), light olive gray (5Y 6/1), and light greenish gray (5GY 8/1), thinly laminated to thin bedded. The contacts between the olive gray, olive black, and greenish gray mudstones are gradational except for several well defined greenish gray zones. Some of these well-defined zones are slightly mottled by bioturbation. A single thin bed at 833.1' fines upward from light greenish gray silty mudstone to greenish gray mudstone. Light olive gray, calcareous siltstone laminations occur throughout the interval. A rippled lamination was noted in mudstone at 834.9'. The dark mudstones contain carbonaceous fragments, fish jaws, spore resin bodies, mica, and pyrite. Pyrite occurs in the dark mudstones as mineralized fecal pellets and as stems at 836.8' and 838.8'; in light mudstones as coatings on <u>Tasmanites</u> spore cases at 832.9'.
840.0' - 850.0' (10.0')	Mudstones and siltstones, olive gray (5Y 4/1) to olive black (5Y 2/1), greenish gray (5GY 6/1), and light olive gray (5Y 6/1), thinly to thickly laminated. The color of the mudstones lightens down core. Bedding contacts between the olive gray, olive black, and greenish gray mudstones are gradational except for several sharply defined greenish gray zones. Some of these sharply defined zones are slightly mottled by bioturbation. A single ripple lamination occurs at 845.1' in a dark mudstone. Light olive gray, highly calcareous siltstone laminations occur throughout; siltstone content increases down core. The dark mudstones contain fish jaws, spore resin bodies, and pyritized fecal pellets. <u>Foerstia</u> fragments were noted in the dark mudstones and are concentrated in the lower 1/2 of the interval.

<u>INTERVAL</u>	<u>DESCRIPTION</u>
850.0' - 860.0' (10.0')	Mudstones and siltstones, olive gray (5Y 4/1) to olive black (5Y 2/1), greenish gray (5GY 6/1), and light olive gray (5Y 6/1), thinly laminated to thin bedded. The contacts between the olive gray, olive black, and greenish gray mudstones are gradational except for several sharply defined greenish gray zones. Some of these sharply defined zones are slightly mottled by bioturbation. Light olive gray, very calcareous siltstone laminations are present. A single ripple lamination was noted at 859.7' in a dark mudstone. The dark mudstones contain carbonaceous plant (?) fragments, spore resin bodies, anhydrite, and mica. <u>Foerstia</u> fragments are present throughout but are concentrated in the dark mudstones. <u>Tasmanites</u> spore cases occur in the light mudstones.
860.0' - 870.0' (10.0')	Mudstones and siltstones, olive gray (5Y 4/1) to olive black (5Y 2/1), greenish gray (5GY 6/1), and light olive gray (5Y 6/1), thinly to thickly laminated. The contacts between the olive gray, olive black, and greenish gray mudstones are gradational except for several sharply defined greenish gray zones. Some of these light zones are mottled by bioturbation. Occasional rippled laminations occur in the mudstones. Light olive gray, highly calcareous siltstone laminations are present throughout. Several of the siltstones contain load casts. The dark mudstones contain spore resin bodies, mica, occasional <u>Foerstia</u> fragments, carbonaceous plant fragments, and conodonts throughout; several fish teeth were noted at 862.5'. The light mudstones contain <u>Tasmanites</u> spore cases. Pyrite also occurs in the mudstones as lenses at 867.7' and 867.9', and as nodules at 869.3'.
870.0' - 880.0' (10.0')	Mudstones and siltstones, dark greenish gray (5GY 4/1), greenish gray (5GY 6/1) to greenish black (5GY 2/1), and dusky yellow (5Y 6/4), thinly laminated to very thin bedded. The contacts between the dark greenish gray, greenish gray, and greenish black mudstones are gradational except for several sharply defined greenish gray zones. Dusky yellow, calcareous siltstone laminations are present throughout; a single siltstone at 872.9' is noncalcareous. The dark mudstones contain spore resin bodies, occasional fish jaws and teeth, occasional conodonts, mica, and anhydrite throughout; a pyritized fecal pellet at 875.2'.
880.0' - 886.8' (6.8')	Mudstones and siltstones, olive gray (5Y 4/1) to olive black (5Y 2/1), greenish gray (5GY 6/1), and dusky yellow (5Y 6/4), thinly laminated to thin bedded. Contacts between the olive gray, olive black, and greenish gray mudstones are gradational except for several sharply defined greenish gray zones.

<u>INTERVAL</u>	<u>DESCRIPTION</u>
880.0' - 886.8' (Continued)	Dusky yellow siltstones occur as isolated thin, calcareous laminations. The dark mudstones contain mica, anhydrite, and spore resin bodies throughout; <u>Foerstia</u> fragments and fish jaws at 881.5' and 882.8' respectively. A single pyrite lens and an isolated fecal pellet occur in dark zones at 880.8' and 882.8'.
886.8' - 895.0' (8.2')	Mudstones and siltstones, greenish gray (5GY 6/1) to light greenish gray (5GY 8/1), olive black (5Y 2/1) to olive gray (5Y 4/1), and yellowish gray (5Y 8/1), thinly laminated to thin bedded. Several heavily bioturbated zones are present in the mudstones. The yellowish gray siltstones occur as thin laminations and are occasionally ripple-laminated. The ripple-laminated siltstones contain several load casts. The siltstones are heavily calcareous throughout the interval. The light mudstones contain ferruginous stains and <u>Tasmanites</u> spore cases at their upper contacts. The dark mudstones contain spore resin bodies and anhydrite throughout. The mudstones contain mica and pyrite; pyrite is present as irregular nodules and laminations.
895.0' - 902.0' (7.0')	Mudstones, greenish gray (5GY 6/1) to light greenish gray (5GY 8/1), and olive black (5Y 2/1) to olive gray (5Y 4/1), thinly laminated to thin bedded. The interval contains definite light and dark mudstones, however, the color changes within these zones are gradational. Zones of bioturbation occur throughout. A rippled lamination occurs at 895.1' in a light mudstone. The dark mudstones contain spore resin bodies throughout; a tree branch cast and a fish tooth at 898.1' and 901.9' respectively. The light mudstones contain ferruginous stains and pyrite. Pyrite occurs in the light zones as nodules, disseminated grains, laminations, and as coatings on <u>Tasmanites</u> spore cases which are concentrated at the top of the light zones. Occasional calcareous stringers are present in the dark mudstones.
902.0' - 910.0' (8.0')	Mudstones and wackestones, olive gray (5Y 4/1) to olive black (5Y 2/1), and greenish gray (5GY 6/1), thickly laminated to thin bedded. Contacts between the olive gray, olive black, and greenish gray mudstones are gradational. Several bioturbated zones are present in the interval. An olive gray lime mudstone containing several calcareous stringers occurs from 902.9' to 904.3'. The dark mudstones contain fish jaws, teeth and scales, carbonaceous plant (?) fragments, <u>Foerstia</u> fragments, mica, anhydrite, and several pyrite nodules throughout. <u>Tasmanites</u> spore cases occur at the top of several of the light mudstones. Calcareous stringers are present in some of the dark zones.

<u>INTERVAL</u>	<u>DESCRIPTION</u>
910.0' - 920.0' (10.0')	Mudstones and siltstones, olive gray (5Y 4/1) to olive black (5Y 2/1), light olive gray (5Y 6/1), and dusky yellow (5Y 6/4), thinly to thickly laminated. Color changes in the mudstones are gradational with the dark colors predominating. Several bioturbated zones are present. The dusky yellow siltstones occur as laminations which are often ripple laminated. The ripple-laminated siltstones contain slump features. Most of the siltstones are calcareous. The dark zones contain fish jaws and scales, occasional <i>Foerstia</i> fragments, spore resin bodies, carbonaceous plant (?) fragments, mica, anhydrite, and pyrite throughout; bone fragments at 912.6'. Pyrite occurs throughout in dark zones as nodules and mineralized fecal pellets, and as a lens and a graded lamination at 919.6' and 917.0', respectively.
920.0' - 929.9' (9.0')	Mudstones and siltstones, olive gray (5Y 4/1) to olive black (5Y 2/1), light olive gray (5Y 6/1), and dusky yellow (5Y 6/4), thinly laminated to thin bedded. The contacts between the olive gray, olive black, and light olive gray mudstones are gradational except for several light olive gray zones with sharp contacts. These light mudstones are mottled by bioturbation. The laminated dusky yellow siltstones are calcareous, ripple-laminated, and contain load casts. The dark mudstones contain small vitrinite (?) fragments, fish scales, mica, biotite, and anhydrite throughout; concentrated fish parts at 922.8'. Pyrite occurs in the dark zones as nodules, mineralized pellets, lenses, and laminations. Some of the pyritized units are calcareous.
929.9' - 941.1' (12.1')	Mudstones and siltstones, olive gray (5Y 4/1) to olive black (5Y 2/1), greenish gray (5GY 6/1) to light greenish gray (5GY 8/1), and dusky yellow (5Y 6/4), thinly laminated to thin bedded. Contacts are sharp between the light and dark mudstones but gradational within these zones. Mudslumps, bioturbation, and fragmented bedding occur in the mudstones between 932.2' and 932.8'; bioturbated zones occur throughout. Dusky yellow, calcareous siltstone laminations occur throughout the interval; some laminations contain load casts. The dark mudstones contain mica and anhydrite throughout, and vitrinite at 929.2'. <i>Tasmanites</i> spore cases, spore casts, and spore resin bodies are present in the mudstones. Pyrite occurs as nodules, mineralized fecal pellets, and laminations throughout the dark zones; as disseminated grains and mineralized burrows in the light zones. Several of the pyritized units are calcareous.

<u>INTERVAL</u>	<u>DESCRIPTION</u>
941.1' - 951.0' (9.9')	Mudstones and siltstones, olive gray (5Y 4/1) to olive black (5Y 2/1), light olive gray (5Y 6/1), and dusky yellow (5Y 6/4), thinly to thickly laminated. Dark mudstone is the dominant lithology. Contacts between the olive gray, olive black, and light olive gray mudstones are gradational. Dusky yellow, calcareous siltstone laminations are present. Dark mudstones containing pyrite, anhydrite, mica, spore resin bodies, and biotite occur throughout. Vitrinite is present at 941.8'. Pyrite is present in the dark mudstones as irregular nodules and laminations. Several of the pyritic laminations are also calcareous.
951.0' - 958.7' (7.7')	Mudstone, olive gray (5Y 4/1) to olive black (5Y 2/1), and greenish gray (5GY 8/1), thickly laminated to thin bedded. Sharp contacts occur between the light and dark mudstones; gradational contacts occur throughout the remainder of the interval. Mudslumps, mud-filled burrow structures, and zones of bioturbation are present within the interval. The dark mudstones contain spore resin bodies, vitreous plant fragments, pyrite, and mica throughout; vitrinite and a single conodont at 953.0' and 952.4', respectively. Pyrite occurs within the dark zones as irregular nodules and laminations. Partially oxidized plant fragments were noted at 956.4' in a light mudstone. Several calcareous stringers are present throughout the dark zones.
958.7' - 967.0' (8.3')	Mudstones, olive gray (5Y 4/1) to olive black (5Y 2/1), and greenish gray (5GY 6/1) to light greenish gray (5GY 8/1), thinly laminated to thin bedded. Bedding contacts vary from sharp between several of the light and dark zones to gradational throughout the remainder of the interval. Bioturbation and mudslumps are present throughout the interval; a mud-filled burrow structure is present at 962.9'. The dark mudstones contain spore resin bodies, several carbonaceous plant (?) fragments, mica, and biotite throughout, and several conodonts at 964.5'. The light mudstones contain partially oxidized plant fragments and iron stains. Pyrite occurs throughout as laminations in the dark mudstones; as burrows and disseminated grains in the light mudstones. The light zones in the upper 1/2 of the interval are calcareous; highly calcareous lenses and stringers are present throughout.
967.0' - 975.2' (8.2')	Mudstones, olive gray (5Y 4/1) to olive black (5Y 2/1), and greenish gray (5GY 6/1) to light greenish gray (5GY 8/1), thinly laminated to thin bedded. Bedding contacts vary from sharp between several of the light and dark mudstones to gradational throughout the remainder of the interval. Several heavily bioturbated zones occur throughout the

<u>INTERVAL</u>	<u>DESCRIPTION</u>
967.0' - 975.2' (Continued)	mudstones. The dark mudstones contain spore resin bodies, mica, biotite, and anhydrite; vitrinite at 975.2'. The light mudstones contain partially oxidized plant stems and iron stains. Pyrite occurs as small nodules, laminations, and mineralized fecal pellets throughout the dark mudstones; as burrow structures, disseminated grains, and partially pyritized stems in the light mudstones. Most of the light zones and pyritic units contained within these zones are calcareous.
975.2' - 985.0' (9.8')	Mudstones, greenish gray (5GY 6/1) to light greenish gray (5GY 8/1), olive black (5Y 2/1) to olive gray (5Y 4/1), and light olive gray (5Y 6/1), thinly laminated to thick bedded. The bedding contacts vary from sharp between several of the light and dark zones to gradational throughout the remainder of the interval. Several heavily bioturbated zones occur throughout. The light mudstones contain partially oxidized plant fragments, iron stains, and pyrite throughout, a single bone fragment at 977.5'. Pyrite occurs as burrow structures in the light zones, laminations in the dark zones, and as nodules throughout. Several of the pyritic units are calcareous. Several olive gray, highly calcareous concretionary bands are present in the light mudstones. Most of the light mudstones are calcareous.
985.0' - 995.0' (10.0')	Mudstones, greenish gray (5GY 6/1) to light greenish gray (5GY 8/1), and olive black (5Y 2/1) to olive gray (5Y 4/1), thinly laminated to thick bedded. The bedding contacts vary from sharp between several light and dark mudstones to gradational throughout the remainder of the interval. Mudslumps and zones of bioturbation occur throughout. The light mudstones contain partially oxidized plant fragments, mud-filled burrow structures, iron stains, and pyrite. The dark mudstones contain spore resin bodies, mica, and pyrite throughout. Pyrite occurs in burrows and as disseminated grains in the light zones, and as laminae in the dark zones; most of the pyritic units are calcareous. Several dark yellowish orange (10YR 6/6), slightly calcareous concretionary bands occur near the center of the interval; a single light olive gray (5Y 6/1), very calcareous concretionary band occurs at 981.1'. The light mudstones in the bottom 1/4 are calcareous.
995.0' - 1,005.0' (10.0')	Mudstones, olive black (5Y 2/1) to olive gray (5Y 4/1), and greenish gray (5GY 6/1) to light greenish gray (5GY 8/1), thickly laminated to thin bedded. Bedding contacts are sharp between several of the light and dark mudstones. Zones containing heavy bioturbation and mudslumps are present.

<u>INTERVAL</u>	<u>DESCRIPTION</u>
995.0' - 1,005.0' (Continued)	The dark mudstones contain spore resin bodies, carbonaceous plant fragments, and mica; vitrinite appears at 993.3' and 998.5'. Iron stains are commonly present in the light mudstones. Pyrite occurs as irregular nodules and laminations throughout the dark mudstones.
1,005.0' - 1,015.0' (10.0')	Mudstones, olive black (5Y 2/1) to olive gray (5Y 4/1), and greenish gray (5GY 6/1) to light greenish gray (5GY 8/1), thickly laminated to thick bedded. Bedding contacts between several of the light and dark mudstones are sharp with gradational color variations occurring within these zones. Zones containing heavy bioturbation and mudslumps are present throughout. A zone (3 mm thick) containing coarse sand grains is present at 1,012.8'. The dark mudstones contain mica and pyrite. The light mudstones contain pyrite throughout and an unidentified shell imprint, and an ostracod occurs at 1,007.7'. Pyrite occurs on <u>Tasmanites</u> spore cases and as disseminated grains in the light mudstones; as laminations, small nodules, and fecal pellets in the dark mudstones. A pyritized burrow structure at 1,012.0' occurs on a bedding contact between a light and dark zone.
1,015.0' - 1,025.0' (10.0')	Mudstones and siltstones, olive black (5Y 2/1) to olive gray (5Y 4/1), greenish gray (5GY 6/1) to light greenish gray (5GY 8/1), and light olive gray (5Y 6/1), thinly laminated to thin bedded. Contacts between several of the light and dark mudstones are sharp with gradational color changes occurring within these zones. Zones containing heavy bioturbation and mudslumps are present throughout. A light olive gray siltstone band (3 mm thick) occurs at 1,017.3'; it is ripple-laminated, highly calcareous, and contains load casts. The dark mudstones contain spore resin bodies, mica, and pyrite (as nodules and laminations) throughout. The light mudstones contain iron stains and pyrite (as burrow structures and disseminated grains) throughout. Several of the pyritic units are calcareous. Frequently the light mudstones are calcareous. The dark mudstones between 1,017.0' and 1,018.0' are highly calcareous.
1,025.0' - 1,034.7' (9.7')	Mudstones, olive black (5Y 2/1) to olive gray (5Y 4/1), greenish gray (5GY 6/1), and light olive gray (5Y 6/1), thickly laminated to thin bedded. Bedding contacts between several of the light and dark mudstones are sharp with gradational color changes occurring within these zones. Zones containing heavy bioturbation and mudslumps are present throughout the interval. The dark mudstones contain spore resin bodies, pyrite, and mica. The light mudstones contain partially oxidized plant fragments, pyrite, and iron stains. Pyrite is present as burrow fillings and disseminated grains throughout in the light mudstones; as mineralized <u>Tasmanites</u> spore cases at the tops of light zones at 1,031.3' and 1,034.2'.

<u>INTERVAL</u>	<u>DESCRIPTION</u>
1,034.7' - 1,035.7' (1.0')	Lime mudstone, light greenish gray (5GY 8/1), greenish gray (5GY 6/1), light olive gray (5Y 6/1), and yellowish gray (5Y 8/1), thin bedded. Color changes in this interval are gradational. Calcite-filled veins are present. Pyrite occurs as vein-fillings along with calcite, and as small irregular nodules.
1,035.7' - 1,040.0' (4.3')	Mudstones, greenish gray (5GY 6/1) to light greenish gray (5GY 8/1), olive black (5Y 2/1) to olive gray (5Y 4/1), and light olive gray (5Y 6/1), thickly laminated to thin bedded. Bedding contacts vary from sharp between several of the light and dark mudstones to gradational throughout the remainder of the interval. Zones containing heavy bioturbation and mudslumps occur throughout. The light mudstones contain partially oxidized plant fragments and pyrite. The dark mudstones contain spore resin bodies and pyrite. Pyrite occurs in the light zones as burrow fillings; in the dark zones as irregular nodules and laminations. Most of the light zones are calcareous.
1,040.0' - 1,050.0' (10.0')	Mudstones, olive black (5Y 2/1) to olive gray (5Y 4/1), light olive gray (5Y 6/1), and greenish gray (5GY 6/1), thickly laminated to thin bedded. Bedding contacts vary from sharp between several of the light and dark zones to gradational throughout the remainder of the interval. Zones containing heavy bioturbation and mudslumps are present throughout. The dark mudstones contain mica. The light mudstones contain <u>Tasmanites</u> spore cases and slickensided surfaces throughout; a <u>Lingula</u> (?) shell fragment and a vitreous fragment encased in pyrite at 1,046.5'. Pyrite occurs in the light zones as spore case coatings; in the dark zones as irregular nodules and laminations. A single olive gray, calcareous concretionary band is present from 1,043.9' to 1,044.9'.
1,050.0' - 1,055.3' (5.3')	Mudstones, olive gray (5Y 4/1), light olive gray (5Y 6/1), and olive black (5Y 2/1), thickly laminated to thick bedded. Bedding contacts are gradational; dark mudstone is the dominant lithology. The light mudstones are heavily disrupted by bioturbation and mudslumps. The dark mudstones contain spore resin bodies, conodonts, carbonaceous plant fragments, mica, pyrite, and anhydrite throughout; vitrinite appears at 1,054.4'. Pyrite occurs as laminations and irregular nodules in the dark zones.

<u>INTERVAL</u>	<u>DESCRIPTION</u>
1,055.3' - 1,066.3' (11.0')	Mudstones, greenish gray (5GY 6/1) to light greenish gray (5GY 8/1), and olive black (5Y 2/1) to olive gray (5Y 4/1), thickly laminated to thin bedded. Bedding contacts vary from sharp between several of the light and dark mudstones to gradational in the remainder of the interval. Zones containing heavy bioturbation and mudslumps are present in the interval. The light mudstones contain partially oxidized plant fragments, iron stains, and pyritized burrows throughout; a <u>Lingula</u> fossil at 1,064.3'. The dark mudstones contain conodonts, carbonaceous plant fragments, anhydrite, and mica throughout. Pyritized burrows (1 mm to 5 cm thick) present in the light mudstones are moderately calcareous.
1,066.3' - 1,074.0' (7.7')	Mudstones, olive black (5Y 2/1) to olive gray (5Y 4/1), greenish gray (5GY 6/1), and light olive gray (5Y 6/1), thickly laminated to thin bedded. Bedding contacts between the light and dark mudstones are disrupted by bioturbation and mudslumps. Mud-filled burrow structures occur throughout. The dark mudstones contain spore resin bodies, conodonts, carbonaceous fragments, pyrite and mica; vitrinite at 1,072.7'. Occasional <u>Lingula</u> fossils are present in the mudstones. Pyrite occurs in the dark zones as mineralized fecal pellets, nodules, and laminations; in the light zones as several pyritized burrow structures.
1,074.0' - 1,078.2' (4.2')	Mudstones and siltstone, olive gray (5Y 4/1) to olive black (5Y 2/1), light olive gray (5Y 6/1), and very light gray (N8), thinly laminated to thin bedded. Contacts between the olive gray, olive black, and light olive gray mudstones are gradational. The light mudstones are disrupted by bioturbation. A single very light gray siltstone, ~3 mm thick, occurs at 1,074.8'. This siltstone is ripple-laminated and contains load casts. The dark mudstones contain spore resin bodies, mica, anhydrite, and conodonts throughout; quartz (?) and vitrinite at 1,077.0' and 1,077.4', respectively.
1,078.2' - 1,079.0' (0.8')	Lime mudstone, light olive gray (5Y 6/1), to olive gray (5Y 4/1), thin bedded. This unit contains gradational color variations. An unidentified shell fragment and carbonaceous plant fragment are noted at 1,078.8'. Spore resin bodies are present at 1,078.85'. A small calcite concretion occurs at 1,078.8'. Pyrite is present as calcified nodules and disseminated grains.
1,079.0' - 1,088.0' (9.0')	Mudstones, olive gray (5Y 4/1) to olive black (5Y 2/1), light olive gray (5Y 6/1), and medium light gray (N6), thinly laminated to thin bedded. Bedding contacts vary from sharp between several of the light and dark mudstones to gradational throughout the remainder of the interval. Light mudstone

<u>INTERVAL</u>	<u>DESCRIPTION</u>
1,079.0' - 1,088.0' (continued)	content increases down core. The interval is disrupted by zones of bioturbation. The light olive gray mudstones from 1,087.3' to 1,087.9' contain abundant mud-filled burrow structures which are medium light gray in color. A slickensided curvilinear fracture is noted at 1,087.9' in a light mudstone. The dark mudstones contain spore resin bodies, carbonaceous plant fragments, conodonts, mica, and pyrite throughout; and vitrinite at 1,085.7'. Pyrite is present in the dark zones as laminations, concentrations of disseminated grains, mineralized fecal pellets and nodules; in the light mudstones as mineralized burrow structures. The light zones in the upper 1/2 are calcareous.
1,088.0' - 1,090.0' (2.0')	Mudstones and silty mudstones, grayish black (N2) and olive black (5Y 2/1), thickly laminated to very thin bedded. Laminae of disseminated pyrite grains are present throughout the interval. Bitumen fragments occur at 1,089.4' and 1,089.6'. The lower 0.2' grades into lighter mudstone, dark greenish gray (5GY 4/1). The interval is noncalcareous and devoid of biogenic structures.
1,090.0' - 1,097.4' (7.4')	Mudstones and silty mudstones, greenish gray (5GY 6/1 and 5G 6/1), thinly laminated to thin bedded. Sparse laminae of disseminated pyrite grains, pyritized spore bodies, and pyrite nodules (<.05' diam) are present throughout the interval. Carbonaceous plant fragments occur rarely in the upper 1/2. A calcareous, siltstone, septarian concretion is present from 1,091.3' to 1,091.6'. The core is thinly banded near the center 1/3. The interval is slightly calcareous.
1,097.4' - 1,103.0' (5.6')	Mudstones and silty mudstones, dark greenish gray (5GY 4/1) and greenish gray (5GY 6/1), thinly laminated to thin bedded. Numerous olive black (5Y 2/1) mudstone laminations occur within the lighter mudstones. Laminae of disseminated pyrite grains and small nodules are present throughout the interval. Pyritized burrow fillings occur between 1,097.4' and 1,097.7'. A bituminous wood fragment (1,097.8') and unidentified fossils (1,100.2') are also present. Soft-sediment deformation features occur at some of the darker mudstone interfaces. A small calcareous concretion is present between 1,102.4' and 1,102.7'. The core is slightly calcareous in zones.
1,103.0' - 1,108.1' (5.1')	Mudstones, silty mudstones, and siltstones, dark greenish gray (5GY 4/1), olive black (5Y 2/1), and greenish gray (5GY 6/1), thinly laminated to thin bedded. The olive black mudstones occur as mottling and burrow fillings in the greenish gray mudstones. A calcareous silty band is present between 1,106.4' and 1,106.8'. Sparse carbonaceous plant fragments occur throughout. Siltstone laminations and pyrite-filled burrows are present in the lower 0.8'. The core is noncalcareous.

<u>INTERVAL</u>	<u>DESCRIPTION</u>
1,108.1' - 1,112.7' (4.6')	Mudstones and silty mudstones, dark greenish gray (5GY 4/1), greenish gray (5GY 6/1), and dark gray (N3), thinly laminated. The dark greenish gray mudstones occur as laminations and thin bands in the lighter mudstones. Mottling, intermittent planar laminae and slight bioturbation is present at some of the interfaces. Sparse carbonaceous plant fragments occur throughout the interval. Pyrite (arsenopyrite 1,111.9') is present as both nodules and burrow fillings. Calcareous laminations are present between 1,111.7' and 1,112.1'.
1,112.7' - 1,128.0' (15.3')	Mudstones and silty mudstones, dark greenish gray (5GY 4/1), medium dark gray (N4), and greenish gray (5GY 6/1), thin to thickly laminated. The darker mudstones occur as laminations and thin bands throughout the interval. Calcareous, silt-filled burrows are present in thick (>1.0') zones and appear to be restricted to the greenish gray mudstones. A few carbonaceous plant fragments and pyritized burrows are present within the interval. Waveform pyrite occurs at various interfaces. A coal flanked, pyritized burrow is present at 1,112.8'. The interval is slightly calcareous in zones.
1,128.0' - 1,137.3' (9.3')	Mudstones and silty mudstones, dark greenish gray (5GY 4/1), dark gray (N3), and greenish gray (5GY 6/1), thinly to thickly laminated. The darker mudstones are present as laminations and bands within the interval. Sparse pyritized and calcareous, silt-filled burrows occur in the light mudstones. Laminae of waveform pyrite are present in the dark mudstones and at various interfaces. Various carbonaceous plant fragments and glauconite and siderite-stained burrows occur throughout the interval. The core is slightly calcareous.
1,137.3' - 1,158.0' (20.7')	Mudstones and silty mudstones, dark greenish gray (5GY 4/1), medium dark gray (N4), and greenish gray (5GY 6/1), thinly laminated to thin bedded. The dark mudstones occur as thin bands and laminations. The greenish gray mudstones contain numerous calcareous, silt-filled burrows. Pyrite occurs as nodules, burrow fillings, and waveform laminae throughout the interval. A small vitrinite stringer (1,154.6') and numerous carbonaceous plant fragments (throughout) are noted. A small scour surface is present at 1,147.3'. The core is slightly calcareous.
1,158.0' - 1,166.4' (8.4')	Mudstones and silty mudstones, dark greenish gray (5GY 4/1), greenish black (5GY 2/1), and dark gray (N3), thinly laminated to thin bedded. The greenish black mudstones are present as bands and sparse laminae. Pyrite occurs as burrow fillings and a few thin laminae. Intermittent planar laminae

<u>INTERVAL</u>	<u>DESCRIPTION</u>
1,158.0' - 1,166.4' (continued)	and sparse scour surfaces occur throughout. A glauconite-rich zone is present between 1,161.0' and 1,163.0'. Numerous carbonaceous plant fragments occur throughout. The core is slightly calcareous in zones.
1,166.4' - 1,175.7' (9.3')	Mudstones and silty mudstones, dark greenish gray (5GY 4/1), medium dark gray (N4), and greenish black (5GY 2/1), thinly laminated to thin bedded. The greenish black mudstone is present as laminations and less prominent thin bands. Both pyritized and calcareous, silt-filled burrows are present throughout the interval. Sparse carbonaceous plant fragments occur within the interval. Four calcareous concretions are present in the upper 6.4'. A single, coiled ammonite is at 1,173.9'. The interval is slightly calcareous in zones.
1,175.7' - 1,186.2' (10.5')	Mudstones and silty mudstones, medium dark gray (N4) and dark greenish gray (5GY 4/1), thinly laminated to thin bedded. The dark gray mudstone occurs as gradational laminae in the upper 2.0'; the remainder is uniform in appearance. Three calcareous siltstone concretions (<.8' thick) occur within the interval. A few carbonaceous plant fragments are present throughout. Siltstone laminae and pyritized burrows occur in the upper 2.0'. The lower 7.5' is moderately calcareous.
1,186.2' - 1,200.0' (13.8')	Mudstones and silty mudstones, medium dark gray (N4) and dark greenish gray (5GY 4/1), thinly laminated to thin bedded. The core is intermittently thin bedded and uniform in appearance. Two calcareous siltstone concretions are present in the lower 4.0'. <u>Spirifer</u> brachiopods and <u>Lingula</u> sp.? occur in the upper ~8.0'. Numerous carbonaceous plant fragments are present throughout the interval. The core is slightly calcareous.
1,200.0' - 1,210.0' (10.0')	Mudstones and silty mudstones, dark gray (N3) and olive black (5Y 2/1) thinly laminated to thin bedded. Three light gray (N7) calcareous silty bands are present in the interval. <u>Stropheodonta</u> sp.? are common in the upper 4.0'. Carbonaceous plant fragments are present, but rare, in the interval. The core is calcareous and devoid of pyrite.
1,210.0' - 1,220.0' (10.0')	Mudstones and silty mudstones, medium dark gray (N4), brownish black (5YR 2/1), and olive gray (5Y 4/1), thinly laminated to thin bedded. Brachiopods (<u>Stropheodonta</u> sp?) are common throughout the interval. Carbonaceous plant fragments are present, but rare. One light gray (N7) silty band occurs between 1,217.6' and 1,217.7'. The interval is devoid of biogenic structures, sedimentary features, and pyrite. The core is calcareous.

<u>INTERVAL</u>	<u>DESCRIPTION</u>
1,220.0' - 1,230.0' (10.0')	Silty mudstones and mudstones, olive black (5Y 2/1) and olive gray (5Y 4/1), thinly laminated to thin bedded. Some mottling occurs in the lighter silty zones. Brachiopods (<u>Stropheodonta</u> sp?) are present throughout. A concretion occurs between 1,224.1' and 1,224.8'. No pyrite or plant fragments are present. The entire interval is calcareous.
1,230.0' - 1,240.0' (10.0')	Mudstones and silty mudstones, olive gray (5Y 4/1), medium dark gray (N4), and brownish black (5YR 2/1), thinly laminated to thin bedded. Sparse plant fragments occur in the lower 1/3. No biogenic structures or pyrite is present. A few fossil fragments are present in the upper 1/2. The core is calcareous.
1,240.0' - 1,250.0' (10.0')	Mudstones and silty mudstones, olive gray (5Y 4/1), brownish gray (5YR 4/1), and brownish black (5YR 2/1), thinly laminated to thin bedded. A few carbonaceous plant fragments and pyritized burrows are present in the upper 1/2. A pyritized <u>Stropheodonta</u> sp.? is present at 1,247.1'. A slightly calcareous concretion is present between 1,247.2' and 1,247.3'. The core is calcareous.
1,250.0' - 1,260.0' (10.0')	Mudstones, silty mudstones, and siltstones, olive gray (5Y 4/1), dark gray (N3), and olive black (5Y 2/1), thinly laminated to thin bedded. Sparse carbonaceous plant fragments are present throughout the interval. Two irregular siltstone lenses containing disseminated pyrite are present at 1,254.4' and 1,259.9'. A single burrow is present at 1,250.8'. The core is calcareous.
1,260.0' - 1,270.0' (10.0')	Mudstones and silty mudstones, olive gray (5Y 4/1), medium dark gray (N4), and brownish black (5YR 2/1), thinly laminated to thin bedded. Numerous brachiopod fragments and an ammonoid cast (1,265.7') are present between 1,265.0' and 1,268.0'. Carbonaceous plant fragments occur throughout. Sparse pyrite nodules occur within the interval. No biogenic structures are present. The core is slightly calcareous.
1,270.0' - 1,279.7' (9.7')	Mudstones and silty mudstones, dusky brown (5YR 2/2), olive black (5Y 2/1), and grayish brown (5YR 3/2) thinly laminated to thin bedded. The upper 5.5' and lower 2.5' are uniform in appearance; the remainder being composed of laminated medium light gray (N6) and olive gray (5Y 4/1) mudstone. Numerous carbonaceous plant fragments are present throughout. Laminae of disseminated pyrite grains, nodules, lenses, and burrow fillings occur within the interval. The core becomes darker and contains more silt near the bottom. The core is calcareous in zones.

INTERVALDESCRIPTION

1,279.7' - 1,280.7'
(1.0')

Wackestone, light olive gray (5Y 6/1) and brownish gray (5YR 4/1), thin bedded and massive in appearance. Sparse silty laminae are present throughout. The upper contact is an erosional unconformity containing small pyrite nodules. No fossils or biogenic structures are present.

APPENDIX B

SYMBOLS, TERMS, AND ABBREVIATIONS USED
IN FRACTURE LOGGING

EGSP-OHIO #5 WELL - LORAIN COUNTY



1. CHARACTER: Specifically, the character of the fracture plane.

(P): Planar
(CP): Curvilinear

2. FRACTURE TYPE: These terms are used to classify the different types of fractures into genetic groups.

(N): Natural

Spl. Jt. (Simple Joint): One discrete fracture plane, no displacement.

Cpd. Jt. (Compound Joint): Two or more parallel, closely spaced (approximately 1 cm or less) fracture planes, no displacement.

Flt. (Fault): A shear fracture with demonstrable displacement indicated by displaced primary features or slickensides.

Mc. Flt. (Micro-Fault): A small-scale shear fracture, generally curvilinear; of the same order of size as the core diameter.

(CI): Coring Induced

PF (Petal Fracture): An oblique fracture, usually planar or slightly curvilinear, which originates at the core margin and terminates against bedding within the core.

PFC (Petal-Centerline Fracture): A fracture originating as a petal fracture which curves down-core and bisects the core as a vertical planar fracture. The strike of the vertical fracture and the petal fracture is identical. The face of the vertical fracture is characterized by regularly spaced arrest lines, convex down-core and symmetrical about the core axis.

DF (Disc Fracture): A subhorizontal fracture originating within the core and displaying hackle plumes radiating from the fracture origin to meet the core margin orthogonally.

- TF (Torsional Fracture): A spiraling or irregular fracture developed when a couple is applied to the core.
- DCS (Disc Fracture with Circular Slickensides): A feature induced by coupling of the inner and outer core barrels, causing core in the barrel to rotate against a stationary core stump.
- KES (Knife Edge Spall): A fracture, typically conchoidal, formed by scribe knives cutting orientation grooves into the core. This fracture type can be used to determine the down-core direction and the relative age of induced fractures.
- CBS (Core Bit Spall): A tiny conchoidal fracture caused by a diamond from the core bit plucking a chip off the edge of a preexisting fracture. When the face of the preexisting fracture is viewed with the core in normal position the spalls should appear along the right-hand margin. This fracture type is useful in inferring relative fracture chronology.

3. FRAC TOGRAPHIC FEATURES:

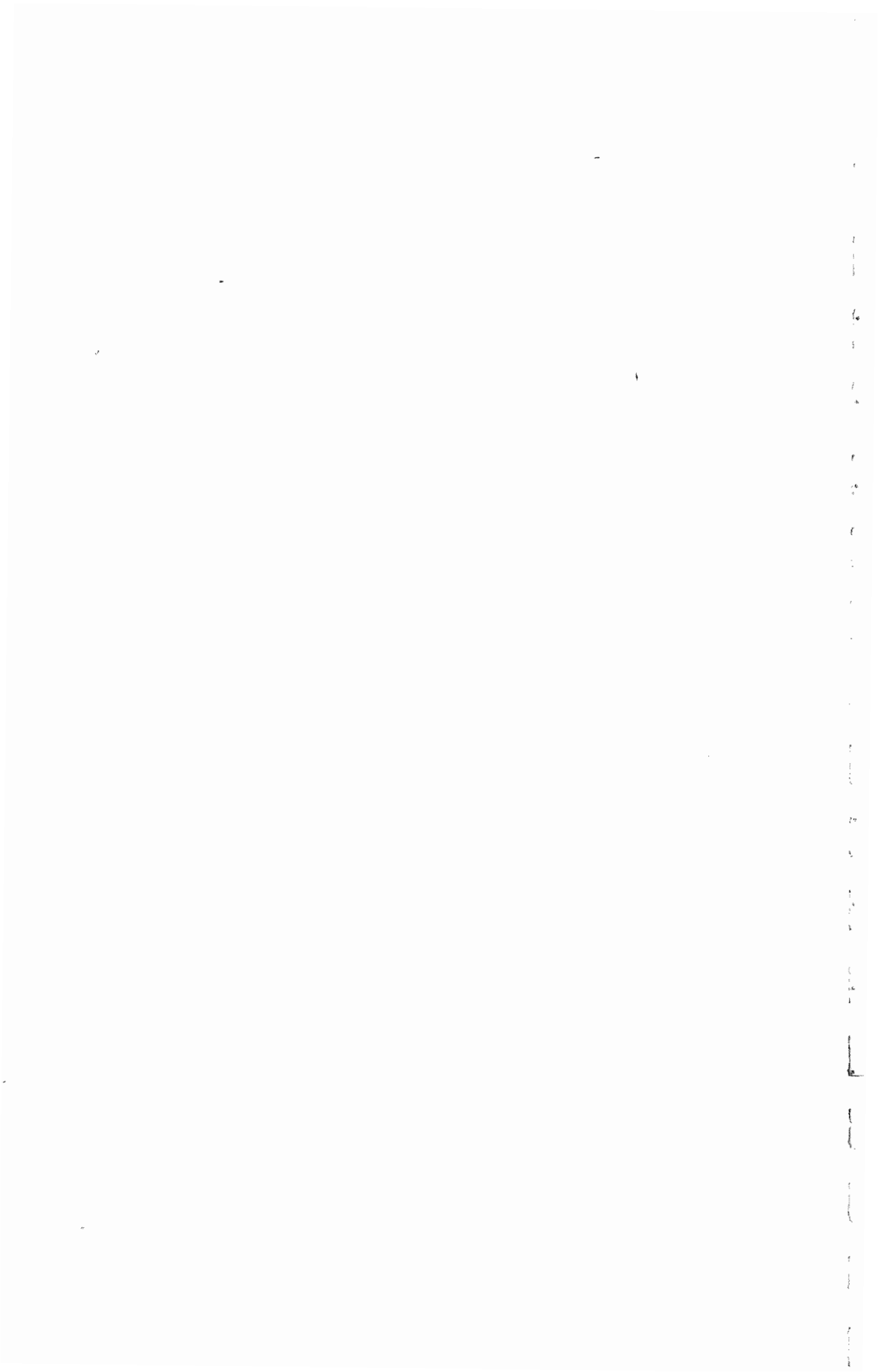
- Org. (Fracture Origin): A discrete fracture surface irregularity from which hackles originate. Fractures may originate at the boundaries of fossils, concretions, preexisting fractures, etc.
- Hkl. (Hackle): A linear marking on a fracture face, similar to a striation, which trends in the direction of fracture propagation. Hackles radiate away from the origin, are perpendicular to arrest lines, and will curve to meet preexisting surfaces orthogonally.
- Fn. Hkl. Plm. (Fine Hackle Plume): A very fine, wispy plumose structure on an otherwise featureless fracture face.
- Incl. Hkl. (Inclusion Hackle): A hackle trailing an inclusion or obstacle on the fracture plane.
- Cs. Tw. Hkl. (Coarse Twist Hackle): A hackle composed of discrete steps generally appearing as a fringe near the edge of of a fracture face.
- Ar. Ln. (Arrest Line): A crescentic feature with a cusp-like profile which marks the still stand of the fracture front. Two types are noted:
 Term. Ar. Ln.: Terminal Arrest Lines.
 Int. Ar. Ln.: Intermediate Arrest Lines.

- Hk. (Hook): The curving of a fracture plane to adjust to a change in the stress field orientation. Fractures hook to meet preexisting free surfaces orthogonally and in the vicinity of the neutral axis developed in bending.
4. TERMINATIONS: These terms are used to describe how a fracture terminates. The upper entry depicts the upper termination, the lower entry depicts the lower.
- M: The fracture exits the margin of the core.
- Ⓜ : A subhorizontal fracture that exits the margin of the core. This symbol is entered only once straddling the dividing line.
- : A fracture that terminates within the core as a dying hairline fracture.
- ↗ : The upper and lower extents of the fracture die out within the core. This symbol is drawn straddling the dividing line.
- ?: Missing or disrupted core prohibits observation of the mode of termination.
- ?/M: Same as above, but the fracture probably exits the core margin.
- ?/ Ⓞ : Same as above, but the fracture probably terminates within the core margin.
- BDG: The fracture terminates along a conspicuous bedding plane indicating an abrupt change in lithology.
- TAL: The fracture terminates as a terminal arrest line which is visible only on the fracture face.
- ⓉAL : The fracture terminates in a terminal arrest line so that the fracture enters one side of the core but does not exit the other. This symbol is entered only once straddling the dividing line.
- F22: This symbol is used when one fracture terminates against another (i.e., fracture 23 terminates against fracture 22).

APPENDIX C

FRACTURE LOGS

EGSP-OHIO #5 WELL - LORAIN COUNTY



EGSP STANDARD CORE FRACTURE LOGGING FORMAT

CORING RUN NO.(S) ALL
 (INDICATE BEGINNING & END)
 CORING DATE: 9/79
 LOG DATE: 3/80

PAGE 1 OF 1
 LOG CLASSIFICATION
 INDIVIDUALS
 INTERV.
 FRACTURE TYPE(S): CI

WELL: EGSP OHIO-5 LORAIN CO.

NUMBER	DEPTH EXTENT	LENGTH	LITHOLOGY	TERMINATIONS	CHARACTER	STRIKE DIP	INTERPRETATION	FRACTURE TYPE	MINERALIZATION	SLICKENSIDES	FRACTOGRAPHIC FEATURES	COMMENTS
1	472.6		Silty Mdst, dk grnsh (5G4/1)	(M)	P		CI	DCS	NONE	NONE		
2	480.0		Silty Mdst, dk Grnsh Grx (5G7/1)	(M)	P		CI	DCS				
3	492.3		Silty Mdst, Grnsh Grx (5G7/1)	(M)	P		CI	DCS				
4	493.0		Silty Mdst, dk Grnsh Grx (5G7/1)	(M)	P		CI	DCS				
5	493.5		Silty Mdst, Lt. ol. Grx (5Y6/1)	M	CP		CI	TF				
6	502.1		A/A	M	CP		CI	TF				
7	550.5		Silty Mdst, dk Grnsh Grx (5G7/1)	M	CP		CI	TF				
8	564.8		A/A	(M)	P		CI	DCS				
9	627.0		Silty Mdst, dk Grnsh Grx (5G7/1)	M	CP		CI	TF				
10	662.7		Silty Mdst, dk Grnsh Grx (5G7/1)	M	CP		CI	TF				
11	667.4		A/A	(M)	P		CI	DCS				
12	726.7		Silty Mdst, ol. blk (5Y2/1)	(M)	P		CI	DCS				
13	784.7		A/A	(M)	P		CI	DCS				
14	815.0		Silty Mdst, dk Grnsh Grx (5G7/1)	M	CP		CI	TF				
15	824.8		Silty Mdst, ol. blk (5Y2/1)	M	CP		CI	PF				
16	843.1		Silty Mdst, brnsh blk (5YR2/1)	M	CP		CI	TF				
17	846.3		Silty Mdst, ol. blk (5Y2/1)	M	CP		CI	TF				
18	889.3		Silty Mdst, dk Grnsh Grx (5G7/1)	(M)	P		CI	DCS				
19	941.9		Silty Mdst, Grnsh blk (5G2/1)	M	CP		CI	TF				
20	960.1	19'	Silty Mdst, Grnsh blk (112)	M	CP		CI	KES				
21	970.7	19'	A/A	M	CP		CI	KES				
22	972.2		A/A	M	CP		CI	TF				
23	1020.9		Silty Mdst, Grnsh blk (112)	(M)	P		CI	DCS				
24	1257.1		Silty Mdst, ol. blk (5Y4/1)	M	CP		CI	TF				

FF-58

EASTERN GAS SHALES PROJECT
DISC FRACTURE FREQUENCY LOG
OHIO #5 - LORAIN COUNTY, OHIO

<u>Feet</u>	<u>Freq/ Foot</u>	<u>Feet</u>	<u>Freq/ Foot</u>	<u>Feet</u>	<u>Freq/ Foot</u>	<u>Feet</u>	<u>Freq/ Foot</u>
400	7.8	620	5.8	840	2.4	1,060	2.4
405	8.4	625	6.6	845	2.2	1,065	3.6
410	3.4	630	5.4	850	1.6	1,070	1.8
415	4.2	635	4.2	855	2.0	1,075	2.0
420	7.0	640	6.2	860	2.2	1,080	1.8
425	9.2	645	3.6	865	3.0	1,085	2.4
430	9.0	650	2.4	870	2.0	1,090	2.2
435	8.8	655	5.0	875	2.0	1,095	2.2
440	4.4	660	4.2	880	2.2	1,100	3.2
445	6.0	665	3.2	885	1.8	1,105	2.8
450	9.2	670	3.6	890	2.6	1,110	2.0
455	10.0	675	3.8	895	2.4	1,115	2.2
460	7.8	680	2.8	900	3.6	1,120	2.0
465	10.8	685	3.6	905	2.4	1,125	2.8
470	8.0	690	4.0	910	2.2	1,130	3.2
475	5.8	695	4.0	915	2.0	1,135	3.8
480	7.0	700	3.0	920	1.6	1,140	3.2
485	6.8	705	2.8	925	2.4	1,145	2.4
490	7.4	710	2.4	930	2.2	1,150	2.6
495	5.4	715	2.8	935	1.6	1,155	3.2
500	5.4	720	2.6	940	2.2	1,160	3.4
505	4.4	725	3.4	945	1.8	1,165	3.0
510	4.6	730	2.4	950	1.8	1,170	2.4
515	5.8	735	3.2	955	1.8	1,175	2.6
520	5.0	740	2.2	960	2.2	1,180	3.6
525	4.0	745	2.8	965	2.2	1,185	2.2
530	5.8	750	2.4	970	2.6	1,190	2.4
535	6.2	755	2.6	975	2.6	1,195	2.8
540	6.0	760	2.4	980	2.2	1,200	5.6
545	6.6	765	2.4	985	2.0	1,205	6.0
550	8.2	770	2.6	990	2.4	1,210	4.8
555	6.6	775	2.6	995	1.8	1,215	4.4
560	6.0	780	3.4	1,000	2.2	1,220	3.2
565	4.8	785	2.0	1,005	2.0	1,225	4.8
570	7.2	790	1.8	1,010	1.4	1,230	6.2
575	5.4	795	2.0	1,015	1.4	1,235	5.0
580	8.8	800	3.2	1,020	1.8	1,240	3.4
585	5.6	805	1.6	1,025	2.4	1,245	3.4
590	4.6	810	2.4	1,030	2.4	1,250	2.6
595	6.0	815	2.4	1,035	2.4	1,255	3.0
600	7.2	820	2.8	1,040	2.2	1,260	2.6
605	4.6	825	2.2	1,045	2.2	1,265	3.8
610	8.2	830	2.2	1,050	1.8	1,270	5.6
615	6.4	835	2.4	1,055	2.6	1,275	4.4
						1,280	END

BIBLIOGRAPHY

Bennison, A. P., 1978, Geological highway map of the Great Lakes Region: Map No. 11, AAPG, Tulsa, Oklahoma.

Dunham, R. J., 1962, Classification of carbonate rocks according to depositional texture: in W. E. Ham (Ed.), Classification of Carbonate Rocks, pp. 108-21, AAPG, Tulsa, Oklahoma.

Evans, M., 1979, Fracture density and orientation study of the Reel Energy #3 D/K core from Mason County, West Virginia: (Unpublished Contract Report, U. S. Department of Energy Contract No. DE-AC21-76MC05194), Morgantown, West Virginia.

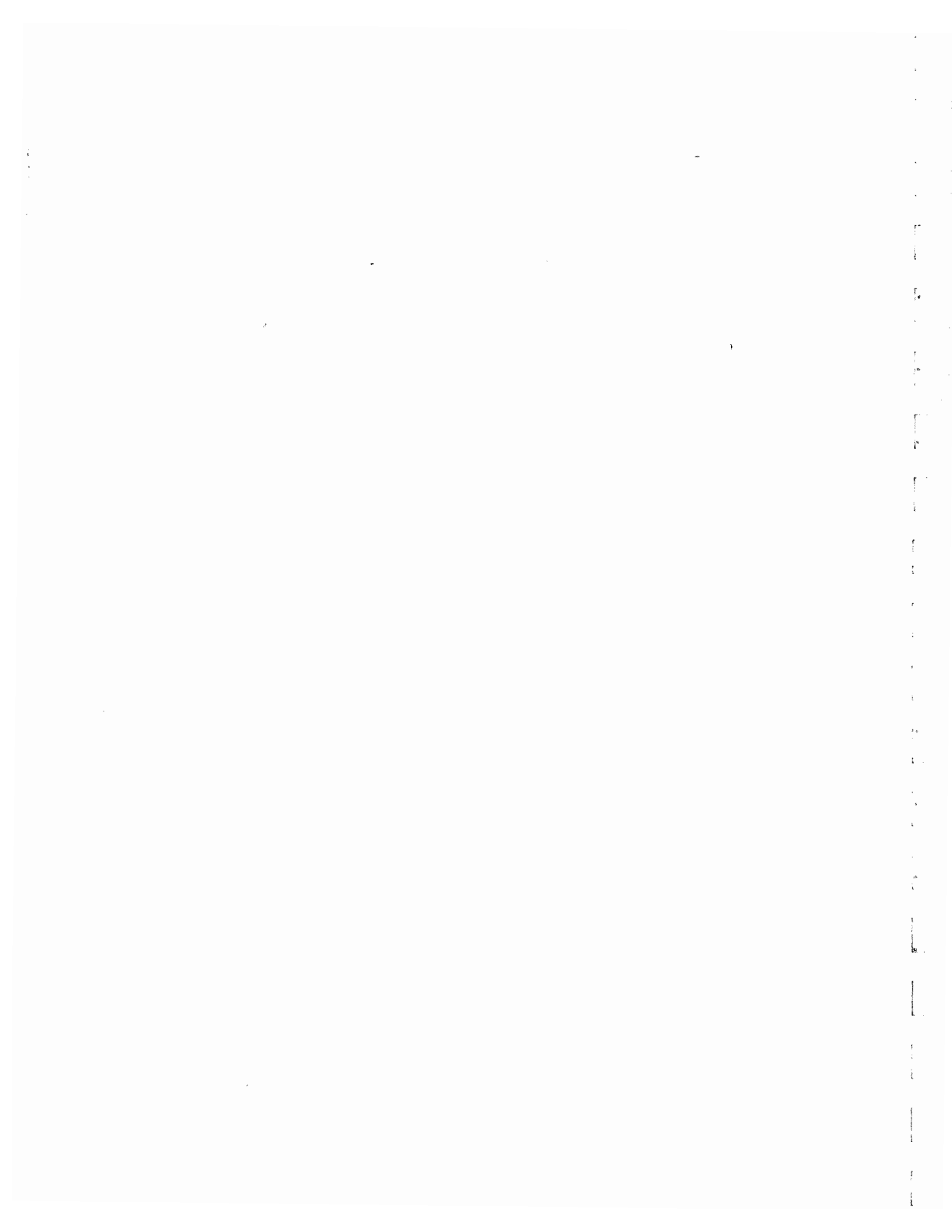
Geological Society of America, 1948, Rock Color Chart: Geological Society of America, Boulder, Colorado.

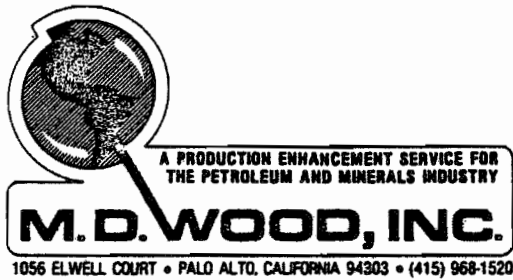
Kulander, B. R., et al, 1977, Fractographic logging for determination of precore and core-induced fractures, Nicholas Combs No. 7239 Well, Hazard, Kentucky: U. S. Department of Energy, MERC/CR-7713, Morgantown, West Virginia.

Ragan, D. M., 1973, Structural Geology, An Introduction to Geometrical Techniques: 2nd Ed., John Wiley & Sons, New York, New York.

APPENDIX F

M. D. Wood, Inc., Final Report
February 27, 1981





FRACTURE CHARACTERIZATION
IN THE DEVONIAN GAS SHALE
UNCONVENTIONAL GAS RECOVERY
PROGRAM.

ANALYSIS OF GROUND DEFORMATIONS
AND DESCRIPTION OF HYDRAULIC
FRACTURES FORMED DURING TREAT-
MENT OF THE COLUMBIA GAS
TRANSMISSION COMPANY WELL 20148-T
(WAKEFIELD) IN LORAIN COUNTY,
OHIO, ON OCTOBER 7, 1980.

WORK PERFORMED UNDER SANDIA
SCIENTIFIC LABORATORIES CONTRACT
13-2371 AT THE DIRECTION OF THE
GAS RESEARCH INSTITUTE IN
COOPERATION WITH THE DEPARTMENT
OF ENERGY.

FINAL REPORT

February 27, 1981

M. D. WOOD, INC.
1056 ELWELL COURT
PALO ALTO, CA 94303

(415) 968-1520

TABLE OF CONTENTS

	<u>PAGE</u>
1.0 EXECUTIVE SUMMARY	1
2.0 INTRODUCTION	2
2.1 Well Environs and Rock Deformational Parameters	4
2.2 Instrumentation and Array Configuration	6
3.0 DATA	8
4.0 ANALYSIS	10
4.1 Dip and Growth of Fracture	12
4.2 Fracture-Forming Fluid Volumes	14
4.3 Modelling Procedure and Data-fit Criterion	16
4.4 Driving Pressure at Shut-in	20
4.5 Post Shut-in Tilting	22
5.0 CONCLUSION	28
6.0 CLOSING REMARKS	30
7.0 BIBLIOGRAPHY	34
8.0 TABLES AND FIGURES	36
9.0 ACKNOWLEDGEMENTS	50

APPENDIX A FRAC-MAP TECHNOLOGY

1.0

EXECUTIVE SUMMARY

Analysis of the tilt data resulted in the following conclusions:

1. The fracture was a near horizontal penny-shaped feature, approximately symmetric about the wellbore, having a slight dip of no more than ten degrees to the north.
2. Depth-to-centre of the fracture was constrained to lie somewhere in the range of 650-740 feet.
3. Bounds imposed on the radius depended upon the depth of the fracture, deeper solutions generally involving shorter fractures. A maximum shut-in radius estimate of 508 feet was obtained for the shallowest (650 feet) solution and a minimum radius estimate of 346 feet was associated with the deepest solution.
4. The excess of shut-in fracture fluid pressure over the formation stress component acting to close the fracture was constrained to the range 20-44 psi for all solution depths.
5. Significant closure, exhibiting an exponential like decay, was inferred to have occurred for some three hours following shut-in. The rapid closure phase was smoothly succeeded by a sustained closure at a very low rate which persisted for a further seven hours at least. Closure was most likely due to a controlled fluid leak-off into tight natural fractures.
6. A final propped fracture volume in excess of 1000bb1 was indicated by the tilt data.
7. Fluid was conducted to the shallow horizontal fracture from the perforation interval (812-1050 feet) by a pre-existing vertical hydraulic fracture, formed two weeks prior to the treatment here reported, which acted as a low impedance conduit. The 'conduit' fracture was not spatially extensive. Most likely the preceding treatment established the horizontal fracture, enlarged during the treatment of interest here, as a breakout from the 'conduit' fracture. Such behavior has previously been observed during treatment of a similar Devonian Shale reservoir.

2.0

INTRODUCTION

Between the hours 15:21 and 16:22 (EDT) on the 7th of October 1980, a fluid mix consisting of a total of 33,000 gallons of gelled water, 61 tons of carbon dioxide (0 deg F, 305 psi) and 88,000 lb of sand proppant was injected into well #20148-T, known locally as the Wakefield well and owned by Columbia Gas Transmission Co. (CGTC). The well penetrates the Devonian shale of the Appalachian Basin in Lorain County, Ohio and was perforated between 816 and 1050 feet in depth. The treatment of the well constituted one of a series of hydraulic fracture characterization studies jointly sponsored by the Department of Energy (DOE) and the Gas Research Institute (GRI) as part of the Eastern Gas Shales Program. Consequently, a number of fracture diagnostic technologies were fielded to supply a data base which could be used to determine the geometry of the induced fracture and provide a consistency check for the various diagnostic systems involved. One such technology present was the FRAC-MAP™ system of M. D. Wood, Inc. (MDWI), a technology which is based on the interpretation of the evolving pattern of surface tilting characteristic of the growing fracture. The object of this report is to present an analysis of the tilt data and thereby deduce the form of

fracturing resulting from the treatment. Provisional results from the other participating technologies, where available, are presented for comparison with the conclusions drawn as a result of tilt data analysis. These data were collected by Sandia National Laboratories (SNL) and include, co-treatment surface potential measurements, post-treatment downhole hydrophone observations and finally downhole three-component geophone observations.

It is important to note that the three-component seismic detection system was operated downhole some two weeks prior to the treatment here reported when a smaller unproped fracture was formed in the well. The treatment involved the injection of 15,000 gallons of dilute HCl solution through the same perforation interval. A fracture of orientation N10 E degrees and unknown height was indicated to have formed by the system (C. Schuster, personal communication). Thus, it should be understood that the well had suffered a sizeable hydraulic fracture a mere two weeks prior to the treatment here reported.

2.1 Well Environs and Rock Deformational Parameters

The shallow lithology about the wellbore is shown in Figure 1. The shale is encountered at a depth of 252 feet and consists of alternating sections of grey and black shales which are organically lean and rich respectively. Bedding is essentially horizontal with a slight dip to the east. Analysis of cores taken from a similar well 2000 feet distant (#20149-T) failed to reveal any spatially extensive natural fractures (Cliff Minerals report 1980). Shale matrix permeability is low and rarely exceeds a few micro-darcies. Density of the shale about the well was found to vary between 2.35 and 2.6 gm/cc with mean value of 2.50 gm/cc (Birdwell Density Compensated Log). The shale is overlain by the Berea Sandstone and extends to a depth of 1246 feet where it finds contact with the Onodaga limestone.

The elastic parameters of Devonian shales, taken from other locations but of similar density, have been measured by a number of workers. Jones et al (unpublished data) found values:

$$\text{Poisson's Ratio} \quad \nu = 0.22 \pm 0.04$$

$$\text{Shear Modulus} \quad \mu = 1.15 \times 10^6 - 1.55 \times 10^6 \text{ psi.}$$

Hert et al. (personal communication), found values similar to the above and noted the shale to be anisotropic, appearing more resistant to fractures opening vertically than those opening horizontally. The correct value of shear modulus applicable to the bulk behavior of the formation (rather than a core sample) is difficult to estimate. The core-determined value is invariably an overestimate attributable to a class of cracks and imperfections in the bulk rock which are not present in the core sample. Bearing these points in mind, the following values will be adopted in this analysis:

Poisson's Ratio: $\nu = 0.25$

Shear Modulus
(Vertical Cracks): $2.5 \times 10^6 > \mu > 1.5 \times 10^6$ psi.

Shear Modulus
(Horizontal Cracks): $1.0 \times 10^6 > \mu > 0.5 \times 10^6$ psi.

Fracture toughness, K_{IC} , of the shale has been measured by Jones et al. (unpublished data) using the burst test (Abou-Sayed, 1978) on unconfined 10 inch diameter specimens. They find a value,

Fracture Toughness: $1000 < K_{IC} < 1200$ psi-inch^{1/2}

Abou-Sayed (1978), however, has reported a twofold increase in the measured K_{IC} value of Indiana limestone in response to an increase in confining pressure from atmospheric to several hundred psi. Consequently, in anticipation of down-hole confining pressures of hundreds of psi, we shall adopt the following range of values for effective fracture toughness:

Fracture Toughness: $1000 < K_{IC} < 1800 \text{ psi-inch}^{\frac{1}{2}}$

2.2 Instrumentation and Array Configuration

Eight tiltmeters circumscribed the wellbore at a radial distance of 400 feet (Figure 2). The radial array was supplemented by an additional four instruments located roughly north, south, east and west of the wellbore at respective distances of 925, 846, 830 and 765 feet. The radius of the radial array was chosen so as to maximize the signal strengths anticipated from a fracture of depth-to-centre 900 feet whereas the more distant instruments were deployed to provide further model-constraining datapoints.

The topography of the site was not severe, and it was possible to choose favorable locations for the instruments without sacrificing symmetry of the array. Water table depth varied with location but was usually encountered at about 12 feet. All sites were cased with 15 foot capped casings which served both to protect the sensor, and to increase the sample length thereby improving stability of the instrument (Davis et al. 1981). Details as to the operation and noise level of the instrument are presented in Appendix A. Sensor outputs were sampled every 30 seconds and recorded on a system of data loggers having absolute time control to better than 1 second.

3.0

DATA

Although all instruments deployed functioned satisfactorily, the data from instrument #12 (Figure 2) was not used in the analysis owing to uncertainty in calibration. Data quality was generally excellent with signal-to-noise ratios often in excess of 100:1. A time series plot of 6 days data from instrument #7 is shown in Figure 3. The record is somewhat typical of those from other instruments. Three features of the data are outstanding; the clear solid earth tide, the large co-frac signal and the immediate post-shutin response which exhibits an exponential-like decay character.

Accurate estimates of co-frac tilting could be made without the removal of the tidal component. The same was not true, however, for the post-frac response whose form was such as to contain significant energy at tidal frequencies. Hence, to permit definition of the form of post frac tilting, a least squares prediction of the tides (at M_2 and O_1 frequencies) during and following the frac was made and subtracted from the observed series. An example of the result of this tidal removal scheme is presented in Figure 4 and shows the tilt residue for both 'X' and 'Y' components at site #7. Clearly, the scheme enjoyed only moderate

success as is revealed by the increasingly significant component of tidal tilts toward the end of the record (Figure 4). The implied divergence of the tidal prediction series from the observed is an artifact of the short (10 days) data span used to generate the tidal estimate and cannot be eliminated. Despite the limitations, sufficient improvement in definition of the evolutionary form of the tiltfield immediately following shutin was obtained to justify the attempt.

4.0

ANALYSIS

The data were analysed according to the following scheme. The tilt vectors developed at each site since the start of injection were calculated at four points in time during the treatment interval. The times chosen occurred 9 min., 24 mins., 39 mins. and 61 mins. (shut-in) following the start of injection (15:21) and the resulting suite of four vector fields, which may be considered as snapshots of the evolving tiltfield, are presented as a time sequence in Figures 5-8 respectively. The fields were then used independently to constrain an appropriate elastic continuum model of the fracture subject to a chosen maximum allowable error-of-fit criterion. Visual inspection of the tilt snapshots clearly revealed the fracture to be a near horizontal feature and hence an idealised penny-shaped horizontal fracture model similar to that given by Sun (1969) was adopted. Free parameters in the data inversion were depth to fracture, d , and the quotient of driving pressure, P_D , with shear modulus, μ . Driving pressure is taken to be the excess of fracture fluid pressure over the formation stress normal to the plane of the fracture. Within the framework of the model, the radius, a , of the fracture is determined once the quotient value, P_D/μ , is known. The " P_D/μ versus

d" solution spaces for each of the four tilt snapshots were then plotted on a common chart and restricted still further by assuming fracture growth to have occurred in a single horizontal plane. Clearly, only those depths which are common to all solution spaces can be considered as candidate solutions.

Application of the above procedure identified those combinations of depth and radius (or alternatively, P_D/μ) which were compatible with the tilt data given the assumptions of the model. Specific knowledge of shear modulus, μ , or fracture toughness, K_{IC} , as given in section 2.1 was not necessary in the scheme. This is an important point, for the two parameters may be used to identify those combinations of driving pressure and radius which are consistent with certain relations drawn from the theory of linear elastic fracture mechanics. The relations pertain to the stability of uniformly pressured penny-shaped fractures of given volume, for a variety of radii, subject to conditions of mechanical equilibrium. The resulting bounds on radius may be compared with those deduced from the surface tilts (which assume only linear elasticity) to provide a consistency test for the analysis.

To conclude the analysis, the nature of the observed post-frac tilting is discussed.

4.1 Dip and Growth of Fracture

The pattern of surface tilting developed up to the time of shut-in is shown in Figure 8. The radial symmetry of the field is immediately striking and unquestionably indicative of a near-horizontal penny-shaped fracture. Indeed, the strong radial pattern is evident on all four snapshots (Figures 5-8) suggesting that the development of near-horizontal fracturing began somewhat less than nine minutes following the start of injection. This conclusion is supported by the absence of any erratic change in tilt rate throughout the period of injection (Figure 4) which argues against any sudden change in the plane of fracture growth during the interval of injection.

Close inspection of the four tiltfields does, however, reveal a consistently small, yet significant, north-south gradient in the amplitudes of the tilt vectors (Table 1). The gradient is such that instruments located to the north of the array experienced somewhat smaller tilting than their counterparts to the south. Assuming lateral elastic

heterogeneity, two explanations for the trend are possible; that it result from the fracture plane having a slight dip to the north, or that it represent the effects of horizontal fracturing assymmetric about the wellbore. The latter hypothesis was extensively tested using the horizontal penny-shaped fracture model of section 4.3 but with the sensor array translated with respect to the fracture center. No model which satisfactorily reproduced the observed surface tilt amplitude distribution could be found. Fracture volume as well as model geometry were varied in the investigation without success. It should also be noted that the pattern of tilting about the array indicated by all four snapshots does suggest that the geometrical center of the fracture remained near the wellbore throughout the treatment. Consequently, we conclude the north-south trend in tilt amplitudes to be an expression of slight fracture dip to the north.

Despite our inability to quantitatively substantiate the above assertion by determining the precise angle of dip required, we may demonstrate the viability of the mechanism for the case of plane-strain fractures. Figure 11 presents the suite of surface tilt patterns generated by plane strain fractures of identical depth-to-center, height and width but

having various dips (Pollard and Holzhausen, 1979). Clearly the dependence on dip is such that a slight dip of several degrees is all that would be required to give rise to the observed strength of the north-south trend in tilt amplitudes. By appeal to this model we estimate the required dip to be less than ten degrees.

4.2 Fracture-Forming Fluid Volumes

For the purpose of estimating fracture forming fluid volumes we have assumed leak-off into the rock matrix and/or joints and fissures during the treatment to be negligible. Fracture volume at a specific instant is thus given by the total volume of fluid (corrected for in-situ temperature and pressure) injected up to that time. Although the low formation permeability and the inferred small population of natural fractures within the area tend to support this assumption, it is known that a sizeable hydraulic fracture, vertical near the wellbore at least, extended from the perforations (section 2.0). Evidence that the vertical sections of this fracture were not inflated appreciably, thereby depriving the principal horizontal structure of fluid, is provided by the absence of a significant vertical-fracture-characteristic component in the surface tiltfield

developed after nine minutes (Figure 5). In fact, we propose that the vertical fracture acted as a low impedance conduit which fed the inflating horizontal fracture. Further evidence to suggest low fluid loss to the formation is provided by the inferred slow collapse of the inflated fracture for several hours following shut-in (section 4.4), a corollary of which is that the fracture system, at shut-in, formed what was essentially a hydraulically closed, albeit leaky, system. Thus, we feel confident that snapshot fracture volumes estimated from the respective injected fluid volumes are essentially correct although some allowance is made in the analysis for the possibility that fluid loss during the first few minutes, in filling the pre-existing artificial fracture, might lead to a significant overestimate of the horizontal fracture volume after 9 minutes.

Total injected fluid volume at the time of shut-in was calculated from the bulk material quantities used in the treatment subject to a correction for anticipated in-situ shut-in conditions (68 deg F and 1000 psi confining pressure). Further cooling of the fluid to a formation temperature of 52 deg F was calculated to result in a fluid volume decrease of 2%. Injected fluid volumes at times

preceding shut-in were estimated from data supplied by CGTC. The specific fracture forming fluid volumes used in the modeling procedure were:

Fracture Volume after 9 minutes = 119bb1
Fracture Volume after 24 minutes = 391bb1
Fracture Volume after 39 minutes = 811bb1
Fracture Volume at shut-in = 1377bb1

4.3 Modelling Procedure and Data-fit Criterion

The model used to invert the tilt data was similar to that given by Sun (1969) and calculated the surface tiltfield resulting from the development at a depth, d , of a penny-shaped horizontal fracture of radius, a , and volume, V , under a driving pressure, P_D , in a homogeneous, isotropic, linear elastic medium having a Poisson's ratio, ν , and shear modulus, μ . The laboratory value for Poisson's ratio of 0.25 (section 2.1) was used throughout the analysis, an assumption justified in view of the comparative insensitivity of the model solution to the parameter. Model parameters sought in the inversion were depth of fracture, ' d ', and the quotient of driving pressure and shear modulus, ' P_D/μ ', which, within the framework of the model, uniquely

defined fracture radius, 'a'. In other words, the problem posed was to find all combinations of values of 'd' and ' ρ_D/μ ' (or equivalently, 'a') which could generate the observed surface tiltfield to within some adopted bounds of error. Before developing a criterion-of-fit for this purpose, however, some account must be taken of the non-radial component of the observed tiltfield which obviously cannot be generated by a radial symmetric model.

Let us assume that the non-radial field is, indeed, predominantly the result of fracture dip (section 4.1) and note that providing the dip is slight, as is certainly the case here, the dip related component of the tiltfield is approximately assymmetric about the wellbore (Figure 11). Then an average of tilt vector amplitudes taken about the wellbore at a fixed distance should be essentially independent of the dip and equal to the radial component of the field at that distance. The eight equispaced sensors which circumscribe the wellbore at a radius of 400 feet provided an excellent ensemble of datapoints for the averaging operation, and the resulting mean tilts at the times of the four snapshots were used as the principal model-constraining datapoints. Furthermore, the confidence level in the estimate of the radial field 400 feet from the wellbore was

substantially improved as a result of the statistical smoothing inherent in the averaging operation. Such smoothing tends to average out the effects of site elastic inhomogeneities which can conspire to modify the response of a sensor to signal tiltfields (King et al. 1976). Expressing datapoint error in terms of the effective uncertainty in system calibration, we feel that the 400 feet datapoint can be trusted to within +/-4% of its specific value. The more distant datapoints, however, must be ascribed greater error, for their different distances and smaller number degrade the benefits of averaging as well as complicate the averaging operation. We have chosen to specify the error margin associated with the more distant instruments (#9, #10 and #11 in Figure 2) in terms of the maximum allowable mean discrepancy between observed and model predicted tilts at the three sites. Specifically, we demand that this average discrepancy be less than 6% of the mean observed tilt averaged over the three sites. This particular criteria of fit was adopted because, quite fortuitously, the configuration of the more distant sensors is such that the effects of fracture dip largely cancel when mean discrepancies from model generated radial fields are considered.

The results of the four tilt snapshot inversions are shown in Figure 9. Each of the four outlined areas bound those combinations of depth and quotient value ' P_D/μ ' which, for a model fracture of volume appropriate to the model snapshot, give rise to a surface tiltfield which replicates that observed to within the adopted error margin; that is, the model reproduces the observed mean tilt at 400 feet to within 4% whilst producing a mean error averaged over the more distant datapoints of less than 6%. Imposing the demand that the horizontal fracture remain at a constant mean depth throughout its development, further constrains the solution spaces to the range of depths which intersect all four solutions spaces. The result is to limit the fracture to lie between 650 and 740 feet in depth-to-center. Corresponding bounds on quotient value ' P_D/μ ', hence radius, a , for each snapshot may be read from the figure and are presented in Table 2. It is important to note that, in contrast to shear modulus which may be taken as a constant, the mean driving pressure will be expected to decrease as the fracture lengthens, thus reducing the effective quotient value ' P_D/μ ' from one snapshot to the next.

4.4 Driving Pressure at Shut-in

Quantitative statements regarding maximum driving pressures permissible for fractures of given radii can be made provided mechanical equilibrium conditions prevail and bounds on material fracture toughness are available. Specifically, in a brittle elastic material, driving pressure and radius are related by the criterion that fracture propagation occurs when stress intensity at the fracture tip is equal to the value of K_{IC} . For the case of a penny-shaped crack in an infinite, homogeneous linear-elastic medium, the relation takes the form,

$$P_D = \frac{\pi K_{IC}}{2a^{1/2}} \quad \dots\dots\dots 1$$

Equation 1 is shown plotted in Figure 10 with the constant K_{IC} taking on the two values which bound the range of likely values, as given in section 2.1. The solution space lies between the curves and is valid provided that mechanical equilibrium conditions prevail, as is the case at shut-in. Additionally, Perkins and Kern (1961) have derived expressions which relate the radius, a , and width, w , of a penny shaped fracture of volume, V , to the driving pressure, P_D , for the fracture contained in an infinite, isotropic,

homogeneous linear-elastic medium of Poisson's ratio, ν , and shear modulus, μ . The relations are given as,

$$\text{radius, } a = \left\{ \frac{3\mu V}{8 P_D(1-\nu)} \right\}^{1/3} \quad \text{..... 2}$$

$$\text{width, } w = \frac{4 P_D (1-\nu) a}{\pi\mu} \quad \text{..... 3}$$

Equation 2 may be used to further constrain the solution space in Figure 10 by plotting radius versus shut-in driving pressure for the two likely extremum values of shear modulus discussed in section 2.1. Poisson's ratio is taken as 0.25 and shut-in fracture volume is adopted as given in section 4.2. The region defined by the intersection of the areas between the two pairs of bounding curves (hatched area in Figure 10) represents the solution space as inferred from fracture physics. The bounds on radius as deduced from the shut-in tiltfield are shown as bold horizontal lines in Figure 10. Agreement between the two is excellent although no significant improvement in the tilt derived radius estimate is achieved. Consistency of the model assumptions within the resolving power of the data is, however, demonstrated. Driving pressure at the time of shut-in is constrained to lie within the range 20-44 psi.

Bounds on maximum fracture width at shut-in may be calculated from equation 3 using the values of radius, 'a', and quotient ' P_D/μ ' given in Table 2. The range of widths, w, which correspond to the range of solution radii, a, is found to be,

$$\begin{array}{l} \text{Maximum width, w:} \quad 0.17 < w < 0.37 \text{ inches} \\ \quad \quad \quad \quad \quad (508 > a > 346 \text{ feet}) \end{array}$$

It should be remembered that wider fractures are largely associated with deeper solutions.

4.5 Post Shut-in Tilting

The pattern of surface tilting developed during the three hours following shut-in is shown in Figure 12. Comparison of the figure with the pattern of co-treatment tilting as established at shut-in reveals the field to represent a partial dissolution of the shut-in tilt field. Fracture closure resulting from either fluid leak-off or continued fracture extension is most likely responsible for the deflation; the question of mechanism shall be investigated shortly.

The form of development of post shut-in tilting as recorded at site #7 can be studied in Figure 12 and the response of the dominant 'Y' component may be taken as typical of that observed at other sites. Both the radial 'X' and tangential 'Y' tilt series shown have been subject to a tidal-prediction filtering operation which reduced but did not eliminate the tidal component from the record (section 3.0). Two distinct phases of post shut-in tilting are evident; that of an initial, pronounced reversal of the co-injection tilt trend which smoothly decays, exponential like over a period of three hours, into the barely discernable sustained tilting at a very low rate which is identified as the second phase. It may reasonably be argued that discrimination between fracture and tidal origins for the second phase of tilting cannot sensibly be made. However, the trend in tilting at all sites for some ten hours following shut-in was consistently toward the wellbore thereby indicating a fracture origin for the trend on grounds of spatial coherence. Thus, tilting was predominantly fracture induced for some seven hours following the quantitatively more significant initial phase. We associate the initial

exponential-like decay in inferred closure rate with the gradual transition from predominantly hydraulic support of the inflated walls to proppant-structure support. Slow closure persisting beyond 3 hours might be explained by creep of the supportive proppant in response to loading. Fracture closure was most certainly complete by the time of flowback, some 18.6 hours after shut-in, as is revealed by the absence of a coincident tilt step in the record of Figure 4.

The inferred change in fracture geometry following shut-in can be explained as resulting from either fluid leak-off into the formation or sustained fracture growth for several hours following shut-in. Both of these models have been quantitatively investigated subject to the constraints imposed by the tilt observations. The mean amplitude of tilting developed in the three hours following shut-in at a distance 400 feet from the wellbore was 1.65 μ Rad (Table 3). Ascribing a 4% error margin to this estimate together with the mean shut-in tilt amplitude, as measured by the same instruments, of 7.4 μ Rad (Table 1) results in an estimated proportional deflation of the shut-in tilt field after 3 hours, ΔT_3 , of

$$0.21 < \Delta T_3 < 0.24.$$

The fluid leak-off model shall be considered first. Assuming fracture growth following shut-in to be negligible, the effective fracture radius throughout the deflation phase is given as a constant and hence any observed surface deformation can only be explained by changes in fracture width. The relation is found to be linear (Sun 1969), hence a proportional deflation of the surface tiltfield, T , implies an identical proportional reduction in maximum fracture width. Furthermore, on rearranging equations 2 and 3 so as to express fracture volume, V , as a function of radius, a , and maximum width, w , we have,

$$V = \frac{2\pi a^2 w}{3}$$

Thus, fracture volume must suffer the same proportional reduction from its shut-in value as do the surface tilts. For a shut-in fracture volume of 1377bb1, a total fluid loss of 330bb1 is implied. Consideration of the leak-off during injection, which has been neglected here, is unlikely to alter this estimate appreciably. The fluid must be lost to the formation by matrix diffusion, natural fracture penetration or both. We have calculated the difference in pore-pressure and fracture-fluid pressure necessary to provide the required vigour of diffusion. Assuming a formation permeability of one microdarcy, we find pressures

of the order of several thousand psi to be required. Matrix diffusion can thus be discounted as a significant mechanism of fracture deflation. If fluid flow from the fracture was, indeed, responsible for the deflation, then escape must have been achieved through controlled leakage into natural fractures.

The alternative to fluid leak-off is that the proportional deflation, ΔT_3 , be principally due to continued fracture growth following shut-in. We have applied the model of Sun (1969) to the problem and find the tilt data to require the following modifications to the shut-in fracture radius estimates derived in the preceding section;

Depth = 653 feet

minimum shut-in radius : 508 feet

minimum radius 3 hours after shut-in: 604 feet

Depth = 740 feet

minimum shut-in radius : 346 feet

minimum radius 3 hours after shut-in: 514 feet

Clearly, the tilt data require post-injection fracture extension to be considerably greater than is popularly believed to occur. The argument against post-injection fracture growth on this scale, however, springs more from the absence of an established time dependent mechanism of

extension rather than an observational basis. Indeed, to our knowledge, no dataset, quantitatively sensitive to possible post-injection fracture growth, has been collected for a fracture which so clearly exhibits the hydraulically-closed character of the fracture discussed here. Nevertheless, we are unable to suggest a time dependant fracture mechanism which might give rise to the required sustained stable advance in such a short time period. Stress corrosion fracturing, possibly facilitated by time dependant fluid penetration to the fracture tips, although a viable mechanism for slow extension of hydraulic fractures (Demarest, 1976) is unlikely to give rise to the rapid extension required by the model. Thus we must reservedly conclude that significant fracture growth was not primarily responsible for the observed post-shut-in tilts and propose fluid leak-off to be the dominant mechanism.

An interesting corollary of the preceding calculations is that a final propped fracture volume in excess of 1000bb1 seemingly finds support from a proppant structure whose bulk volume is a mere 158bb1 (calculated assuming a packed sand density of 1.6 gm/cc). The probable departure of fracture geometry on closure from the form of a uniformly pressurized crack as assumed in the calculation, is unlikely to change this estimate of propped volume appreciably.

5.0

CONCLUSION

Analysis of the tilt data permitted the following conclusions to be drawn. The fracture was a near horizontal penny-shaped feature approximately symmetric about the wellbore, exhibiting a slight dip of certainly no more than ten degrees to the north. Depth-to-centre was constrained by the data to lie somewhere in the range 650-740 feet. Bounds on fracture geometry depended upon the specific depth of the solution. Deeper solutions generally involved greater driving pressures and consequently shorter fractures. A maximum shut-in radius estimate of 508 feet was obtained for the shallowest (650 feet) solution whereas the minimum radius estimate of 346 feet was associated with the deepest solution. The solutions were shown to be consistent with the predictions of a fracture mechanics analysis of the problem provided that the laboratory determined values of fracture toughness and shear modulus were subject to reasoned corrections for in-situ conditions and scaling respectively. Driving pressure at shut-in was constrained to the range 20-44 psi for all depth solutions.

Following shut-in, significantly rapid diminution of the established surface tiltfield was observed for some three

hours, after which the rate lessened appreciably, yet detectably persisted, for a further seven hours. The deflation is most certainly due to fracture closure. The initial rapid deflation phase exhibited a smooth exponential-like decay and is interpreted as resulting from the transition from predominantly hydraulic support of the fracture walls to that of proppant structure support. The inferred continued slight closure after three hours might be due to proppant-creep in response to loading. The mechanism responsible for closure is not resolved, although fluid leak-off into the shale matrix can be discounted in view of the exceedingly low permeability. Continued fracture growth following shut-in is capable of satisfying the tilt observations but is not considered an attractive candidate owing to the large extension required. Fluid leak-off into the formation through tight natural fractures is favored as being the most orthodox explanation of the deflation. The final propped fracture volume was found to be in excess of 1000bb1, a figure which contrasts remarkably with the 158bb1 volume of proppant injected.

6.0

CLOSING REMARKS

To close this report we would like to comment on several points which arise from the analysis. Firstly, we find the inferred behavior of the vertical fracture near the wellbore to be remarkable. The assertion that the fracture acted as a conduit in response to injection thereby conducting fluid to shallower horizons is, we feel, almost certainly correct. Furthermore, inspection of the evolving tiltfield reveals that horizontal fracturing began minutes after the start of injection and provides no evidence to suggest significant opening of a vertical fracture. Thus, it would seem that the exploited pre-existing vertical fracture was either open, or was of very small spatial extent, presenting essentially a narrow conductive corridor to more shallow horizons. We favor the latter, and add that it is most likely that the initial treatment, performed some two weeks prior to that discussed here, produced the initial breakout from the vertical into the horizontal plane. For support, we cite the provisional results of co-injection surface electric potential measurements (Carl Schuster, personal communication) which indicate that the extension of the vertical fracture had effectively ceased after one minute of injection. It is difficult to explain breakout into a

horizontal plane with such small fluid volumes unless the horizontal fracture was simply being reworked. It is of note that almost identical behavior, involving significant upward extension of a vertical fracture until horizontal breakout can be achieved, has been reported by Evans et al. (1980) for a very similar well penetrating Devonian shale subject to a nitrogen hydraulic fracturing treatment.

Of additional note is the observed initial shut-in pressure (ISIP) of 740 psi. Such a high value must be taken as indicating that the vertical 'conduit' fracture suffered total closure as soon as the wellbore pressure dropped to the downhole shut-in value, thereby hydraulically isolating the horizontal fracture from the wellbore. For permitting hydraulic communication between the horizontal fracture and the wellbore would require a fracture depth of about 1050 feet in order to satisfy the ISIP data and this was most certainly not the case. Assuming the vertical fracture to have intersected the wellbore at a depth of 1000 feet, as is indicated by post injection downhole hydrophone observations (C. Schuster, personal communication), the resulting estimate of hydrostatic loading due to wellbore fluids leads to an inferred downhole fluid pressure of about 1150 psi. We propose that this figure, in fact, represents the minimum

horizontal principal stress at a depth of 1000 feet. A horizontal fracture at a depth of 700 feet is calculated to be capable of producing a fluid pressure within the vertical 'conduit' fracture at a depth of 1000 feet of no more than 940 psi. Ascribing a shallower depth to the horizontal fracture reduces this fluid pressure estimate still further. Thus, at shut-in, about 160 psi excess stress was available at a depth of 1000 feet to close the vertical fracture. We conjecture that continued monitoring of wellbore pressure for several hours following shut-in might have revealed a slow pressure reduction, amounting to about 160 psi, as wellbore fluids penetrated the closed but leaky vertical fracture until hydrostatic equilibrium condition's within the entire fracture system had been achieved.

Finally, mention must be made of the detection of post-injection microseismic activity at a depth of 500 feet. The observations were made with downhole hydrophones and must be taken as suggestive that fracturing occurred at that depth. No significant activity was recorded in the interval 650-740 feet which corresponded to the range of possible fracture depths indicated by the tilt data. We are unable to account for the discrepancy. We must stress, however, that despite exhaustive modelling involving lateral translation of the

fracture centre from the wellbore as well as variable fracture volume, no model could be found which satisfactorily reproduced the observed surface tiltfield using a 500 feet deep horizontal penny-shaped source.

7.0

BIBLIOGRAPHY

- Abou-Sayed, A.S., 1978. An experimental technique for measuring the fracture toughness of rocks under downhole stress conditions. 6th Intl. Conf. on Exp. Stress Analysis, Sept. 18th-22nd, Munich, W. Germany.
- Cliffs Minerals, Inc., Granville, West Virginia. Work performed under DOE contract #DE-AC21-78MC08199. Semi-annual report for the Unconventional Gas Recovery Program, June 1980, p. 3-16: Morgantown Energy Technology Centre, Morgantown, West-Virginia.
- Davis, P.M., King, G.C.P., Evans, K.F. and J.A.C. Horsfall, 1981. Spatial averaging of deformation fields as a function of spectral content, instrument length and depth of burial, submitted to Bull. Seis. Soc. Am.
- Demarest, H.H., 1976. Application of stress corrosion to geothermal reservoirs, Informal report LA-6148-MS, Los Alamos Sci. Lab, Los Alamos, N. Mex.
- Evans, K. F., Holzhausen, G. R. and M. D. Wood, 1980. The mapping of nitrogen gas induced hydraulic fractures in Devonian shale by observation of the associated Surface deformation. SPE/DOE paper #8933, presented at 1980 SPE/DOE symposium on Unconventional Gas Recovery, Pittsburg, Penn., May 18-21.
- Hert, H, Lawrence Livermore Laboratories, Livermore, California.
- Jones, A. H., Terra Tek, Inc., Salt Lake City, Utah. Work performed under DOE contract #DE-AC21-80MC12093. Semi-annual report for the Unconventional Gas Recovery Program, June 1980, p3-87: Morgantown Energy Technology Centre, Morgantown, West Virginia.
- King, G. C. P., Zurn, W., Evans, J. R. and D. Emter, - 1976. Site correction for long period seismometers, tiltmeters and strainmeters. Geoph. J. Roy. Ast. Soc., 44, 405-411.
- Perkins, T. K. and L. R. Kern, 1961. Widths of hydraulic fractures. J. Petr. Tech, Sept, 937-949.

Pollard, D. D., and G. R. Holzhausen, 1979. On the mechanical interaction between a fluid-filled fracture and the Earth's crust. *Tectonophysics*, 53, 27-57. -

Sun, R. J., 1969. Theoretical size of hydraulically induced fractures and corresponding surface uplift in an idealized medium, *J. Geoph. Res.*, 74, 5995-6001.

Schuster, C., Sandia National Laboratories, Albuquerque, New Mexico.

8.0

TABLES AND FIGURES

Tilt Amplitudes at Snapshot Times: (μ Rad)

Instrument #	9 mins	24 mins	39 mins	61 mins (Shut-in)
1	0.80	2.4	4.3	6.15
2	0.75	2.5	4.4	6.2
3	1.15	3.2	5.9	8.45
4	1.10	3.0	5.7	8.3
5	1.00	2.9	5.6	8.6
6	0.75	2.6	5.0	7.8
7	0.85	2.6	4.9	7.2
8	0.85	2.5	4.5	6.7
Mean (#1-8)	0.90	2.7	5.05	7.4
9	0.20	0.75	1.5	2.5
10	0.225	0.70	1.5	2.8
11	0.25	0.90	1.9	3.4

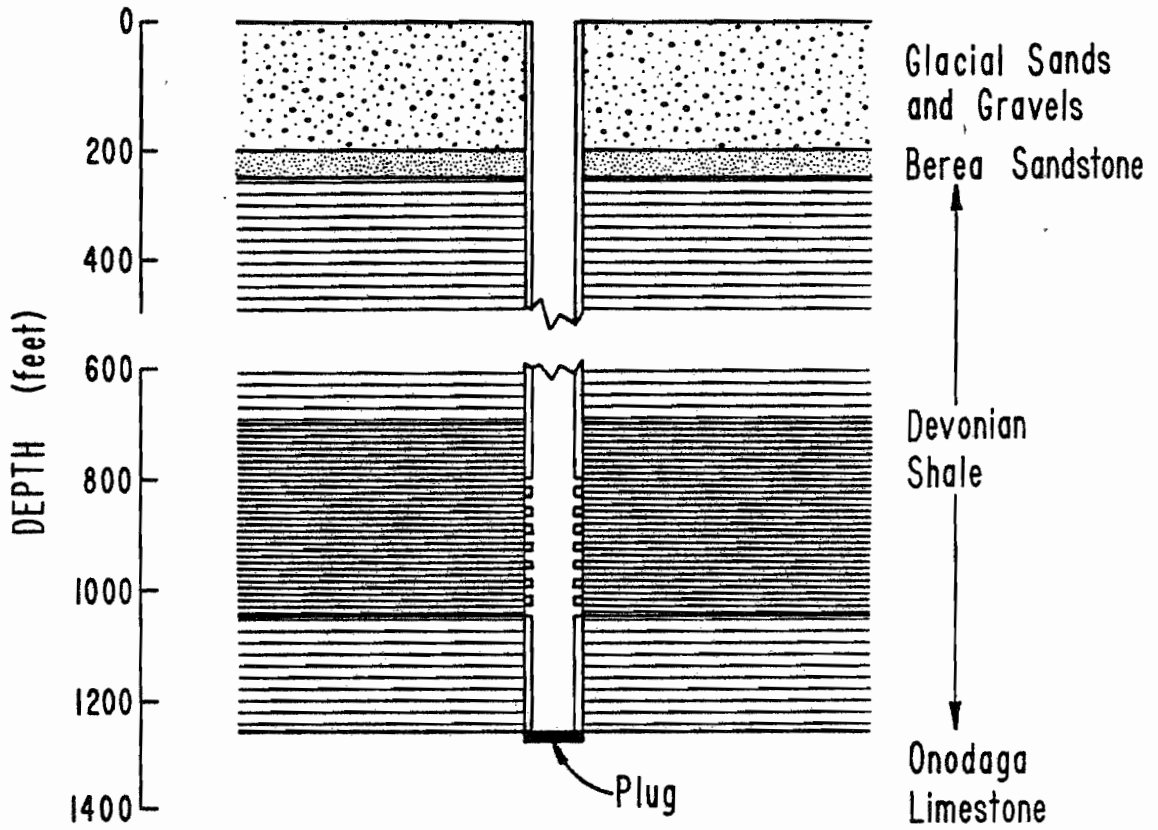
Table 1. Tilt amplitudes developed about the array from the start of injection up to the various snapshot times. Also entered is the mean value of tilting at a distance 400 feet from the wellbore as averaged over instruments #1-8.

Snapshot Time	Bounds on $P_D/\mu \times 10^6$ (653 < depth < 743 feet)	Bounds on radius 'a' (feet) (653 < depth < 743)
9 minutes	17 < P_D/μ < ∞	270 > a > 0
24 minutes	18.5 < P_D/μ < ∞	390 > a > 0
39 minutes	28 < P_D/μ < 185	433 > a > 231
61 minutes	29.5 < P_D/μ < 93	508 > a > 346

Table 2. Bounds imposed on quotient value ' P_D/μ ' and radius by limiting the fracture to the depth range 653-743 feet. Deeper fractures generally require larger ' P_D/μ ' values to satisfy the observed surface tilting and hence are associated with shorter fractures.

Instrument #	3-hour post Shut-in tilts
1	1.15
2	1.55
3	2.05
4	1.90
5	1.80
6	1.70
7	1.80
8	1.25
Mean (#1-8)	1.65

Table 3. Tilt amplitudes developed at the eight sites located 400 feet from the wellbore during the three hour period following shut-in of the well.



Explanation

- 
 Band of black shale (organically rich) within the predominantly grey (organically lean) sequence
- 
 Cased : Unperforated
- 
 Cased : Perforated

Figure 1. Shallow lithology about the Wakefield well, Lorain County, Ohio.

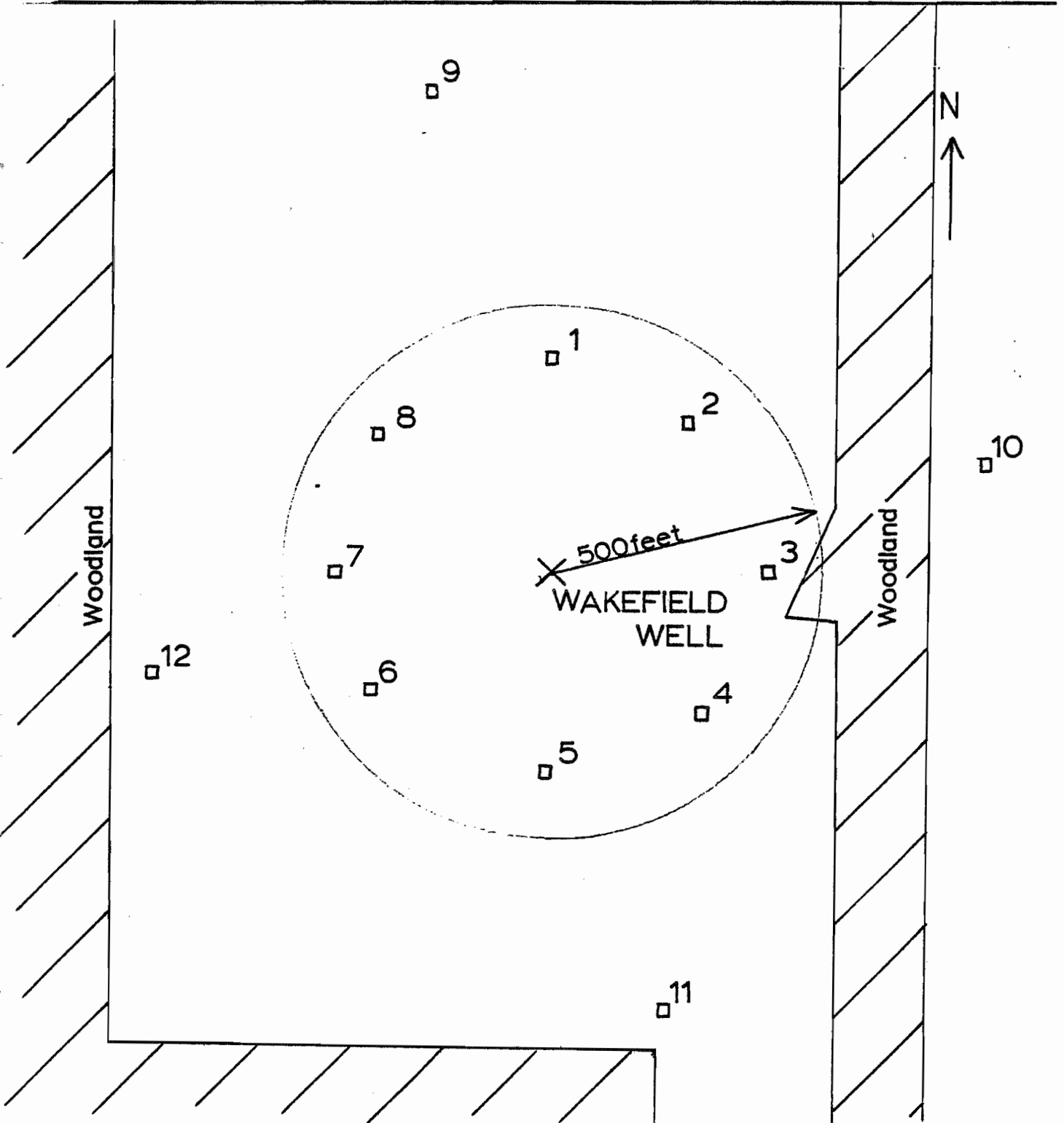


Figure 2. Plan view of the Wakefield Well and its surrounds. Tiltmeter sites are denoted by a square with the site number indicated alongside.

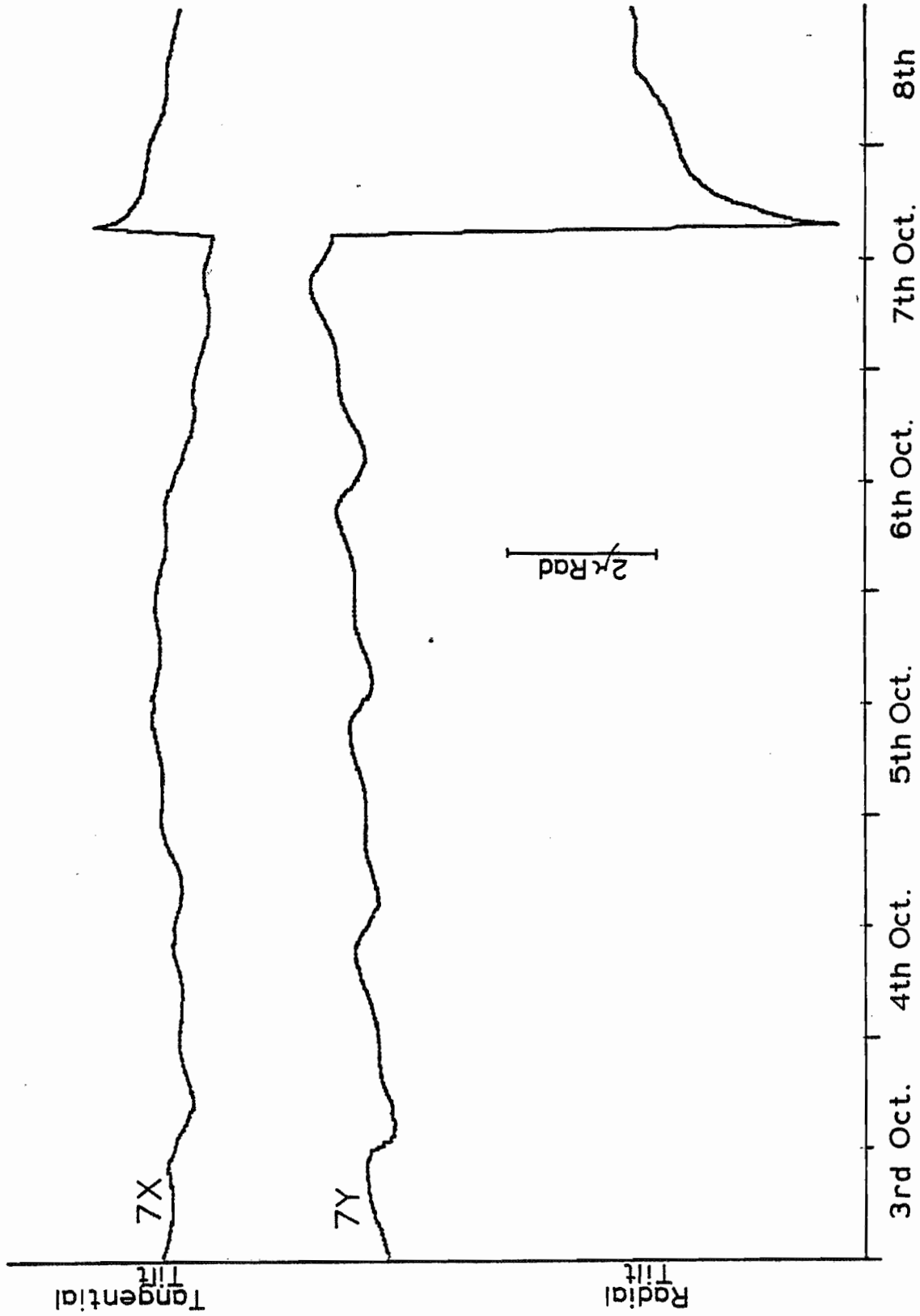


Figure 3. 5 1/2 days raw data collected at tiltmeter site #7. Positive trending 'Y' indicates that the instrument is undergoing a rotation such that the top of the sonde moves towards the wellbore with respect to the bottom. Similarly, positive trending 'X' indicates a movement of the top of the sonde anticlockwise about the wellbore when viewed from above.

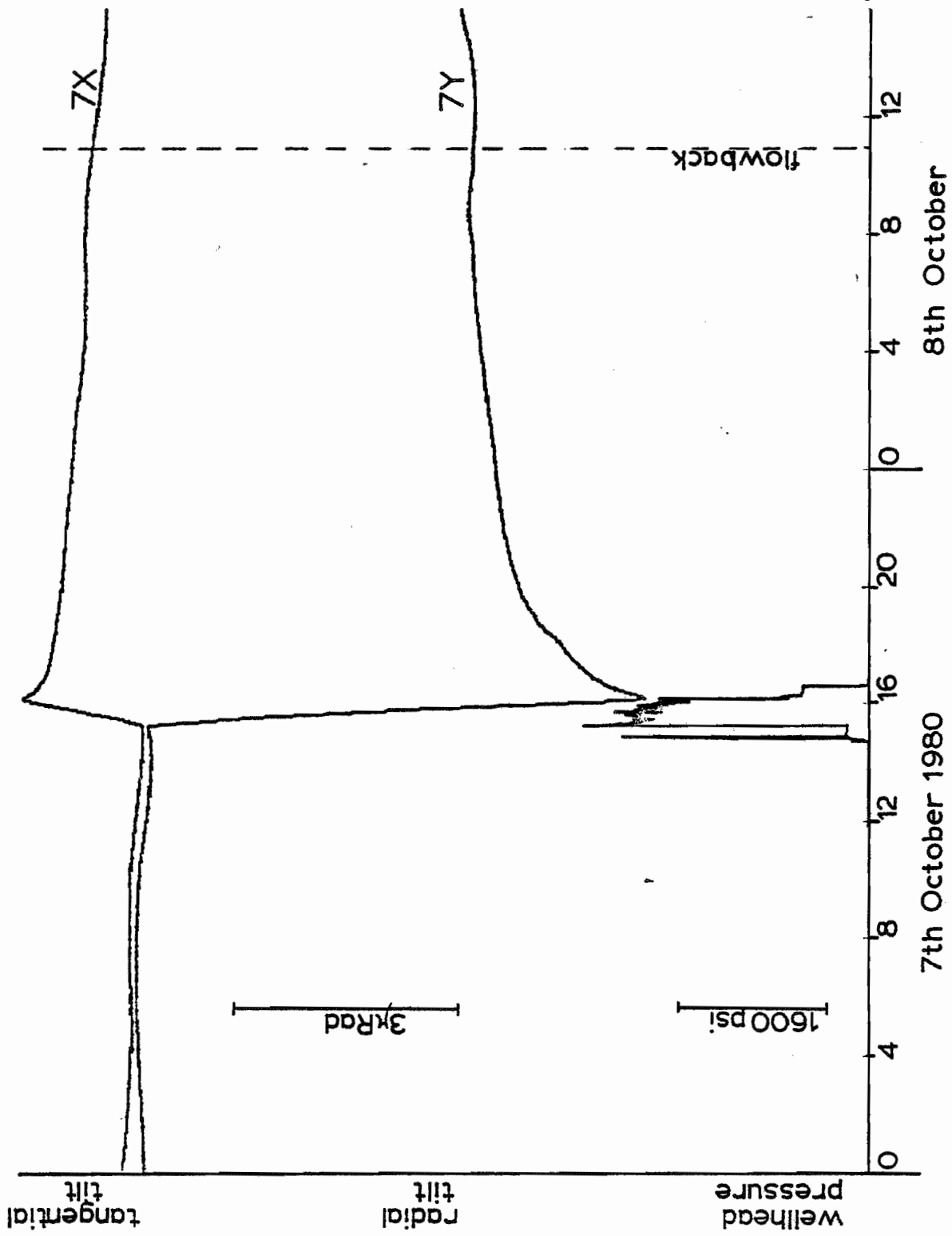
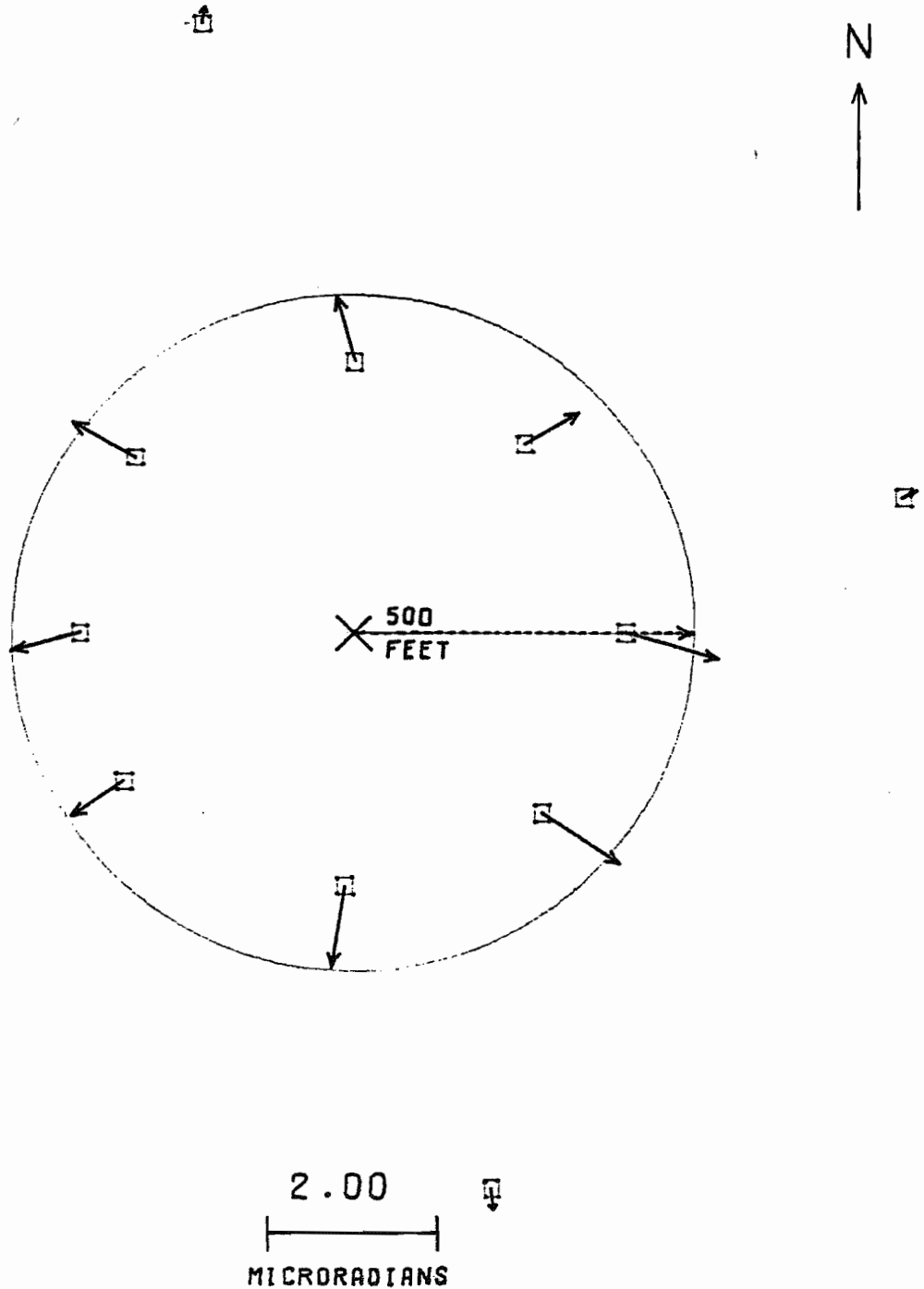


Figure 4. 40 hours tidally filtered tilt residuals from instrument #7. The frac window can be identified from the wellhead pressure record shown below the two residual tilt series.

WAKEFIELD #1: TILT 15:21 - 15:30

M.D.WOOD. INC.

DATE OF TREATMENT: 07-OCT-80



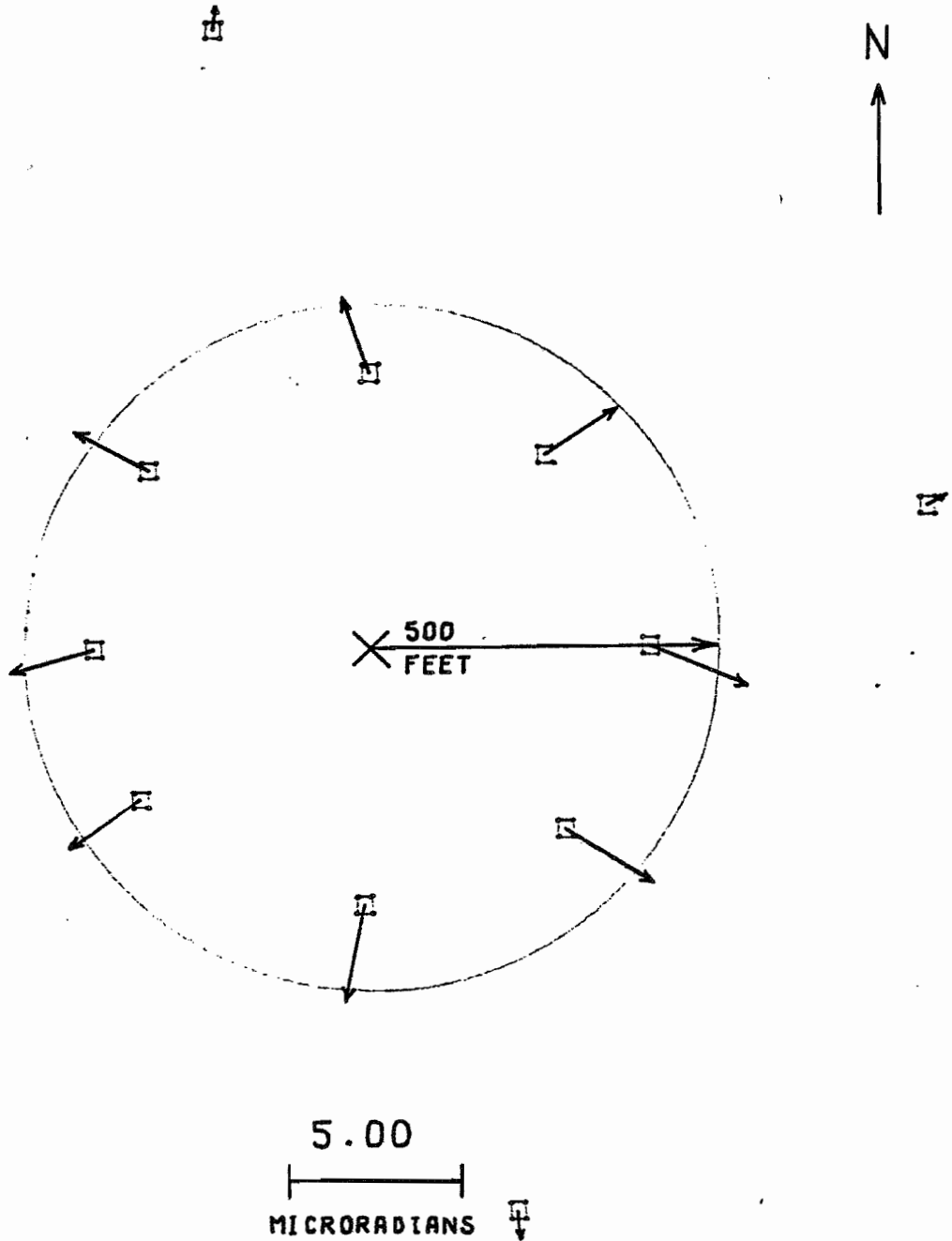
VECTOR FIELD PLOT

Figure 5. Pattern of surface tilting developed 9 minutes after the start of injection. The vectors can be taken as indicating the direction of displacement of the top of the sonde with respect to the bottom as viewed from above.

ROB TILT 15:21 - 15:45

M.D.WOOD, INC.

DATE OF TREATMENT: 07-OCT-80



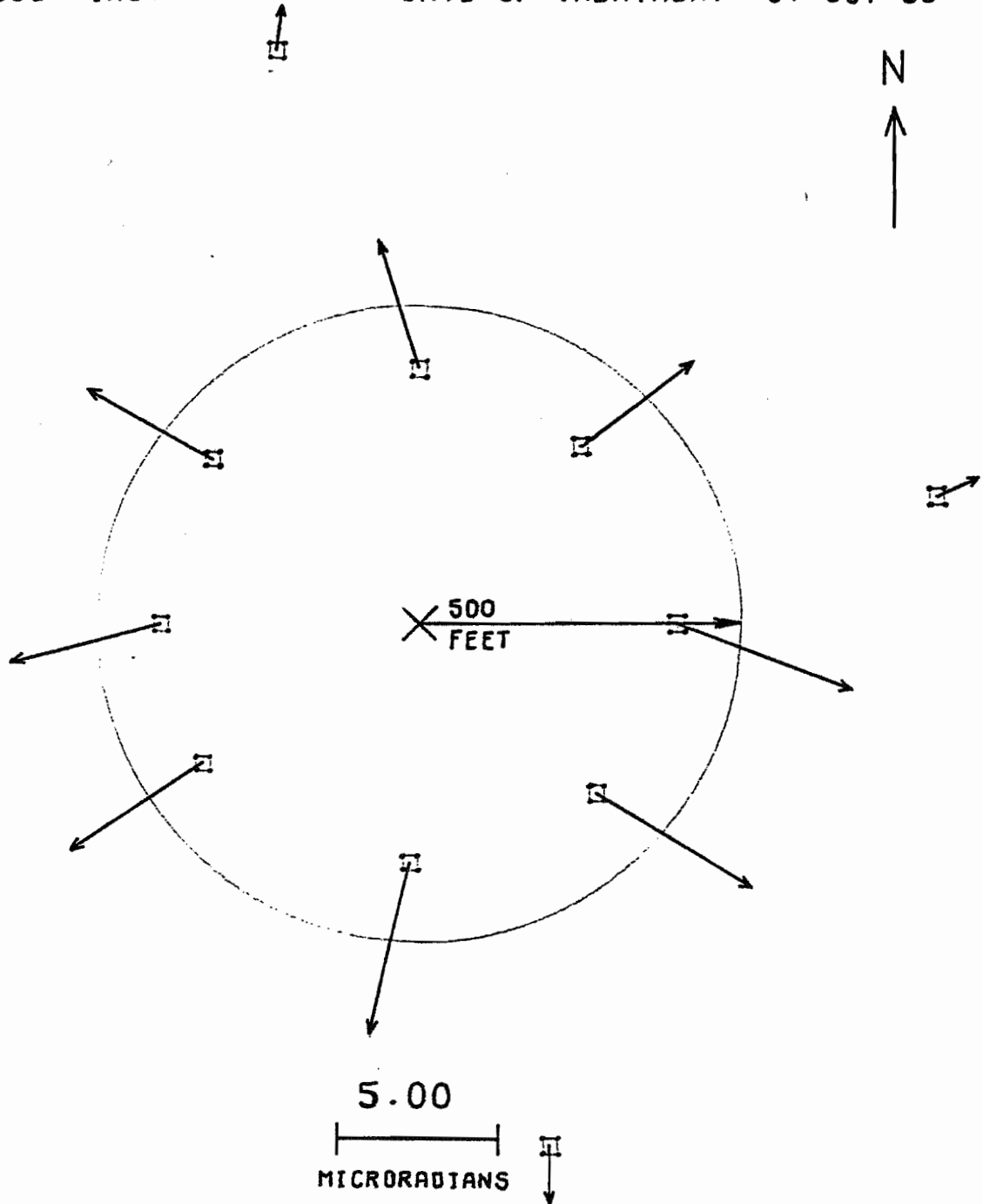
VECTOR FIELD PLOT

Figure 6. Pattern of surface tilting developed 24 minutes after the start of injection.

AOB TILT 15:21 - 16:00

M.D.WOOD. INC.

DATE OF TREATMENT: 07-OCT-80



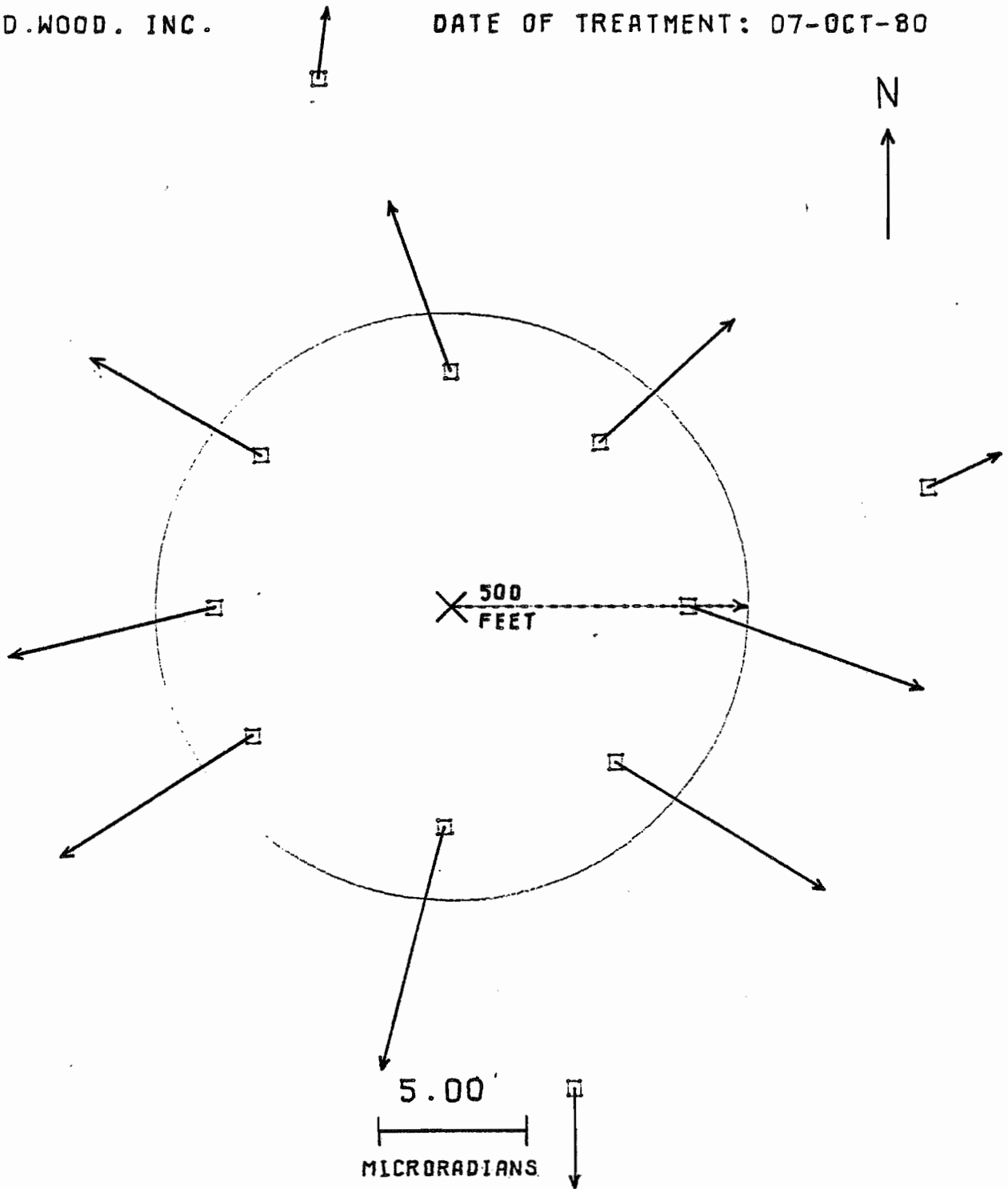
VECTOR FIELD PLOT

Figure 7. Pattern of surface tilting developed after 39 minutes of injection.

WAKEFIELD #1: TILT 15:21 - 16:22

M.D.WOOD. INC.

DATE OF TREATMENT: 07-OCT-80



VECTOR FIELD PLOT

Figure 8. Pattern of surface tilting developed at the time of shut-in of the well.

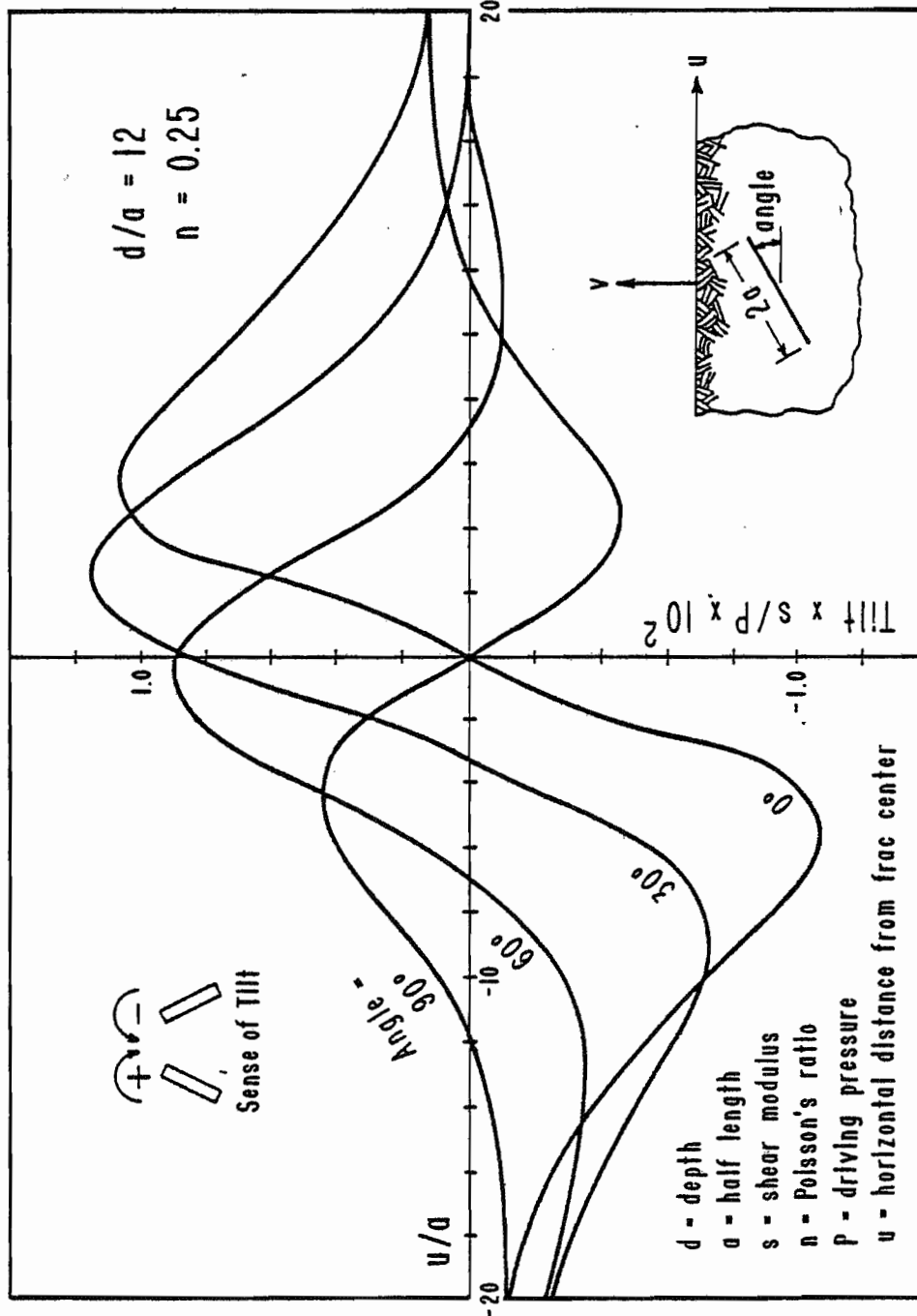
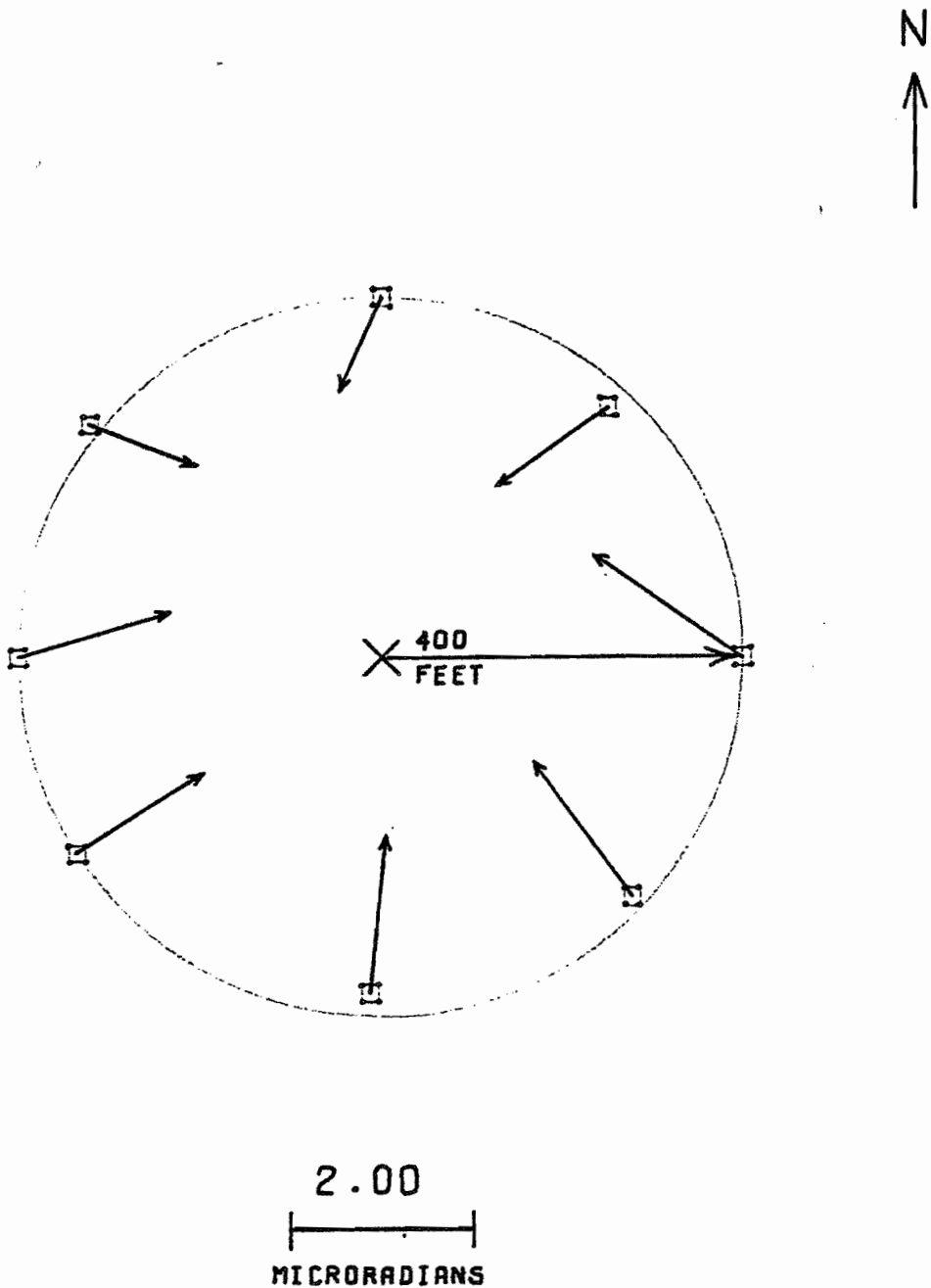


Figure 11. Free-surface tilt profiles taken across the strike of a plane strain fracture for a variety of fracture dips. The marked asymmetry in the profile about the centre which ensues from a 30 degree inclination to the horizontal should be noted. The profiles were calculated from the model given by Pollard and Holzhausen (1979).

AOB POST SHUT-IN (3 HOUR) TILTS

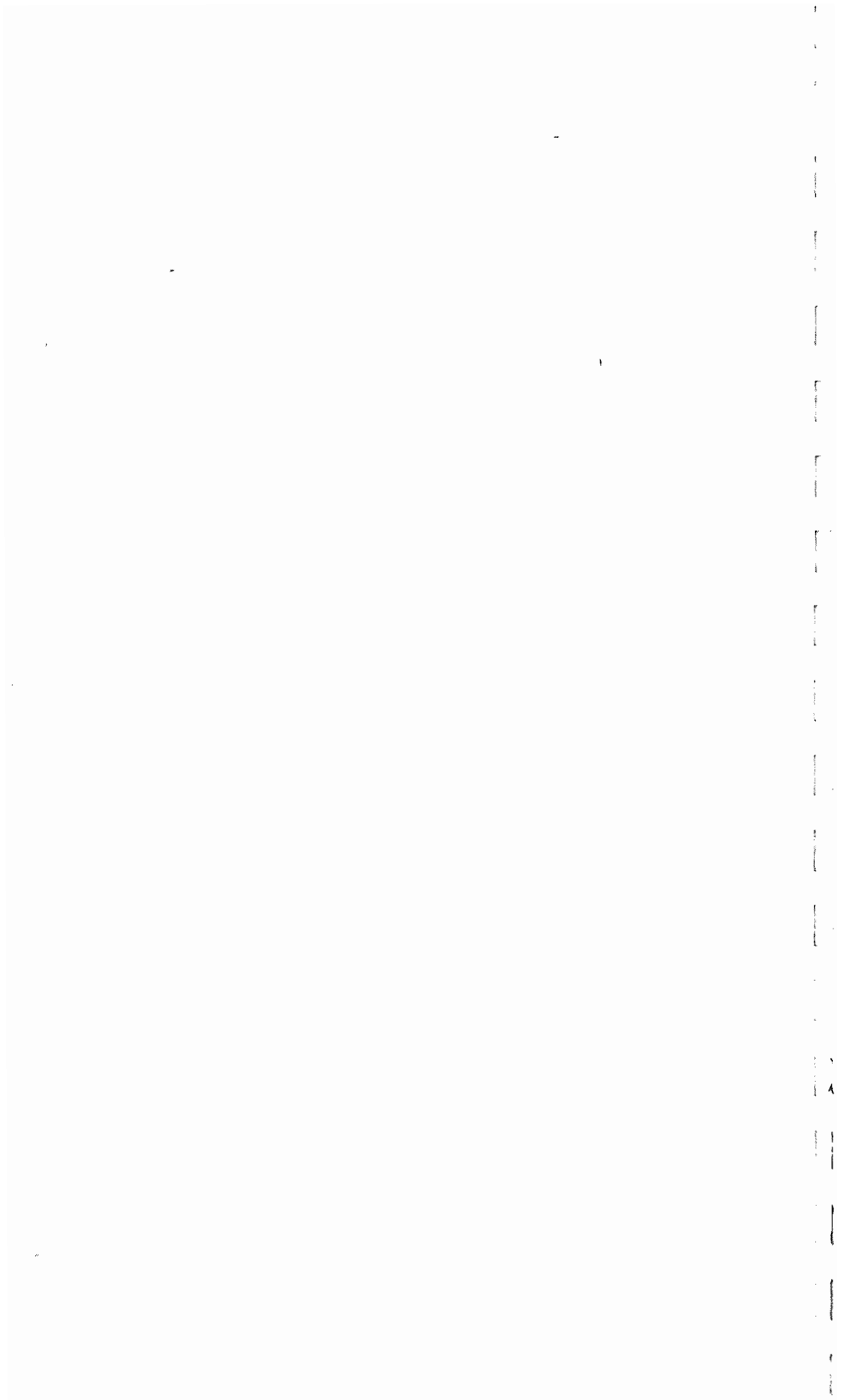
M.D.WOOD. INC.

DATE OF TREATMENT: 07-OCT-80



VECTOR FIELD PLOT

Figure 12. The pattern of surface tilting developed during the course of the three hour period which immediately followed shut-in.



PHYSICAL BASIS OF FRAC-MAP™ TECHNOLOGY

FRAC-MAP™ is a technique for mapping fractures and other subsurface deformations by measuring and interpreting ground response to subsurface displacements. The technique is based on the fact that the earth deforms under applied forces. The forces may be of mechanical origin, such as those due to fluid pressure on the walls of an hydraulic fracture; of thermal origin, such as those associated with a subsurface burn front; or gravitational, resulting for example from the removal of fluids from the pore space of a rock. Depending on the rock type and the conditions of force application, the deformations may be elastic, in which the crust returns to its original shape after removal of the force; plastic, in which the deformation is permanent; or viscous, in which the amount of permanent deformation is proportional to force magnitude and duration.

In general, deformations at a point are proportional to the size of the source region, and inversely proportional to the distance or an exponential power of the distance between the source and the point. In commercial practice deformations of the ground surface are small but can be detected by measurement of a variety of physical parameters. Among these are vertical displacement of the ground surface,

1
2
3
4
5
6
7
8
9
10
11
12
13
14
15
16
17
18
19
20
21
22
23
24
25
26
27
28
29
30
31
32
33
34
35
36
37
38
39
40
41
42
43
44
45
46
47
48
49
50
51
52
53
54
55
56
57
58
59
60
61
62
63
64
65
66
67
68
69
70
71
72
73
74
75
76
77
78
79
80
81
82
83
84
85
86
87
88
89
90
91
92
93
94
95
96
97
98
99
100

strain parallel to the surface, and rotation (tilt) of the surface (Figure 1A). With some knowledge of the mechanical properties of the earth at the test site, the depth of the source, and the applied forces, the measurements can be interpreted using appropriate physical models.

FRAC-MAP™ has been applied in a variety of jobs with source regions in tight oil and gas sands, heavy oil and tar sands, salt, and welded tuff at depths ranging from 100 to 10,000 feet. Injected fluids have included water, gel, steam, foam, gas, and slurried explosives. Among these jobs are many cases of independent verification of the results of the technique.

The M. D. Wood Company has patents pending in the area of fracture mapping and FRAC-MAP is a registered trademark of the M. D. Wood Company.

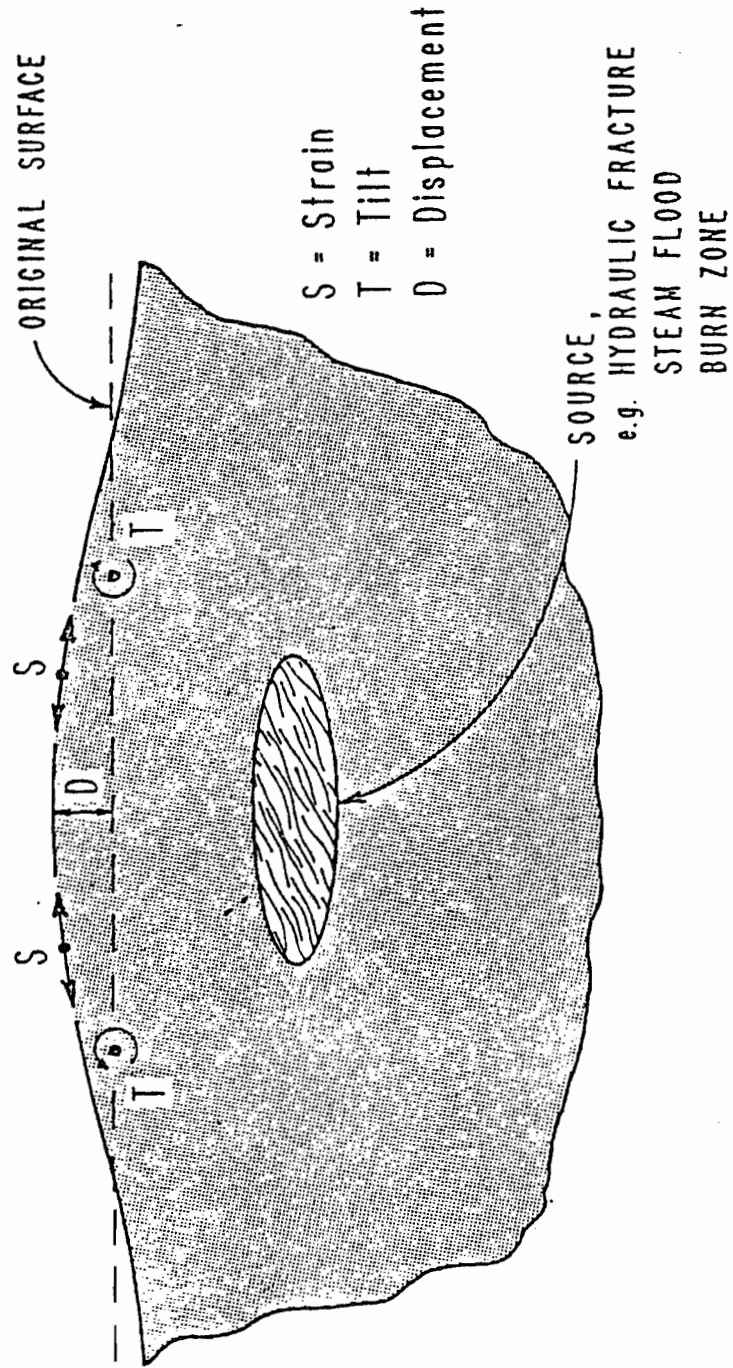


Figure 1A

F-57
INSTRUMENTATION SYSTEM

The complete FLEX-MAPTM instrumentation system consists of an array of sensors with on-site recording and transmitting unit for each sensor, and a central receiving and recording station where all data can be monitored and recorded for subsequent reduction and computer analysis. The actual configuration of the system varies according to the specific requirements of a particular operation.

Sensors

The deformation sensor used is an extremely sensitive modified tiltmeter and has considerable advantage over other forms of available instrumentation. Specifically, it is both practical to install and is capable of detecting signals resulting from a broad range of source sizes and depths, such as the rates of deformation associated with the hydraulically induced fractures in commercial treatments of the oil and gas wells. The smallest tilt resolvable by the instrument is set by the noise level of the sonde instrument environment and not by the sonde itself. The design of the sonde provides for a minimum detectable signal strength of the sonde of 5×10^{-9} radians along the axes. Consider for example the detector sonde to be mounted at the intersection of two orthogonal rigid beams extending the distance between

New York and California in one direction and between Denver and Alaska in the other, the sonde is capable of detecting a change in the height of one end of either beam, with respect to the other end, of as small as 1 inch. In addition, it can determine which beam has moved.

The noise resulting principally from the near-surface environment of the instrument will generally reduce the signal resolution, but may be countered in part by the installation of the instrument below the surface in especially prepared shallow boreholes and to some extent by the employment of elaborate signal analysis techniques. Data treatments and their efficiency are discussed in a later section. The cylindrical geometry of the sonde is designed for operation in cased or uncased holes. The accurate installation of the device in the borehole is determined by its response to a convenient and precise local reference, i.e. the local gravity vector. In principle the sensor can be operated at any depth; however, current operation is limited to depths less than 10 meters. Ultimately the sensor should be deployable at any depth where temperatures and pressures do not exceed 50 degrees Celsius and 200 psi. A later version is planned for 100 degrees Celsius and 3,000 psi.

Data Loggers

Field measurements are permanently recorded on data loggers, which are self-powered, self-contained recording units, each of which is controlled by an internal microcomputer and clock. Each unit can monitor up to 32 channels of data with a selectable scan interval ranging from one second to 30 hours. Up to two megabits of data or 128,000 data points may be recorded on each cassette tape.

Field Transmission

Data is currently taken from the sensors which are installed in their boreholes and is transmitted to the data loggers by the use of a network of armored field cable. In the future a two-way telemetry network will replace the use of the armored cable.

Data Recording Sequences

Figure 2A exhibits the flow of events in the data recording operations. The instruments are deployed at their appropriate position about 10 days prior to treatment operations and 2 to 3 days are allowed for settling of the instrument and

good coupling with the ground. Recording of background information begins about 7 days before the frac and continues to one or two days after the frac. In the earlier stages, tapes are transferred to M. D. Woods headquarters for quality control. Should one or more sites indicate malfunctioning instruments, those instruments are repaired or replaced as soon as possible. Along with the continuous recording of tiltmeter outputs and temperature data, pressure is also recorded during, and if possible, after the fracturing operations.

Data Recording
F-61

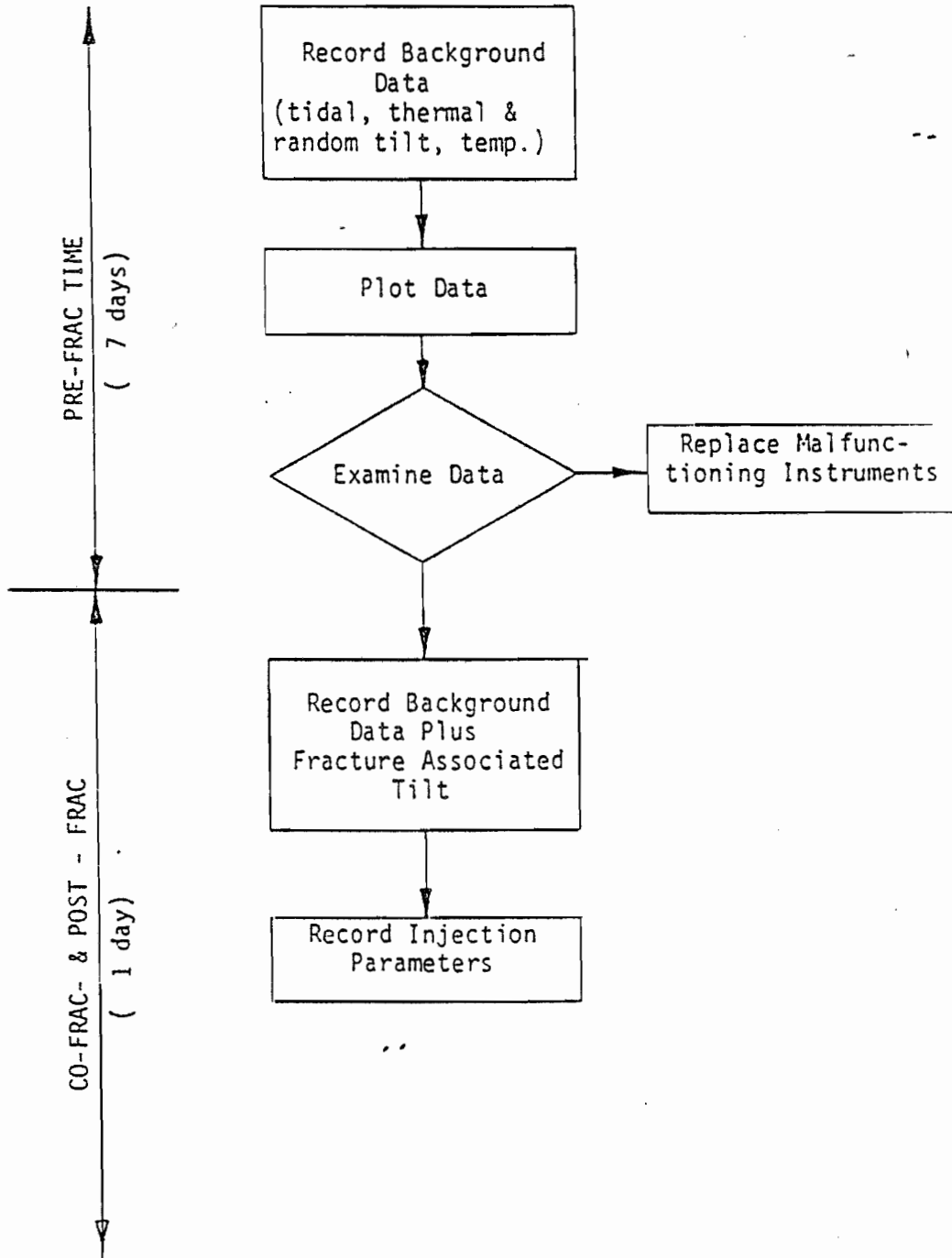
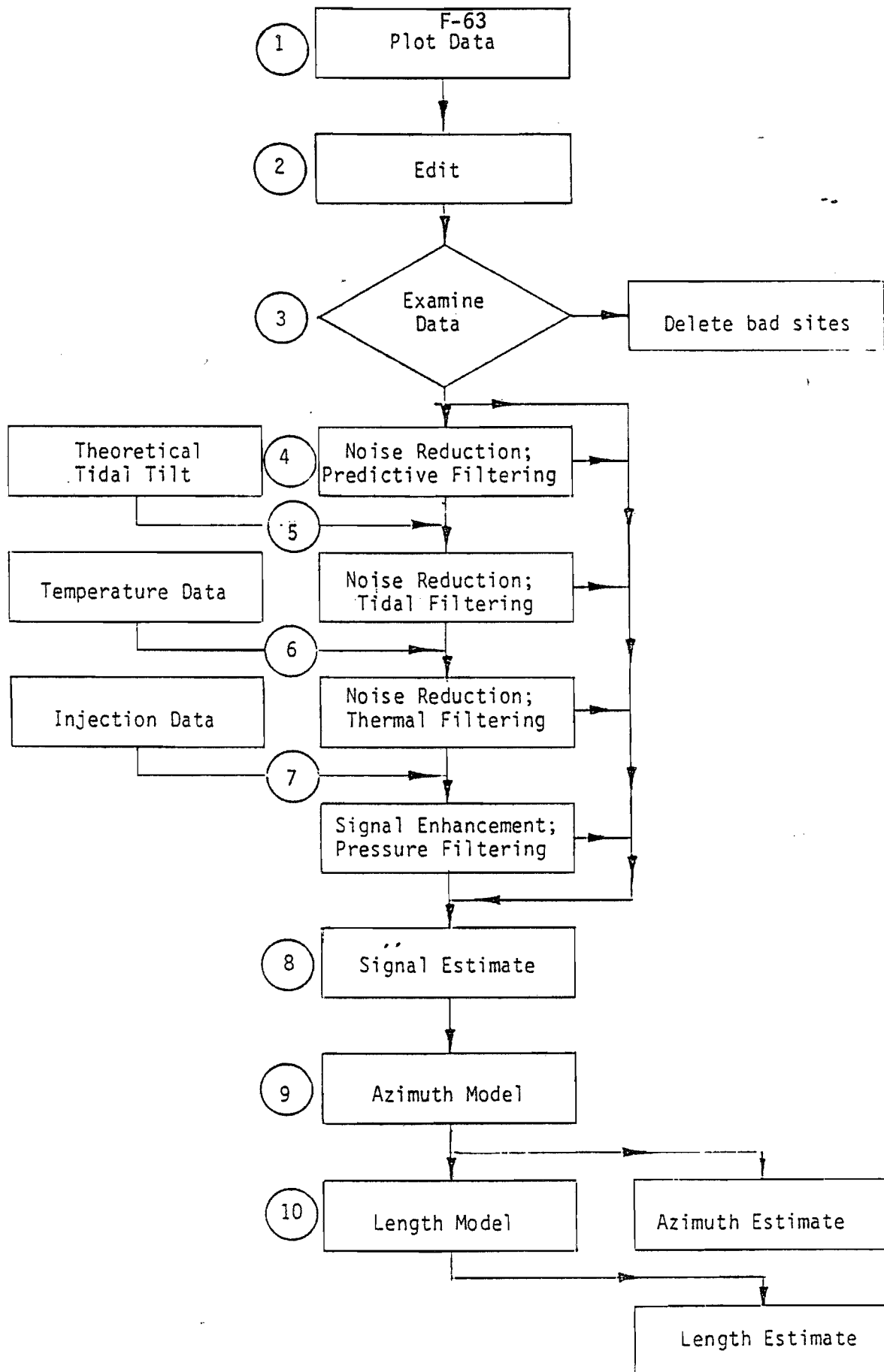


Figure 2A

DATA PROCESSING

Current data processing techniques at M. D. Wood, Inc. consist of 10 individual stages as shown in Figure 3A. A brief description of each stage is given below. Depending on the quality and strength of the signal, steps 5, 6, and 7 may not be necessary.

Figure 3A



1. Plotting of the Data

Once the data are transcribed from data logger cassettes onto discs, a hard copy plot of the tilt time series is produced. These plots are used for quality control and design of editing parameters.

2. Editing

Editing consists of the removal of extraneous events such as steps, spikes, and gaps caused by the re-zeroing of instruments, incidents at or near the site, electrical interference, changing of batteries etc.

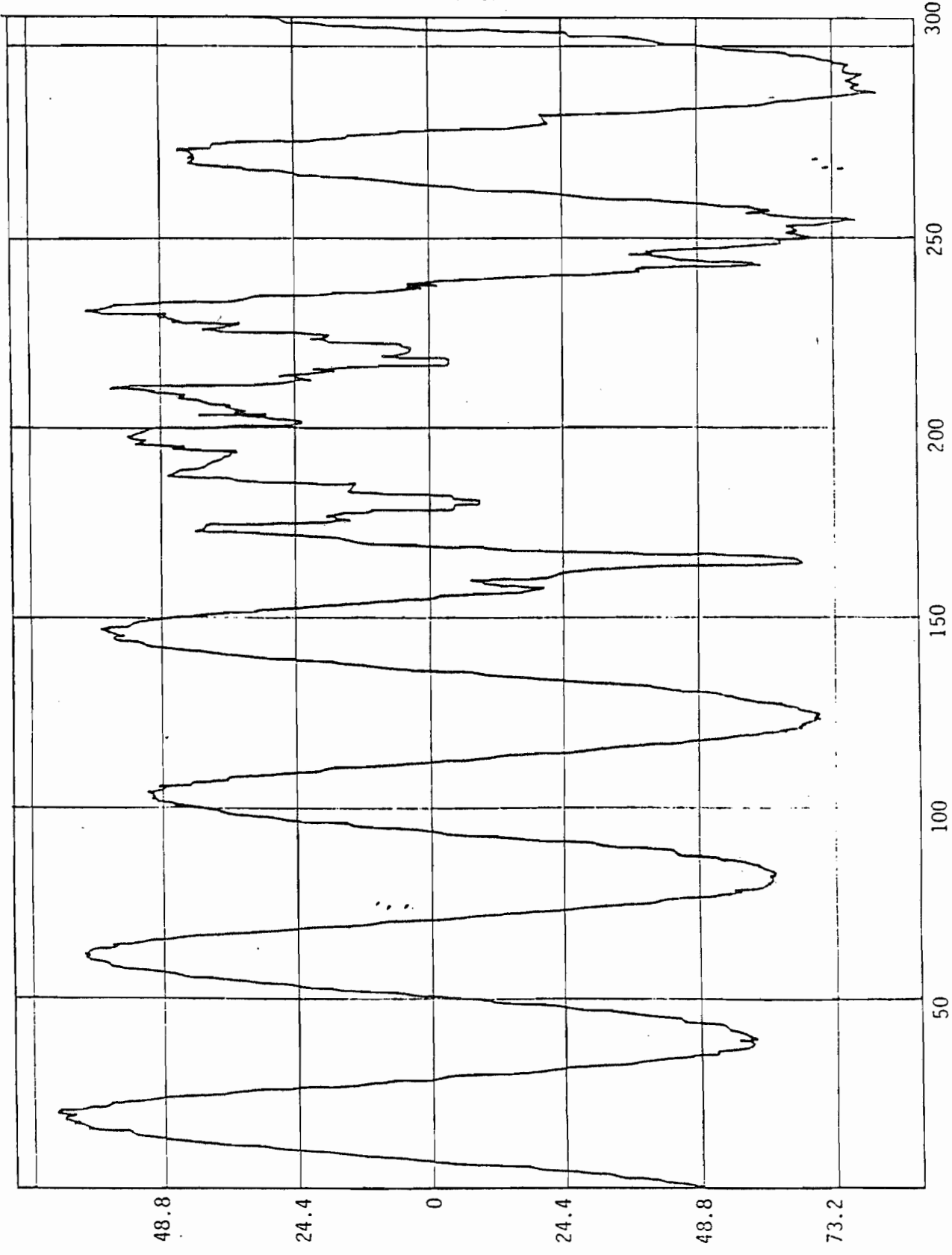
3. Examination of Data

The edited data is examined for effectiveness of editing and quality control. The data from malfunctioning instruments is removed from the data set.

4. Noise Reduction; Predictive Filtering

In this operation, a numerical filter is designed from the background data that when applied will attenuate that part of the noise which appears as "predictable" to the filter. In practice, the continuous record of tilt components for a period of up to seven days prior to the fracturing time is used to establish a filter which predicts what the tilt-meter would observe during the fracturing period if there was not fracturing taking place. The difference between the predicted frac-free tilt and actual data can thus be taken as the tilt associated with the fracturing process. The effectiveness of this filtering operations depends on the nature of the noise and the length of the background time series. Theoretically, this filter should be able to remove the tidal and thermoelastic tilt as well as other periodical noise provided that appropriate time windows are used in the design of the filter. However, should this not be possible, the data will go through the following additional processing steps discussed under steps 5 and 6.

Figures 4A through 9A are examples illustrating the effectiveness of the autoprediction filtering resulting in excellent attenuation of the noise. These figures exhibit raw data i.e. Noise plus Signal (Figures 4A and 7A), estimated noise or predicted background (Figures 5A and 8A), and the residual signal (Figures 6A and 9A) after the removal of the noise from the raw data for site 1, channel X and site 8, channel Y in a fracture mapping project carried out in conjunction with an MHF treatment at a depth in excess of 10,000 feet. It will be interesting to note that the noise in these two sites have been of totally different nature. The noise at site 1 is of high frequency nature originated from a man-made source, perhaps a pump, while the noise at site 8 is of almost pure thermoelastic nature. The autoprediction filter has been equally effective in both cases which occupy the extreme ends of the noise spectrum in our work.



CHANNEL 1X, UNCHANGED RAW DATA

Figure 4A

AMPLITUDE IN MILLIVOLTS

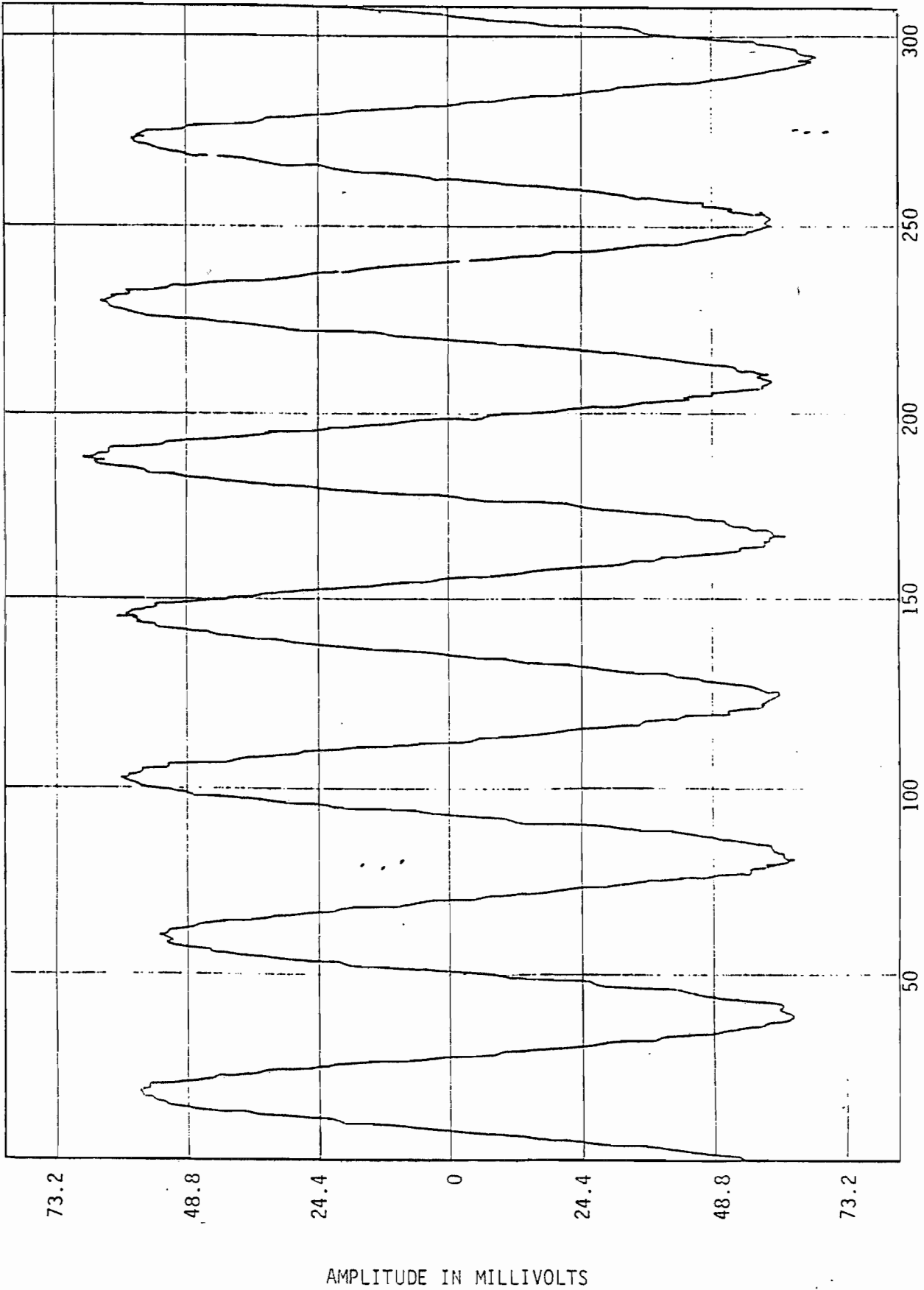


Figure 5A
CHANNEL IX, PREDICTED BACKGROUND

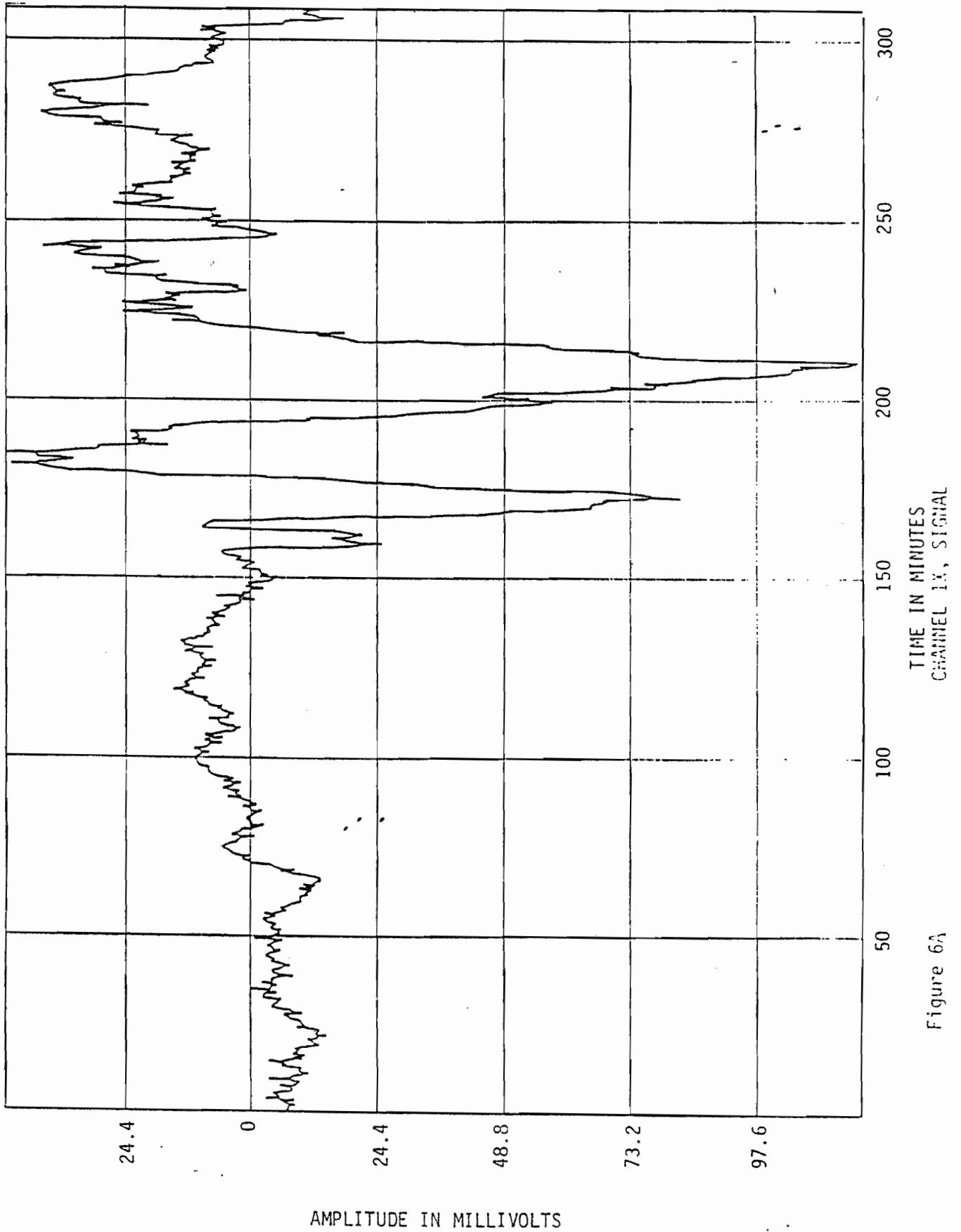
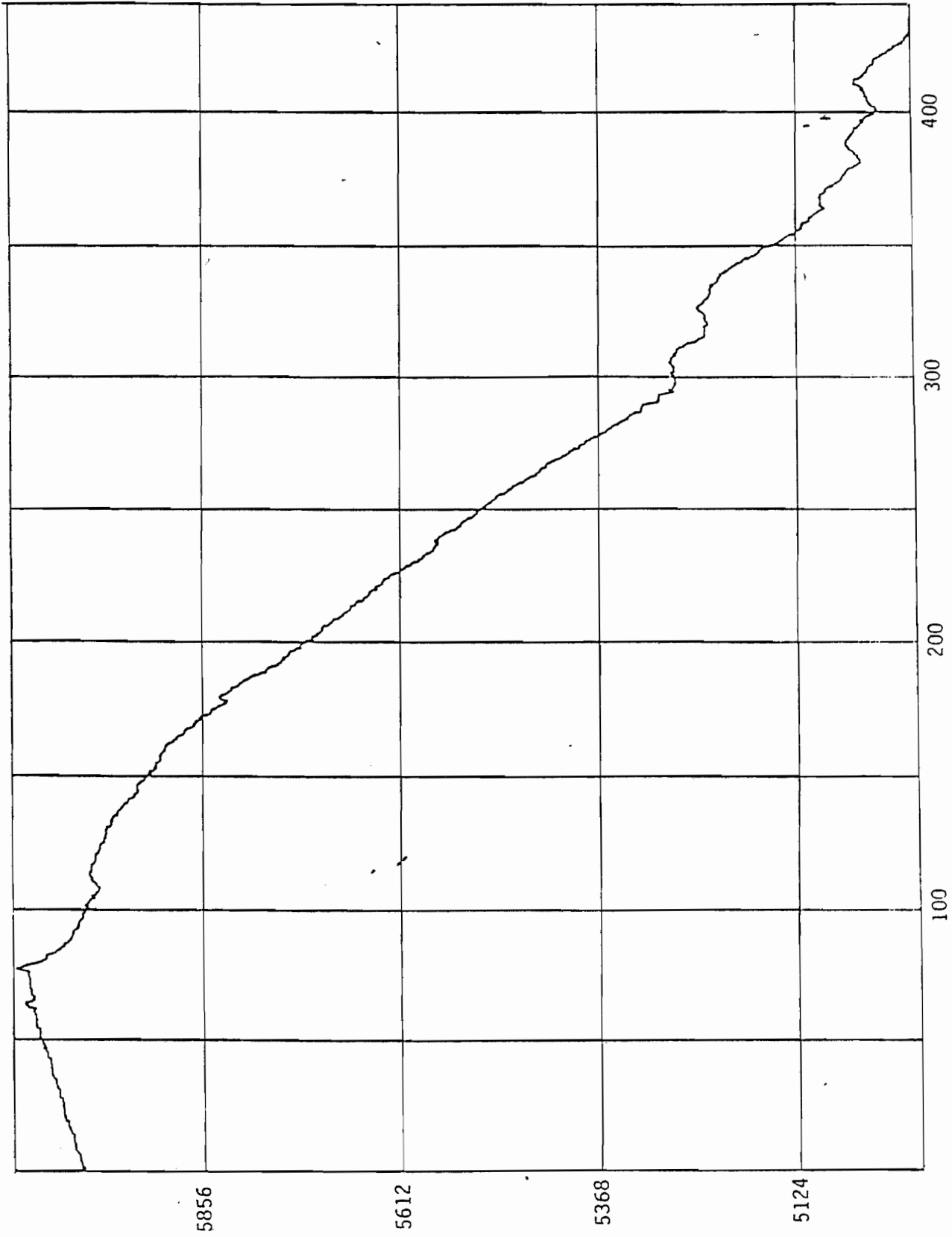


Figure 6A

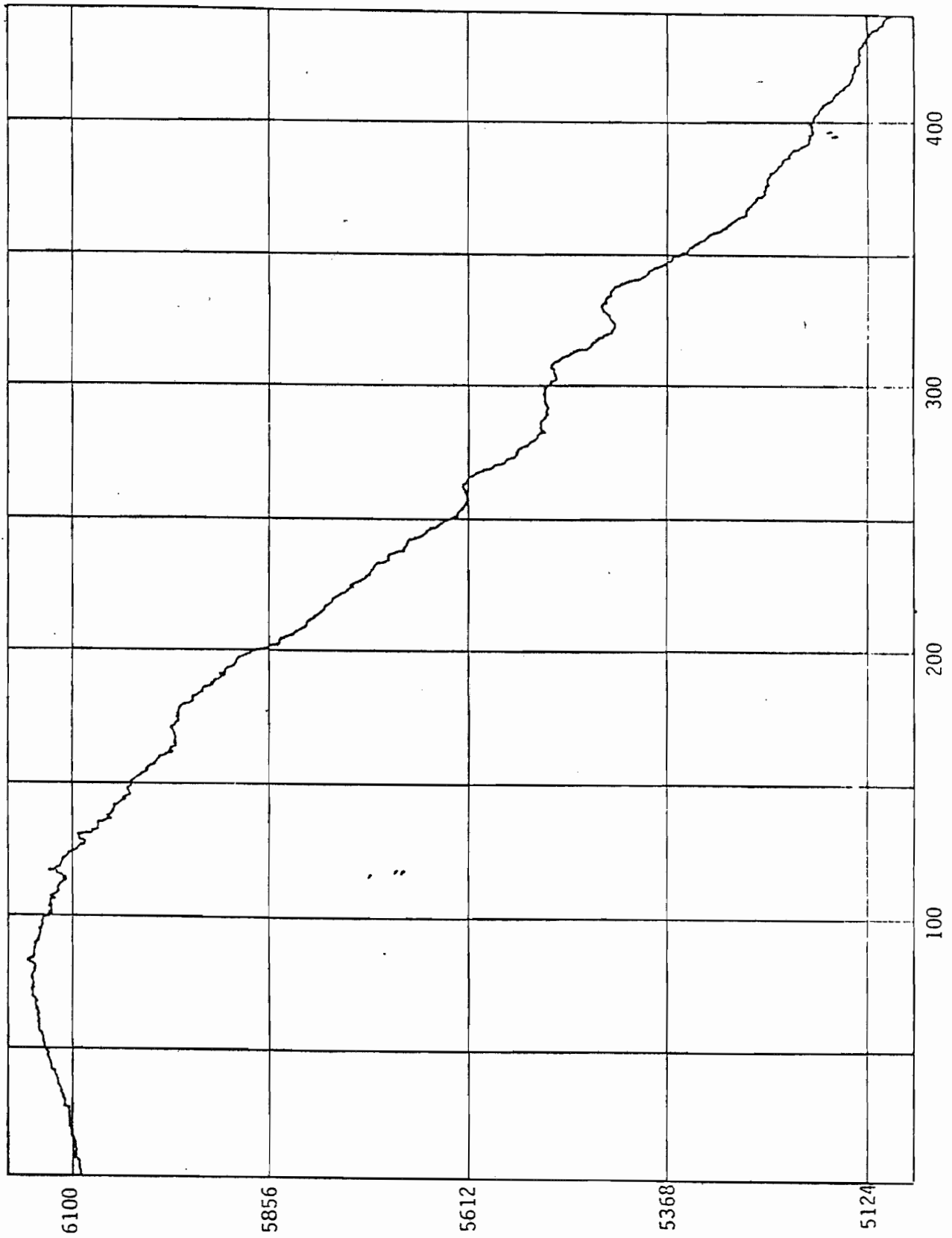
AMPLITUDE IN MILLIVOLTS



TIME IN MINUTES
CHANNEL 8Y, RAW DATA

Figure 7A

AMPLITUDE IN MILLIVOLTS



CHANNEL 8Y, PREDICTED BACKGROUND

Figure 8A

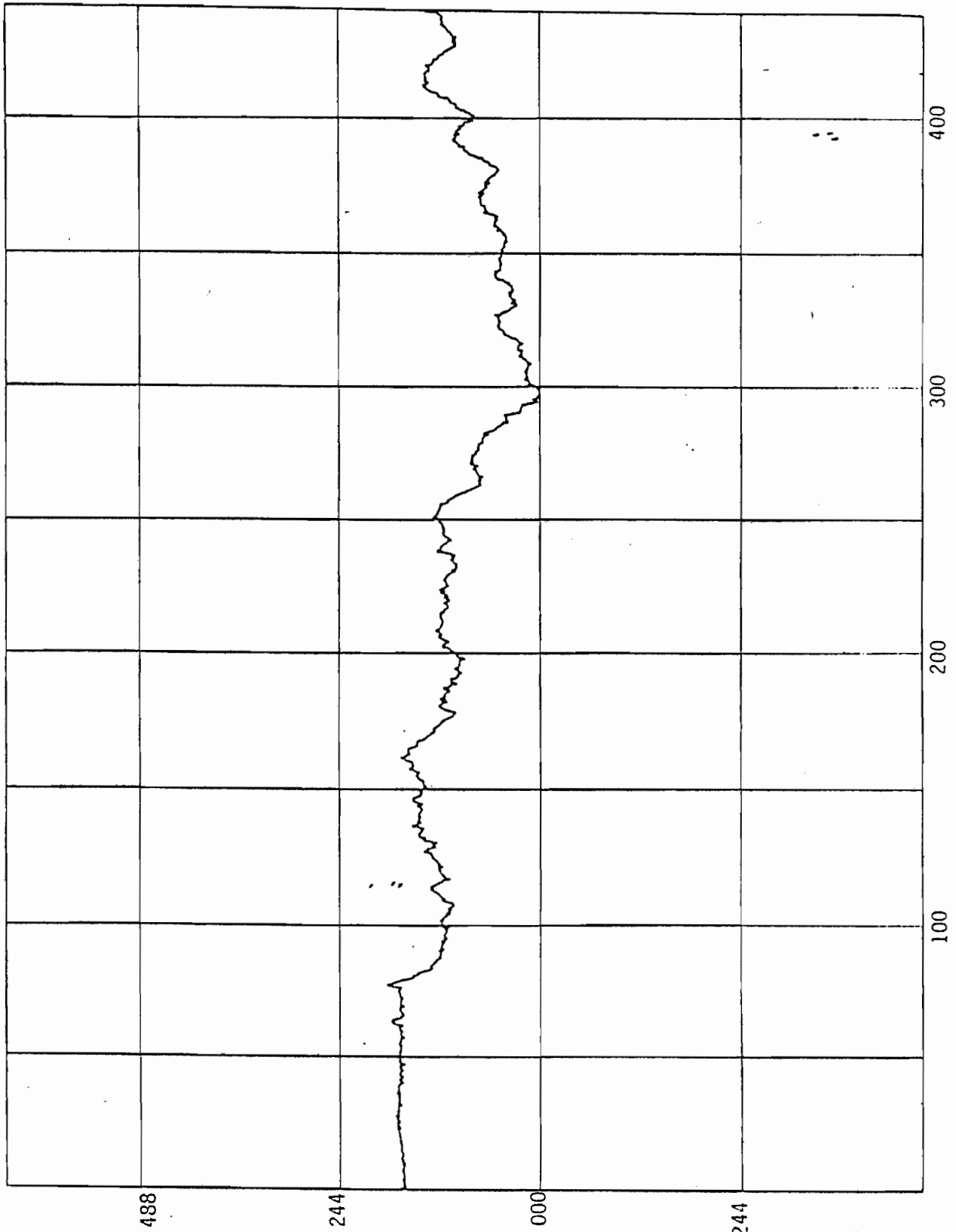


Figure 9A

AMPLITUDE IN MILLIVOLTS

It is worthwhile mentioning again here that the extent of data processing may vary from one data set to another in that in one particular survey a signal estimate might be readily available without any noise reduction, in other cases all four stages of noise reduction and signal enhancement operations may be necessary.

5. Noise Reduction, Tidal Filtering

Should the predictive filtering prove inefficient in removing the noise with tidal frequencies this type of noise is removed by a least square fit process removing the tidal harmonics.

6. Noise Reduction, Thermal Filtering

M. D. Wood, Inc. has recently completed a computer program which establishes the covariance between the temperature fluctuations and the thermoelastic tilt using field recorded temperatures. It is thus possible to apply a filter constructed from the mentioned covariance to attenuate the thermoelastic tilt, should it be necessary.

7. Signal Enhancement; Convolution With Pressure Record

The relationship between the injection pressure and fracturing associated tilt has been well established. Although a perfectly linear relation between the short period surface pressure fluctuation and tilt is rather unlikely, an overall "Cause and effect" relationship is by no means unexpected. In the absence of a bottom hole pressure record, which is usually free of short period events normal to the surface pressure record, the surface pressure record can be used as an input to a filter which is constructed from the covariance between the pressure record and the tilt record. The only risk in this operation is an accidental correspondence between the high frequency contents of the surface pressure record and the high frequency remanent noise in the tilt record. In severe cases, a Hi-cut filtered is applied to the pressure record prior to its application as a signal enhancement filter.

It must be emphasized here that the filter designed from the pressure record is by no means capable of creating a "psuedo" signal but its power is limited to the enhancement of that part of the tilt data which will be co-spectral with the pressure record.

8. Signal Estimate

Signal estimates are possible either by direct amplitude measurements from the plotted data or by the RMS averaging method.

9. Azimuth Model

The azimuth model is an iterative computer program that finds an azimuth which best satisfies the collective responses of all tiltmeters. Under an absolutely noise free condition the model is capable of computing a unique fracture azimuth that satisfies the observed tilt as a result of fracturing; However, since no such conditions will ever exist

in the real world the presence of some re-
manent noise in the tilt record will result
in some degree of uncertainty. It is felt
that as the number of field instruments in-
creases and as the elaborate noise reduction
signal enhancement operations are carried out,
the reliability of the estimated azimuth ap-
proaches its theoretical bounds.

10. Length Model

In cases of proper field instrumentation for
estimation of the fracture length, the last
stage of the data processing operation is the
calculation of the fracture length through a
computer program which is basically similar to
the azimuth model. This program is being cur-
rently tested and will be commercially avail-
able in very near future.

SIGNAL PROCESSING

Needless to say, there are a number of qualitative and statistical tests that are carried out upon completion of each stage of the data processing. It is rather unlikely and highly undesirable that any geophysical interpretation work will ever be totally automatic. The tests at the end of each data processing stage provides the interpretation geophysicist with means to evaluate each output before it is used as an input to the next stage.

Some of the jobs that are monitored and mapped by M. D. WOOD, INC. originate at depths as great as 10,000 feet. In these instances, the theoretical surface displacements associated with deep, commercial size treatments are on the order of microns. Our experience indicates that gradients of the vertical displacement field are easier to measure than the displacements themselves at the deformational signal periods (minutes to hours) and magnitudes (nanoradians to microradians) that occur during the treatments. Such small measurements have previously been possible only in an observatory environment.

FLEX-MAP™ attempts, within the bounds of commercial practice, to record all signal and noise inputs and the instrument responses to these inputs. Deep and elaborate, observatory-type site preparation that would enhance the signal-to-noise ratio is not economically feasible. Thus, monitoring is done in the noisy near-surface environment. This environment requires recording of surface meteorological data as the primary noise input. Reservoir stimulation parameters (e.g. injection pressures and flow rates in the case of hydraulic-fracture treatments) and, most importantly, the tilt response of the earth's surface to all of the above inputs are also recorded. This strategy is followed to varying degrees in all monitoring programs, but is most important when the signal source is deep and the signal-to-noise ratio is small.

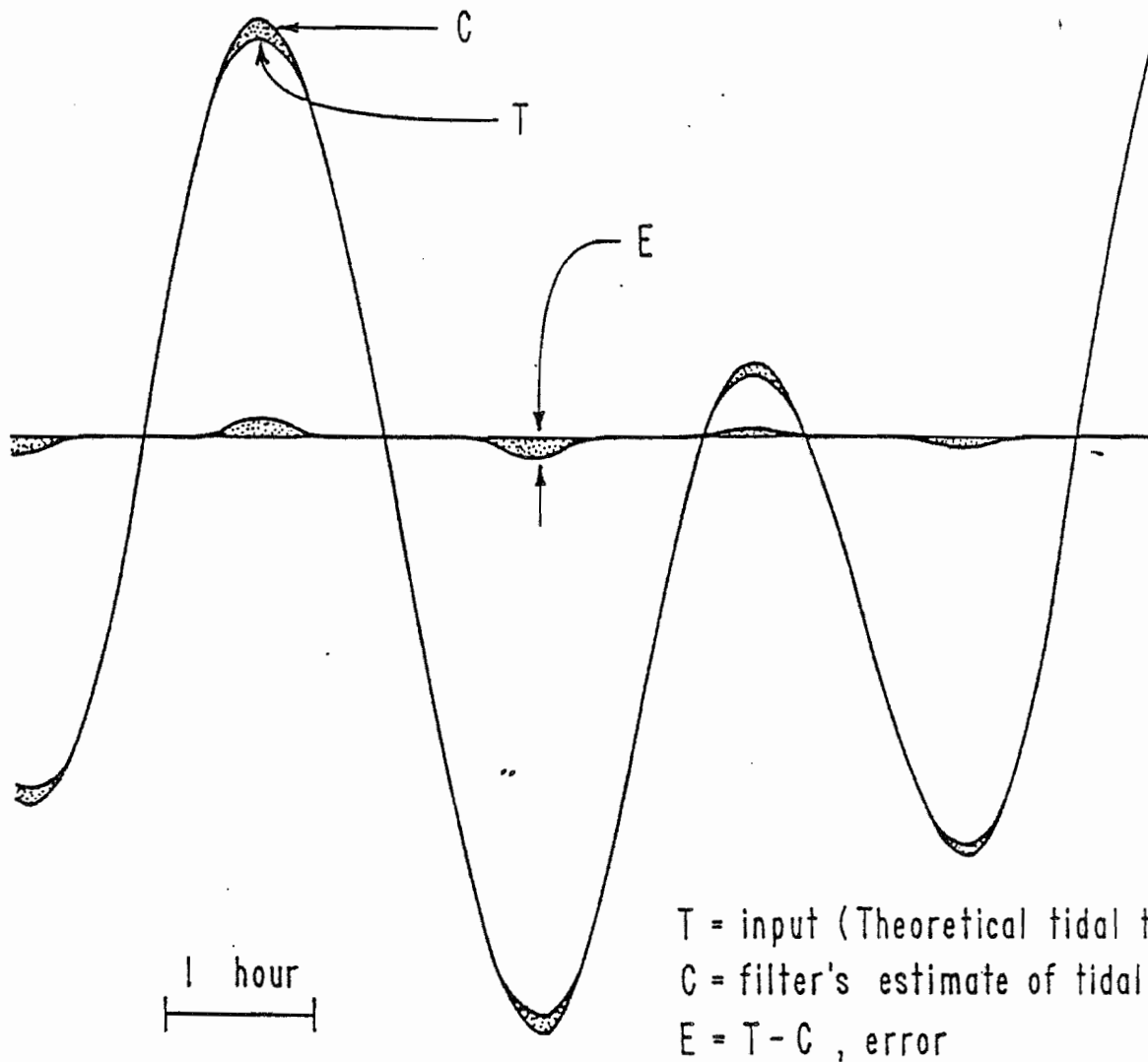
The accuracy of the instrument response to the weak signal produced by the treatment is of paramount concern. Fortunately, a natural and continuous calibration signal is produced at microradian and microhertz levels by the tidal deformation of the earth by the sun and moon. The solid earth tides are the most predictable and precisely known of all geophysical phenomena. Figures 10A and 11A are repre-

sentative of data recorded in the Denver basin associated with monitoring of hydraulic fracturing at 8,000 and 5,000 feet, respectively. These data illustrate a well defined tidal response at diurnal and semi-diurnal periods that is also contaminated by thermal strains of predominantly a diurnal period as induced by the sun. Thermally-induced strains are most often an order of magnitude greater than tidal strains and tilts at the same frequency and hence, clear recognition of the diurnal tide is not always possible. The semi-diurnal tide, however, should be detectable, and the identification of such in the data provides a necessary and sufficient quality control on the instrument's reliability. This lends credibility to its sensitivity to the small fracture-related signals. A signal of 1×10^{-7} radian or less, produced by a deep fracture, is not easily recognized in the raw data, and is inadequate for direct determination of fracture geometry and azimuth. Figure 11A illustrates this problem for a job monitored at 5,000 feet depth. Without knowledge of the exact period of fracturing, the slope changes in the sinusoidal diurnal deformation curve due to fracture deformation would not be recognized and would, in any event, be difficult to use in fracture mapping. Sophisticated noise analysis and signal enhancement are required for mapping deep fractures.

tidal frequencies. The dataset used is a record consisting of theoretically predicted earth tides from an arbitrary location. The filter has removed all but one percent of the theoretical earth tides, showing the efficacy of this technique.

The next stage of data treatment consists of removing the meteorological noise from the data. Contamination of the record due to diurnal thermal strains, wind, barometric fluctuations, and moisture changes are the most serious and difficult sources of noise to eliminate. It is especially important to separate these inputs in the study of long-term, in-situ processing schemes. As discussed above, the extraction of the earth tides removes thermal strains at solar frequencies from the raw data. Thereafter the weather-driven contaminants remaining are aperiodic and consist of rainfall effects (ground settling or swelling from water absorption), local temperature changes, and wind effects (ground deformation due to swaying trees, etc.).

A comparison (E) of the theoretical tidal tilt (T) with the nine principal tidal constituents (C) filtered from (T)



There have been situations where favorable signal-to-weather noise ratios have been obtained without meteorological filtering. In some situations we have found that improved site preparation for deeper emplacements and improvements in remote manipulation of the sensor with site excavation have largely decoupled the sensor from significant surface noise conditions.

R
F
F
I
I
I
C
L
L
E
E
C
L
E
I

INTERPRETATION OF EARTH DEFORMATIONS

Once the signal attributable to the source has been isolated from the noise, it is interpreted with selected models derived within the framework of continuum mechanics. Interpretation makes use of all data available from a particular project, e.g. wellhead pressures, injection rates, downhole pressures, fluid viscosities, total volume injected, mechanical properties of the earth at the site, and depth of the source. In general, the displacement gradient (tilt) at a point at the earth's surface is a function of the coordinates of the point, the pressure distribution in the source region, the depth, to the center of the source, the earth's material properties (elastic moduli, yield point, coefficients of thermal expansion, permeability to various fluids, etc.), and source geometry and dimensions.

If there are initial limitations on the structure of the source, e.g. it is known to be an hydraulic fracture, the analysis is considerably simplified. The general orientation of the fracture can be derived from the symmetry of the measured tilt field (Figure 13A) and fracture radii can be estimated using functional relationships between tilt and fracture geometry. This surface deformation varies with the

position of the sensor relative to the fracture. Figure 13A shows theoretical surface tilts as a function of position above a 2-dimension vertical fracture. It follows that tilts produced by fracture flexure are greatest at points perpendicular to the fracture azimuth at distances equal to approximately one-half of the injection depth. This maximum decays smoothly as a line directly above the strike of the fracture is approached. Based on such theoretical considerations, the optimum instrumentation array can be chosen for each job. The procedure for finding the azimuth of a deep fracture is based on the statistical errors from the filtering process, making use of the average fracture deformation tilt seen by a tilt channel during a treatment.

Azimuth determination assumes that each tiltmeter site is as likely as another to receive fracture deformation energy (i.e., assumes no prior knowledge of preferred fracture azimuth), and hence requires a circular instrument array. If the actual array is noncircular, applying an appropriate mathematical transformation will make that array appear circular to the azimuth-finding procedure.

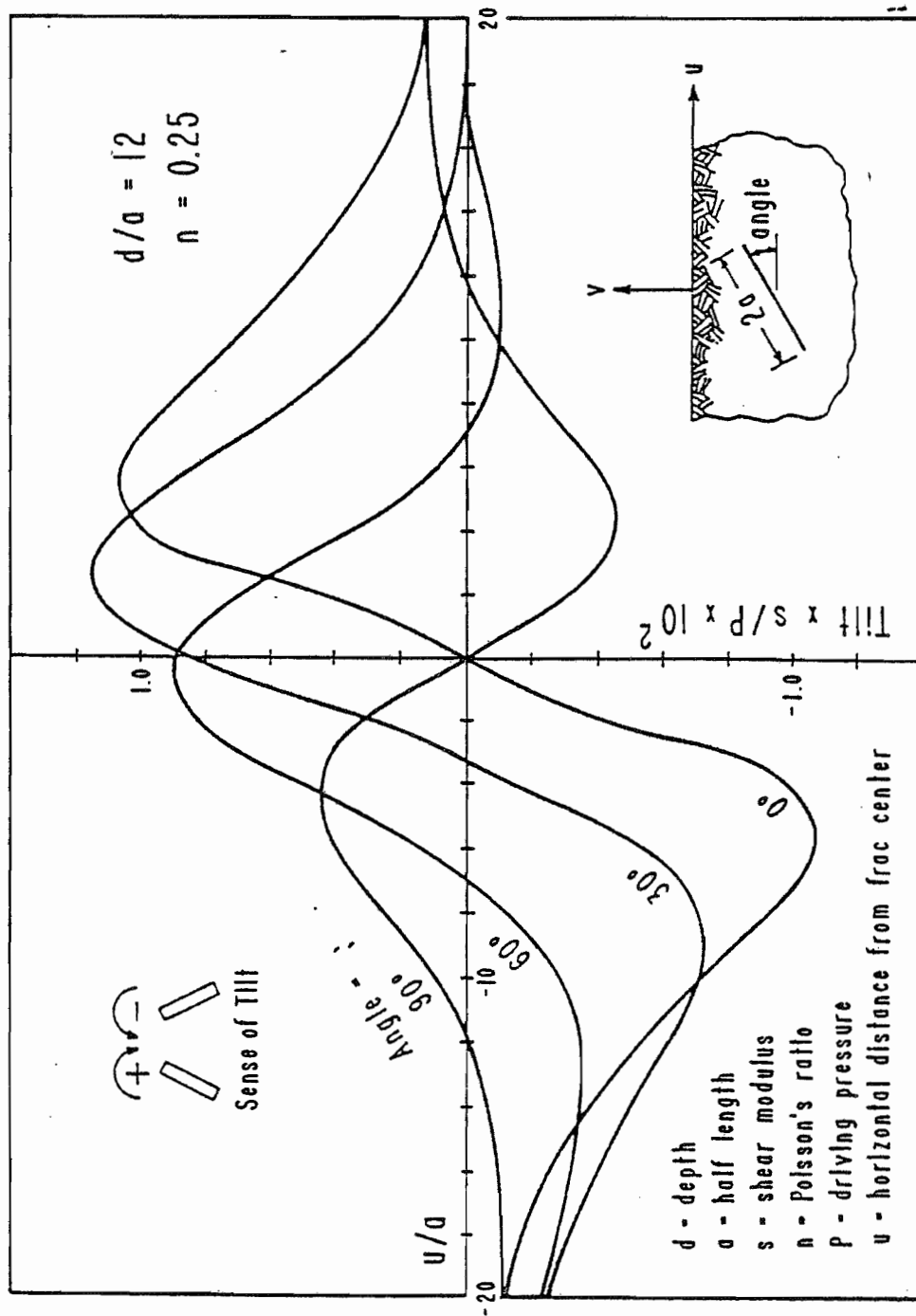


Figure 13A

If general source structure and geometry is not known beforehand (as in some thermal recovery schemes, for example) choosing a physical model for interpretation of the measurements is more difficult. Nonetheless, considerable useful information can be obtained on the basis of the symmetry and overall magnitude of the tilt field. These features may indicate whether the source is predominantly equidimensional, elongate, or flattened. Physical models for the deformation become progressively more accurate with increasing experience at a particular locality or with a particular source.

DETERMINING FRACTURE AZIMUTH AND LENGTH

Under ideal circumstances, three sites could accurately define the azimuth of a biwinged fracture. In practice, the noise filtering and signal filtering operations are imperfect, and the results are nonuniform across an array. For these reasons, the array size is usually eight or more instruments, uniformly deployed about the injection well. The solution for fracture azimuth is then a mathematical least squares weighting based on the theoretically expected energy distribution in the vicinity of the fracture plane.

The problem of determining the complete fracture vector (i.e. both azimuth and length) results from limited array size. A generalized solution would be a dense grid of instruments as the fracture vector must be bounded. In principle, with a limited set of instruments, a precise fracture length determination demands a linear array extending beyond the predicted length of the fracture, paralleling the assumed azimuth of the fractures. Currently, estimating the fracture azimuth is determined with a circular instrument array from a nearby well. However, since previous azimuth

information is seldom available, two or more circular array's of instruments can be used for determination of length provided the fracture length to depth ratio is not very small.

CONCLUSIONS

Significant progress has been made in delineating both fracture azimuth and length.

Confidence in the fracture azimuth technique is due in large measure to the reproducibility of the results from well to well in the same field in the same production zone, with the same hydraulic-fracture treatment volumes and rates. The results have been substantiated by other geophysical results derived from the same wells. For example, the agreement of FRAC-MAP™ results with laboratory determinations of preferred fracture orientation from oriented cores tends to confirm our azimuth determinations. The field near Denver, Colorado, has provided an excellent field test site where these results could be verified. We are equally confident that over time our fracture length techniques will receive similar verification.

Similarly, we now see fracture asymmetry in our fracture length analysis. The presence of fracture asymmetry adds the necessary detail for fracture mapping to be considered as an integral part of the completion program for intensive infill spacing and location of new wells. It should, in fact, be

employed to determine the placement of wells where azimuth, geometry, and dimensions of previously-fractured neighboring wells deviate from earlier assumptions that guided the initial pattern of well placement. Information distributed over, say, every tenth well that has a FRAC-MAP™, might be sufficient to recover fully 15% more of the resource that would have been otherwise lost on improper well placement.

In the future, when real-time monitoring with FRAC-MAP™ is fully developed anomalous conditions in the reservoir leading to a possible screenout can be identified and perhaps measures taken to change the condition and to allow the job to reach completion. It is not possible to steer a fracture, but FRAC-MAP™ can certainly point out when the azimuth has steered itself to an undesirable orientation and length, and at that moment terminate the treatment. At that point fracturing operations will be able to improve with FRAC-MAP™ information feedback. The treatment company should then be capable of tailoring procedures to the idiosyncrasies of the particular reservoir.